e-ISSN:2651-4060

June 2023
Volume 6
Issue 3

SABİAD

SAĞLIK BİLİMLERİNDE İLERİ ARAŞTIRMALAR DERGİSİ

JOURNAL OF ADVANCED RESEARCH IN HEALTH SCIENCES

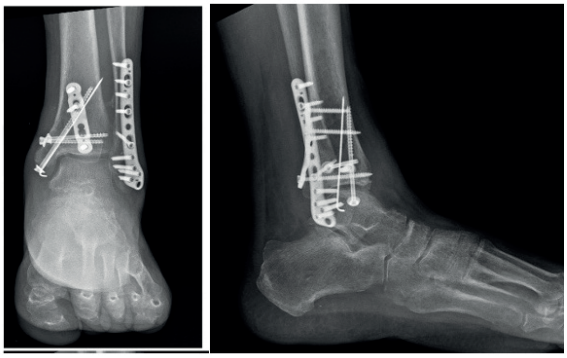

RESEARCH ARTICLE

İSTANBUL UNIVERSITY PRESS

Indexing and Abstracting

ULAKBİM TR Dizin

CAB Abstracts

CABI Global Health

CABI Nutrition and Food Sciences

EBSCO CINAHL Ultimate

EBSCO Central & Eastern European Academic Source

ASOS Index

DOAJ

SABİAD
SAĞLIK BİLİMLERİNDE İLERİ ARAŞTIRMALAR DERGİSİ
JOURNAL OF ADVANCED RESEARCH IN HEALTH SCIENCES
June 2023, Volume 6, Issue 3 e-ISSN:2651-4060

Owner
Prof. Dr. Yahya GÜLDİKEN
Istanbul University, Institute of Graduate Studies in Health Sciences, Istanbul, Turkiye

Responsible Manager
Prof. Dr. Yahya GÜLDİKEN
Istanbul University, Institute of Graduate Studies in Health Sciences, Istanbul, Turkiye

Correspondence Address
İstanbul Üniversitesi, Sağlık Bilimleri Enstitüsü,
Bozdoğan Kemeri Cad. No: 4 Vezneciler Hamamı Sk.
Vezneciler, Fatih 34126 İstanbul, Türkiye
Telefon / Phone: +90 (212) 440 00 00 (14131)
Faks / Fax: +90 (212) 414 30 16
E-mail: sabiad@istanbul.edu.tr
https://dergipark.org.tr/sabiad
http://iupress.istanbul.edu.tr/tr/journal/jarhs/home

Publisher
Istanbul University Press
İstanbul Üniversitesi Merkez Kampüsü, 34452 Beyazıt,
Fatih / İstanbul, Türkiye
Telefon / Phone: +90 (212) 440 00 00

Cover photo
Dr. İbrahim SUNGUR

The publication language of the journal is English.

This is a scholarly, international, peer-reviewed and open-access journal published triannually in February, June and October.

Publication Type: Periodical

SABİAD
SAĞLIK BİLİMLERİNDE İLERİ ARAŞTIRMALAR DERGİSİ
JOURNAL OF ADVANCED RESEARCH IN HEALTH SCIENCES
June 2023, Volume 6, Issue 3 e-ISSN:2651-4060

EDITORIAL MANAGEMENT BOARD

SABİAD
SAĞLIK BİLİMLERİNDE İLERİ ARAŞTIRMALAR DERGİSİ
JOURNAL OF ADVANCED RESEARCH IN HEALTH SCIENCES
June 2023, Volume 6, Issue 3 e-ISSN:2651-4060

EDITORIAL BOARD

From the Editor

Dear readers of the Journal of Advanced Studies in Health Sciences, welcome to last issue of this year. The Journal of Advanced Studies in Health Sciences is one of Istanbul University's journals and is published triannually in February, June, and October according to international standards. The journal provides a wide range of services in the field of health. Our journal started its publication life in 2018 and has been included in national and international indexes since 2021. There are 18 research articles, 7 of which are basic science and 11 are clinical, in the October 2023 issue of our journal. Our journal aims to participate SCI. In this context, only publications in English accepted to our journal as of June 2023. We are waiting for your research, we will be stronger with you, thank you to the scientists who contributed, with our respect.

Editörden

Sağlık Bilimleri İleri Araştırmalar Dergisi'nin değerli okuyucuları, bu yılın son sayısına hoş geldiniz. Sağlık Bilimleri İleri Araştırmalar Dergisi, İstanbul Üniversitesi'nin dergilerinden biri olup, uluslararası standartlara uygun olarak yılda üç kez Şubat, Haziran ve Ekim aylarında yayımlanır.

Dergi sağlık alanında geniş bir yelpazede hizmet sunmaktadır. Dergimiz 2018 yılında yayın hayatına başlamış olup 2021 yılından itibaren ulusal ve uluslararası indekslerde yer almaktadır. Dergimizin Ekim 2023 sayısında 7'si temel bilim, 11'i klinik olmak üzere 18 araştırma makalesi bulunmaktadır. Dergimiz SCI'a katılmayı hedeflemektedir. Bu bağlamda dergimize Haziran 2023 itibarıyla yalnızca İngilizce yayınlar kabul edilmektedir.

Araştırmalarınızı bekliyoruz, sizlerle daha güçlü olacağız, emeği geçen bilim insanlarına teşekkür eder, saygılarımızı sunarız.

Prof. Dr. Zeynep Karakaş

CONTENTS

CONTENTS

CONTENTS

İSTANBUL UNIVERSITY PRESS

RESEARCH ARTICLE / ARAŞTIRMA MAKALESİ
Journal of Advanced Research in Health Sciences / Sağlık Bilimlerinde İleri Araştırmalar Dergisi 2023
DOI: 10.26650/JARHS2023-1346155

TNFRSF13B VARIANTS ACT AS MODIFIERS TO CLINICAL PHENOTYPES IN COMMON VARIABLE IMMUNE DEFICIENCY DISORDERS

TNFRSF13B VARYANTLARI, YAYGIN DEĞİŞKEN İMMÜN YETMEZLİK KLİNİK FENOTİPİNİN DÜZENLENMESİNDE ROL OYNAR

Sinem FIRTINA[1], Aslı KUTLU[2], Begüm IŞIKGİL[3], Medinenur YOZLU[4], Beyza Nur CEPECİ[4], Hülya YILMAZ[5], Yuk Yin NG[6], Özden HATIRNAZ NG[7], Ayça KIYKIM[8], Esra YÜCEL ÖZEK[9], Elif AYDINER[10], Safa BARIŞ[10], Ahmet Oğuzhan ÖZEN[10], Serdar NEPESOV[11], Yıldız ÇAMCIOĞLU[8], İsmail REİSLİ[12], Muhlis Cem AR[5], Müge SAYİTOĞLU[13]

[1]Istanbul University-Cerrahpasa, Cerrahpasa Faculty of Medicine, Department of Medical Genetics, Istanbul, Turkiye
[2]Istinye University, Engineering and Natural Science Faculty, Department of Molecular Biology and Genetics, Istanbul, Turkiye
[3]Istinye University, Institute for Graduate Education, Department of Medical Biology and Genetics, Istanbul, Turkiye
[4]Gebze Technical University, Science Faculty, Department of Molecular Biology and Genetics, Kocaeli, Turkiye
[5]Istanbul University-Cerrahpasa, Cerrahpasa Faculty of Medicine, Department of Internal Medicine, Division Hematology, Istanbul, Turkiye
[6]Bilgi University, Engineering and Natural Science Faculty, Department of Genetics and Bioengineering, Istanbul, Turkiye
[7]Acibadem Mehmet Ali Aydinlar University, Faculty of Medicine, Department of Medical Genetics, Istanbul, Turkiye
[8]Istanbul University-Cerrahpasa, Cerrahpasa Faculty of Medicine, Department of Infectious Diseases, Division Allergy and Clinical Immunology, Istanbul, Turkiye
[9]Istanbul University, Istanbul Faculty of Medicine, Department of Pediatrics, Division Pediatric Allergy and Immunology, Istanbul, Turkiye
[10]Marmara University, Faculty of Medicine, Department of Pediatrics, Division Pediatric Allergy and Immunology, Istanbul, Turkiye
[11]Medical Park Goztepe Hospital, Clinic of Pediatrics, Division of Pediatric Allergy and Immunology, Istanbul, Turkiye
[12]Necmettin Erbakan University, Faculty of Medicine, Department of Pediatrics, Division Pediatric Allergy and Immunology, Istanbul, Turkiye
[13]Istanbul University, Aziz Sancar Institute of Experimental Medicine, Department of Genetics, Istanbul, Turkiye

ORCID ID: S.F. 0000-0002-3370-8545; A.K. 0000-0002-9169-388X; B.I. 0000-0002-7541-4596; M.Y. 0000-0002-3580-7280; B.N.C. 0000-0001-9417-2943; H.Y. 0000-0001-5664-5893; Y.Y.N. 0000-0001-9755-6045; Ö.H.N. 0000-0001-7728-6527; A.K. 0000-0001-5821-3963; E.Y.Ö. 0000-0003-3712-2522; E.A. 0000-0003-4150-5200; S.B. 0000-0002-4730-9422;A.O.Ö. 0000-0002-9065-1901; S.N. 0000-0002-4551-5433; Y.Ç. 0000-0002-4796-6828; İ.R. 0000-0001-8247-6405; M.C.A. 0000-0002-0332-9253; M.S. 0000-0002-8648-213X

Citation/Atıf: Firtina S, Kutlu A, Isikligil B, Yozlu M, Cepeci BN, Yilmaz H, et al. TNFRSF13B variants act as modifiers to clinical phenotypes in common variable immune deficiency disorders. Journal of Advanced Research in Health Sciences 2023;6(3):210-218. https://doi.org/10.26650/JARHS2023-1346155

ABSTRACT

Objective: The TNF receptor gene 13B (*TNFSRF13B*) is a member of the TNF superfamily which is crucial for B cell maturation, plasma cell differentiation, and antibody response. Impaired expression of the *TNFRSF13B* gene is associated with common variable immune deficiency (CVID), autoimmunity, and lymphoproliferation disorders. Besides the disease-causing variants of this gene, its different isoforms are associated with strong and weak *TNFRSF13B* expression that leads to an unbalanced B cell response.

Materials and Methods: The study detected 26 variants (three synonymous, five missenses, eleven UTR, and seven intronic variants) in the *TNFRSF13B* gene by screening 68 CVID patients with targeted next generation sequencing. An integrative bioinformatics approach was utilized to provide a plausible explanation for CVID associations from different perspectives and to investigate the associations from the clinical findings.

Results: Fifty-eight percent (15/26) of the detected variants were altered regulatory elements, such as transcription factor binding, miRNA binding sites, splice site regions or the thermodynamic impact on protein. We observed that patients who suffered from the potential splicing variants had significantly low IgA levels *(p=0.009)*, autoimmunity *(p=0.02)* and gastrointestinal findings *(p=0.05)*. In addition, the c.*79A>G 3-UTR variant was found with the low IgA and IgE levels. Thirteen variants found to have at least tenfold increased allele frequencies as compared to global databases indicating that the *TNFRSF13B* variants, which have a potential regulatory effect, are more common in CVID patients.

Conclusions: All findings suggested that these variants may not be the causative variant for the CVID phenotype but the unbalanced *TNFRSF13B* alternative splices could contribute to the pathogenesis of patients independent from the underlying genetic background of CVID.

Keywords: *TNFRSF13B*, *in silico* analysis, CVID, integrated bioinformatics, PID

ÖZ

Amaç: TNF reseptör üst ailesi üyesi 13B (*TNFSRF13B*), B hücre olgunlaşması, plazma hücresi farklılaşması ve antikor yanıtı için kritik olan TNF üst ailesinin bir üyesidir. *TNFRSF13B* geninin bozulmuş ifadesi, yaygın değişken immün yetmezlik (YDİY), otoimmünite ve lenfoproliferasyon bozuklukları ile ilişkilendirilir. Bu genin hastalığa neden olan varyantlarının yanı sıra bazı farklı izoformlarınında B hücre yanıtını değiştirdiği gösterilmiştir.

Gereç ve Yöntemler: Bu çalışmada, 68 YDİY hastası yeni nesil dizileme yöntemi ile taranarak *TNFRSF13B* geninde 26 varyant (üç sinonim, beş yanlış anlamlı, on bir UTR ve yedi intronik varyant) saptanmıştır. Tespit edilen varyantlar etkilerine göre biyoinformatik araçlar ile modellenmiş, etkili olduğu gösterilen varyantların klinik bulgular ile ilişkisi araştırılmıştır.

Bulgular: Saptanan varyantların (15/26) %58'i, transkripsiyon faktörü ya da miRNA bağlama bölgeleri, kırpılma bölgeleri veya protein üzerinde termodinamik etkisi olabileceği gösterilen varyantlardır. Biyoinformatik olarak kırpılma bölgesini değiştirdiği düşünülen varyantlara sahip hastalarda, diğer hastalara göre anlamlı derecede düşük IgA düzeylerinin *(p=0,009)*, otoimmünite varlığının *(p=0,02)* ve gastrointestinal bulgular *(p=0,05)* gibi YDİY fenotipinde görülen bulguların olduğunu gözlemledik. Ayrıca c.*79A>G 3-UTR varyantının düşük IgA ve IgE seviyeleri ile ilişkili olduğu bulunmuştur. Global veritabanlarına kıyasla on üç varyantın en az on kat artmış alel frekanslarına sahip olduğu bulundu. Bu fark potansiyel düzenleyici etkiye sahip *TNFRSF13B* varyantlarının YDİY hastalarında daha yaygın olduğunu göstermektedir.

Sonuçlar: Bu bulgular, *TNFRSF13B*'deki varyantların YDİY fenotipini açıklamasa da, kırpılma bölgesini değiştirme potansiyeli olan varyantların YDİY'in altında yatan genetik arka plandan bağımsız olarak hastaların patogenezine katkıda bulunabileceğini göstermiştir.

Anahtar Kelimeler: *TNFRSF13B*, *in siliko* analiz, YDİY, entegre biyoinformatik, PİY

Corresponding Author/Sorumlu Yazar: Sinem FIRTINA **E-mail:** snmfirtina@gmail.com

Submitted/Başvuru: 19.08.2023 • **Revision Requested/Revizyon Talebi:** 31.08.2023 • **Last Revision Received/Son Revizyon:** 31.08.2023 • **Accepted/Kabul:** 01.09.2023 • **Published Online/Online Yayın:** 20.10.2023

INTRODUCTION

Common variable immune deficiency (CVID) is the one of the most common types of primary immune deficiencies (PID) with a 1:25.000 frequency in adults (1). CVID is characterized by recurrent infections, low levels of immunoglobulins and predisposition to autoimmunity, cancer, and allergy. The genetic etiology of CVID is complicated. Unlike other types of PID, only 20% of CVID patients, mostly familiar cases, have a chance to define the causative genetic variant. This highlights the importance of not only monogenic inheritance but also complex/polygenic inheritance and/or epigenetic factors. The TNF receptor superfamily member 13B (*TNFSRF13B*) gene variant is one of the most well-known CVID associated genes which is detected in up to 10% of all CVID patients (2).

The *TNFSRF13B* encodes the transmembrane activator calcium modulator, and the cyclophilin ligand-calcium modulating ligand (CAML) interactor (TACI) protein that binds *CAML, TNFRSF13 (APRIL),* and *TNFSF13B (BAFF)* ligands and activates the NFkB signaling pathway (3). The *TNFRSF13B* has an important role in the isotype switching of IgM to other immunoglobulins, plasma cell differentiation, survival of memory B cells, and T cell-independent B cell response (4). The *TNFRSF13B* controls the autoreactive antibody production by downregulating the inducible T cell costimulator (ICOS) gene expression on B cells and maintenance of the homeostasis of B cell tolerance by upregulating the apoptosis and increasing the expression of Fas and FasL (5, 6).

The *TNFRSF13B* gene gives rise to three dominant protein-coding splice variants of TNFRSF13B-201 (293 aa), TNFRSF13B-203 (156 aa) and TNFRSF13B-206 (247 aa). Full-length isoform TNFRSF13B-201 contains four domains; two cysteine-rich domains (CRD1, CRD2), a stalk region; and a transmembrane domain, while TNFRSF13B-206 only has one functional CRD domain and TNFRSF13B-203 has a soluble form with no CRD domain. Studies showed that different isoforms of TACI proteins have different functions. While the short isoform of TACI is found in memory B cells and associated with the classical NFkB signaling activation, the dominant (long) isoform is found in the cell surface of resting B cells and increased expression of the CD19 and IgG (7).

The Biallelic and/or monoallelic *TNFRSF13B* variants are associated with CVID, selective IgA deficiency, lymphoproliferation, and some autoimmunity disorders like systemic lupus erythematosus (SLE). CVID-associated monoallelic variants are characterized by null or dominant-negative effects and cause haploinsufficiency of the *TNFRSF13B* by impaired ligand binding and lack of NFkB signaling activation (8).

Studies indicated that the *TNFRSF13B* variants act as a modifier gene rather than a causative gene and modifying variants of the *TNFRSF13B* contribute to the clinical phenotype in some patients (9). The Epistatic effects of *TNFRSF13B* variants with other CVID-associated genes like *TCF3* trigger autoimmunity in CVID patients (10). In addition, some specific variants cause the downregulation of TACI expression, but this is not a complete loss. Autoimmune diseases with this CVID phenotype provides another example of the modifying effects of *TNFRSF13B* variants (11) (Figure 1).

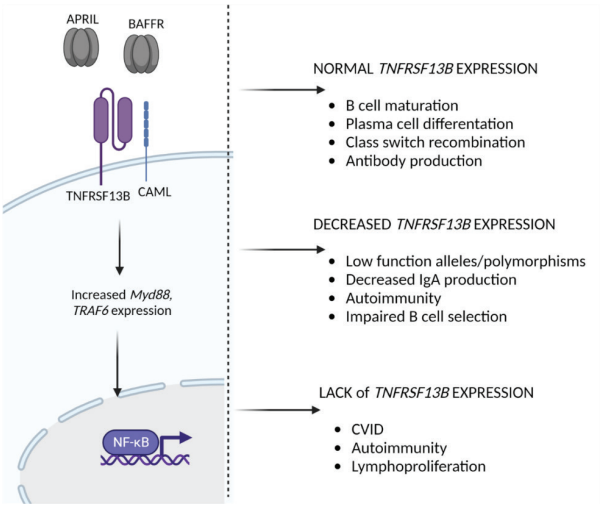

Figure 1: Schematic overview of the *TNFRSF13B* signaling pathway in B-cells and summarize the effects of strong or very *TNFRSF13B* expression in immune response. TNFRSF13B receptor binds to soluble BAFF and/or APRIL ligands and this engagement activates MYD88 and TRAF6 expression. This activation mediates NFkB signaling pathway

We previously screened disease-causing variants in pediatric primary antibody deficiency (PAD) and severe combined immune deficiency (SCID) and discovered that the genetic background is clearer in SCID patients (12, 13). Due to the genetic heterogeneity of CVID, in this study we aimed to sequence the *TNFRSF13B* gene via next generation sequencing methods in pediatric and adult CVID patients and evaluatethe modifying effects of non-disease-causing variants on this clinical phenotype. An integrative informatic analysis was performed to determine potential miRNA and/or transcription factor binding sites for 3-UTR and 5-UTR variants, to evaluate the effects of synonymous variants on RNA folding, to check the presence of splice site effects of missense and synonymous variants, and to reveal any structural and functional impacts of missense variants. We wanted to reveal more about the associations of the *TNFRSF13B* gene variants from different perspectives according to the types of variants.

MATERIAL and METHODS

Screening of *TNFRSF13B* variants

Sixty-eight pediatric and adult CVID patients (twenty-eight females, forty male) were enrolled in this study. The mean age was 20.26 years (min 3-max 68 years), and the mean age of symptom onset was 6.4 years. Forty-three patients were pediatric, and twenty-five patients were adults. Clinical findings

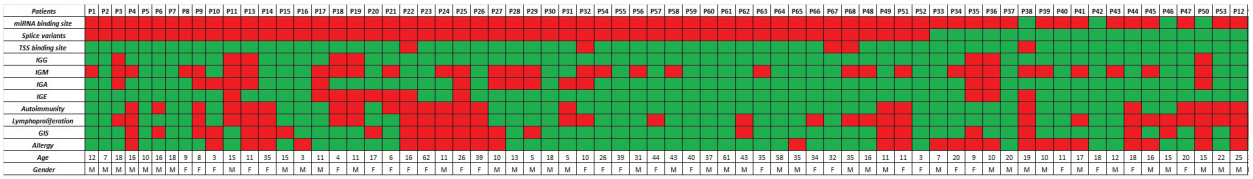

Figure 2: Heat map showing the occurrence of clinical signs and variants in CVID patients. Red boxes indicates that the relevant information is present in the patient. Green boxes indicates that the relevant information is absent in the patient. M: Male F: Female, GIS: Gastrointestinal system, TSS: Transcription start site

are shown in Figure 2. This study was approved by the Ethics Committee of the Cerrahpasa Faculty of Medicine (Date: 01.03.2016, No: A-61). Diagnosis time samples were collected between the years of 2017-2019 and the genomic DNA was extracted using the Qiamp DNA Blood Kit (Qiagen) according to the manufacturer's instructions. Quantification of sequencing libraries was prepared by the Qubit dsDNA HS assay kit (Invitrogen, USA) using the Qubit 4 Fluorometer (Invitrogen, USA). The promotor and the exonic region of the *TNFRSF13B* gene was sequenced by the Illumina Miseq (Illumina USA) sequencer. Quality control parameters and variant analysis were checked by Seq v7.0 (Genomize, Turkey). The *TNFRSF13B* (ENST00000261652.2) variants were filtered and included in the study according to passed filter quality (>Q30) and read depth (>50X) scores. The standard analysis of variant interpretation is given in Figure 3. For further analysis, all variants were checked by several *in silico* prediction tools after categorizing them according to their types. The mirDB, airbase, and TargetScan for 3'-UTR prime variants were used for the determination of *TNFRSF13B* miRNA binding sites; the Human splice finder and Gene Splicer were used for intronic variants to understand the potential alternative splices; the Missense 3D and Visual Molecular Dynamics (VMD) were used for annotation of missense variants, and the RNA fold (http://rna.tbi.univie.ac.at/) was used for checking the effects of synonymous variants to RNA secondary structure and stability (14-20). The Fabian (https://www.genecascade.org/fabian) and Regulation Spotter were used for predicting the effects of variants on the transcription factor binding sites (21).

Structural analysis

The full crystal structure of the TACI protein was not reported in the literature but the partial crystal structure of the TACI protein between residues 68 and 109 was determined by X-Ray (PDB id: 1XU1 / Chain R/S/T) and the NMR (PDB id: 1XUT/ Chain A) (22). To provide a full understanding, the AlphaFold predicted structure of the TACI protein (AF-O14836-F1) was used due to compromising all residues. Prior to analyzing the structural impacts of missense variants, a quality check of the AF-O14836-F1) was performed via the Saves 6.0 tool, compromising five different structure validation tools, e.g., PROCHECK, WHAT_CHECK, ERRAT, VERIFY 3D and PROVE (23-28). To

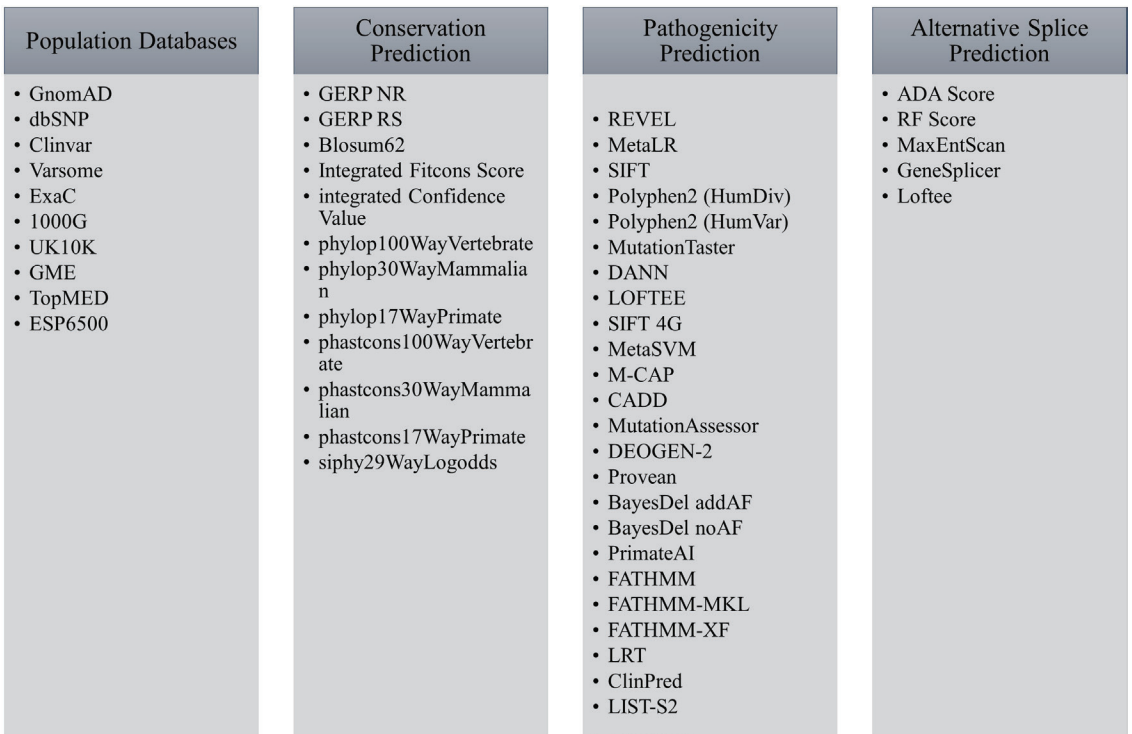

Figure 3: Standard analysis of variant interpretation by Genomize Seq Platform

Table 1: *TNFRSF13B* variants in the patients

Variation Type	Variant *GRcH37	dbSNP	cDNA	AA change	ACMG classification	VAF (*in house*/ global)	VAF fold change	Predicted regulatory effect
3 Prime UTR	17:16842688C>T	rs56153623	c.*173G>A	N/A	B	0.4397 / 0.2482	2 +	miRNA binding site
3 Prime UTR	17:16842774CAT>C	rs150068036	c.*86_*88delTG	N/A	VUS	0.0357 / 0.0557	0.6 -	miRNA binding site
3 Prime UTR	17:16842782T>C	rs1183784784	c.*79A>G	N/A	VUS	0.01 / 0.001	10 +	miRNA binding site
3 Prime UTR	17:16842602G>GCCTCTCT	rs1378399485	c.*252_*259dupCCCTCTCTG	N/A	VUS	0.0129 / 0.0007	18.5 +	miRNA binding site
3 Prime UTR	17:16842661G>C	rs373632897	c.*200C>G	N/A	VUS	0.1379 / 0.0060	23 +	miRNA binding site
3 Prime UTR	17:16842645G>C	rs1597655978	c.*216C>G	N/A	VUS	0.1940 / 0.0070	28 +	miRNA binding site
3 Prime UTR	17:16842777A>C	rs1375454146	c.*84T>G	N/A	VUS	0.0202 / 0.0003	67 +	miRNA binding site
3 Prime UTR	17:16842796A>C	rs1337965516	c.*65T>G	N/A	VUS	0.4343 / 0.0054	80 +	miRNA binding site, splice medium loss donor
3 Prime UTR	17:16842447C>A	rs55701306	c.*414G>A	N/A	B	0.1625 / 0.0817	2 +	No change
3 Prime UTR	17:16842824A>C	rs188626884	c.*37T>G	N/A	VUS	0.0167 / 0.0002	83.5 +	No change
5 Prime UTR	17:16875407A>C	rs1478747037	c.-18T>G	N/A	VUS	0.0156 / 0.0001	156 +	TSS binding site
Intronic	17:16843171A>G	rs11652811	c.632-60T>C	N/A	B	0.1125 / 0.2416	0.4656 -	No change
Intronic	17:16852027T>C	rs2274892	c.445+25A>C	N/A	B	0.4697 / 0.4400	1 +	No change
Intronic	17:16852367G>A	rs537951875	c.200-70C>T	N/A	VUS	0.0619 / 0.0028	22 +	No change
Intronic	17:16852377G>A	rs1397554467	c.200-80C>T	N/A	VUS	0.0177 / 0.0002	88 +	No change
Intronic	17:16852388TA>T	rs67234667	c.200-83del	N/A	VUS	0.1549 / 0.0165	9 +	No change
Intronic	17:16852410G>A	rs1459501406	c.200-113C>T	N/A	VUS	0.0275 / 0.0003	91 +	No change
Intronic	17:16875264G>A	rs1359249090	c.61+65C>T	N/A	VUS	0.0042 / 0.00007	60 +	TSS binding site
Missense	17:16778660A>C	NA	c.44T>G	V15G	VUS	0.0147 / NA		ESE/ESS splice
Missense	17:16842991G>A	rs34562254	c.752C>T	P251L	B	0.1667 / 0.1454	1.146 -	Thermodynamic impact
Missense	17:16852133G>A	rs201124889	c.364C>T	R122W	LB	0.0140 / 0.0003	46 +	Thermodynamic impact
Missense	17:16778693A>C	NA	c.11T>G	L4R	VUS	0.0041 / NA		No change
Missense	17:16843084A>G	rs56063729	c.659T>C	V220A	LB	0.0109 / 0.0101	1.079 -	Splice medium loss donor
Synonymous	17:16855878C>T	rs8072293	c.81G>A	T27=	B	0.6891 / 0.7270	0.9478 +	New Acceptor splice site
Synonymous	17:16842912A>C	rs11078355	c.831T>C	S277=	B	0.5875 / 0.4981	1 +	No change
Synonymous	17:16852206A>C	rs35062843	c.291T>G	P51=	LB	0.0160 / 0.0392	0.408 +	No change

AA: Amino acid, VAF: Variant allele frequency, VUS: Variant of Unknown Significance, LB: Likely Benign, B: Benign, ACMG: The American College of Medical Genetics and Genomics variant classification, ESS: Exonic splicing silencers, ESE: Exonic splicing enhancers, N/A: Not Available

create and visualize mutant TACI protein structures, the Visual Molecular Dynamics (VMD) tool was used to assess the changes in intramolecular interactions, the salt bridge interactions with 3.2 Å oxygen-nitrogen distance cut-off distance were also calculated by VMD. The PremPS and Cupsat tools were used to assess the effects of missense variants on thermodynamic stability by performing Ala-scanning and calculating changes in destabilization tendencies (29, 30). The Stride web tool was used to track changes in the secondary structure between the native and mutant forms (31).

Statistical analysis

Clinical findings between patients with or without the *TNFRSF13B* variants were statistically compared by Pearson's χ2 or Fisher's exact and p<0.05 was considered as statistically significant. We evaluated the correlation between the *TNFRSF13B* variants and the clinical characteristics such as gender (male vs female), Lymphocyte count (>50000 vs <50000), B lymphocyte percentage (<20% vs >20%), immunoglobulin levels (normal vs decreased age-dependent IgG, IgM, IgG and IgA levels), autoimmunity (presence vs absence), lymphoproliferation (presence vs absence), allergy (presence vs absence), and gastrointestinal findings (presence vs absence) (32). All statistical analyses were done by the IBM SPSS statistics 20 (IBM Corp. Armonk, NY, USA).

RESULTS

We screened the *TNFRSF13B* variants in sixty-eight CVID patients via next-generation panel sequencing and found twenty-six monoallelic variants. No pathogenic or likely pathogenic variants were detected. Seven variants were classified as benign, three were likely benign and sixteen variants were classified as a variant of unknown significance (VUS) according to ACMG classification criteria. There were ten variants consisting of 3-UTR and one 5-UTR variants, eight coding sequence (three synonymous, five missense) variants, and seven intronic variants. The detailed information about detected variants is provided in Table 1.

We observed increased minor allele frequencies in several variants as compared to The Genome Aggregation Database (gnomAD) and the Exome Sequencing Project (ExAC) population frequency databases. One likely benign and twelve VUS variants were found to have at least tenfold increased allele frequencies when compared to the global databases (Table 1).

Impact of missense variants

Out of twenty-six variants, we reported five missenses; L4R, V15G, R122W, P251L, and V220A. We performed visualization of the TACI protein structure by displaying the locations of all missense variants according to the CRD1 and CRD2 domains and checked the presence of salt bridge interactions in native and mutant TACI protein complexes, but we reported neither the formation of new salt bridge interactions nor the loss of existing ones (Figure 4).

Secondly, we evaluated the thermodynamic changes in our missense variants and found that only the P251L replacement caused a decrease in the destabilization tendency (-0.38 kcal/mole) out of the five missense variants. To assess the impact of variants from thermodynamic points of view, Ala-Scanning and destabilization tendencies calculations were performed. Based on the Ala-scanning results by the PremPs tool, we determined that only the R122W and P251L variants were favorably reported to contribute to torsion (Table 2).

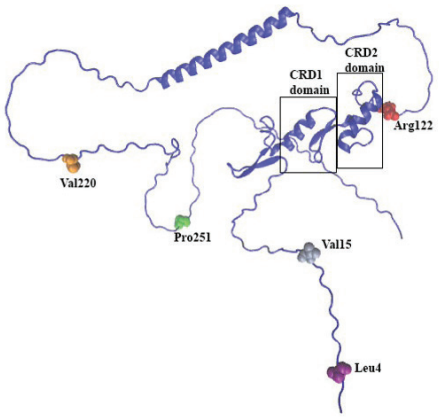

Figure 4: The locations of detected missense variants in 3D TACI protein structure (AlphaFold ID: AF-O14836-F1) CRD: cysteine-rich domains

Table 2: The change in destabilization tendencies upon the presence of missense mutations via PremPs and CUPSAT tools

Variants	PRemPs tool mutation analysis ΔΔG (kcal/mole)	PRemPs tool Ala-scanning ΔΔG (kcal/mole)	CUPSAT tool mutation analysis ΔΔG (kcal/mole)
L4R	0.27	0.32	2.53
V15G	0.31	0.36	0.77
R122W	**0.31**	**0.54**	**-3.41**
V220A	0.28	0.28	0.44
P251L	**-0.38**	0.20	**-1.74**

Besides evaluating the structural and thermodynamic changes of missense variants, we also identified the splice site effects of the missense variants and determined that the V15G variant was predicted as changing the exon splicing enhancer/silencer (ESE/ESS) site and the V174A variant caused the loss of donor site (score 5.5).

Regulatory effects of UTR variants

To understand the effects of 3-UTR variants, we described the potential miRNA-binding sites on the 3-UTR prime of the *TNFRSF13B* gene using the TargetScan 7.1. tool. Candidate miRNAs were chosen if the predicted context++ score percentile was higher than 95%. We investigated eight of ten 3-UTR variants (c.*65T>G, c.*79A>G, c.*84T>G, c.*86_*88delTG, c.*173G>A,

Table 3: Detailed information about *TNFRSF13B* variants and miRNA target pairing in the seed regions.

Variants	miRNA	Predicted position of target region (bp)	Alignment	Context++ score	Context++ score percentile
c.*65T>G	hsa-miR-1224-3p	62-68	5' ...GGGAGAGAGAAAGAGAGGUGGGG... |||||| |||||| 3' GACUCCUCUCUCC---UCCACCCC	-0.33	97
c.*79A>G	hsa-miR-7110-3p	76-83	5' ...GAGGUGGGGAGAGGGGAGAGAGA... |||| |||||| 3' GACGUCCCUUCACCCUCUCUCU	-0.61	99
c.*79A>G	hsa-miR-6873-3p	77-83	5' ...AGGUGGGGAGAGGGG-AGAGAGAU... |||| |||||| 3' GACUCUCUCUUUCUGUCUCUCUU	-0.38	98
c.*79A>G **c.*84T>**G	hsa-miR-3675-3p	79-85	5' ...GUGGGGAGAGGGGAGAGAGAUAU... |||||| |||||| 3' AACCCCCUCAAGGAA-UCUCUAC	-0.26	98
c.*86_*88delTG	hsa-miR-4279	87-93	5' ...AGGGGAGAGAGAUAUGAGGAGAG... ||||||| 3' CUUCGGCCCUCCUCUC	-0.33	98
c.*173G>A	hsa-miR-2276-5p	168-174	5' ...AGAGGGAGAGAGAGACAGAGGGG... ||||||| 3' GCAGACGUUCCACUGUCUCCCG	-0.26	97
c.*173G>A	hsa-miR-6826-3p	170-177	5' ...AGGGAGAGAGAGACAGAGGGGAA... ||||||| 3' GACUUGUCCUUUCUCUCCCCUC	-0.55	99
c.*173G>A	hsa-miR-6795-3p	170-176	5' ...AGGGAGAGAGAGACAGAGGGGAA... |||||| 3' GACCCCCUUCUUUGCUCCCCA	-0.31	98
c.*200C>G	hsa-miR-2682-3p	194-201	5' ...AGAGGCAGAGAGGGAAAGAGGCA... ||| |||||| 3' CCUUCUGUCGCGAC--UUCUCCGC	-0.50	99
c.*200C>G	hsa-miR-6781-3p	194-201	5' ...AGAGGCAGAGAGGGAAAGAGGCA... ||||| |||||| 3' GACUCCGGCACCUU--UUCUCCGU	-0.48	99
c.*200C>G	hsa-miR-5001-3p	197-203	5' ...GGCAGAGAGGGAAAGAGGCAGAG... ||||||| 3' UUCCUGGACCUGUCUCCGUCUU	-0.26	95
c.*216C>G	hsa-miR-6895-3p	211-217	5' ...GAGGCAGAGAAGGAA-AGAGACAG... |||| |||||| 3' GAUUCCGGUUCCCGCUCUCUGU	-0.39	98
c.*216C>G	hsa-miR-593-3p	211-217	5' ...GAGGCAGAGAAGGAAAGAGACAG... |||||| 3' UCUUUGGGGUCGUCUCUGU	-0.36	98
c.*216C>G	hsa-miR-6818-3p	211-217	5' ...GAGGCAGAGAAGGAA--AGAGACAG... ||||| |||||| 3' GACACACUCCUUGUUCUCUGUU	-0.27	96
c.*216C>G	hsa-miR-5699-3p	213-219	5' ...GGCAGAGAAGGAAAGAGACAGGC... |||||| |||||| 3' CGAGGUUGUUCCUU--UCUGUCCU	-0.35	97
c.*216C>G	hsa-miR-214-5p	214-221	5' ...GCAGAGAAGGAAAGAGACAGGCA... ||| |||||| 3' CGUGUCGUUCACAU--CUGUCCGU	-0.56	99
c.*216C>G	hsa-miR-6514-3p	215-221	5' ...CAGAGAAGGAAAGAGACAGGCAG... |||| |||||| 3' GACCUCACCUUCU--UGUCCGUC	-0.26	97
c.*252_*259dupCCCTCTCTG	hsa-miR-6769b-3p	253-259	5' ...GAGAGGGAGAGAGGCAGAGAGGG... ||||||| 3' GAUACCCACCCUGUCUCUCCC	-0.27	96
c.*252_*259dupCCCTCTCTG	hsa-miR-4723-3p	253-259	5' ...GAGAGGGAGAGAGGCAGAGAGGG... ||||| |||||| 3' AAACCCCUCCUCGG-UCUCUCCC	-0.31	96
c.*252_*259dupCCCTCTCTG	hsa-miR-3183	253-259	5' ...GAGAGGGAGAGAGGCAGAGAGGG... ||||||| 3' AGGCUCGCUGAGGCUCUCUCCG	-0.22	96
c.*252_*259dupCCCTCTCTG	hsa-miR-6892-3p	254-261	5' ...AGAGGGAGAGAGGCAGAGAGGGA... ||||||| 3' GACGUUCCCCACCCUCUCCCU	-0.59	99
c.*252_*259dupCCCTCTCTG	hsa-miR-4469	256-263	5' ...AGGGAGAGAGGCAGAGAGGGAGA... ||||||| 3' AGGCUCGCUGGGAUCUCCCUCG	-0.45	99

c.*200C>G, c.*216C>G and c.*252_*259dupCCCTCTCTG) which were located on a potential miRNA binding site of 22 different miRNAs (Table 3).

In addition, we predicted the impact of our variants on the known transcription factor (TF) binding site by the Fabian (ePOSSUM2) tool and found that the c.-18T>G and c.61+65C>T variants were located on the known TF binding site of the *TNFRSF13B* gene. The c.-18T>G in is located in the promotor region of the *TNFRSF13B* and leads to a potential gain in the binding ability *EGR1* and the loss of the *POU2F2* transcription factor. This variant was seen in only four allele in the global databases (C=0.000015 (4/264690, TOPMED), C=0.00000 (0/14050, ALFA)). In our unit, we detected this variant in three of our patients (MAF=0.01). Secondly, a previously known intronic variant (c.61+65C>T) was found in one individual, which caused a potential loss of the *EGR1* binding region, and led to the enhancement of the *POU2F2* binding ability on the *TNFRSF13B* gene.

***In silico* analysis of synonymous variants**

For the next step of this study, we evaluated the possible effects of three synonymous variants (S277S, T27T, and P51P) on the secondary structure of RNA by calculating the changes in minimum free energy (MFE) value. Based on this calculation, we reported almost no change in all replacements; 2% in S277S, 0.7% in T27T, and 1.2% in P51P as compared to native. These little changes suggested that there is no significant change in the secondary structure of RNA in terms of altering binding dynamics. Lastly, we evaluated the alterations on the splice site region, and only reported the T27T variant as a cause of possible activation of the cryptic acceptor site (HSF 56.45%).

Clinical significance of *TNFRSF13B* variants

In order to understand the effects of variants, the relationship between clinical findings and variants was evaluated by statistical analysis. Variants were evaluated both individually and by classifying them according to their types; 'splice effects', 'UTR site', 'TSS binding site', 'miRNA binding site' and 'prior' variants which were VUS classified, increased (>20 times) *in house* allele frequency and have at least one potential effect (c.*65T>G, c.-18T>G, c.61+65C>T and c.364C>T).

We observed that patients who suffered from potential splicing variants (c.44T>G; V15G, c.659T>C; V220A, c.81G>A; T27T, c.*65T>G; n=35) had significantly low IgA levels (*p=0.009*), autoimmunity (*p=0.02*) and gastrointestinal findings (*p=0.05*). In addition, the c.*79A>G 3 prime UTR variant (n=19) that was associated with low IgA (*p=0.05*) and IgE levels (*p=0.007*). c.752C>T (P251L, n=8) was also associated with significantly low IgG levels (*p=0.04*). However, no other clinical correlation was found between other variant types and clinical findings. A heat map showing the occurrence of clinical signs and variants in CVID patients is presented in Table 3.

DISCUSSION

The *TNFRSF13B* gene regulates T-cell-dependent B lymphocyte signaling, antibody production, and plasma cell differentiation by activating the NFkB pathway (8). Besides this classical way, the *TNFRSF13B* receptor also promotes immunoglobulin production by interacting with Toll-Like Receptors (TLRs) in B cells (33). Studies showed that monoallelic variants of the *TNFRSF13B* gene were mostly sporadic and characterized by incomplete penetrance and lack of segregation which leads to low-IgA levels, lymphoproliferation, autoimmunity and dysregulated immune response (34).

In this study, we detected twenty-six monoallelic *TNFRSF13B* variants classified as B, LB, or VUS in sixty-eight CVID patients. Within the scope of this paper, we explained the disease associations of twenty-six variants existing in the *TNFRSF13B* gene related to CVID. According to the types of variants, we questioned their possible associations from different perspectives, e.g., missense variants from the structural and thermodynamical point of view, UTR variants from regulatory issues, synonymous variants in RNA binding perspectives and checked out the correlation of these variants with clinical features.

Within the scope of this research no patient was diagnosed with a TACI deficiency but *in silico* analysis of the variants showed that 58% (15/26) have at least one potential regulatory effect on TACI protein. In addition, thirteen variants were found to have at least ten-fold increased allele frequencies when compared to global databases. These high-frequent variants were categorized as VUS classification except for one likely benign R122W missense variant, and 69% of these variants (9/13) could have a potential effect on TACI protein. Based on these results, we indicated that the *TNFRSF13B* variants, which are thought to have a modifying effect on protein, are more common in CVID patients.

Then we evaluated the potential splice site effects of missense, intronic and synonymous *TNFRSF13B* variants and found that the V15G, T27T, V220A and c.*65T>G variants have a potential splice site effect. These variants were also associated with significantly low level IgA, autoimmunity, and GIS findings. In view of the fact of the importance of *TNFRSF13B* splice variants on its function, this data indicates that the alternative splice effects could change the ratio of long/short isoform of the *TNFRSF13B* gene. Unbalanced *TNFRSF13B* alternative splices might contribute to the pathogenesis of patients independent from underlying genetic background of CVID. Evaluating the ratio of the long/short isoform of the *TNFRSF13B* gene on patients might be helpful for understanding the balance of alternative isoforms of TACI and their function.

Additionally, we showed the impact of UTR variants and found two variants (c.-18T>G and c.61+65C>T variants), that are located in known TF binding sites, which might affect the binding ability of *EGR1* and *POU2F2* TFs according to the *in silico* analysis. We did not detect any association between these two variants and clinical findings, but we showed that the 3-prime UTR c.*79A>G (rs1183784784) variant was associated with low IgA and IgE levels. This UTR variant had 10-fold increased allele frequency when compared to the global databases in our research. GWAS studies showed that UTR primer variants of the *TNFRSF13B* gene are associated with low IgG levels (35). Moreover, the P251L variant was also associated with low IgG

levels. Speletas et al. previously showed that patients who suffered from this variant, had increased risk of recurrent infections (36). We showed the association between regulatory variants and immunoglobulin levels that may be helpful to understand the mechanism of modified *TNFRSF13B* variants in primary immunodeficiency.

Even though all these findings covered the possible impacts of detected variants on TACI deficiency from different perspectives, the most important limitation of our study is the lack of experimental studies conducted to reveal the changes in mRNA and protein expression levels.

The fact that patients who are not diagnosed with TACI deficiency but have potential splice site variants in the *TNFRSF13B* gene have lower IgA and autoimmunity findings, suggesting the potential effect of these variants on TACI protein. This study discussed that *TNFRSF13B* gene variants do not cause CVID but it does not explain the phenotype of the diseasethat may be associated with minimal or moderate regulatory effects and which could accompany the pathogenesis of the disease. Here, it is important to emphasize that even though all this provided information is not sufficient to explain the whole etiology of TACI deficiency, it points out the importance of focusing on variants having minimal/moderate regulatory impacts since they were seen more frequently in CVID patients within this study.

Acknowledgements: We would like to thank to Dr. Ozkan Ozdemir for his interpretation for creating a graphical figure 1 with Biorender program.

Ethics Committee Approval: This study was approved by Cerrahpasa Faculty of Medicine Clinical Research Ethics Committee (Date: 01.03.2016, No: A-61).

Peer Review: Externally peer-reviewed.

Author Contributions: Conception/Design of Study- S.F., A.K.; Data Acquisition- H.Y., Y.Y.N., Ö.H.N., A.K., E.Y.Ö., E.A., S.B., A.O.Ö., S.N., Y.Ç., İ.R., B.N.C., M.Y.; Data Analysis/Interpretation- S.F., A.K.; Drafting Manuscript- S.F., A.K.; Critical Revision of Manuscript- M.S., M.C.A.; Final Approval and Accountability- S.F.; Material and Technical Support- S.F., A.K., B.İ.; Supervision- M.S., M.C.A.

Conflict of Interest: The authors have no conflict of interest to declare.

Financial Disclosure: This project was supported by Istanbul University-Cerrahpasa Research Fund (Project no: TYO-2017-24271).

REFERENCES

1. Fried AJ, Bonilla FA. Pathogenesis, diagnosis, and management of primary antibody deficiencies and infections. Clin Microbiol Rev 2009;22(3):396-414.
2. Karaca NE, Severcan EU, Guven B, Azarsiz E, Aksu G, Kutukculer N. TNFRSF13B/TACI Alterations in Turkish Patients with Common Variable Immunodeficiency and IgA Deficiency. Avicenna J Med Biotechnol 2018;10(3):192-5.
3. Wu Y, Bressette D, Carrell JA, Kaufman T, Feng P, Taylor K, et al. Tumor necrosis factor (TNF) receptor superfamily member TACI is a high affinity receptor for TNF family members APRIL and BLyS. J Biol Chem 2000;275(45):35478-85.
4. Salzer U, Jennings S, Grimbacher B. To switch or not to switch--the opposing roles of TACI in terminal B cell differentiation. Eur J Immunol 2007;37(1):17-20.
5. Ou X, Xu S, Lam KP. Deficiency in TNFRSF13B (TACI) expands T-follicular helper and germinal center B cells via increased ICOS-ligand expression but impairs plasma cell survival. Proc Natl Acad Sci U S A 2012;109(38):15401-6.
6. Figgett WA, Fairfax K, Vincent FB, Le Page MA, Katik I, Deliyanti D, et al. The TACI receptor regulates T-cell-independent marginal zone B cell responses through innate activation-induced cell death. Immunity 2013;39(3):573-83.
7. Salzer U, Grimbacher B. TACI deficiency - a complex system out of balance. Curr Opin Immunol 2021;71:81-8.
8. He B, Santamaria R, Xu W, Cols M, Chen K, Puga I, et al. The transmembrane activator TACI triggers immunoglobulin class switching by activating B cells through the adaptor MyD88. Nat Immunol 2010;11(9):836-45.
9. Bogaert DJ, Dullaers M, Lambrecht BN, Vermaelen KY, De Baere E, Haerynck F. Genes associated with common variable immunodeficiency: one diagnosis to rule them all? J Med Genet 2016;53(9):575-90.
10. Ameratunga R, Koopmans W, Woon ST, Leung E, Lehnert K, Slade CA, et al. Epistatic interactions between mutations of TACI (TNFRSF13B) and TCF3 result in a severe primary immunodeficiency disorder and systemic lupus erythematosus. Clin Transl Immunology 2017;6(10):159-65.
11. Platt JL, de Mattos Barbosa MG, Huynh D, Lefferts AR, Katta J, Kharas C, et al. TNFRSF13B polymorphisms counter microbial adaptation to enteric IgA. JCI Insight 2021;(6):14-7.
12. Firtina S, Ng YY, Ng OH, Kiykim A, Ozek EY, Kara M, et al. Primary antibody deficiencies in Turkey: molecular and clinical aspects. Immunol Res 2022;70(1):44-55.
13. Firtina S, Yin Ng Y, Hatirnaz Ng O, Kiykim A, Aydiner E, Nepesov S, et al. Mutational landscape of severe combined immunodeficiency patients from Turkey. Int J Immunogenet 2020;47(6):529-38.
14. Chen Y, Wang X. miRDB: an online database for prediction of functional microRNA targets. Nucleic Acids Res 2020;48(1):127-31.
15. Kozomara A, Birgaoanu M, and Griffiths-Jones S. miRBase: from microRNA sequences to function. Nucleic Acids Res 2019;47(1):155-62.
16. Agarwal V, Bell GW, Nam JW, Bartel DP. Predicting effective microRNA target sites in mammalian mRNAs. Elife 2015;(4):1-3.
17. Desmet FO, Hamroun D, Lalande M, Collod-Beroud G, Claustres M, Beroud C. Human Splicing Finder: an online bioinformatics tool to predict splicing signals. Nucleic Acids Res 2009;37(9):67-70.
18. Pertea M, Lin X, Salzberg SL. GeneSplicer: a new computational method for splice site prediction. Nucleic Acids Res 2001;29(5):1185-90.
19. Ittisoponpisan S, Islam SA, Khanna T, Alhuzimi E, David A, Sternberg MJE. Can Predicted Protein 3D Structures Provide Reliable Insights into whether Missense Variants Are Disease Associated? J Mol Biol

2019;431(11):2197-212.

20. Humphrey W, Dalke A, Schulten K. VMD: visual molecular dynamics. J Mol Graph 1996;14(1):27-33.
21. Schwarz JM, Hombach D, Kohler S, Cooper DN, Schuelke M, Seelow D. RegulationSpotter: annotation and interpretation of extratranscriptic DNA variants. Nucleic Acids Res 2019;47(1):106-13.
22. Hymowitz SG, Patel DR, Wallweber HJ, Runyon S, Yan M, Yin J, et al. Structures of APRIL-receptor complexes: like BCMA, TACI employs only a single cysteine-rich domain for high affinity ligand binding. J Biol Chem 2005;280(8):7218-27.
23. Colovos C, Yeates TO. Verification of protein structures: patterns of nonbonded atomic interactions. Protein Sci 1993;2(9):1511-9.
24. Bowie JU, Luthy R, Eisenberg D. A method to identify protein sequences that fold into a known three-dimensional structure. Science 1991;253(5016):164-70.
25. Luthy R, Bowie JU, Eisenberg D. Assessment of protein models with three-dimensional profiles. Nature 1992;356(6364):83-5.
26. Pontius J, Richelle J, Wodak SJ. Deviations from standard atomic volumes as a quality measure for protein crystal structures. J Mol Biol 1996;264(1):121-36.
27. Laskowski RA, Rullmannn JA, MacArthur MW, Kaptein R, Thornton JM. AQUA and PROCHECK-NMR: programs for checking the quality of protein structures solved by NMR. J Biomol NMR 1996;8(4):477-86.
28. Hooft RW, Vriend G, Sander C, and Abola EE. Errors in protein structures. Nature 1996;381(6):272-6.
29. Parthiban V, Gromiha MM, and Schomburg D. CUPSAT: prediction of protein stability upon point mutations. Nucleic Acids Res 2006;34(Web Server issue):W239-42.
30. Chen Y, Lu H, Zhang N, Zhu Z, Wang S, Li M. PremPS: Predicting the impact of missense mutations on protein stability. PLoS Comput Biol 2020;16(12):100-5.
31. Frishman D, Argos P. Knowledge-based protein secondary structure assignment. Proteins 1995;23(4):566-79.
32. Aksu G, Genel F, Koturoglu G, Kurugol Z, Kutukculer N. Serum immunoglobulin (IgG, IgM, IgA) and IgG subclass concentrations in healthy children: a study using nephelometric technique. Turk J Pediatr 2006;48(1):19-24.
33. Ozcan E, Rauter I, Garibyan L, Dillon SR, Geha RS. Toll-like receptor 9, transmembrane activator and calcium-modulating cyclophilin ligand interactor, and CD40 synergize in causing B-cell activation. J Allergy Clin Immunol 2011;128(3):601-9.
34. Salzer U, Bacchelli C, Buckridge S, Pan-Hammarstrom Q, Jennings S, Lougaris V, et al. Relevance of biallelic versus monoallelic TNFRSF13B mutations in distinguishing disease-causing from risk-increasing TNFRSF13B variants in antibody deficiency syndromes. Blood 2009;113(9):1967-76.
35. Liao M, Ye F, Zhang B, Huang L, Xiao Q, Qin M, et al. Genome-wide association study identifies common variants at TNFRSF13B associated with IgG level in a healthy Chinese male population. Genes Immun 2012;13(6):509-13.
36. Speletas M, Mamara A, Papadopoulou-Alataki E, Iordanakis G, Liadaki K, Bardaka F, et al. TNFRSF13B/TACI alterations in Greek patients with antibody deficiencies. J Clin Immunol 2011;31(4):550-9.

RESEARCH ARTICLE / ARAŞTIRMA MAKALESİ
Journal of Advanced Research in Health Sciences /
Sağlık Bilimlerinde İleri Araştırmalar Dergisi 2023
DOI: 10.26650/JARHS2023-1349345

THE FREQUENCY AND FITNESS OF m6A-ASSOCIATED VARIANTS COULD BE MODULATED BY THE THERMODYNAMIC STABILITY OF AN OVERLAPPING G-QUADRUPLEX

m6A İLE İLİŞKİLİ VARYANTLARIN SIKLIĞI, ÖRTÜŞTÜĞÜ G-KUADRUPLEKS YAPISININ TERMODİNAMİK KARARLILIĞI İLE DEĞİŞEBİLİR

Çağrı GÜLEÇ[1]

[1] Istanbul University, Istanbul Faculty of Medicine, Department of Medical Genetics, Istanbul, Turkiye

ORCID ID: C.G. 0000-0002-1256-9574

Citation/Atıf: Gulec C. The frequency and fitness of m6A-associated variants could be modulated by the thermodynamic stability of an overlapping G-quadruplex. Journal of Advanced Research in Health Sciences 2023;6(3):219-228. https://doi.org/10.26650/JARHS2023-1349345

ABSTRACT

Objective: Post-transcriptional modifications like m6A (N6-methyladenosine) and secondary structures like G-quadruplex (G4) are formations that play a vital role in RNA processing. Their synergy also has functional consequences. Since m6A is known to be enzymatically created in the DRACH-motif, and that genetic variants can create a novel DRACH-motif or abolish a pre-existing DRACH-motif, we can hypothesize that variants which affect the gene product level through modulating m6A-G4 colocalization, may also consequently affect fitness and change the allele frequency. To test this hypothesis, the rare and common variants in selected human genes were investigated to determine their effect on DRACH-G4 colocalization.

Material and Methods: Genomic sequences and variant information were retrieved from the GRCh37/hg19 and Biomart-Ensembl databases. Experimentally determined G4 sequences were obtained from two different studies.

Results: Common variants leading to the formation of a novel DRACH-motif were found to be significantly higher inside the G4 structure than outside. In contrast, rare variants with the same feature were higher outside the G4-structure and had uneven distribution alongside the pre-mRNA. The uneven distribution of the DRACH-creating rare variants was observed to correlate with their effect on thermodynamic stability of the overlapping G4.

Conclusion: Selective DRACH-G4 colocalization suggests that m6A is evolutionally favorable when overlapping with G4. The thermodynamic stability could lead to uneven distribution of DRACH-G4 colocalization, favorable in 3-prime-side, but not in 5-prime-side. We can conclude that the fitness, and consequently frequency of a DRACH-creating variant is prone to become higher or lower depending in its position and effect on the overlapping-G4 stability.

Keywords: RNA modification, N6-methyladenosine, G-quadruplex, allele frequency

ÖZ

Amaç: M6A (N6-metiladenozin) gibi post-transtranskripsiyonel modifikasyonlar ve G-kuadrupleks (G4) gibi ikincil yapılar, RNA işlenmesinde önemli rol oynayan oluşumlardır. Bu iki oluşumun birlikteliğinin de işlevsel sonuçları vardır. M6A oluşumunun DRACH motifi üzerinde enzimatik olarak meydana geldiği, genetik varyantların yeni DRACH motifi oluşturabildiği veya var olan bir DRACH motifini ortadan kaldırabildiği dikkate alındığında, bu tür varyantların, mRNA üzerinde m6A-G4 örtüşme durumunu değiştirerek gen ürün düzeyini etkileyebileceğini, bunun da nesiller boyunca ilgili varyantın alel sıklığını değiştireceğini varsayabiliriz. Bu hipotezi test etmek için seçilmiş hastalık ilişkili genlerdeki nadir ve sık varyantlar DRACH-G4 örtüşmesi yönünden incelendi.

Gereç ve Yöntemler: Genomik diziler ve varyant bilgileri sırasıyla GRCh37/hg19 ve Biomart-Ensembl veritabanlarından çekildi. Deneysel olarak saptanmış G4 dizileri iki farklı çalışmadan elde edildi.

Bulgular: Yeni bir DRACH motifi oluşumuna yol açan yaygın varyantlar, G4 yapısı içinde yüksek bulundu. Aynı özelliğe sahip nadir varyantlar ise G4 yapısı dışında yüksek bulunurken, pre-mRNA üzerinde eşit dağılım göstermedikleri belirlendi. Yeni bir DRACH motifi oluşumuna yol açan nadir varyantların eşit olmayan dağılımı, örtüştüğü G4 yapısının termodinamik kararlılığı üzerindeki etkisi ile ilişkili bulundu.

Sonuç: Beklenenden sık gözlenen DRACH-G4 örtüşmesi, m6A modifikasyonunun G4 ile örtüştüğü durumların evrimsel bir avantaj sağlıyor olabileceğini düşündürmektedir. Nadir varyantlara bağlı ortaya çıkan DRACH-G4 örtüşmelerinin pre-mRNA'da eşit dağılım göstermemesi ise, m6A'nın G4 termodinamik kararlılığını değiştirmesi ve bu değişikliğin pre-mRNA'nın 5' kısmına göre 3' kısmında daha fazla tolere ediliyor olmasına bağlı görünmektedir. Sonuç olarak, DRACH motifi oluşturan varyantların seçilim baskısı ve bunun sonucunda biçimlenen alel sıklığı, bu varyantın pre-mRNA üzerindeki konumuna ve örtüştüğü G4 oluşumunun kararlılığı üzerindeki etkisine göre değişiklik göstermektedir.

Anahtar kelimeler: RNA modifikasyonu, N6-metiladenozin, G-kuadrupleks, alel sıklığı

Corresponding Author/Sorumlu Yazar: Çağrı GÜLEÇ **E-mail:** cagri@istanbul.edu.tr

Submitted/Başvuru: 25.08.2023 • **Revision Requested/Revizyon Talebi:** 25.08.2023 • **Last Revision Received/Son Revizyon:** 01.09.2023 • **Accepted/Kabul:** 01.09.2023 • **Published Online/Online Yayın:** 13.10.2023

INTRODUCTION

The genetic variants in protein-coding genes display their impact on the phenotype mostly through quantitative and qualitative fluctuation in protein products. In this respect, post-transcriptional RNA modifications play a significant role, especially in a quantitative manner. To date, more than 150 chemical modifications have been identified in RNAs (1, 2). Though most of these modifications are found in non-coding RNAs (rRNA, tRNA, snRNA and long-non-coding RNAs), it has been shown that coding RNAs are also subject to modifications (3). N6-methyladenosine (m6A) is one of the most abundant chemical modifications found in mRNAs (4, 5). The function of m6A was elucidated long after its discovery (6, 7). We now know that m6A plays a significant role in processing, nuclear export, translational regulation, and decay of mRNAs (8, 9). In line with these functions, m6A modification displays an unequal distribution throughout mRNA (4, 5, 10).

In addition to post-transcriptional modifications, secondary structures have a key role in translational efficiency of mRNAs. One of these secondary structures is the G-quadruplex (G4) which is spontaneously formed in guanine-rich (G-rich) sequences in DNA or RNA. This structure is formed via Hoogsten base pairing of adjacent guanines in G-rich sequences (11). Although Hoogsten hydrogen binds between G bases are essential for G4 structure, there are many additional factors that could affect G4 folding in a G-rich sequence, like the length of the sequence, the presence of an alternative Watson-Crick pair-based stable structure and free metal cations (12-15). Bioinformatic studies which are based on the acknowledged consensus sequence and experimental genome-wide studies using G4 specific probes revealed a non-random distribution of G4 structure throughout the genome and transcriptome (16). These studies demonstrated that the G4 sequences are enriched at the telomeres, promoter regions and replication origins in genomic DNA, and UTRs (Untranslated Region) in mRNA. Though G4 structures are formed both in DNA and RNA, it has been shown that G4 structures in RNA are more stable and have less topological diversity than G4 structures in DNA (17). Searching the canonical consensus sequence (5'-$G_3N_{1-7}G_3N_{1-7}G_3N_{1-7}G_3$-3' where N is A, C, G, T, or U) from which a typical G4 structure is known to form, putative G4 structures were found to be present in 5'UTR of more than 9.000, and in 3'UTR of more than 8.000 human genes (15, 18, 19, 20-22). Moreover, it showed that more than 1.600 human genes have G4 structures in their ORFs (Open Reading Frame) (23). G4 structures in RNAs are supposed to play a role in stability, splicing, and translation of RNAs through binding specific proteins like eIF4G, LARK, SLIRP, AFF3, AFF4, eIF4A and hnRNP A2 (24-30).

Despite the enormous difference in their formation and structure, m6A modification and the G4 structure seem to share common functional consequences in RNA processing. Both are separately shown to modulate splicing, nuclear export, translation, and decay of the RNAs. Although mutual or synergic activities of the m6A and G4 are not well understood, recent studies revealed that m6A modification can modulate G4 structure formation and vice versa. The m6A modification was found to modulate the G4 structure through affecting its stability as shown in R-loops, while the G4 structure was demonstrated to modulate m6A modification through facilitating the adenine N6-methylation in target motif as shown in viral RNAs (31, 32). Their synergic activity is supported by overlapping m6A-G4 in eukaryotic mRNAs (33, 34).

MATERIAL and METHODS

Aim: Considering previous studies, this study aimed to investigate whether the functional consequences of overlapping m6A-G4 have selective pressure on the variants that lead to colocalization of m6A and G4. To address this question, defined single nucleotide variants in selected disease-associated human genes were investigated to determine their effect on the colocalization of m6A and G4.

Reference sequence data: Human genome sequence (GRCh37/hg19) was downloaded from NCBI (https://www.ncbi.nlm.nih.gov/assembly/GCF_000001405.25) and recorded as a sql database using Sqlite3 library of Python3.7. The name list and exonic coordinates of disease associated human genes (28,250 transcripts from 3,306 MIM genes) and genomic coordinates, alleles, and allele frequencies of the variants within these regions were fetched from Ensembl (Biomart; http://grch37.ensembl.org/biomart/martview/c4f6ef5ffc88cf1d9a00b63173228cda) and UCSC Genome Browser (https://genome.ucsc.edu/cgi-bin/hgTables).

Real G4 data: Genomic coordinates of experimentally identified G4 regions were yielded from two GEO datasets (GSE77282 and GSE181373) (37, 38). The neighboring gene name, SNP (Single Nucleotide Polymorphism) record name, variant alleles, and allele frequency of the variants within these coordinates were fetched from the UCSC Genome Browser and recorded as text files.

Artificial variant sequences: Considering their genomic position, strand, alleles and allele frequency, each single nucleotide variant and their flanking reference sequence was retrieved from a hg19-sql database, and separately stored as 'wild-type sequence pieces'. By replacing the reference base with a variant base, a 'variant sequence piece' was produced for each corresponding 'wild-type sequence piece.' Each 'variant sequence piece was tagged as 'common' or 'rare' regarding the minor allele frequency (MAF) ('common' for alleles with MAF ≥0.01, and 'rare' for alleles with MAF <0.01) of the corresponding variant. Variants with no recorded MAF value in the database were evaluated as rare variants.

Searching and counting the putative G4 structures and m6A motifs: Both wild-type and matched variant sequence pieces were evaluated with 're' module and 'Pandas' library of the Python3.7, for the presence and count of a putative G4-forming sequence ($G_{1-3}[N_{1-7}G_{1-3}]_3$), for putative G4 structures and consensus DRACH motif ([A/G/U][A/G]AC[A/C/U]), and for putative

m6A modification sites. The effect of the variant on the m6A (DRACH) motif number was evaluated according to putative DRACH motif Number (n) in the presence of a reference allele. The resulting effect was assessed as inert (change from 'n' to 'n'), augmentative (from 'n' to 'n+1') or reductive (from 'n' to 'n-1').

Thermodynamic stability: Minimum free energy (MFE) value of each sequence piece was calculated with 'seqfold' library of the Python3.7.

Statistical analysis: The Chi-square, t-test, Z-test, and correlation test were performed with the 'statsmodels' library of the Python3.7.

RESULTS

The number of common variants creating the DRACH (m6A) motif inside the G4 structure are higher than the rare variants. Since, both m6A and G4 found in pre-mRNA are known to affect splicing, localization, translational efficiency, and decay of the RNAs, variants in a non-spliced sequence of the selected MIM genes were evaluated in terms of their effect on a m6A motif Number within putative G4 structures. While most of the variants (94,6%, 50,933 variants) were found not to relate to the m6A motif (n→n;inert variants), 75% (2,009 variants) of the remaining variants created a novel m6A motif (n→n+1;augmentative variants), and 25% (851 variants) abolished a preexisting m6A motif (n→n-1;reductive) inside a putative G4-structure (Supplementary File 1). The research found that the number of rare variants which create a novel m6A motif or increase the number of preexisting m6A motifs inside a G4 structure were statistically lower (p=3.02e-6) than that of the common variants (Table 1).

To clarify whether this situation is limited to G4-included regions, the variants which have a flanking region that is not included in any putative G4 (G4-not-included regions) were analyzed. Contrary to G4-included regions, the number of rare augmentative variants, which created a novel m6A motif or increased the number of preexisting m6A motifs inside G4-not-included regions, were found statistically higher (p=6.98e-30) than that of common variants (Table 1).

Since both the m6A modification and G4 structures participated in the translational rate, localization and stability of mRNA, variants were evaluated in the spliced RNA sequence, as well. While the difference between rare and common variants in G4-not-included regions remained statistically significant (p<0.001), there was no statistical significance in the distribution of variant counts inside G4 (Table 2).

Rare variants creating the DRACH (m6A) motif inside G4 avoid being close to 3'-side and prefer to be near 5'-side of pre-mRNAs.
Independent of their frequency, both inert and reductive variants displayed an equal distribution throughout pre-mRNAs. The distribution of augmentative rare variants displayed a statistically significant shift from 3'-end to 5'-end of the pre-mRNAs (Figure 1).

Table 1: Count of variants which decrease (n ->n-1), increase (n ->n+1) or do not change (n ->n) the m6A motif number (n) inside or outside the G4 structure in pre-mRNA. Rare variants (MAF<0.01) increasing the m6A motif number were significantly higher outside the G4 structure, while common variants (MAF ≥0.01) increasing the m6A motif number were significantly higher inside the G4 structure

m^{6}A motif location	m^{6}A motif number		MAF value	Variant count		Chi-square
	Reference allele	Variant allele		Observed	Expected	
Inside G4-motif	n	n-1	<0.01	509	529.913	0.82
			≥0.01	763	742.087	0.58
	n	n	<0.01	31,814	31,661.47	0.73
			≥0.01	44,186	44,338.53	0.52
	n	n+1	<0.01	1,174	1,305.619	13.26*
			≥0.01	1,960	1,828.381	9.47*
Outside G4-motif	n	n-1	<0.01	994	919.87	5.97
			≥0.01	7,913	7,987.12	0.68
	n	n	<0.01	23,410	23,836.62	7.63
			≥0.01	207,396	206,969.37	0.87
	n	n+1	<0.01	1,516	1,163.5	106.79**
			≥0.01	9,750	10,102.49	12.29**

* p=3.02e-6, Total chi-square:25.41, df=2, ** p=6.98e-30, Total chi-square: 134.26, df=2

Table 2: Count of variants which decrease (n ->n-1), increase (n ->n+1) or does not change (n ->n) the m6A motif number (n) inside or outside the G4 structure in mRNA. Rare variants (MAF<0.01) increasing the m6A motif number were significantly higher outside the G4 structure, while common variants (MAF≥0.01) were lower

m^{6}A motif location	m^{6}A motif number		MAF value	Variant count		Chi-square
	Reference allele	Variant allele		Observed	Expected	
Inside G4-motif	n	n-1	<0.01	0	1.09	0.128
			≥0.01	13	11.9	1.395
	n	n	<0.01	71	68.2	7.995
			≥0.01	737	739.79	86.728
	n	n+1	<0.01	1	2.73	0.320
			≥0.01	31	29.29	3.434
Outside G4-motif	n	n-1	<0.01	695	655.42	2.39
			≥0.01	5,443	5,482.57	0.28
	n	n	<0.01	12,698	12,857.69	1.98
			≥0.01	107,714	107,554.3	0.23
	n	n+1	<0.01	756	635.88	22.69*
			≥0.01	5,199	5,319.11	2.71*

* p<0.0001, Total chi-square: 30.299, df=2

Because the total length and exon-intron contents of each transcript are different, relative position rather than absolute position of the variants is more appropriate for the comparison of their position-dependent effect in pre-mRNAs. To investigate the position-dependent effect of the variants on m6A-G4 colocalization in more detail, their relative positions were clustered as positional quartiles. Distribution of the rare variant ratio through positional quartiles revealed that the ratio of inert variants displayed an equal distribution throughout pre-mRNAs. Except for the second quartile, the ratio of reductive variants displayed an equal distribution. In the second quartile, the ratio of reductive rare variants was found to be significantly lower than expected. The ratio of augmentative variants displayed unequal distribution in all quartiles. In the first quartile, the ratio of augmentative rare variants was higher than expected, howerver in the last quartile it was lower than expected (Figure 2).

To evaluate whether there is a difference between the distribution of variant positions throughout the G4 structure, the relative position of variants in the G4 sequence were compared. There was no difference found between the over-G4 distribution of the variants (Data not shown.).

Colocalization of m6A and G4 seems to increase the thermodynamic stability of the G4 structure.

Because of the crucial involvement of thermodynamic stability in G4-structure formation, minimum free energy (MFE) values of the putative G4-structures were compared considering the variants and m6A motif numbers.

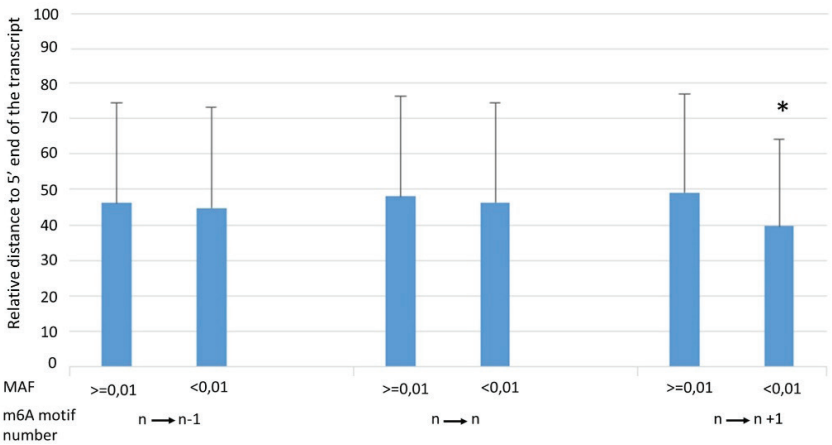

Figure 1: Comparison of mean distribution of common (MAF≥0.01) and rare (MAF<0.01) variants regarding their effect on m6A-motif number inside the putative G4 motifs. Distribution of the rare variants that increase m6A number have closer location to 5'-side. *p<0.001

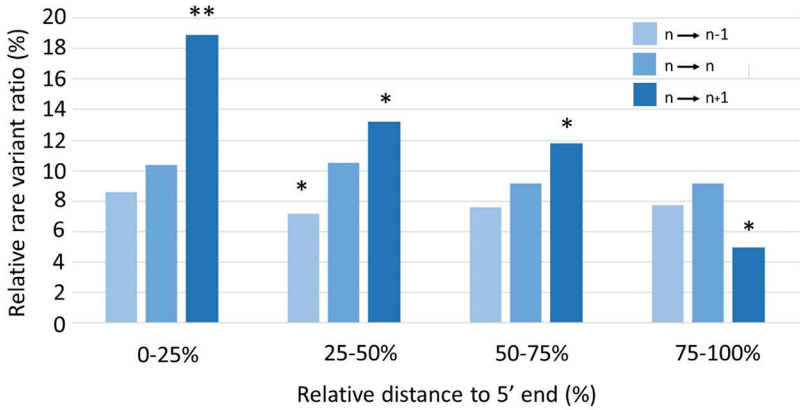

Figure 2: Distribution of rare variant/common variant ratio throughout relative position quartiles. The rare variants that increase m6A number display a gradually decreasing pattern from 5'- to 3'- side. *p<0.001, **p<0.0001

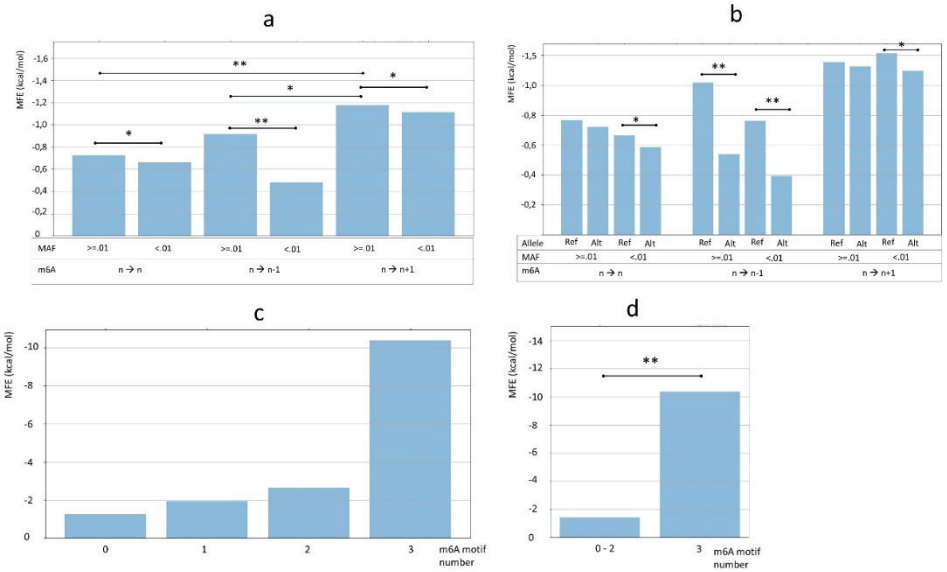

Figure 3: Distribution of G4-MFE values throughout relative position quartiles (a, b) and the effect of m6A number on G4-MFE value (c, d). The effect of m6A on MFE value depends on frequency (a), alleles (b) and m6A number (c), especially three m6As (d). *p<0.001, **p<0.0001

Rare variants were shown to have lower MFE values, especially in reductive variants (Figure 3a). When reference and variant bases were considered, it was observed that the alternative variant had a lower MFE than the reference allele in each group (Figure 3b). While reductive rare variants were found to have the lowest MFE, augmentative common variants were found to have the highest MFE value (Figure 3a). To evaluate whether this result was due to the presence of the m6A motif, the MFE values of G4 sequences were compared to the m6A motif number. The MFE values were observed to be inversely related to the m6A motif count (Figure 3c). Putative G4 structures with three m6A motifs were found to have the lowest MFE values (Figure 3d).

Overlapping m6A-G4 could modulate the G4 stability in a position-dependent manner.

Due to position-dependent colocalization of m6A-G4 and m6A-dependent stability of G4, we can hypothesize that G4-stability could also be modulated in a position-dependent manner. Additionally, because of the relationship between overlapping m6A-G4 and allele frequency, it is possible that G4-stability could depend on allele frequency of the variants. To test this theory, the MFE values of putative G4 structures were compared while considering the relative position and minor allele frequency of the variants that created the m6A motif.

Distribution of the MFE values over positional quartiles showed that MFE values were likely to decrease from the 5'-end to the

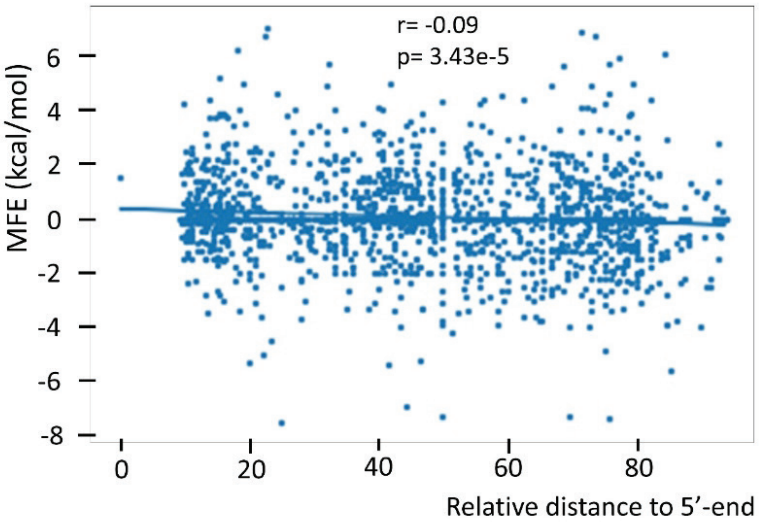

Figure 4: Correlation between G4-MFE values led by m6A-creating variants and their relative position. Decreasing MFE value suggests an increased stability of G4 from 5'- to 3'-end.

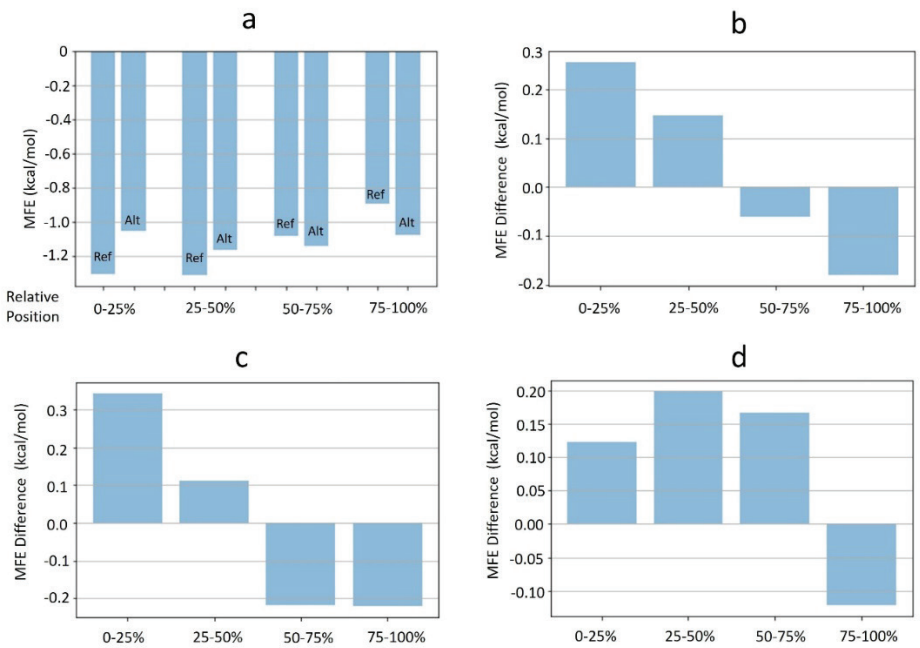

Figure 5: Position-dependent decrease in MFE values shows difference between reference (Ref) and alternative (Alt) allele of the variants (a). The position dependency of MFE values is clearer when MFE differences between Ref and Alt alleles are considered (b). MFE differences of common variants (c) and rare variants (d) have different distribution patterns.

3'-end of pre-mRNAs (Figure 4). To see whether this position-dependent decrease depended on variant alleles, the MFE values were evaluated in terms of alleles. The effect of variant alleles on the MFE values was found to depend on their relative position (Figure 5a). The difference between MFE values of the variant allele and reference allele showed a dependence on relative position (Figure 5b). The MFE-difference (Variant allele MFE minus reference allele MFE) value had a decreasing pattern throughout pre-mRNA. When the distribution of the MFE-difference was reevaluated considering the frequency of variant alleles, it revealed that the decrease in the MFE-difference started closer to the 5'-end with common alleles (Figure 5c), and closer to the 3'-end with rare variants (Figure 5d).

Real Data Analysis

To evaluate the validity of the findings, experimental

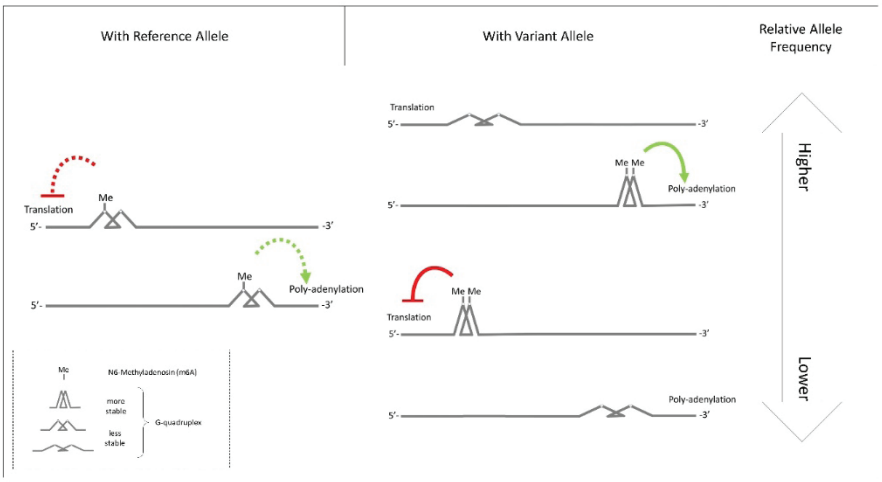

Figure 6: A hypothetical model to explain the position-dependent effect of m6A-G4 colocalization. A variant that creates m6A motif overlapping with G4 is prone to have higher allele frequency in 3'-side, because G4 supports poly-adenylation. In 5'-side, however, it is prone to have lower allele frequency to allow translation.

G-quadruplex data were analyzed. The first set of data included 13,423 genomic coordinates of G-quadruplex regions yielded from the HeLa human transcriptome study dataset, GSE77282 (35). The second set was retrieved from the GSE181373 dataset that obtained single-cell mapping of DNA G-quadruplex structures in three human cancer cell lines (K562, MCF7 and U2OS), and included 223,696 genomic regions (36). All the SNPs and their flanking sequences located inside these genomic coordinates were gotten from the USCS Browser (https://genome.ucsc.edu/).

The first dataset included 13,360 unique genomic regions in 6,613 genes. A total of 15,169 known variants were found within these regions. When the regions with extreme length (median length: 11,657 bp, min length: 10 bp, maximum length: 110,841 bp) were filtered out, 823 regions covering at least one variant were yielded (Supplementary File-2). Of these regions, only 110 (13.36%) were found to have classical G4-quadruplex motifs ($G_{1-3}[N_{1-7}G_{1-3}]_3$). The G4-quadruplex motif-included sequences that were evaluated in terms of DRACH (m6A) motif number with variant alleles. Approximately 10% of them were found to have a changed DRACH motif number; From 0 to 1:21 variants, from 1 to 2:13 variants, from 2 to 3:2 variants, from 1 to 0: 15 variants and from 2 to 1:4 variants.

The second dataset included 223,696 genomic regions of which 198,959 were unique. Of these experimentally detected quadruplex regions, which had a 2,939.46 bp length in mean (median 1,766 bp), 1,5487 (43.5%) were found to have at least one classical G4-quadruplex motif. Though 34,482 variants (35,603 alleles) were identified to be covered by these regions, only 406 (1.14%) were located inside a classical G4-quadruplex motif. While 81 variants were found to remove a pre-existing classical G4-quadruplex motif, 117 were observed to create a novel classical G4-quadruplex motif. Of the remaining 299 variants, which did not affect the G4-motif, 288 did not change the m6A-motif number within the G4-quadruplex motif. Only six variants were found to increase the m6A-motif number within the G4-quadruplex motif, while five variants decreased the m6A-motif number.

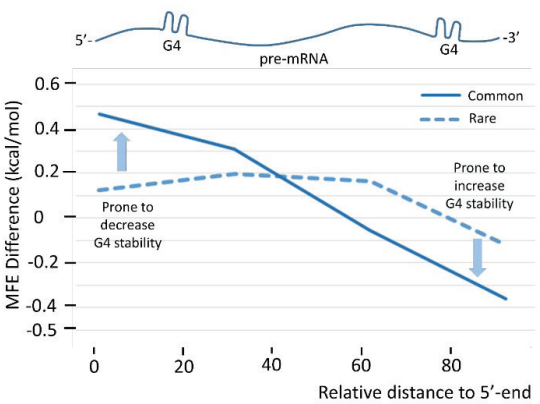

Figure 7: The position-dependent effect of m6A-G4 colocalization can be explained by MFE difference. The variants that create m6A motif overlapping with G4 may have better fitness due to decreased G4 stability near 5'-side and increased G4 stability near 3'-side.

When the allele frequency was considered, no significant difference was found in the distribution of the m6A motif counts (Supplementary Table-1). On the other hand, the statistically significant relationships observed in the data yielded from the presumed G4-motifs that we were not able to evaluate in the real data, because the count of rare variants were not sufficient (Supplementary File-2).

DISCUSSION

Post-transcriptional modifications like m6A, and secondary structures like G-quadruplex, are principal actors in RNA processing. While the m6A modification is controlled by specific enzymes, the formation of G4 structures relies on physico-chemical conditions and thermodynamic rules. Both lead to similar consequences in terms of their effects on RNA processing, but with different manners. The dependence on a consensus sequence is another common feature of the m6A and G4. While the m6A modification targets the adenine in the third position of the DRACH ([A/G/U][A/G]AC[A/C/U]) motif, the G4 structure is formed from the sequence with $G_{1-3}[N_{1-7}G_{1-3}]_3$ motif (15, 18, 19, 37).

Besides the separate roles of the m6A modification and G4 structure, their colocalization has been shown to have functional importance. The crosstalk between the m6A modification and G4 structures seems bidirectional. For instance, the m6A modification is shown to affect the stability of the R-loop, and a G4 structure formed by DNA: RNA hybrid strands (31, 32). Mutually, the G4 structures are shown to modulate m6A modification in some viral genomes like HIV, Zika, Hepatitis B, and SV40 (34). If we suppose that a variant within the G4-forming sequence can create or abolish the m6A motif (DRACH), this variant could be under selective pressure depending on the functional effect of the resulting overlapping m6a-G4 status. In this respect, we can expect a correlation between the frequency and colocalization ability of the variants. In this study, the impact of the m6A-G4 colocalization on the variant frequency was investigated. For this purpose, the single nucleotide variants in selected disease-associated human genes were evaluated for their allele frequency and m6A-G4 colocalization ability.

The outstanding result of this study is that the variants creating the m6A motif inside a G4 structure are prone to have a higher frequency. In contrast, such variants have lower frequency if located outside of the G4 structure. The Colocalization-dependent higher allele frequency of such variants suggest that overlapping m6A-G4 could have a protective role.

To understand how a variant creating m6A motif inside a G4 structure may play a protective role and gain a favorable feature, distribution of the colocalization-leading variants throughout pre-mRNAs was evaluated, since both the m6A modification and G4 structure display their functional effects in a position-dependent manner (38).

The results showed that the position of the colocalization-leading variants has importance for the underlying mechanism. Previous studies, showed that the m6A motif distribution throughout RNA molecules was not equal. Many studies observed that the m6A residues were enriched in 5'UTRs, around stop codons and in 3' UTRs adjacent to stop codons in mammalian mRNAs (4, 5, 39). Similarly, the G4 structures were also reported to be overrepresented in 5'- and 3'-UTRs (20, 40).

Findings of this study suggest that the functional consequence of the m6A-G4 colocalization may have selective pressure on the colocalization-leading variants in a position-dependent manner. While the G4 structures hosting a m6A motif created by a common variant showed equal distribution throughout the pre-mRNA, G4 structures overlapping with m6A motifs created by a rare variant are likely to avoid the 3'-side of the pre-mRNAs. This result could mean that the m6A-G4 colocalization can be tolerated when found near the 3'-side, but not in the central region and especially near the 5'-side of the pre-mRNA. Then, it can be deduced that any variant that creates a novel m6A motif inside a G4 structure could become favorable, and display an increased population frequency, if found near the 3'-side. On the other hand, the same type of variant would not bepreferable if found in the transcript body, and undesirable if found near the 5'-side of the pre-mRNA. The latter is expected to display a decreasing allele frequency. The favorability of a m6A-G4 colocalization in the 3'-side is due to the supported function of the pre-existing G4 structure. For instance, as represented in Fig 6, the G4 structure supported by the m6A in 5'UTR may reduce the translational efficiency of mRNA, since G4 structures in 5'UTR are known to affect cap-dependent and cap-independent translation (41). Similarly, the G4 structure supported by an overlapping m6A in the 3'-side may enable the transcript to produce alternative products, through modulating alternative splicing and alternative poly-adenilation of pre-mRNA (21, 41). It is also possible that the m6A can modulate miRNA binding through stabilizing the G4 structure after splicing (40).

There could be consequences for the m6A-G4 colocalization. The creation of novel docking sites for specific proteins must be considered in this respect. Both m6A and G4 structures are known to be recognized by specific proteins (24, 43, 44). Therefore, colocalization of the m6A modification and G4 structure may lead to competitive or cooperative interaction between these proteins. Evaluating these possibilities requires experimental methods dealing *in vitro* RNA-protein interactions. Another consequence of the m6A-G4 colocalization is the changing thermodynamic properties of the structure. Thermodynamic stability is crucial for the formation of G4 structures (45). In contrast, m6A formation is regulated by specific enzymes rather than the thermodynamic status of the flanking sequence (46). However, m6A modification can affect the thermodynamic stability of RNA, and marginally reduce the stability of an A: U base pairing (47). Similarly, in recent studies, the colocalization of m6A and G4 was shown to alter the stability of the DNA: RNA hybrid quadruplexes, known as R-loop (31, 32). Some studies reported that the m6A promoted G4 folding, while others demonstrated that the m6A downregulated the G4 formation. These contradictory findings are still discussed. The G4 was also disputed to modulate the m6A modification in viral RNAs (32). The overlapping m6A and G4 in 3'UTR of viral RNAs revealed that the folded G4 structures may guide the enzymatic adenine methylation in the DRACH motifs (34). Moreover, enrichment of the overlapping m6A and G4 in viral RNAs are reported to be critical for the impact of the m6A on viral fitness; as shown in HIV-1 (48). In eukaryotes, the overlapping m6A and G4 are shown in the 3'UTRs of mRNAs, as well (33, 49).

Based on previous studies that suggested the synergy between m6A and G4, we can deduce that significance in the distribution of variants leading to the m6A-G4 colocalization may result from the changed stability of the G4 structures. To assess this possibility, the MFE values of G4 structures were calculated. DRACH (m6A) motifs were observed to cause a decreased MFE, which means increased thermodynamic stability of the G4 structure. The number of m6A motifs inside the G4 structure also seems crucial for the degree of stability.

The position-dependency of overlapping m6A-G4 may explain the mechanism responsible for difference in allele frequency among the variants leading to m6A-G4 colocalization. Based on the findings of this study, we can suppose that a m6A-G4 colocalization-leading variant will prone to have higher allele frequency, if decreases G4 stability when located near 5'-side and increases it when located near 5'-side of the pre-mRNA (Figure 7).

The preliminary results of this study suggest that m6A overlapping with G4 structure may have functional consequences with an unknown mechanism. At least, it seems likely that this mechanism needs position-dependent stability of the G4 structure.

Since all findings of the study need to be validated with real data, sequences yielded from genomic coordinates of experimentally identified quadruplex regions in two GEO datasets were also investigated for the covered variants and putative m6A motif numbers. However, because the counts of the experimentally detected quadruplex regions which had classical motif ($G_{1-3}[N_{1-7}G_{1-3}]_3$) were not sufficient for further statistical analysis, findings of the study could not be supported or disproved by the real data. Choosing the classical G4-quadruplex motif was a limitation of recent study, so the theoretical findings of this study were restricted to the classical G4-quadruplex motif, which seems not to be common in the real quadruplex pools. Therefore, different subtypes of the G4-quadruplex motifs, together with the $G_{1-3}[N_{1-7}G_{1-3}]_3$ motifs, should be considered in further studies to manage the synergy of the overlapping G4-m6A motifs and allele frequency of the m6A-related variants.

In summary, we conclude that the fitness, and consequently the frequency of a variant creating the m6A motif is prone to become higher or lower depending on whether it is located inside or outside the classical G4 structure. Furthermore, the frequency of these variants may depend on both their position and their effect on the thermodynamic stability of the overlapping G4 structure. If located near the 5'-side it destabilizes the G4 structure or if located near the 3'-side it stabilizes the G4, a variant creating m6A motif is prone to have higher fitness and frequency.

Study limitations: The recent study included only the selected MIM genes, and the known SNPs reported in these genes. Findings revealed from the available experimental data were insufficient to evaluate theoretical findings of the study.

CONCLUSION

The starting point of this study was a suspicion as to whether there is a functional crosstalk between chemical modifications (like m6A) and secondary structures (like G4-quadruplex) in RNA. In case of such a crosstalk, the genetic variations at the chemically modified base are expected to have functional consequences, which create selective pressure on the variant allele. Though the lack of experimental validation and supports, the findings of this study suggest that the fluctuation in allele frequency of the human SNP's could be a consequence of the crosstalk between the m6A and G4-quadruplex. In addition to the potential contribution to population genetics and evolutionary genetics, such a crosstalk between the m6A and G4-quadruplex also has the potential to help us understand the polygenic nature of the complex disorders and the modifying genetic factors in the single-gene disorders.

Ethics Committee Approval: The author declared that an ethics committee approval is not required for this study.

Peer Review: Externally peer-reviewed.

Conflict of Interest: The authors have no conflict of interest to declare.

Financial Disclosure: The authors declared that this study has received no financial support.

REFERENCES

1- Motorin Y, Helm M. RNA nucleotide methylation. Wiley Interdiscip Rev RNA 2011;2(5):611-31.
2- Machnicka MA, Milanowska K, Oglou OO, Purta E, Kurkowska M, Olchowik A, et al. MODOMICS: a database of RNA modification pathways--2013 update. Nucleic Acids Res 2013;41(Database issue):D262-7.
3- Desrosiers R, Friderici K, Rottman F. Identification of methylated nucleosides in messenger RNA from Novikoff hepatoma cells. Proc Natl Acad Sci U S A 1974;71(10):3971-5.
4- Dominissini D, Moshitch-Moshkovitz S, Schwartz S, Salmon-Divon M, Ungar L, Osenberg S, et al. Topology of the human and mouse m6A RNA methylomes revealed by m6A-seq. Nature 2012;485(7397):201-6.
5- Meyer KD, Saletore Y, Zumbo P, Elemento O, Mason CE, Jaffrey SR. Comprehensive analysis of mRNA methylation reveals enrichment in 30 UTRs and near stop codons. Cell 2012;149(7); 1635-46.
6- Roundtree IA, Evans ME, Pan T, He C. Dynamic RNA modifications in gene expression regulation. Cell 2017;169(7):1187-200.
7- Zhao BS, Roundtree IA, He C. Post-transcriptional gene regulation by mRNA modifications. Nat Rev Mol Cell Biol 2017;18(1):31-42.
8- Shi H, Wang X, Lu Z, Zhao BS, Ma H, Hsu PJ, et al. YTHDF3 facilitates translation and decay of N6-methyladenosine-modified RNA. Cell Res 2017;27(3):315-28.
9- Roignant JY, Soller M. m6A in mRNA: an ancient mechanism for fine-tuning gene expression. Trends Genet 2017;33(6):380-90.
10- Gilbert WV, Bell TA, Schaening C. Messenger RNA modifications: form, distribution, and function. Science 2016;352(6292):1408-12.
11- Bochman ML, Paeschke K, Zakian VA. DNA secondary structures: stability and function of G-quadruplex structures. Nat Rev Genet 2012;13(11):770-80.

12- Rachwal PA, Brown T, Fox KR. Effect of G-tract length on the topology and stability of intramolecular DNA quadruplexes. Biochemistry 2007;46(11):3036-44.
13- Rachwal PA, Fox KR. Quadruplex melting. Methods 2007;43(4):291-301.
14- Rachwal PA, Brown T, Fox KR. Sequence effects of single base loops in intramolecular quadruplex DNA. FEBS Lett 2007;581(8):1657-60.
15- Mukundan VT, Phan AT. Bulges in G-quadruplexes: broadening the definition of G-quadruplex-forming sequences. J Am Chem Soc 2013;135(13):5017-28.
16- Lam EY, Beraldi D, Tannahill D, Balasubramanian S. G-quadruplex structures are stable and detectable in human genomic DNA. Nat Commun 2013;4:1796.
17- Bugaut A, Murat P, Balasubramanian S. An RNA hairpin to G-quadruplex conformational transition. J Am Chem Soc 2012;134(49):19953-6.
18- Huppert JL, Balasubramanian S. G-quadruplexes in promoters throughout the human genome. Nucleic Acids Res 2007;35(2):406-13.
19- Huppert JL. Hunting G-quadruplexes. Biochimie 2008;90(8):1140-8.
20- Kumari S, Bugaut A, Huppert JL, Balasubramanian S. An RNA G-quadruplex in the 5' UTR of the NRAS proto-oncogene modulates translation. Nat Chem Biol 2007;3(4):218-21.
21- Beaudoin JD, Perreault JP. 5'-UTR G-quadruplex structures acting as translational repressors. Nucleic Acids Res 2010;38(20):7022-36.
22- Huppert JL, Bugaut A, Kumari S, Balasubramanian S. G-quadruplexes: the beginning and end of UTRs. Nucleic Acids Res 2008;36(19):6260-8.
23- Thandapani P, Song J, Gandin V, Cai Y, Rouleau SG, Garant JM, et al. Aven recognition of RNA G-quadruplexes regulates translation of the mixed lineage leukemia protooncogenes. Elife 2015;4:e06234.
24- Brázda V, Hároníková L, Liao JC, Fojta M. DNA and RNA quadruplex-binding proteins. Int J Mol Sci 2014;15(10):17493-517.
25- Lyons SM, Kharel P, Akiyama Y, Ojha S, Dave D, Tsvetkov V, et al. eIF4G has intrinsic G-quadruplex binding activity that is required for tiRNA function. Nucleic Acids Res 2020;48(11):6223-33.
26- Niu K, Xiang L, Jin Y, Peng Y, Wu F, Tang W, et al. Identification of LARK as a novel and conserved G-quadruplex binding protein in invertebrates and vertebrates. Nucleic Acids Res 2019;47(14):7306-20.
27- Williams P, Li L, Dong X, Wang Y. Identification of SLIRP as a G Quadruplex-Binding Protein. J Am Chem Soc 2017;139(36):12426-9.
28- Serikawa T, Spanos C, von Hacht A, Budisa N, Rappsilber J, Kurreck J. Comprehensive identification of proteins binding to RNA G-quadruplex motifs in the 5' UTR of tumor-associated mRNAs. Biochimie 2018;144:169-84.
29- Lyonnais S, Tarrés-Solé A, Rubio-Cosials A, Cuppari A, Brito R, Jaumot J, et al. The human mitochondrial transcription factor A is a versatile G-quadruplex binding protein. Sci Rep 2017;7:43992.
30- Khateb S, Weisman-Shomer P, Hershco-Shani I, Ludwig AL, Fry M. The tetraplex (CGG)n destabilizing proteins hnRNP A2 and CBF-A enhance the in vivo translation of fragile X premutation mRNA. Nucleic Acids Res 2007;35(17):5775-88.
31- Yang X, Liu QL, Xu W, Zhang YC, Yang Y, Ju LF, et al. m6A promotes R-loop formation to facilitate transcription termination. Cell Res 2019;29(12):1035-8.
32- Abakir A, Giles TC, Cristini A, Foster JM, Dai N, Starczak M, et al. N6-methyladenosine regulates the stability of RNA:DNA hybrids in human cells. Nat Genet 2020;52(1):48-55.
33- Jara-Espejo M, Fleming AM, Burrows CJ. potential G-quadruplex forming sequences and N6-methyladenosine colocalize at human Pre-mRNA intron splice sites. ACS Chem Biol 2020;15(6):1292-130.
34- Fleming AM, Nguyen NLB, Burrows CJ. colocalization of m6A and G-Quadruplex-Forming sequences in Viral RNA (HIV, Zika, hepatitis B, and SV40) suggests topological control of adenosine N6-methylation. ACS Cent Sci 2019;5(2):218-28.
35- Kwok CK, Marsico G, Sahakyan AB, Chambers VS, Balasubramanian S. rG4-seq reveals widespread formation of G-quadruplex structures in the human transcriptome. Nat Methods 2016;13(10):841-4.
36- Hui WWI, Simeone A, Zyner KG, Tannahill D, Balasubramanian S. Single-cell mapping of DNA G-quadruplex structures in human cancer cells. Sci Rep 2021;11(1):23641.
37- Csepany T, Lin A, Baldick CJ Jr, Beemon K. Sequence specificity of mRNA N6-adenosine methyltransferase. J Biol Chem 1990;265(33):20117-22.
38- Bushkin GG, Pincus D, Morgan JT, Richardson K, Lewis C, Chan SH, et al. m6A modification of a 3' UTR site reduces RME1 mRNA levels to promote meiosis. Nat Commun 2019;10(1):3414.
39- Batista PJ, Molinie B, Wang J, Qu K, Zhang J, Li L, et al. m(6)A RNA modification controls cell fate transition in mammalian embryonic stem cells. Cell Stem Cell 2014;15(6):707-19.
40- Rouleau S, Glouzon JS, Brumwell A, Bisaillon M, Perreault JP. 3' UTR G-quadruplexes regulate miRNA binding. RNA 2017;23(8):1172-9.
41- Jodoin R, Carrier JC, Rivard N, Bisaillon M, Perreault JP. G-quadruplex located in the 5'UTR of the BAG-1 mRNA affects both its cap-dependent and cap-independent translation through global secondary structure maintenance. Nucleic Acids Res 2019;47(19):10247-66.
42- Song J, Perreault JP, Topisirovic I, Richard S. RNA G-quadruplexes and their potential regulatory roles in translation. Translation (Austin) 2016;4(2):e1244031.
43- von Hacht A, Seifert O, Menger M, Schütze T, Arora A, Konthur Z, et al. Identification and characterization of RNA guanine-quadruplex binding proteins. Nucleic Acids Res 2014;42(10):6630-44.
44- Roundtree IA, He C. Nuclear m(6)A Reader YTHDC1 Regulates mRNA Splicing. Trends Genet 2016;32(6):320-1.
45- Xue Y, Liu JQ, Zheng KW, Kan ZY, Hao YH, Tan Z. Kinetic and thermodynamic control of G-quadruplex folding. Angew Chem Int Ed Engl 2011;50(35):8046-50.
46- Song Y, Xu Q, Wei Z, Zhen D, Su J, Chen K, Meng J. Predict Epitranscriptome Targets and Regulatory Functions of N6-Methyladenosine (m6A) Writers and Erasers. Evol Bioinform Online 2019;15:1176934319871290.
47- Kierzek E, Kierzek R. The thermodynamic stability of RNA duplexes and hairpins containing N6-alkyladenosines and 2-methylthio-N6-alkyladenosines. Nucleic Acids Res 2003;31(15):4472-80.
48- Kennedy EM, Bogerd HP, Kornepati AVR, Kang D, Ghoshal D, Marshall JB, et al. posttranscriptional m6A editing of HIV-1 mRNAs enhances viral gene expression. Cell Host Microbe 2017;22(6):830.
49- Jenjaroenpun P, Wongsurawat T, Wadley TD, Wassenaar TM, Liu J, Dai Q, et al. Decoding the epitranscriptional landscape from native RNA sequences. Nucleic Acids Res 2021;49(2):e7.

İSTANBUL UNIVERSITY PRESS

RESEARCH ARTICLE / ARAŞTIRMA MAKALESİ
Journal of Advanced Research in Health Sciences /
Sağlık Bilimlerinde İleri Araştırmalar Dergisi 2023
DOI: 10.26650/JARHS2023-1231512

ESTIMATION OF HEALTHY AND LIVER DISEASED INDIVIDUALS BY A LINEAR REGRESSION CLASSIFICATION ALGORITHM

SAĞLIKLI VE KARACİĞER HASTALIĞI OLAN BİREYLERİN DOĞRUSAL REGRESYON SINIFLANDIRMA ALGORİTMASIYLA TAHMİN EDİLMESİ

Handan TANYILDIZI KÖKKÜLÜNK[1]

[1]Altınbas University, Vocational School of Health Sciences, Radiotherapy Program, Istanbul, Turkiye

ORCID ID: H.T.K. 0000-0001-5231-2768

Citation/Atıf: Tanyildizi-Kokkulunk H. Estimation of healthy and liver diseased individuals by a linear regression classification algorithm. Journal of Advanced Research in Health Sciences 2023;6(3):229-233. https://doi.org/10.26650/JARHS2023-1231512

ABSTRACT

Objective: In this study, the aim was to make a categorical estimation of the absent/presence of liver disease by using some blood biochemistry parameters (ALB, ALP, ALT, AST, BIL, CHE, CHOL, CREA, GGT, and PROT), gender and the age of healthy individuals, and those with liver disease.

Material and methods: The prediction was obtained with multiple linear regression of machine learning in the R Studio program. Machine learning was improved by selecting parameters that have a high contribution to the prediction by using the Akaike information criterion.

Results: The three strongest parameters with a positive effect on the estimation were AST, BIL, and GGT, respectively; The three strongest parameters with negative effects were CHOL, CHE, and ALB, respectively. The accuracy of the model used was 91%, the precision was 99%, the recall was 0.91, and the F score was 94%. When the correlation relationship graph was examined, it was determined that AST was a strong differential parameter in healthy/liver diseased individuals.

Conclusion: Multiple linear regression is a preferable method for categorical disease classification.

Keywords: Machine learning, liver, classification

ÖZ

Amaç: Bu çalışmada sağlıklı ve karaciğer hastalığı olan bireylere ait bazı kan biyokimya parametreleri (ALB, ALP, ALT, AST, BIL, CHE, CHOL, CREA, GGT ve PROT), cinsiyet ve yaş bilgileri kullanılarak karaciğer hastalığı yok/var kategorik tahmini yapılması amaçlanmıştır.

Gereç ve Yöntem: R Studio programında makine öğrenmesine ait çoklu doğrusal regresyon ile tahmin elde edilmiştir. Akaike bilgi kriteri kullanılarak tahmin üzerine yüksek katkısı olan parametreler seçilerek makine öğrenmesinde iyileştirilmeye gidilmiştir.

Bulgular: Tahmine pozitif yönlü etkisi olan en güçlü 3 parametre sırasıyla AST, BIL ve GGT; negatif yönlü etkisi olan en güçlü 3 parametre sırasıyla CHOL, CHE ve ALB bulunmuştur. Kullanılan modelin doğruluğu %91, kesinlik %99, geri çağırma 0,91 ve F skoru %94 olarak bulunmuştur. Korelasyon ilişkisi grafiği incelendiğinde AST 'nin sağlıklı/karaciğer hastası bireylerde güçlü bir ayırıcı parametre olduğu tespit edilmiştir.

Sonuç: Çoklu doğrusal regresyonun, kategorik hastalık sınıflandırması için tercih edilebilir bir yöntem olduğu bulunmuştur.

Anahtar Kelimeler: Makine öğrenmesi, karaciğer, sınıflandırma

INTRODUCTION

Machine learning offers strategies, techniques, and resources that can assist in resolving diagnostic and prognostic issues in a range of medical specialties. The significance of clinical indicators and their combinations for prognosis is examined using machine learning. It has developed into a method that is often used to gather medical data for things like planning treatments, outcome studies, and estimating illness progression. Additionally, machine learning is employed for data analysis in the form of smart alerts, continuous data interpretation in intensive care units, and the replication of inaccurate or missing data based on pattern discovery in the available data. It is well recognized that when machine learning techniques are successfully deployed, they aid in the integration of computer-based healthcare systems, present chances to facilitate and enhance the work of medical professionals, and ultimately improve the effectiveness and caliber of medical care (1). Machine learning is being used in the healthcare industry not to replace doctors, but to reduce their workload and give patients feedback more quickly and efficiently.

Machine learning has several important applications in the field of medical diagnosis (2,3). In this approach, doctor-based techniques are used to create hypotheses from patient data. In order to do this, the system is enhanced with symbolic learning

Corresponding Author/Sorumlu Yazar: Handan TANYILDIZI KÖKKÜLÜNKK **E-mail:** handan.kokkulunk@altinbas.edu.tr

Submitted/Başvuru: 09.01.2023 • **Revision Requested/Revizyon Talebi:** 17.01.2023 • **Last Revision Received/Son Revizyon:** 06.07.2023 • **Accepted/Kabul:** 24.07.2023 • **Published Online/Online Yayın:** 10.10.2023

techniques and knowledge management capabilities that are appropriate for the doctor's interpretation of the case. As a result, the forecast is generated using straightforward rules or, most often, a decision tree. The reporting of a medical imaging as a certain radiologist using machine learning is an illustration of this.

Biomedical signal processing is an additional application area (4). With the use of machine learning techniques, it is feasible to model the linear or non-linear relationships that exist between the data and find the fundamental features and information that are concealed in physiological signals or that are likely to be disregarded. Additionally, machine learning is employed in radiography, magnetic resonance imaging, endoscopy, confocal microscopy, computer tomography, and other imaging techniques, particularly for the detection of cancerous regions. In addition to all of these uses, the most typical application of machine learning is to forecast diseases using categorical classification algorithms and patient data (5-7).

The most accessible and practical way for identifying biomarkers that can be used to predict disease is through blood biochemistry characteristics. Some disorders, including diabetes, hypertension, heart disease, hormonal diseases, blood diseases, and liver diseases, can be preliminarily diagnosed using it (8,9). When examining liver illnesses, the blood sample is tested for the presence of biomarkers including ALB, ALP, ALT, AST, BIL, CHE, CHOL, CREA, GGT, and PROT (10). ALB acts as a source of amino acids, carries things through the blood, and aids in osmotic pressure maintenance. The liver contains the enzymes ALP, ALT, AST, CHE, and GGT. BIL is a yellow pigment created when red blood cells are broken down. A lipid molecule called CHOL is necessary for a number of physiological activities. A byproduct of muscle metabolism called CREA is eliminated by the kidneys. ALB and other globulins are included in the PROT measurement of the blood's overall protein concentration. Abnormalities in these biomarkers indicate liver disease (11).

In this study, it was aimed to estimate the presence or absence of liver disease by using liver-related parameters, gender and age information from blood biochemistry results of individuals without liver disease (healthy) and diagnosed with liver disease (patient).

MATERIAL and METHODS

A. Dataset and machine learning preparation

The data set was acquired from the open source Kaggle website and included 615 people who were categorized as healthy, hepatitis, fibrosis, and cirrhotic people (12). Age, gender, ALB, ALP, ALT, AST, BIL, CHE, CHOL, CREA, GGT, and PROT values are all attributes in the data stack that was used. Class values were divided categorically as only healthy (1) and patient (2). By averaging the appropriate column, missing measurements in the dataset were filled in. Detailed information about the attributes in the dataset is given in Table 1.

In the study, the xlsx extension data set was used to code machine learning algorithms through the R Studio program. An amount of 80% of the data set was used to train the algorithm, and 20% of the data set was used in the test set to control the accuracy of the prediction and to evaluate the performance.

B. Forecast ModeL

Machine learning includes a variety of categorization and regression estimation techniques. Multiple linear regression (MLR) was chosen among machine learning regression methods for estimation since the dependent variable in the data set utilized in this study must be estimated as a categorical data type.

B. 1. Multiple Linear Regression (MLR)

One technique for determining the relationship between multiple independent variables (x1–xn) and a dependent variable, y, is known as multiple linear regression (MLR).

Table 1: Some information about the attributes in the dataset

Category		Health (n=540)	Liver Disease (n=75)
		Min-max values	Min-max values
Age	Age	32-77	19-75
Sex	Sex (371 M, 244 F)	-	-
ALB	Albumin Blood Test (g/dL)	14.9-82.2	20-50
ALP	Alkaline phosphatase (U/L)	27-208.2	11.3-416.6
ALT	Alanine Transaminase (U/L)	2.5-325.3	0.9-258
AST	Aspartate Transaminase (U/L)	10.6-188.7	16.7-324
BIL	Bilirubin (mg/dL)	0.8-59.1	5-254
CHE	Acetylcholinesterase (U/g)	3.44-15.43	1.42-16.41
CHOL	Cholesterol (mg/dL)	2.61-9.43	1.43-9.67
CREA	Creatinine (mg/dL)	8-170	45.4-1079,1
GGT	Gamma Glutamyl Transferase (U/L)	4.5-345.6	11.5-650.9
PROT	Protein (g/dL)	44.8-86.5	54.2-90

Multiple linear regression is cited as a typical technique for estimating an unknown variable's value from the known values of two or more other variables (13). The following Eq. 1 for n independent variables, which might be linear or linearized, often expresses this relationship (14).

$$y = b_0 + b_1x_1 + b_2x_2 + \cdots + b_nx_n \quad (1)$$

By adjusting the input parameters, 4 alternative fit operations were performed in the study. It is intended to obtain the input parameters with the greatest impact on the estimation using these 4 various procedures. For each fit procedure, the Akaike information criterion (AIC) is determined (15). The AIC is a single numerical value that can be used to identify the best model for a given dataset among the various models. A better forecast is made by the model with the lower AIC value than by the other models.

C. Performance evaluation criteria

Efficiency research of machine learning classification algorithms is measured using metrics such as accuracy, precision, recall, and F-score (16). After making an estimate, the complexity matrix will be determined for this. It displays TP true positive, TN true negative, FP false positive, and FN false negative in order to depict the positive healthy people and the negative persons with liver disease in the complexity matrix and metrics. As a result, Eq. 2-5, as illustrated in the table below, is used to calculate accuracy, precision (P), recall (R), and F-score.

$$Accuracy = \frac{TN+TP}{TP+TN+FP+FN} \quad (2)$$

$$Precision = \frac{TP}{TP+FP} \quad (3)$$

$$Recall = \frac{TP}{TP+FN} \quad (4)$$

$$Fscore = \frac{2(R*P)}{R+P} \quad (5)$$

In order to assess how much the data contribute to the prediction of disease, the correlation matrix, which is the table of correlation coefficients between various factors, will also be visualized using the corrplot tool.

RESULTS and DISCUSSION

ALB, ALP, ALT, AST, BIL, CHE, CHOL, CREA, GGT and PROT parameters were used in the study, while the search for the presence of liver disease through hemogram biochemistry results was carried out with machine learning. While these parameters are within the typical reference range for healthy people, they do not match the reference range for sick people. In the adult population, the following normal reference ranges are used: 35-52 for ALB, 30-120 for ALP, 0-45 and 0-31 for ALT (male and female), 0-35 and 0-31 for AST (male and female), BIL 3-13, 8-18 for CHE, 0-5.2 for CHOL, 50-110 for CREA, 0-55 and 0-38 (male and female) for GGT, and PROT 60-83 U/L (17). In the data included in the study, the mean age, the ALB, ALP, ALT, AST, BIL, CHE, CHOL, CREA, GGT and PROT values for healthy individuals were calculated as 42.00, 68.86, 27.61, 27.12, 8.47, 8.38, 5.48, 78.75, 30.62 and 71.87 U/L, respectively. These mean values were calculated as 38.70, 61.35, 34.48, 89.94, 32.41, 6.83, 4.52, 99.53, 103.67 and 73.23 U/L for sick individuals, respectively. The ALB, ALP, ALT, CHOL, CREA, and PROT readings of patients with liver illness were determined to be normal when the hemogram findings were compared with normal reference values. Additionally, it was shown that liver patients had low CHE values and high AST, BIL, and GGT values.

Figure 1 presents a graph illustrating the relationship between machine learning and the features used to predict liver disease. The use of the correlation relationship graph to reduce the amount of features and to exclude those that have little to no impact on the prediction are examples of intermediate operations that may be used to improve machine learning. Since most of the factors that have a strong link with the estimate of the features will be incorporated in the algorithm, increasing the results of metrics like accuracy and precision in machine learning, Figure 1 was also employed as a parameter analysis. It was discovered that the three strongest parameters that have a negative effect on the estimation indicated in red are CHOL, CHE, and ALB, respectively. The three strongest parameters that have a favorable influence on the forecast shown in blue are AST, BIL, and GGT, respectively. It was discovered that other factors contributed less positively or negatively to liver prediction.

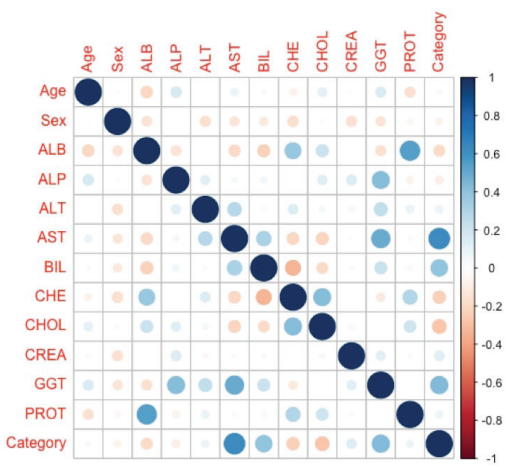

Figure 1. Correlation relationship graph of features with each other. ALB:Albumin, ALP: Alkaline phosphatase, ALT: Alanine Transaminase, AST: Aspartate Transaminase, BIL: Bilirubin, CHE: Acetylcholinesterase, CHOL: Cholesterol, CREA: Creatinine, GGT: Gamma Glutamyl Transferase, PROT: Protein

The glm.fit algorithm was used on 4 different feature collections taking into account the findings of the feature analysis. Table 2 provides details on the glm.fit techniques utilized and the derived AIC results.

Table 2: Machine learning improvement step results

glm.fit number	Attributes	AIC
glm.fit.0	Age + Gender + ALB + ALP + ALT + AST + BIL + CHE + CHOL + CREA + GGT + PROT	151.14
glm.fit.1	Gender + ALB + ALP + ALT + AST + BIL + CHOL + CREA + GGT + PROT	147.82
glm.fit.2	Gender + ALP + ALT + AST + BIL + CHOL + CREA + GGT + PROT	148.41
glm.fit.3	Age + Gender + ALP + ALT + AST + BIL + CHOL + CREA + GGT + PROT	150.33

ALB: Albumin, ALP: Alkaline phosphatase, ALT: Alanine Transaminase, AST: Aspartate Transaminase, BIL: Bilirubin, CHE: Acetylcholinesterase, CHOL: Cholesterol, CREA: Creatinine, GGT: Gamma Glutamyl Transferase, PROT: Protein, glm: General linear model

It is advised to choose the model with the lowest AIC value for predicting the disease. Due to this, the estimation was performed using the features from glm.fit.1, which produced the AIC result with the lowest value (147.82).

Gender, ALB, ALP, ALT, AST, BIL, CHOL, CREA, GGT, and PROT characteristics were used in machine learning utilizing MLR as a healthy/patient estimation method. Table 3 contains the complexity matrix that was produced as a result of the estimation.

The success of the model used to predict healthy individuals with liver illness using the multiple linear regression algorithm of machine learning was found to be 91%. It was determined to be 99% accurate, which indicates how many of the values we anticipated as positive truly are positive. The results showed that the recall and F score were 0.91 and 94%, respectively.

Among the features that excluded AST, Teke discovered that direct bilirubin had the highest correlation with the prediction of liver illness, with a score of 0.87. Additionally, they discovered that the machine learning he created using the logistic regression model had a training accuracy of 87%, test accuracy of 84%, precision of 89%, a F score of 0.78%, and recall of 76% (18). AST was a useful distinguishing characteristic, according to Akter et al., who investigated the liver disease prediction model with machine learning from biochemical test data (19). The accuracy of the random forest and classification-regression trees algorithms was 94% and 95%, respectively (19). Another study used decision trees, logistic regression, random forest, support vector machines, k-near neighbor, and Naive Bayes algorithms to make predictions. The corresponding accuracy percentages for these forecasts were 75%, 74%, 69%, 64%, 62%, and 53% (20). While diagnosing liver disease in machine learning, a comparison of classifications was made with the support vector method or the Naive Bayes-support vector method using several biomarkers (21,22). Similarly, in various studies, methods such as random forest, functional tree, and logistic regression were tried and various liver disease predictions were made using a small number of biomarkers, and the highest success was found to be 82% and the highest accuracy was found to be 87% (18,23).

Table 3: Complexity matrix for MLR estimation of the healthy/patient population

glm.pred_test	Positive	Negative
Positive	110	1
Negative	2	10

glm.pred.test: General linear model predictive test, MLR: Multiple linear regression

The metric having the greatest impact on liver disease was discovered to be AST, and our study was found to be consistent with the literature that uses machine learning to predict liver disease using similar features. Contrary to the literature, the employment of MLR algorithms in machine learning led to the greatest values being attained in all performance evaluation criteria, particularly accuracy. It is believed that getting high accuracy also depends on the quantity of the dataset.

CONCLUSION

The MLR classification algorithm, which is based on machine learning, was used in this study to predict disease based on the categorical classification of healthy/liver disease according to age, gender, and various hemogram biochemical values. The correlation association graph was studied, and it was shown that the AST was a significant differential parameter between healthy and liver-ill people.

The accuracy, precision, recall, and F score of the prediction made by machine learning using the complexity matrix were 91%, 99%, 0.91, and 94%, respectively. Although there are many studies on estimation methods, it has been observed that high success has been achieved by including the features that have a high positive or negative effect on the estimation with the glim.fit function proposed in our study. On this occasion, more efficient results can be obtained even if a single algorithm is used for estimation. If the used model is run on more data, improved accuracy will be possible.

Acknowledgements: I would like to thank Res. Assist. Fatih Okumuş for his valuable suggestions and contributions during the development of this research study.

Ethics Committee Approval: The author declared that this study does not require ethics committee approval.

Peer Review: Externally peer-reviewed.

Conflict of Interest: The author has no conflict of interest to declare.

Financial Disclosure: The author declared that this study has received no financial support.

REFERENCES

1. Magoulas GD, Prentza A. Machine learning in medical applications. In: Paliouras G, Karkaletsis V, Spyropoulos CD, editors. Machine learning and its applications: advanced lectures. Berlin, Heidelberg: Springer; 2001 (cited 2022) p.300–7. (Lecture Notes in Computer Science). https://doi.org/10.1007/3-540-44673-7_19.
2. Stausberg J, Person M. A process model of diagnostic reasoning in medicine. Int J Med Inform 1999;54(1):9-23.
3. B. Zupan, J. Halter, M. Bohanec. Qualitative model approach to computer assisted reasoning in physiology. Computer Science 1998 (cited 2022 September 2) https://www.semanticscholar.org/paper/Qualitative-Model-Approach-to-Computer-Assisted-in-Zupan-Halter/4197bc7fc5af6754e99d39c204eef80a99e324c3
4. Gindi GR, Darken CJ, O'Brien KM, Stetz ML, Deckelbaum LI. Neural network and conventional classifiers for fluorescence-guided laser angioplasty. IEEE Trans Biomed Eng 1991;38(3):246-52.
5. Srinivas S. A machine learning-based approach for predicting patient punctuality in ambulatory care centers. Int J Environ Health Res 2020;17(10):3703.
6. Anusuya V, Gomathi V. An efficient technique for disease prediction by using enhanced machine learning algorithms for categorical medical dataset. I Inf Technol Control 2021;50(1) :102-22.
7. Uddin S, Khan A, Hossain ME, Moni MA. Comparing different supervised machine learning algorithms for disease prediction. BMC Medical Inform Decis Mak 2019;19(1):281.
8. Petrie JR, Guzik TJ, Touyz RM. Diabetes, hypertension, and cardiovascular disease: clinical insights and vascular mechanisms. Can J Cardiol 2018;34(5):575-84.
9. Parkin DM, Bray F, Ferlay J, Pisani P. Global cancer statistics, 2002. CA Cancer J Clin 2005;55(2):74-108.
10. Jayaswal ANA, Levick C, Selvaraj EA, Dennis A, Booth JC, Collier J, et al. Prognostic value of multiparametric magnetic resonance imaging, transient elastography and blood-based fibrosis markers in patients with chronic liver disease. Liver Int 2020;40(12):3071-82.
11. Abebe M, Melku M, Enawgaw B, Birhan W, Deressa T, Terefe B, et al. Reference intervals of routine clinical chemistry parameters among apparently healthy young adults in Amhara National Regional State, Ethiopia. Plos one 2018;13(8):e0201782.
12. Hepatitis c prediction dataset. 2021 (cited 2022 August 1): 1(1):(1 screen). https://www.kaggle.com/datasets/fedesoriano/hepatitis-c-dataset.
13. Yee MM, Aung EE, Khaing YM. Forecasting stock market using multiple linear regression. IJTSRD 2019;3(5):2174-6.
14. Giacomino A, Abollino O, Malandrino M, Mentasti E. The role of chemometrics in single and sequential extraction assays: a review. Part II. Cluster analysis, multiple linear regression, mixture resolution, experimental design and other techniques. Anal Chim Acta 2011;688(2):122-39.
15. Khalid A, Sarwat AI. Unified univariate-neural network models for lithium-ion battery state-of-charge forecasting using minimized akaike information criterion algorithm. IEEE Access 2021;9:39154-70.
16. Hasan M, Islam MdM, Zarif MII, Hashem MMA. Attack and anomaly detection in IoT sensors in IoT sites using machine learning approaches. Internet of Things 2019;7:100059.
17. Reference ranges for blood tests. In: Wikipedia. 2022 (cited 2022 September 1). https://en.wikipedia.org/w/index.php?title=Reference_ranges_for_blood_tests&oldid=1109845763.
18. Teke M. Prediction of liver diseases with machine learning method. SMUTGD 2022;5(1):115-22.
19. Akter S, Shekhar HU, Akhteruzzaman S. Application of biochemical tests and machine learning techniques to diagnose and evaluate liver disease. Adv Biosci Biotechnol 2021;12(6):154-72.
20. Rahman AKM, Shamrat FM, Tasnim Z, Roy J, Hossain S. A comparative study on liver disease prediction using supervised machine learning algorithms. Int J Sci Technol Res 2019;8(11):419-22.
21. Schiff ER, Maddrey WC, Reddy KR. Schiff's Diseases of the Liver. 12th Edition. USA: Wiley-Blackwell; 2017. pp.135-218.
22. Sorich MJ, Miners JO, McKinnon RA, Winkler DA, Burden FR, Smith PA. Comparison of linear and nonlinear classification algorithms for the prediction of drug and chemical metabolism by human udp-glucuronosyltransferase isoforms. J Chem Inf Comput Sci 2003;43(6):2019-24.
23. Saygın E, Baykara M. Karaciğer yetmezliği teşhisinde özellik seçimi kullanarak makine öğrenmesi yöntemlerinin başarılarının ölçülmesi. FÜMBD 2021;33(2):367-77.

İSTANBUL UNIVERSITY PRESS

RESEARCH ARTICLE / ARAŞTIRMA MAKALESİ
Journal of Advanced Research in Health Sciences /
Sağlık Bilimlerinde İleri Araştırmalar Dergisi 2023
DOI: 10.26650/JARHS2023-1320786

THE EFFECT OF SCREW FIXATION AND BUTTRESS PLATE FIXATION ON CLINICAL AND RADIOLOGICAL RESULTS IN THE SURGICAL TREATMENT OF POSTERIOR MALLEOLAR FRACTURES

POSTERİOR MALLEOL KIRIKLARININ CERRAHİ TEDAVİSİNDE VİDA SABİTLEME VE DESTEK PLAKASI SABİTLEMESİNİN KLİNİK VE RADYOLOJİK SONUÇLAR ÜZERİNDEKİ ETKİSİ

İbrahim SUNGUR[1], Kadri ENCU[1], Mahmud AYDIN[1], Serkan SÜRÜCÜ[2], Sercan ÇAPKIN[3]

[1] Sultangazi Haseki Training and Research Hospital, Clinic of Orthopaedics and Traumatology, Istanbul, Turkiye
[2] Yale University, School of Medicine, Department of Orthopaedics and Rehabilitation, Connecticut, USA
[3] Aksaray University Education Research Hospital, Department of Orthopaedics and Traumatology, Aksaray, Turkiye

ORCID ID: İ.S. 0000 0001 5950 1713; K.E. 0009-0009-5992-4930; M.A. 0000-0002-2235-1480; S.S. 0000-0003-1551-4525; S.Ç. 0000-0001-6957-5927

Citation/Atıf: Sungur I, Encu K, Aydin M, Surucu S, Capkim S. The effect of screw fixation and buttress plate fixation on clinical and radiological results in the surgical treatment of posterior malleolar fractures. Journal of Advanced Research in Health Sciences 2023;6(3):234-238. https://doi.org/10.26650/JARHS2023-1320786

ABSTRACT

Objective: Posterior malleolar fractures (PMF) are common among ankle fractures and their proper management is crucial to maintaining ankle stability. The purpose of this study was to compare the clinical and radiological effects of screw versus support plate fixation in the surgical treatment of PMF.

Material and Methods: Between December 2016 and February 2018, 82 patients who underwent surgical treatment for PMF were analyzed retrospectively. Patients were divided into two groups based on the type of fixation material used: screws and buttress plates. Using the American Orthopaedic Foot and Ankle Society (AOFAS) ankle-hindfoot score, range of motion measurements, and radiographic evaluations, clinical evaluations were conducted.

Results: A total of 60 patients were included in the study, 33 of whom were treated with plate osteosynthesis and 27 with screw osteosynthesis. The demographic and clinical characteristics were similar between the groups. The AOFAS scores, range of motion measurements, and complication rates were comparable between the screw and plate fixation groups. The radiological evaluation showed no significant difference in posttraumatic arthritis levels between the two groups.

Conclusion: The screw fixation alone provides similar clinical and radiological results compared to buttress plate fixation in the surgical treatment of PMF. These results are in advance of the growing evidence supporting screw-only osteosynthesis for Haraguchi type 1 and 2 posterior malleolus fractures.

Keywords: Ankle fracture, bone screw, posterior malleolar fracture, surgical procedures

ÖZ

Amaç: Posterior malleol kırıkları (PMF) ayak bileği kırıkları arasında yaygındır ve uygun tedavileri ayak bileği stabilitesini korumak için çok önemlidir. Bu çalışmanın amacı, PMF'nin cerrahi tedavisinde vida ile destek plağı tespitinin klinik ve radyolojik etkilerini karşılaştırmaktır.

Gereç ve Yöntemler: Aralık 2016 ile Şubat 2018 tarihleri arasında PMF nedeniyle cerrahi tedavi uygulanan 82 hasta retrospektif olarak analiz edildi. Hastalar kullanılan fiksasyon materyalinin türüne göre iki gruba ayrıldı: vidalar ve destek plakları. Amerikan Ortopedik Ayak ve Ayak Bileği Derneği (AOFAS) ayak bileği-arka ayak skoru, hareket açıklığı ölçümleri ve radyografik değerlendirmeler kullanılarak klinik değerlendirmeler yapıldı.

Bulgular: Çalışmaya 33'ü plak osteosentezi ve 27'si vida osteosentezi ile tedavi edilen toplam 60 hasta dâhil edildi. Demografik ve klinik özellikler gruplar arasında benzerdi. AOFAS skorları, hareket açıklığı ölçümleri ve komplikasyon oranları vida ve plak fiksasyon grupları arasında karşılaştırılabilirdi. Radyolojik değerlendirmede iki grup arasında posttravmatik artrit düzeyleri açısından anlamlı bir fark saptanmadı.

Sonuç: PMF'nin cerrahi tedavisinde tek başına vida tespiti, butress plak tespiti ile karşılaştırıldığında benzer klinik ve radyolojik sonuçlar sağlamaktadır. Bu sonuçlar, Haraguchi tip 1 ve 2 posterior malleol kırıkları için sadece vida osteosentezini destekleyen artan kanıtların ilerisindedir.

Anahtar kelimeler: Ayak bileği kırığı, kortikal vida, posterior malleol kırığı, cerrahi prosedürler

Corresponding Author/Sorumlu Yazar: İbrahim SUNGUR **E-mail:** sungurhaseki@gmail.com

Submitted/Başvuru: 28.06.2023 • **Revision Requested/Revizyon Talebi:** 06.07.2023 • **Last Revision Received/Son Revizyon:** 28.08.2023 • **Accepted/Kabul:** 28.08.2023

INTRODUCTION

Ankle fractures frequently include PMF. The form of these fractures varies; they might range from minor posterolateral avulsion injuries to major displaced fracture fragments (1). PMF can occur in conjunction with lateral and medial malleolar fractures or in isolation following ankle rotational traumas; they account for 7 to 40% of all ankle fractures (2–5). The fracture patterns of PMF are widely variable (6,7). Haraguchi et al. Suggested a classification system based on computed tomography (CT) to accurately assess the percentage of fragmentation (8).

The posterior inferior tibiofibular ligament (PITFL) provides syndesmosis-based rotatory support to the ankle joint, and it attaches to the posterior malleolus (9). The distal tibiofibular syndesmosis is essential for joint stability and mortise congruency. If the syndesmosis is not reduced, the joint is more likely to develop long-term problems, including pain, ankle instability, and arthritis (10).

Which type of fractures should be treated surgically is a matter of debate today. It is widely accepted by many surgeons that surgical treatment is necessary for fractures involving more than one-third of the articular surface and in which fragments are displaced more than 2 mm (11,12). In addition, some biomechanical studies suggest no fixation for fragments of 25% and smaller (13). However, Langenhuijsen et al. suggested that anatomical reduction of the posterior fragment with internal fixation should be performed in fractures involving 10% or more of the tibial articular surface (14). Both percutaneous and open surgical methods can be used in the treatment of PMF (15). The body of literature reveals very few studies on the effect of different fixation methods on clinical outcomes.

The purpose of this study was to evaluate the effect of screw and plate fixation techniques on the clinical and radiological outcomes of PMF treated surgically. The hypothesis was that fixation with screws alone would be sufficient for satisfactory clinical results.

MATERIALS and METHOD

Study design

The study was conducted retrospectively in keeping with the ethical standards of the Clinical Research Ethics Committee of the SBU Haseki Training and Research Hospital. All patients included in the study gave informed consent and the study was approved by a local ethics committee (Date:26.04.2023, No:84-2023). 82 patients with PMF who had received surgical treatment between December 2016 and February 2018 were reviewed retrospectively. Institutional trauma registries were screened. Bimalleolus and trimalleolus fractures with posterior malleolus subtype fractures were included in the analysis, and all ankle fractures were radiographically confirmed. The Haraguchi classification was used to classify the PMF. Inclusion criteria were Haraguchi types 1 and 2 PMF and a minimum follow-up of 24 months. Exclusion criteria were patients younger than 18 years of age, open and pathological fractures, history of previous lower extremity fractures, additional injury, <12 (12 or 24) months follow-up, and missing data. The medical records were used to collect patient demographic, perioperative, and postoperative characteristics. Following the exclusion of 20 patients according to the exclusion criteria, the remaining patients were divided into two groups regarding the fixation material. An anti-glide plate was used for osteosynthesis in 32 patients and screws alone were used in 30 patients.

Surgical technique

A senior orthopedic surgeon who is an expert in foot and ankle surgery performed all surgeries under general or epidural anesthesia. Patients were positioned in the prone position and a tourniquet was applied to the upper thigh. We utilized a posterolateral technique. Between the Achilles tendon and the fibula, a longitudinal incision was made. Careful dissection along the lateral border of the Achilles tendon was performed to prevent damage to the sural nerve. Under direct view, the pieces were reduced by traction of the foot and dorsiflexion of the ankle, and then secured with a sharp reduction clamp. In the screw group, after the fixation of the fragments temporarily by Kirschner wires, one or two 3.5 mm lag screws were administered from the posterior to the anterior direction (Figure 1). In the plate group, a buttress plate was used to attach the posterior malleolus to the tibia's posterior surface (Figure 2).

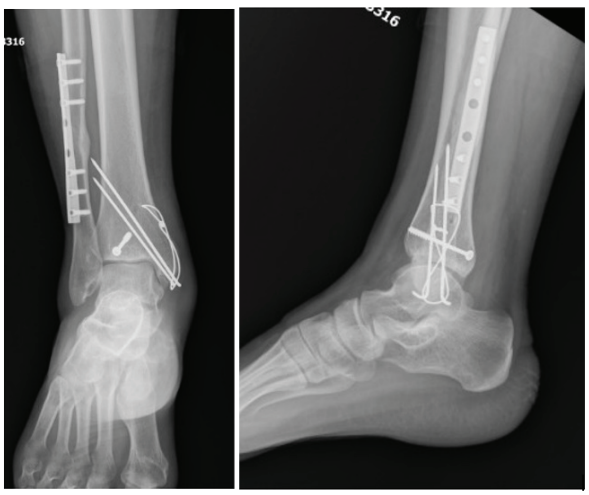

Figure 1: Radiographs AP and lateral with posterior Malleolar Screw fixation

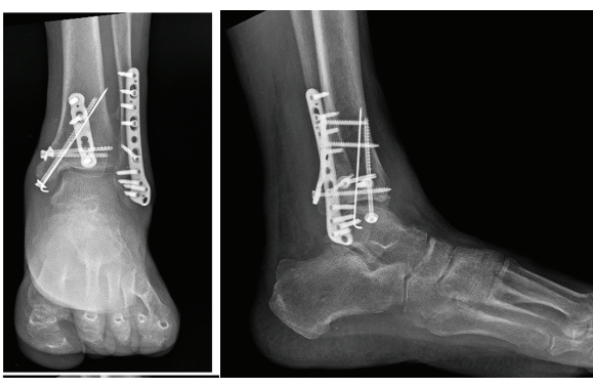

Figure 2: Radiographs AP and lateral PMF fixation with plate osteosynthesis.

Clinical evaluation

All patients were evaluated on the 3rd, 6th, and 12th months, as well as every 6 months throughout the second year. After two weeks of immobilization with a splint, both active and passive movements were initiated. By the fourth week, partial weight-bearing was encouraged, followed by full weight-bearing in the sixth week, allowing patients to be mobilized. Two independent observers assessed clinical results based on the AOFAS score. According to the AOFAS score, 90-100 points define excellent, 80-89 defines good, 70-79 defines moderate, and <70 defines poor results. At the final follow-up, we examined the ankle's range of motion and compared it to the unaffected side.

Radiological evaluation

Before surgery, AP, lateral, and mortise X-rays and 3D CT scans of the injured ankle were performed for all patients (Figure 3). Based on x-rays during the most recent follow-up, the Bargon reference criteria were utilized to determine the severity of posttraumatic arthritis (16).

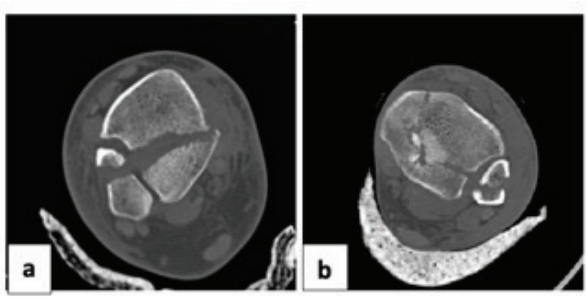

Figure 3: Preoperative axial section computed tomography images of patients. a) Radiographs type 1 Haraguchi posterior malleolus fracture, b) Radiographs type 2 Haraguchi posterior malleolus fracture

Statistical analysis

The statistical analysis was conducted using SPSS 15.0. Numbers and percentages were provided for categorical variables, while the mean, standard deviation, minimum, and maximum were provided for numerical variables. The Mann-Whitney U test was used to compare numerical data between two independent groups because the normal distribution assumption was not met. The Chi-Square Test was utilized to examine the ratio disparity and risk effect between the groups. The significance level for alpha was accepted as $p<0.05$.

RESULTS

There was a total of 60 patients who participated in this study: 27 (45%) women and 33 (55%) men. The mean age was 42.90 (range, 26-54). Thirty-three patients were treated with plate osteosynthesis and the remaining 27 patients were treated with screw osteosynthesis. Both groups consisted of similar demographic and clinical characteristics (Table 1). All patients were followed for at least 24 months (mean 36.2±4.6 months; range, 24–44 months). The rate of clinical and radiological outcomes and complications is detailed in Table 2. According to the AOFAS scoring system, the results were similar between the two groups (p=0.593). Complication rates were also similar between the two groups. (p=0.560). There was no significant difference between groups in terms of active range of motion (Table 3).

Table 1: Demographic and clinical characteristics of patients in both groups

	Plate (n= 33)	Screw (n= 27)	P value
Age (Years)[a]	41.9±7.2 (26-54)	44.1±6.0 (32-52)	0.232*
Sex			
Female (%)	17 (51.5)	10 (37.0)	0.262**
Male (%)	16 (48.5)	17 (63.0)	
Type of fracture			
Bimalleolar (%)	28 (84.8)	24 (88.9)	0.719**
Trimalleolar (%)	5 (15.2)	3 (11.1)	
Haraguchi classification			
Type 1 (%)	18 (54.5)	14 (51.9)	0.835**
Type 2 (%)	15 (45.5)	13 (48.1)	
Time from injury to surgery (days)[a]	1.2±0.5 (1-3)	1.3±0.6 (1-3)	0.291*
Follow-up (months)[a]	35.6±5.3 (24-44)	37.0±3.5 (30-42)	0.367*

Mean±standard deviation, *Independent samples t-test, **Pearson's chi-square test

Table 2: Clinical and radiological results of patients in both groups

	Plate (n= 33)	Screw (n= 27)	P value
AOFAS score	92.4±7.4 (70-100)	92.3±8.1 (70-100)	0.810*
Bargon classification			
Stage 0 (%)	5 (18.5)	7 (25.9)	0.560**
Stage 1 (%)	1 (3.7)	17 (63.0)	
Stage 2 (%)	1 (3.7)	2 (7.4)	
Stage 3 (%)	0 (0.0)	1 (3.7)	
Complication			
Infection (%)	3 (9.1)	5 (18.5)	0.593**
Nonunion (%)	2 (6.1)	1 (3.7)	
Malunion (%)	0 (0.0)	1 (3.7)	
Neurovasculardeficiency (%)	1 (3.0)	0 (0.0)	

Mean±standard deviation, AOFAS: The American Orthopaedic Foot&Ankle Society, *Independent samples t-test, **Pearson's chi-square test

Table 3: Results of joint range of motion measurements of patients in both groups

	Plate (n=33)	Screw (n=27)	P value
Fractured side dorsiflexion	14.1±1.8 (10-18) (14)	14.0±1.6 (12-18) (14)	0.988*
Non-injured side dorsiflexion	17.9±2.0 (14-22) (18)	18.4±2.0 (15-22) (18)	0.413*
Fractured side plantar flexion	36.6±1.9 (30-40) (36)	36.9±2.0 (34-42) (36)	0.932*
Non-injured side plantar flexion	41.5±2.5 (36-46) (42)	40.6±2.7 (36-45) (40)	0.178*
Fractured side inversion	17.0±1.6 (14-20) (17)	17.4±1.4 (14-20) (18)	0.327*
Non-injured side inversion	23.1±1.9 (20-26) (24)	22.2±2.7 (16-26) (22)	0.225*
Fractured side eversion	15.3±1.8 (10-18) (16)	15.5±1.9 (10-19) (16)	0.554*
	17.8±1.6 (15-22) (18)	17.6±1.2 (15-20) (18)	0.523*

Mean±standard deviation, *Independent samples t-test.

DISCUSSION

We discovered that screw fixation alone gives comparable stability to anti-glide plate fixation for PMF. This finding is significant in light of the present amount of literature on the subject. However, it should be noted that our study contributes novel information as it specifically focuses on the comparison of different fixation materials used for stabilizing posterior malleolar fractures. This aspect of our study adds to the existing knowledge and supports the growing body of evidence in favor of screw-only osteosynthesis for Haraguchi type 1 and 2 PMF.

The findings are comparable with those of earlier research evaluating various surgical procedures for treating PMF. Miller et al. compared the outcomes of unstable ankle fractures treated with open posterior malleolar fixation versus locked syndesmotic screws in the absence of a PMF. Fixation of unstable ankle fractures, such as PMF fragments with intact PITFL, was observed to be more stable than trans-syndesmotic screws (17). Similarly, this study supports the importance of direct reduction and screw fixation of the posterior malleolus in achieving stability and positive clinical outcomes.

Fu et al., in their review article, highlighted the lack of consensus regarding the size of the PMF that would lead to ankle instability and affect prognosis. They recommended the use of CT scans for accurate assessment of fragment morphology and supported direct posterior malleolus fixation to stabilize syndesmotic injuries (18). While their conclusions lean towards buttress plate osteosynthesis, our findings demonstrate that direct reduction and screw-only fixation of the posterior malleolar fragment yield comparable stability and clinical outcomes, as evidenced by similar AOFAS scores and radiological evaluation.

Regarding the impact on the existing knowledge, our findings are in line with previous studies that have also reported positive outcomes with screw fixation (18). This consistency across studies reinforces the effectiveness of screw-only fixation and supports its consideration as a preferred treatment option for Haraguchi type 1 and 2 PMF.

It is important to note that while our findings align with the current body of literature, there may still be varying opinions and approaches in the field. Some studies have advocated for buttress plate osteosynthesis (18). However, our results demonstrate that direct reduction and screw-only fixation yield comparable stability and clinical outcomes without the need for additional soft tissue dissection and more complex surgery. This contributes to the ongoing discussion and adds valuable insights to the decision-making process when it comes to posterior malleolar stabilization.

One of the strengths of our study is that it contributes to the limited body of literature comparing different fixation materials used for the stabilization of PMF. However, our study has some limitations as well. First, as a retrospective analysis, inherent selection bias and confounding variables may have influenced the results. Furthermore, it should be noted that factors that could potentially impact patients' clinical outcomes, notably osteoporosis, diabetes, and smoking habits, have not been extensively addressed within our study. The effects of osteoporosis on bone health and healing, the potential influences of diabetes on fracture recovery, and the adverse impact of smoking on bone health are well-documented in the scientific literature. The lack of comprehensive exploration of these factors in our fundamental study could limit the generalizability and interpretation of our findings.

CONCLUSION

Screw fixation alone offers the advantages of smaller incisions and less soft tissue dissection while providing stability similar to plate fixation in PMF. These results add to the growing

literature on the management of PMF and provide valuable information for clinical decision-making.

Ethics Committee Approval: This study was approved by Clinical Research Ethics Committee of Haseki Training and Research Hospital (Date:26.04.2023, No:84-2023).

Peer Review: Externally peer-reviewed.

Author Contributions: Conception/Design of Study- İ.S., M.A.; Data Acquisition- K.E., S.S., S.Ç.; Data Analysis/Interpretation- M.A., K.E.; Drafting Manuscript- İ.S., M.A., K.E.; Critical Revision of Manuscript- M.A., S.S., S.Ç.; Final Approval and Accountability- İ.S., M.A., K.E., S.S., S.Ç.

Conflict of Interest: The authors have no conflict of interest to declare.

Financial Disclosure: The authors declared that this study has received no financial support.

REFERENCES

1. Irvin TA, Lien J, Kadakia AR. Posterior malleolus fracture. J Am Acad Orthop Surg 2013;21(1):32-40.
2. Hong CC, Nashi N, Roy SP, Tan KJ. Impact of trimalleolar ankle fractures: How do patients fare post-operatively? Foot Ankle Surg 2014;20(1):48-51.
3. Lui TH, Ip K, Chow HT. Comparison of radiologic and arthroscopic diagnoses of distal tibiofibular syndesmosis disruption in acute ankle fracture. Arthroscopy 2005;21(11):1370-74.
4. Jaskulka RA, Ittner G, Schedl R. Fractures of the posterior tibial margin: their role in the prognosis of malleolar fractures. J Trauma 1989;29(11):1565-70.
5. Koval KJ, Lurie J, Zhou W, Sparks MB, Cantu RV, Sporer SM, Weinstein J. Ankle fractures in the elderly: what you get depends on where you live and who you see. J Orthop Trauma 2005;19(9):635-9.
6. Bartoníček J, Rammelt S, Kostlivý K, Vaněček V, Klika D, Trešl I. Anatomy and classification of the posterior tibial fragment in ankle fractures. Arch Orthop Trauma Surg 2015;135(4):505-16.
7. Alexandropoulos C, Tsourvakas S, Papachristos J, Tselios A, Soukouli P. Ankle fracture classification: An evaluation of three classification systems: Lauge-Hansen, AO, Broos-Bisschop. Acta Orthop Belg 2010;76(4):521-5.
8. Haraguchi N, Haruyama H, Toga H, Kato F. Pathoanatomy of posterior malleolar fractures of the ankle. J Bone Joint Surg Am 2006;88(5):1085-92.
9. Behery OA, Narayanan R, Konda SR, Tejwani NC, Kenneth AE. Posterior malleolar fixation reduces the incidence of trans-syndesmotic fixation in rotational ankle fracture repair. Iowa Orthop J 2021;41(1):121-5.
10. Pogliocomi F, De Filippo M, Casalini D, Longhi A, Tacci F, Perotta R, et al. Acute syndesmotic injuries in ankle fractures: from diagnosis to treatment and current concepts. World J Orthop 2021;12(5):270-91.
11. Odak S, Ahluwalia R, Unnikrishnan P, Hennessy M, Platt S. Management of Posterior Malleolar Fractures: a systematic review. J Foot Ankle Surg. 2016;55(1):140-5.
12. Barbosa P, Bonnaire F, Kojima K. AO foundation. http://www2.aofoundation.org. 2013.
13. Hartford JM, Gorczyca JT, McNamara JL, Mayor MB. Tibiotalar contact area. Contribution of posterior malleolus and deltoid ligament. Clin Orthop Relat Res 1995;(320):182-7.
14. Langenhuijsen JF, Heetveld MJ, Ultee JM, Steller EP, Butzelaar RM. Results of ankle fractures with involvement of the posterior tibial margin. J Trauma 2002;53(1):55-60.
15. Broos PL, Bisschop AP. Operative treatment of ankle fractures in adults: correlation between types of fracture and final results. Injury 1991;22(5):403-6.
16. Bargon G. Röntgenmorphologische Gradeinteilung der posttraumatischen Arthrose im oberen Sprunggelenk. HefteUnfallheilkd 1978;133:28-34.
17. Miller AN, Carroll EA, Parker RJ. Posterior malleolar stabilization of syndesmoticinjuries is equivalent to screw fixation. Clin Orthop Relat Res 2010;468(4):1129-35.
18. Fu S, Zou ZY, Mei G. Advances and disputes of posterior malleolus fracture. Chin Med J (Engl) 2013;126(20):3972-77.

İSTANBUL UNIVERSITY PRESS

RESEARCH ARTICLE / ARAŞTIRMA MAKALESİ
Journal of Advanced Research in Health Sciences / Sağlık Bilimlerinde İleri Araştırmalar Dergisi 2023
DOI: 10.26650/JARHS2023-1294442

EXPRESSION OF ANGIOPOETIN ON THE KIDNEY TRANSPLANT WAITING LIST: A SINGLE-CENTER STUDY

BÖBREK NAKLİ BEKLEME LİSTESİNDEKİ HASTALARDA ANJİYOPOETİN'İN İFADESİ: TEK MERKEZLİ BİR ÇALIŞMA

Süleyman Rüştü OĞUZ[1, 2], Ayşe SİNANGİL[3], Demet KIVANÇ İZGİ[4,5], Soykan BARLAS[6,7], Hayriye ŞENTÜRK ÇİFTÇİ[4], Kıymet Güzin ŞEN[2], Tevfik ECDER[3], Barış AKIN[6]

[1] Demiroglu Bilim University, Faculty of Medicine, Group Florence Nightingale Hospital, Department of Medical Biology and Genetics, Istanbul, Turkiye
[2] Demiroglu Bilim University, Faculty of Medicine, Group Florence Nightingale Hospital, Tissue Typing Laboratory, Istanbul, Turkiye
[3] Demiroglu Bilim University, Faculty of Medicine, Group Florence Nightingale Hospital, Department of Nephrology, Istanbul, Turkiye
[4] Istanbul University, Istanbul Faculty of Medicine, Department of Medical Biology, Istanbul, Turkiye
[5] İstanbul University, Institute of Graduate Studies in Health Sciences Department of Medical Biology, Istanbul, Turkiye
[6] Demiroglu Bilim University, Faculty of Medicine, Group Florence Nightingale Hospital, Department of General Surgery, Istanbul, Turkiye
[7] Goztepe Medicalpark Hospital, Department of General Surgery, Istanbul, Turkiye

ORCID ID: S.R.O. 0000-0002-5854-1163; A.S. 0000-0003-4001-6376; D.K.İ. 0000-0002-2451-5709; S.B. 0000-0003-0422-4960; H.Ş.Ç. 0000-0001-5160-5227; K.G.Ş. 0009-0005-6665-8803; T.E. 0000-0003-3394-5775; B.A. 0000-0002-7410-3614

Citation/Atıf: Oguz SR, Sinangil A, Kivanc Izgi D, Barlas S, Senturk Ciftci H, Sen KG, et al. Expression of angiopoetin on the kidney transplant waiting list: a single-center study. Journal of Advanced Research in Health Sciences 2023;6(3):239-243. https://doi.org/10.26650/JARHS2023-1294442

ABSTRACT

Objective: Angiopoietin-2 (Ang-2) is a growth factor belonging to the angiopoietin (Ang)/Tie signaling pathway. Plasma levels of especially Ang-2, are thought to be significantly increased in patients with acute kidney injury (AKI), independent of inflammation. Ang-2 is also important in dialysis and transplantation, as it plays an important role in the disruption of endothelial homeostasis. Our study aimed to investigate the relationship between anti-HLA antibody loads and Ang levels in patients with end-stage renal disease (ESRD) who are on the organ transplant waiting list.

Material and Method: 80 ESRD patients who were on the waiting list between 2018 and 2020 and whose panel reactive antibody (PRA) screening and identification test were studied participated in our study. First, the PRA screening test was performed on the patients, and the class I-II identification tests were studied on the patients who were positive for PRA. The Ang-2 level was evaluated by the ELISA method. The relationship between Ang-2 levels and PRA percentages in PRA positive and negative patients was evaluated.

Results: A positive correlation was found between anti-HLA antibody and Ang-2 levels in patients with ESRD (class I, p=0.024; class II, p=0.032), and a statistically significant increase in Ang-2 level was found in patients with PRA ≥50% positive (class I, p=0.038) This finding suggests that Ang-2 may have an important role in the progression of chronic renal failure and may be effective in predicting graft survival after transplantation.

Conclusions: Further studies will be required to fully elucidate the effect of Ang-2 on renal progression.

Keyword: Angiopoetin-2, anti-HLA antibody, kidney transplantation

ÖZ

Amaç: Anjiyopoietin-2 (Ang-2), anjiyopoietin (Ang)/Tie sinyal yolağına ait bir büyüme faktörüdür. Akut böbrek hasarı (AKH) olan hastalarda inflamasyondan bağımsız olarak özellikle Ang-2'nin plazma düzeylerinin önemli ölçüde arttığı düşünülmektedir. Ang-2, endotel homeostazının bozulmasında önemli bir rol oynadığı için diyaliz ve transplantasyonda da önemlidir. Çalışmamızda organ nakli bekleme listesinde olan son dönem böbrek hastalığı (SDBY) hastalarında anti-HLA antikor yükleri ile Ang düzeyleri arasındaki ilişkinin araştırılması amaçlandı.

Gereç ve Yöntem: Çalışmamıza 2018-2020 yılları arasında panel reaktif antikor (PRA) tarama ve tanımlama testi çalışılmış bekleme listesinde bulunan 80 SDBY (son dönem böbrek yetmezliği) hastası katıldı. Hastalara önce PRA tarama testi, PRA pozitif çıkan hastalara sınıf I-II tanımlama testleri çalışıldı. Ang-2 düzeyi ELISA yöntemi ile değerlendirildi. PRA pozitif ve negatif hastalarda Ang-2 düzeyleri ile PRA yüzdeleri arasındaki ilişki değerlendirildi.

Bulgular: SDBY olan hastalarda anti-HLA antikoru ile Ang-2 düzeyleri arasında pozitif korelasyon (sınıf I, p=0,024; sınıf II, p=0,032) ve PRA ≥%50 pozitif olan hastalarda Ang-2 düzeyinde istatistiksel olarak anlamlı bir artış bulundu (sınıf I, p=0,038). Bu bulgu, Ang-2'nin kronik böbrek yetmezliğinin ilerlemesinde önemli bir rolü olabileceğini ve nakil sonrası greft sağkalımını tahmin etmede etkili olabileceğini düşündürmektedir.

Sonuç: Ang-2'nin renal progresyon üzerindeki etkisini tam olarak aydınlatmak için daha ileri çalışmalara ihtiyaç duyulmaktadır.

Anahtar kelimeler: Anjiyopoetin-2, anti-HLA antikoru, böbrek nakli

Corresponding Author/Sorumlu Yazar: Süleyman Rüştü OĞUZ **E-mail:** rustu.oguz@florence.com.tr

Submitted/Başvuru: 09.05.2023 • **Revision Requested/Revizyon Talebi:** 18.05.2023 • **Last Revision Received/Son Revizyon:** 01.06.2023 • **Accepted/Kabul:** 05.06.2023 • **Published Online/Online Yayın:** 10.10.2023

INTRODUCTION

Angiopoietins (Angs) are an important vascular growth factor family which is composed of the members Ang-1, Ang-2, Ang-3, and Ang-4 and is involved in multiple cellular functions related to cell survival, cell growth, and cell migration. The best-characterized members of this family are Ang-1 and Ang-2, and their activities are mediated by tyrosine kinase receptors (Tie-1 and Tie-2). Ang-1 is a strong angiogenesis growth factor, which transmits signals by way of Tie-2, while Ang-2 is a growth factor belonging to the angiopoietin (Ang)/Tie signaling pathway, which is one of the main pathways involved in angiogenesis. It has been reported that Ang-2 binds to the Tie-2 receptor with a similar binding affinity and induces its inhibitory role, while it does not bind to Tie-1 (1-3).

The Ang/Tie-2 signaling axis is an important modulator of vascular integrity, and Tie-2 receptors are extensively expressed in endothelial cells (4). Activation of Tie-2 signaling strengthens interendothelial junctions and reduces the expression of leukocyte adhesion molecules (5). Studies have reported that Ang-2 can antagonize the stability action of Ang-1 by competitively binding to Tie-2 in pathological conditions, and thus, it can lead to vascular instability, reduce cell-to-cell adhesion, and activate beta-1 integrin to encourage endothelial inflammation by disrupting the protective Ang-1/Tie-2 signaling pathway (6,7). The Ang-2 expression may be triggered by inflammatory mediators (8,9). Studies which used targeted manipulations of Ang/Tie-2 signaling by way of tools such as genetic approaches, antibodies, and RNA intervention showed that end-organ injury and hemodynamic changes occurring in experimental sepsis and hepatic disease were associated with an excessive increase in Ang-2 (10).

Angs, belonging to the vascular growth factor family, is widely expressed in the kidneys and is thought to maintain the structure of the glomerular filtration barrier. Studies in the literature have reported that Ang-Tie signaling is important for the efficient functioning of the renal microvascular system. In a study conducted with patients, who had lupus nephritis, it was reported that Ang-2 protein expression was prominent in glomerular endothelium, and serum Ang-2 levels were closely associated with the severity of systemic lupus erythematosus (SLE) (11). In addition, the same researchers showed that serum Ang-2 levels were significantly higher in patients with ANCA-related vasculitis and renal involvement compared to healthy individuals (11). The results of these studies suggest that inflammatory damage to the kidneys may result in the release of Ang-2 from the renal endothelium. Acute kidney injury (AKI) is closely associated with sepsis (12). Ang-2 level increases in response to sepsis, and as a result, the endothelial barrier structure is disrupted, and microvascular permeability increases (13). Studies have reported that plasma levels of especially Ang-2, among endothelial biomarkers, significantly increase independent of inflammation in critical patients with AKI, and Ang-2 is associated with the development of late-onset AKI (14).

Ang-2 is also important in dialysis and transplantation, as it is effective in disrupting endothelial homeostasis. Studies show that circulating Ang-2 levels increase in patients receiving dialysis treatment, and these results suggest that Ang-2 can be used as a marker to detect cardiovascular disorders that occur during dialysis, especially in childhood (15,16).

During organ transplantation, ischemia-reperfusion (I/R) injury may occur to a great extent. It is thought that endothelial irregularity is an important pathogenic outcome of I/R injury, and this complication plays an important role in patient/graft survival (17).

In a study using the renal I/R model, it was reported that the imbalance in the Ang-1/Ang-2 ratio caused an increase in pericyte proliferation, endothelial cell loss, and fibrosis (18). In studies conducted with patients with I/R injuries and undergoing dialysis, it has been reported that the increase in Ang-2 promotes plasma and leukocyte leakage by causing a loss in the endothelial glycocalyx (eGC) (19).

Fibrosis is a complication that may result in disease progression and graft loss after kidney transplantation. It occurs especially in the first three months after transplantation is triggered by inflammation following reperfusion injury and continues with a sustained inflammatory immune response that supports the progression of kidney disease (20). The presence of anti-human leukocyte antigen (HLA) antibodies in the recipient increases the risk of antibody-mediated rejection (AMR) after kidney transplantation (21). Subclinical AMR, which may occur with the presence of donor-specific antibodies, is a strong profibrotic stimulus and may provide a prediction of graft loss (20). Therapeutic strategies used to minimize the risk of progression of fibrosis in renal grafts have reduced the incidence of clinical rejection developing in the first few years following transplantation, and early fibrosis markers have become important markers for renal function and graft survival.

In our study, we aimed to investigate the relationship between anti-HLA antibody loads and Ang levels in patients included on organ transplant waiting lists because of end-stage renal disease (ESRD).

MATERIAL and METHOD

Eighty patients with ESRD, who were included on the renal transplant waiting list between 2018 and 2020 and underwent panel reactive antibody (PRA) screening and identification test, were included in our study. PRA screening test was primarily performed in all patients using life codes kits (immucor Medizinische Diagnostik GmbH Robert-Bosch-Strasse, Dreicich Germany). In 40 patients whose screening tests were found to be positive, class I and class II identification tests were performed again using lifecodes kits (immucor Medizinische Diagnostik GmbH Robert-Bosch-Strasse, Dreicich Germany) with the Luminex method in accordance with the manufacturer's instructions. In PRA screening and identification tests, a mean fluorescence intensity (MFI) value of >1000 was considered positive.

Table 1: Ang-2 levels in PRA positive and negative patients

		PRA positive	PRA negative		p
Ang-2		888.54±287.58	866.57±239.93		0.548
			PRA positive patients		
	Group	**Class I positive**	**p**	**Class II positive**	**p**
Ang-2	**1. group ≤30**	785.29±289.63	1 vs 2 p=0.898 1 vs 3 p=0.089 2 vs 3 **p=0.046***	754.39±300.51	1 vs 2 p=0.994 1 vs 3 p=0.483 2 vs 3 p=0.976
	2. group 31-60	711.87±242.68		840.46±257.75	
	3. group 61-100	969.20±341.76		932.82±291.31	
	Group	**Class I positive**	**p**	**Class II positive**	**p**
Ang-2	**≤50**	750.25±346.45	**0.038***	804.68±251.44	0.197
	≥50	944.50±258.33		923.07±302.53	

Ang-2: Angiopoetin-2, PRA: Panel reactive antibody

In addition, the Ang-2 level was studied and evaluated using the ELISA (Enzyme-Linked ImmunoSorbent Assay) method (Invitrogen-ThermoFisher Scientific-catalogue number: KHC1641) in accordance with the manufacturer's instructions (Range; 2.236-621 pg/mL) in the sera in which PRA identification tests were studied. The PRA-positive patients included in our study were primarily divided into 3 groups (Group 1=≤30%; Group 2=31%-60%; Group 3= 61%-100%) and later divided into two groups (Group 1=0%-50%; Group 2=50%-100%) according to PRA positivity percentage values. The relationships between Ang-2 levels and PRA percentages in each group were evaluated as well.

This study was approved by Demiroglu Bilim University Clinical Research Ethics Committee (Date: 02.08.2022, No: 2022-15-02).

RESULTS

Among the 80 patients with ESRD who were included in the study, 57.5% (n:46) were female, and 42.5% (n:34) were male. The mean age was 49.54±19.43 years in the whole patient group, 39.50±21.09 years in the female patients, and 35.80±33.20 years in the male patients.

The PRA screening and identification tests were found to be positive in 50% of the patients (n:40) (MFI>1000) and negative in the other 50% (n:40) (MFI<1000). Class I PRA was found to be positive in all 40 patients (100%) who had a positive PRA result. Class II PRA was found to be positive in 39 (97.5%) patients and negative in 1 patient (2.5%). There was no statistically significant difference in Ang-2 levels between PRA-positive patients and PRA-negative patients (p=0.548). The PRA-positive patients included in our study were divided into 3 groups according to PRA positivity percentage values (Group 1=≤30%; Group 2=31%-60%; Group 3=61%-100%), and the relationship between Ang-2 levels and PRA percentages was evaluated in each group. Oneway Anova post hoc test (Bonferroni) was used for the evaluation of Class I and Class II PRA positivity percentages, and when the relationship between PRA positivity percentages and Ang-2 levels was examined, it was found to be significant with class I, but no significant relation was found with class II (respectively class I; p=0.049, class II; p=0.335) (Table 1). Considering the Ang-2 levels between the 3 groups in Class I PRA, a significant difference was found between the 2nd group and the 3rd group (p=0.046).

When the PRA-positive patients were divided into two groups according to positivity percentage (Group 1=0%-50%; 2. Group 2=50%-100%) and the relationships between PRA positivity percentages and Ang-2 levels were compared using the Independent Sample t-test, it was found that Ang-2 levels were significantly higher in the patients whose class I PRA percentages were higher than 50% (p=0.038). A difference reaching statistical significance could not be found between the two groups for the relationship between class II PRA percentages and Ang-2 levels (p=0.197) (Table 1).

When the correlation between Ang-2 levels and class I and class II PRA positivity percentages was evaluated in the PRA positive group, a significant positive correlation (Pearson correlation) was found between Ang-2 and class I positivity (r=0.362, p=0.024) and class II positivity (p=0.348, p=0.032) (Table 2).

Table 2: Correlation between Ang-2 levels and Class I and Class II PRA positivity percentages

PRA positive patients	Ang-2	Class I	Class II
Pearson Correlation (r)	1	0.362	0.348
p		0.024	0.032
N		40	39

Ang-2: Angiopoetin-2, PRA: Panel reactive antibody

DISCUSSION

Angs are vascular growth factors whose functions are mediated by Tie tyrosine kinase receptors. Competitive binding of Ang-2 to the Tie-2 receptor disrupts the vasculature and basal lamina (22). Although it is known that Ang-2 is mostly synthesized by endothelial cells, which have important effects on vascular development, it can also be synthesized and released by other cell types. The release of Ang-2 leads to inflammation. Therefore, it has been associated with many pathological conditions (23).

It is thought that Ang-2 levels are associated with systemic inflammation markers/mediators in patients with chronic renal failure (CRF). In addition, it has been reported in various studies that Ang-2 levels increase in dialysis patients due to the progression of chronic kidney disease (CKD) (17,18). In studies with preclinical glomerulonephritis models, it has been reported that glomerular Ang-2 is up-regulated, and this causes proteinuria (24). It is known that the CVD incidence is higher in patients with ESRD who receive hemodialysis. In studies conducted with ESRD patients undergoing hemodialysis, it has been reported that endothelial dysfunction is associated with an increased incidence of CVD (17,18). One study reported a strong and consistent association between serum Ang-2 levels and mortality, even when most risk factors were excluded (25).

Anti-HLA donor-specific antibodies are the most important factor leading to AMR. The PRA test generally predicts the percentage of potential donors who possess a recipient's HLA antibodies and approximately displays the risk of positive crossmatching. When compared with solid phase tests, it is more sensitive for antibodies with lower titers and allows more precise specification of specific HLA antigens and alleles (26). In association with negative kidney graft results, a few non-HLA antibodies have been identified (endothelial antibodies, epithelial antibodies, or antibodies to various proteins). Most data related to non-HLA antibodies in liver transplantation originate from observational studies in which antibodies to antigens were identified (Table 1) (27). It is thought that the ability of non-HLA antibodies to mediate allograft injury may be associated with their affinity and strength (titer), target specificity, the intensity of target antigen, and synergy with donor-specific HLA antibodies.

The initial studies regarding Ang showed that Ang-1 stabilized newly formed vessels and reduced vascular permeability when the Tie-2 receptor of Ang-2 blocked Ang-1 activation. On the other hand, current studies included in the literature have reported that Ang-2 can directly induce Tie-2, and both Ang-1 and Ang-2 may be pro-inflammatory. Ang/Tie-2 biology is modified by vascular endothelial growth factor and Tie-1, which is a receptor associated with vascular endothelial growth factor. In healthy individuals, Tie-1 and Tie-2 are expressed in glomerular endothelium, while Ang-1 is expressed in podocytes. In vitro studies have shown that exogenous Ang-l increases the formation of capillary vessels in developing glomerules (25). In some studies on diabetic glomerulopathy and immune-mediated glomerulonephritis, it has been reported that glomerular Ang-2 expression is increased in these diseases (24, 28). In light of these data, it was presumed that Ang-2 might have important roles in the pathobiology of glomerular disease.

The literature does still not involve sufficient experimental data to definitely associate Angs with in-vivo glomerular functions. Thus, it will be useful to examine the effects of the downregulation of Ang-1 levels in healthy animals and the effects of the downregulation of Ang-2 in glomerular disease in future studies.

Although Ang-2 is known to be highly effective in endothelial dysfunction, it is unclear whether it is associated with the progression of renal dysfunction in patients with CKD. In our study, there was a positive correlation between the anti-HLA antibody loads of the patients on the kidney transplant waiting list with the diagnosis of end-stage renal disease and the serum Ang-2 levels of the same patients, and a statistically significant Ang-2 level in patients with a PRA positivity rate of 50% or higher significant increase was found. This finding suggests that Ang-2 may have an important role in the progression of CKD and may be effective in predicting graft survival after transplantation. Further studies will be required to evaluate the pathogenic role of Ang-2 in renal progression and to establish beneficial kidney function by targeting Ang-2.

Ethics Committee Approval: This study was approved by Demiroglu Bilim University Clinical Research Ethics Committee (Date: 02.08.2022, No: 2022-15-02).

Peer Review: Externally peer-reviewed.

Author Contributions: Conception/Design of Study- S.R.O., H.Ş.Ç., T.E., B.A.; Data Acquisition- S.R.O., K.G.Ş.; Data Analysis/Interpretation- A.S., S.B., S.R.O., H.Ş.Ç., D.K.İ.; Drafting Manuscript- S.R.O., H.Ş.Ç., D.K.İ.; Critical Revision of Manuscript- S.R.O., S.B., A.S., T.E., B.A.; Final Approval and Accountability- S.R.O., A.S., S.B., T.E., B.A., H.Ş.Ç., D.K.İ., K.G.Ş.; Material and Technical Support- D.K.İ., K.G.Ş.; Supervision- S.R.O., A.S., S.B., T.E., B.A.

Conflict of Interest: The authors have no conflict of interest to declare.

Financial Disclosure: The authors declared that this study has received no financial support.

REFERENCES

1. Kim KL, Shin IS, Kim JM, Choi JH, Byun J, Jeon ES, et al. Interaction between Tie receptors modulates angiogenic activity of angiopoietin2 in endothelial progenitor cells. Cardiovasc Res 2006;72(3):394-402.
2. Xu J, Lan D, Li T, Yang G, Liu L. Angiopoietins regulate vascular reactivity after haemorrhagic shock in rats through the Tie2-nitric oxide pathway. Cardiovasc Res 2012;96(2):308-19.
3. Maisonpierre PC, Suri C, Jones PF, Bartunkova S, Wiegand SJ, Radziejewski C, et al. Angiopoietin-2, a natural antagonist for Tie2 that disrupts in vivo angiogenesis. Science 1997; 277(5322):55-60.

4. Yuan HT, Khankin EV, Karumanchi SA, Parikh SM. Angiopoietin 2 is a partial agonist/antagonist of Tie2 signaling in the endothelium. Mol Cell Biol 2009;29(8):2011-22.
5. Korhonen EA, Lampinen, A, Giri H, Anisimov A, Kim M, Allen B, et al. Tie1 controls angiopoietin function in vascular remodeling and inflammation. J Clin Investig 2016;126(9):3495-510.
6. He FF, Zhang Di, Chen Q, Zhao Y, Wu L, Li ZQ, et el. Angiopoietin-Tie signaling in kidney disease: an updated review FEBS Lett 2019;593(19):2706-15.
7. Biel NM, Siemann DW. Targeting the Angiopoietin-2/Tie-2 axis in conjunction with VEGF signal interference. Cancer Lett 2016;380(2):525-33.
8. Rathnakumar K, Savant S, Giri H, Ghost A, Fisslthaler B, Fleming I. et al. Angiopoietin-2 mediates thrombin-induced monocyte adhesion and endothelial permeability J Thromb Haemost 2016;14(8):1655-67.
9. Fagiani E, Christofori G. Angiopoietins in angiogenesis. Cancer Lett 2013;328(1):18-26.
10. Yuan HT, Suri C, Yancopoulos GD, Woolf AS. Expression of angiopoietin-1, angiopoietin-2, and the Tie-2 receptor tyrosine kinase during mouse kidney maturation. J Am Soc Nephrol 1999;10(8):1722-36.
11. Kolatsi-Joannou M, Li XZ, Suda T, Yuan HT, Woolf AS. Expression and potential role of angiopoietins and Tie-2 in early development of the mouse metanephros. Develop Dynam 2001;222(1):120-26.
12. Woolf AS, Yuan HT. Angiopoietin growth factors and Tie receptor tyrosine kinases in renal vascular development. Pediat Nephrol 2001;16(2):177-84.
13. Kümpers P, David S, Haubitz M, Hellpap J, Horn R, Bröcker V, et al. The Tie2 receptor antagonist angiopoietin 2 facilitates vascular inflammation in systemic lupus erythematosus. Ann Rheum Dis 2009;68(10):1638-43.
14. Peters E, Antonelli M, Wittebole X, Nanchal R, François B, Sakr Y, et al. Worldwide multicentre evaluation of the influence of deterioration or improvement of acute kidney injury on clinical outcome in critically ill patients with and without sepsis at ICU admission: results from. The Intensive Care Over Nations audit. Crit Care 2018;22(1):188.
15. Leligdowicz A, Richard-Greenblatt M, Wright J, Crowley VM, Kain KC. Endothelial activation: the ang/tie axis in sepsis. Front Immunol 2018;9:838.
16. Yu WK, McNeil JB, Wickersham NE, Shaver CM, Bastarache JA, Ware LB. Angiopoietin-2 outperforms other endothelial biomarkers associated with severe acute kidney injury in patients with severe sepsis and respiratory failure. Crit Care 2021;25(1):48.
17. Shroff RC, Price KL, Kolatsi-Joannou M, Todd AF, Wells D, Deanfield J, et al. Circulating angiopoietin-2 is a marker for early cardiovascular disease in children on chronic dialysis. PLoS ONE 2013;8(2):e56273. doi:10.1371/journal.pone.0056273.
18. David S, Kumpers P, Hellpap J, Horn R, Leitolf H, Haller H, et al. Angiopoietin 2 and cardiovascular disease in dialysis and kidney transplantation. Am J Kidney Dis 2009;53(5):770-8.
19. de Vries DK, Khairoun M, Lindeman JH, Bajema IM, de Heer E, Roest M, et al. Renal ischemia-reperfusion induces release of angiopoietin-2 from human grafts of living and deceased donors. Transplant 2013;96(3):282-9
20. Khairoun M, van der Pol P, de Vries DK, Lievers E, Schlagwein N, de Boer HC, et al. Renal ischemia-reperfusion induces a dysbalance of angiopoietins, accompanied by proliferation of pericytes and fibrosis. Am J Physiol Renal Physiol 2013;305(6):901-10.
21. Vlahu CA, Lemkes BA, Struijk DG, Koopman MG, Krediet RT, Vink H. Damage of the endothelial glycocalyx in dialysis patients. J Am Soc Nephrol 2012;23(11):1900-8.
22. Parikh SM. The angiopoietin-Tie2 signaling axis in systemic inflammation. J Am Soc Nephrol 2017;28(7):1973-82.
23. He FF, Zhang D, Chen Q, Zhao Y, Wu L, Li, ZQ, et al. Angiopoietin-Tie signaling in kidney diseases: an updated review. FEBS Lett 2019;593(19):2706-15.
22. Lim HS, Lip GY, Blann AD. Angiopoietin-1 and angiopoietin-2 in diabetes mellitus: relationship to VEGF, glycaemic control, endothelial damage/dysfunction and atherosclerosis. Atherosclerosis 2005;180(1):113-8.
23. Tsai YC, Lee CS, Chiu YW, Kuo HT, Lee SC, Hwanget SJ, et al. Angiopoietin-2, angiopoietin-1 and subclinical cardiovascular disease in chronic kidney disease. Sci Rep 2016;6:39400.
24. Yuan HT, Tipping PG, Li XZ, Long DA, Woolfet AS. Angiopoietin correlates with glomerular capillary loss in anti-glomerular basement membrane glomerulonephritis. Kidney Int 2002;61(6):2078-89
25. Hillege HL, Fidler V, Diercks GF, van Gilst WK, de Zeeuw D, van Veldhuisen DJ, et al. Urinary albumin excretion predicts cardiovascular and noncardiovascular mortality in general population. Circulation 2002;106(14):1777-82.
26. Zhang Q, Reed QZEF. The importance of non-HLA antibodies in transplantation. Nat Rev Nephrol 2016;12(8):484-95.
27. Kamburova EG, Kardol-Hoefnagel T, Wisse BW, Joosten I, Allebes WA, Van Der Meer A, et al. Development and Validation of a Multiplex Non-HLA Antibody Assay for the Screening of Kidney Transplant Recipients. Front Immunol 2018;9:3002.
28. Davis B, Dei Cas A, Long DA, White KE, Hayward A, Kuet CH, et al. Podocyte-specific expression of angiopoietin-2 causes proteinuria and apoptosis of glomerular endothelia. J Am Soc Nephrol 2007;18(8):2320-9.

İSTANBUL UNIVERSITY PRESS

RESEARCH ARTICLE / ARAŞTIRMA MAKALESİ
Journal of Advanced Research in Health Sciences /
Sağlık Bilimlerinde İleri Araştırmalar Dergisi 2023
DOI: 10.26650/JARHS2023-1266518

INVESTIGATION OF THE FAT MASS AND OBESITY-ASSOCIATED (*FTO*) GENE IN PRESCHOOL CHILDREN

YAĞ KİTLESİ VE OBEZİTE İLİŞKİLİ (*FTO*) GENİN OKUL ÖNCESİ ÇOCUKLARDA ARAŞTIRILMASI

Şeref Buğra TUNÇER[1], Duygu GÜRLEYİK[2], H. Melis YAVUZ[3,4], İbrahim ACAR[5]

[1] Istanbul University, Oncology Institute, Department of Cancer Genetics, Istanbul, Turkiye
[2] Ozyegin University, Faculty of Social Sciences, Department of Psychology, Sports and Exercise Psychology, Istanbul, Turkiye
[3] Algoma University, Faculty of Humanities and Social Sciences, Department of Psychology, Toronto, Canada
[4] University Of Toronto Mississauga, Department of Psychology, Toronto, Canada
[5] Ozyegin University, Faculty of Social Sciences, Department of Psychology, Child, Youth and Family Studies, Istanbul, Turkiye

ORCID ID: Ş.B.T. 0000-0001-8023-3223 2; D.G. 0000-0003-1405-8513; H.M.Y. 0000-0002-2780-1962; İ.A. 0000-0003-4007-5691

Citation/Atıf: Tuncer SB, Gurleyik D, Yavuz HM, Acar I. Investigation of the fat mass and obesity associated (FTO) gene in preschool children. Journal of Advanced Research in Health Sciences 2023;6(3):244-249. https://doi.org/10.26650/JARHS2023-1266518

ABSTRACT

Objective: Obesity is a complex disease defined as being overweight. Previous studies have highlighted familial, environmental, and genetic factors as effective predictors of high body mass index (BMI) and obesity in the preschool period. These studies particularly emphasized that habits acquired in the preschool years affect BMI and obesity. In this population-based case-control study, it was aimed to reveal for the first time the relationship between fat mass and obesity-related (FTO) gene expression and BMI and obesity in preschool children aged 2-6 living in Turkey.

Materials and Methods: Buccal mucosal swabs were collected from 54 preschool children from 3 kindergartens located in Istanbul, Turkey. In the study, the *FTO* gene expression level in a total of 54 (n=25 girls and n=29 boys) children who were obese (n=14) and non-obese (n=40) according to the International BMI index was determined by the 'Quantitative Polymerase Chain Reaction' (qPCR) technique.

Result: A correlation was found between *FTO* gene expression and BMI and obesity in obese and non-obese children with a Mann-Whitney U test (p=0.005).

Conclusion: Additional research is needed to better understand the function and prevalence of the *FTO* gene mutations by performing sequencing analysis of the gene simultaneously in preschool children in Turkey.

Keywords: *FTO* gene, obesity, overweight, preschool children, BMI

ÖZ

Amaç: Obezite fazla kilolu olma olarak tanımlanan çok faktörlü bir hastalıktır. Önceki çalışmalar ailesel, çevresel ve genetik faktörlerin okul öncesi dönemde vücut kitle indeksi (VKİ) ve obezitenin etkili belirleyicileri olarak bulunmuştur. Özellikle okul öncesi yıllarda kazanılan alışkanlıkların VKİ ve obezite üzerinde etkisi olduğu vurgulanmıştır. Bu nüfusa dayalı vaka kontrol çalışmasında, Türkiye'de yaşayan yaşları 2-6 arasında değişen okul öncesi çocuklarda yağ kütlesi ve obezite ile ilişkili (*FTO*) gen ekspresyonu ile VKİ ve obezite arasındaki ilişkinin ilk defa açığa çıkarılması amaçlanmıştır.

Gereç ve Yöntem: İstanbul, Türkiye'de yaşayan 3 adet anaokuluna kayıtlı, yaşları 2-6 arasında olan toplam 54 okul öncesi çocuktan bukkal mukoza sürüntüleri toplandı. Çalışmada, uluslararası VKİ indeksine göre obez olan (n=14), obez olmayan (n=40) toplam 54 (n=25 kız ve n=29 erkek) çocukta *FTO* gen ekspresyon düzeyi 'Quantitative Polymerase Chain Reaction' (qPCR) tekniği kullanılarak incelendi.

Bulgular: Obez olan ve olmayan çocukların *FTO* gen ekspresyonu ve obezite arasında anlamlı ilişki $2^{-\Delta\Delta CT}$ formülü ile Mann-Whitney U testi kullanılarak bulundu (p=0,005).

Sonuç: Okul öncesi çağında olan çocuklarda *FTO* geninin işlevini daha iyi anlamak için daha fazla bireyle gen dizileme analizi araştırmalarına ihtiyaç olduğu düşünülmektedir.

Anahtar kelimeler: *FTO* geni, obezite, fazla kilo, okul öncesi, VKİ

Corresponding Author/Sorumlu Yazar: Şeref Buğra TUNÇER **E-mail:** seref.tuncer@istanbul.edu.tr

Submitted/Başvuru: 22.03.2023 • **Revision Requested/Revizyon Talebi:** 04.05.2023 • **Last Revision Received/Son Revizyon:** 17.07.2023 • **Accepted/Kabul:** 19.07.2023 • **Published Online/Online Yayın:** 13.10.2023

INTRODUCTION

The alarming increase in childhood obesity is impacting both developed and developing countries (1). The World Health Organization has reported that around 60% of adults and one in three school-age children in Europe are currently affected by obesity whereas, in the US, obesity affects more than 17% of children (2). Due to childhood obesity, some children are at risk of developing certain diseases that were previously thought to be adult diseases, such as obstructive sleep apnea, hypertension, type 2 diabetes mellitus, dyslipidemia, and other comorbidities (3). Also, these children are more vulnerable to feelings of low self-esteem, despair, and anxiety, and some experience bullying, which has an impact on their psychological and emotional well-being (4). Furthermore, the risk of suffering from an obesity-related disease is linked to an increased risk of early death and increased healthcare spending (5). For all these reasons, research which seeks to detect the factors underlying childhood obesity is very important.

Genetics have a remarkable influence on obesity in an adipogenic environment and childhood obesity is the result of an interaction of genetic factors and environmental effects (3,6). The combination of these factors leads to energy imbalance, i.e. excessive calorie intake compared to the amount of energy consumed, resulting in excessive accumulation of adipose tissue (7). The fat mass and obesity-associated (*FTO*) gene was the first gene that showed consistent associations with overall obesity in adults and children from different ethnic backgrounds (8). In a longitudinal study of twins, researchers found that the impact of a common variant of the *FTO* gene on BMI becomes more pronounced with increasing age in childhood (9). In terms of obesity onset, age-related differences were observed between the studies. The evidence suggests that the relationship between *FTO* variants and obesity-related traits may be age-dependent (10). Lopez-Bermejo et. al. indicated the onset of obesity in the neonatal period (11). In another study, childhood was indicated as the onset period of obesity (12). In addition, Rutters et. al. pointed to adolescence as the period in which the onset of obesity-related traits is seen (13). But these studies were done entirely on individuals of European descent. The pattern and age of onset of obesity, and the association between *FTO* gene expression and childhood BMI/obesity in the Turkish population are not clear. In 2022, a multicenter study in Turkey investigated potential genes and mutations in children with non-syndromic early-onset severe obesity (onset<7 and BMI-SDS>3) and confirmed any pathogenic variants of any mutations in *FTO* intron (14). But another study conducted by Agagunduz et. al. among Turkish adults demonstrated that only *FTO* polymorphism was associated with whole-body fat accumulation, and not abdominal fat accumulation (15).

To our knowledge, no studies have examined the age and sex-specific associations of BMI and *FTO* gene expression patterns in relation to BMI and obesity in preschool children in a population-based in Turkey. Here in this study, we investigate the associations between the *FTO* gene expression and BMI and obesity in preschool children living in Turkey and examine the interactions of this gene expression pattern with gender, food allergy, and familial factors.

MATERIAL and METHOD

Study Population

In this population-based case-control study, preschool children (aged between 2-6 enrolled in 3 kindergartens) living in Istanbul, Turkey, were assessed for body size parameters. A total of 54 (n=25 girls and n=29 boys) children who were obese (n=14) and non-obese (n=40) according to the international BMI index were included in the study. The age and sex-specific BMI cut points recommended by the International Obesity Task Force were used (IOTF)(16). Buccal mucosa samples were collected from 54 preschool children.

The study was approved by the MEF University Ethics Committee (The approval date was 20.02.2019) to collect the swap samples from preschool children. Istanbul University, Istanbul Faculty of Medicine, and the Clinical Research Ethics Committee approved doing the experimental procedure at the Oncology Institute (Date: 03.03.2023, No: 5). Written consent was obtained from the parents prior to the study. A power analysis was used to determine the minimum number of study groups. The result of the power analysis showed that Type I Error=0.09 and Test Power (Confidence Interval) =80% for patient analysis. It was calculated that the minimum number of subjects in our patient group should be 54.

Anthropometric measurements

Anthropometric measurements including weight, height, and fat mass percentage were calculated using a stadiometer; each participant's height was calculated to the nearest centimeter. On common medical scales set to the nearest 0.1 kg, subjects wearing light indoor attire were weighed. To determine BMI, the formula BMI= weight(kg)/height^2 (m) was used. Using age and sex-specific BMI cut-off values suggested by Cole et al., overweight and obesity status were identified (16). Lifestyle habits (eating habits), nationality, food allergy status, breastfeeding duration, and the obesity status of each child were determined using a questionnaire. Oral swabs were used to gather the biological material needed by the study group from the mouth's cheek region. The *FTO* gene's expression in the collected sample was examined.

Gene expression analysis

To isolate RNA from the buccal mucosal swap samples, Zymo Research's Quick-RNA MiniPrep Kit (Quick-RNA-TM MiniPrep, USA) was used according to the manufacturer's instructions. Buccal mucosal swabs were fixed in a DNase/RNase-free solution and 300 µL of RNA lysis buffer was added and then centrifuged for 30 s at 10,000 g. The supernatant was transferred into a Spin-Away Filter collection tube and centrifuged for one minute at 10,000 g. 5 µL of DNase I and 75 µL of DNA digestion buffer were added and transferred into a collecting tube and filled with 400 µL of RNA preparation buffer and centrifuged at 10,000 g for 30 seconds. This was washed with 700 µL of RNA

wash buffer twice and centrifuged. The column was placed in a new 1.5 mL micro-centrifuge tube and 700 µL of QIAzole solution was added and left at room temperature for 5 minutes. 140 µL of chloroform was added and centrifuged at +40°C for 15 minutes at 12,000g. The top phase was transferred into a collection tube and 525 µL of 100% ethanol was added and centrifuged at 8000 g for 15 seconds. 700 µL of RWT buffer was added and centrifuged at 8000 g for 15 seconds. Then the columns were filled with 500 µL of RPE buffer and centrifuged at 8000 g for 1 minute and RNA was isolated. The purity and concentration of RNAs were determined by electrophoresis on a 1.5% agarose gel at 150 V. A NanoDrop 2000 spectrophotometer (Thermo Scientific, USA) was used. RNA was determined by measuring absorbance at 260 and 280 nm wavelengths.

A 'Bioline SensiFAST cDNA Synthesis Kit' (Meridian, Bioline, ABD) was used to create the cDNA. After adding 1 ng, 1 µL of template RNA, 4 µL of TransAmp buffer, and 1 µL of Reverse Transcriptase, the total volume was brought to 20 µL by adding RNAse DNAse-free water and a BioRad PCR (BioRas, Singapore) device was used for cDNA synthesis.

qPCR was conducted using the 'SensiFAST SYBR®No-ROXKit-Bioline'(Meridian, Bioline, ABD) kit in Mic PCR Biomolecular Systems (Queensland, Australia) device. 10 µL Sybr Green, 400 nM 1 µL *FTO* Reverse Primer 400 nM, 1 µL *FTO* Forward Primer, 6 µL template cDNA, and 2 µL DNAase/ RNAase Free water were added respectively and the total volume of 20 µL was distributed into Mic PCR tubes. The qPCR procedure was performed at 95 °C for 5 minutes, then at 60°C for 2 minutes, and at 60 °C for 30 seconds. The $2^{-\Delta\Delta CT}$ method was used to analyze the relative changes in obese and non-obese children (17). *GAPDH* gene expression assay was used as the housekeeping gene. *FTO* gene expression was determined.

Statistical Analysis: *FTO* gene expression levels in obese and non-obese preschool children were investigated. The descriptive statistics of the qualitative variables in the study were given as numbers and percentages, and the descriptive statistics of the quantitative variables were given as mean, standard deviation, median, minimum, and maximum. The assumption of normal distribution was examined with the Shapiro-Wilk test. The Mann-Whitney U test was used to compare the mean of two independent groups. The Spearman correlation coefficient was used when examining the relationships between quantitative variables. All statistical analyses were performed using the SPSS program (SPSS version 26; SPSS Science, Chicago, USA), and a p-value=0.005 was considered statistically significant.

RESULTS

The demographic features of the children are shown in Table 1. In this population-based case-control study 54 preschool children aged between 2-6 were selected for an investigation of the expression level of *FTO* gene expression. Of the children, 51 (94%) were from the Marmara Region of Turkey and 3 (6%) were from Bulgaria (self-reported). We used the $2^{-\Delta\Delta CT}$ method to analyze the *FTO* gene expression in buccal mucosal swabs from obese and non-obese children. To analyze the statistical difference in the expression of the *FTO* gene between obese children and non-obese children, a Mann-Whitney U test was performed.

Table 1: Demographic features of the children

Variables	Children (n=54)
Age (years)	
2 years old	3 (5.5%)
3 years old	7 (13%)
4 years old	12 (22.2%)
5 years old	25 (46.3%)
6 years old	7 (13%)
Gender	
Female	25 (46.3%)
Male	25 (46.3%)
Nationality	
Turkish	51 (94.4%)
Others	3 (5.6%)
Food allergy of children	
Yes	7 (7.4%)
No	47 (92.6%)
Breastfeeding duration	
6 months	9 (16.7%)
6-12 months	18 (33.3%)
12 months and over	27 (50%)
Obesity/Overweight	
Obese	14 (26 %)
Non-obese	40 (74%)

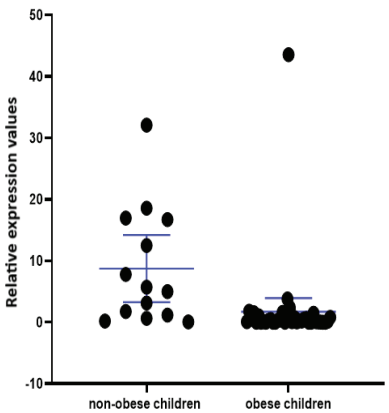

p=0.0001 5.5360 (0.6600-16.97)

Figure 1: Quantitation plots of expression levels of non-obese and obese children. Data are expressed as relative expression units. The bars represent the standard error of the mean (SEM). p value < 0.05 was considered statistically significant using the Mann-Whitney U test.

We also used a Mann-Whitney U test to analyze the data revealing the difference in expression of the obese group from the non-obese group and to determine whether this was statistically significant. The results showed a difference in *FTO* gene

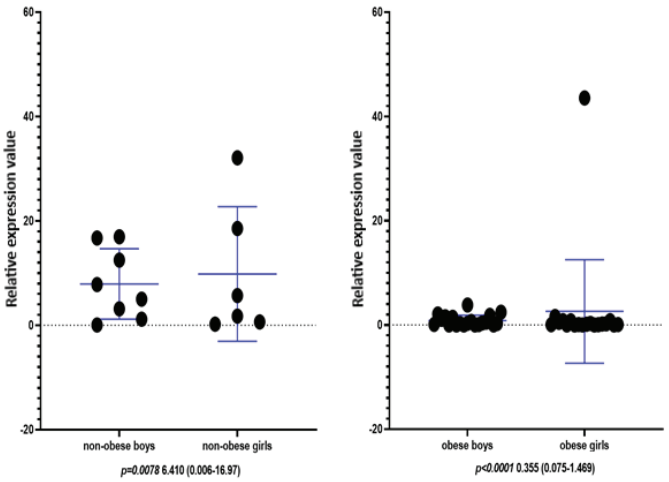

Figure 2: Quantitation plots of expression levels of boys and girls of non-obese (a) and obese (b) children. Data are expressed as relative expression units. The bars represent the standard error of the mean (SEM). p value<0.05 was considered statistically significant using the Mann-Whitney U test.

Table 2: *FTO* gene expression correlation with the parents' weight-height, pregnancy weight of mother, birth weight-height of the children, and breast-feeding duration.

	Mother'sweight	Mother's height	Father's weight	Father's height	Pregnancy weight	Birth weight of the children	Birth height of the children	Breast-feeding duration
FTO gene expression p value	0.919	0.437	0.362	0.745	0.983	0.852	0.565	0.218
r value	0.017	-0.130	0.152	-0.055	0.004	-0.031	-0.096	0.214

Spearman correlation analysis

Table 3: *FTO* gene expression analysis of preschool children with or without food allergy

Food Allergy	N	Mean	Median	Std. Deviation	Minimum	Maximum	p
No	47	12.468	1.1847	43.43699	0.06	255.83	0.085
Yes	7	0.320	0.1686	0.29247	0.13	0.66	

Mann-Whitney U test

Table 4: *FTO* gene expression analysis of obese children between 4-6 months and older than 6 months of age.

Obese children	Mean	Median	Std. Deviation	Minimum	Maximum	p
Between 4-6 months	5.6667	1.0751	9.56681	0.08	32.10	0.788
After 6 months	14.5470	0.8262	51.14744	0.06	255.83	

Mann-Whitney U test

expression levels in obese versus non-obese children shown in Figure 1. The results showed a difference in the gene expression levels in obese versus non-obese, and in boys versus girls in the obese/non-obese groups (Figure 2).

FTO gene expression levels were evaluated in terms of gender, as well as in quantitation plots of expression levels of boys and girls of non-obese (Figure 2a) and obese (Figure 2b) children and there was a difference between the boys versus girls in the obese/non-obese children as shown in Figure 2.

The correlation with the *FTO* gene expression and parents' weight-height, pregnancy weight of mother, birth weight-height of

the children, and breast-feeding duration was also investigated. There was no significant correlation observed between them (p=0.218) as shown in Table 2.

We also evaluated *FTO* gene expression in preschool children with or without food allergy. There was no significant difference between the *FTO* gene expression in children with or without food allergy, and (p=0.085) was detected as shown in Table 3.

We also compared the percentage of obese children aged between 4-6 months and those older than 6 months of age. No significant relationship was detected between obese preschool children who were aged 4-6 months and those older than 6 months of age (p=0.788), as shown in Table 4.

DISCUSSION

This is the first study in Turkey to examine the association between *FTO* gene expression and BMI and obesity in preschool children (aged between 2-6). We found a moderate correlation between *FTO* gene expression and BMI and obesity in prescchool children.

Several studies have shown that the *FTO* gene is known as a susceptibility gene for polygenic obesity. In European populations, the effect of the *FTO* gene on BMI varies at different stages of life (18). However, the results regarding the age of onset of the association have been inconsistent. In this present study, the preschool associations of *FTO* gene expression with BMI and obesity and the risk factors for obesity are investigated for the first time in Turkey. The finding of this study confirms previous research conducted on mice and adult humans which demonstrated an association between *FTO* and the occurrence of obesity. Villalobos et. al. investigated the FTO gene expression level in mestizo Mexican adults and obese individuals who were found to have higher expression of FTO in their subcutaneous adipose tissue compared to healthy individuals (19). In another study, using a mouse model, the researchers discovered that additional copies of the *FTO* gene resulted in increased FTO expression, which in turn promoted the development of obesity. The mice carrying an additional copy of *FTO* exhibited an increase in body weight; furthermore, *FTO* was found to be directly related to the food intake and metabolism of the mice, as an increase in the expression of *FTO* leads to an increase in food intake and body fat (20). Another study indicated that the mRNA level of *FTO* showed a correlation with the BMI of European descent adults, implying that its expression could be influenced by the accumulation of body fat. Notably, the expression of *FTO* in visceral tissues may play a role in the onset of obesity (21). In accordance with the literature findings from different nations, we found a positive association between *FTO* gene expression and obesity in preschool children (22).

Heritable variables are thought to account for 30% to 50% of obese status (23). According to the literature, if both parents are obese, the likelihood of their child being overweight increases by two to three times, and in some cases by as much as fifteen times. In this present study, of the 14 obese preschool children, five of them had obese parents, indicating a possible role of hereditary factors in childhood obesity.

There is growing evidence that these differences in childhood obesity rates are primarily due to inequalities in the physical and social environments in which children grow up (24). For example, the prevalence of obesity among all children in the United States has increased by 10%, while children from households with lower educational attainment, lower income, and higher unemployment have experienced a significant increase in obesity rates, ranging from 23% to 33% from 2003 to 2007 (25). In addition, lower-income families are less likely to recognize their child's obesity or feel the need to intervene in their child's eating and exercise habits (26). Furthermore, low-income communities face several barriers to improving their health conditions (27). As Turkey is a low-income country and obesity is increasingly becoming a major problem, we investigated the expression level of the *FTO* gene expression for the first time in 54 preschool children in the Marmara region (n=51) in Turkey and the Balkans (from Bulgaria, n=3). We analyzed the data taken from obese and non-obese preschool children (2–6 years old) using the Mann-Whitney U test and found it to have a relatively high *FTO* gene expression level (p=0.005).

Childhood obesity has become one of the most serious medical and public health problems of the 21st century. According to statistics, up to 58% of the world's adult population will be obese by 2030 (28). The etiology of obesity is the result of multiple genetic, environmental, and biological effects. Genetic variations also cause the increase in the expression level of specific genes to be one of the main reasons for obesity. This study has both strengths and limitations. One of the limitations has to do with the finding that children from families with obese parents are more likely to be obese. In order to follow this through, however, our study should have continued with an investigation of an additional number of children of different ages, and a mutation analysis performed by sequencing the *FTO* genes should have been conducted.

Acknowledgements: TUBİTAK

Ethics Committee Approval: This study was approved by Istanbul University Istanbul Faculty of Medicine Clinical Research Ethics Committee (Date: 03.03.2023, No: 5).

Peer Review: Externally peer-reviewed.

Author Contributions: Conception/Design of Study- H.M.Y., D.G., Ş.B.T.; Data Acquisition- H.M.Y., D.G., İ.A., Ş.B.T.; Data Analysis/Interpretation- Ş.B.T.; Drafting Manuscript- Ş.B.T.; Critical Revision of Manuscript- H.M.Y., D.G., İ.A., Ş.B.T.; Final Approval and Accountability- H.M.Y., D.G., İ.A., Ş.B.T.; Material and Technical Support- D.G., Ş.B.T.; Supervision- D.G., Ş.B.T.

Conflict of Interest: The authors have no conflict of interest to declare.

Financial Disclosure: This study was supported by TUBİTAK

within the scope of the Scientific and Technological Research Projects Funding Program (Project number: 119K359)

REFERENCES

1. Ogden CL, Carroll MD, Kit BK, Flegal KM. Prevalence of childhood and adult obesity in the United States, 2011-2012. JAMA 2014;311(8):806-14.
2. McNally S, Scarlett McNally. Obesity is a community issue, not just an individual one. BMJ 2023;380:702.
3. Kumar S, Kelly AS. Review of Childhood Obesity: From Epidemiology, Etiology, and Comorbidities to Clinical Assessment and Treatment. Mayo Clin Proc 2017;92(2):251-65.
4. Sahoo K, et al. Childhood obesity: causes and consequences. J Family Med Prim Care 2015. 4(2):187-92.
5. Berkowitz RI, Daniels S. Now is the time to improve access and healthcare systems for childhood obesity treatment. Obesity (Silver Spring) 2017;25(1):13-4.
6. Wardle J, Carnell S, Haworth CM, Plomin R. Evidence for a strong genetic influence on childhood adiposity despite the force of the obesogenic environment. Am J Clin Nutr 2008;87(2):398-404.
7. Bradfield JP, et al. A trans-ancestral meta-analysis of genome-wide association studies reveals loci associated with childhood obesity. Hum Mol Genet 2019;28(19):3327-38.
8. Frayling TM, Timpson NJ, Weedon MN, Zeggini E, Freathy RM, Lindgrenet CM, et al. A common variant in the FTO gene is associated with body mass index and predisposes to childhood and adult obesity. Science 2007;316(5826):889-94.
9. Haworth CM, Carnell S, Meaburn EL, Davis OSP, Plomin R, Wardle J. Increasing heritability of BMI and stronger associations with the FTO gene over childhood. Obesity (Silver Spring) 2008;16(12):2663-8.
10. Wang J, Mei H, Chen W, Jiang Y, Sun W, Li F, et al. Study of eight GWAS-identified common variants for association with obesity-related indices in Chinese children at puberty. Int J Obes (Lond) 2012;36(4):542-7.
11. Lopez-Bermejo A, Petry CJ, Díaz M, Sebastiani G, Zegher Fde, Dunger DB, et al. The association between the FTO gene and fat mass in humans develops by the postnatal age of two weeks. J Clin Endocrinol Metab 2008;93(4):1501-5.
12. Hakanen M, Raitakari OT, Lehtimäki T, Peltonen N, Pahkala K, Sillanmäki L, et al. FTO genotype is associated with body mass index after the age of seven years but not with energy intake or leisure-time physical activity. J Clin Endocrinol Metab 2009;94(4):1281-7.
13. Rutters F, Nieuwenhuizen AG, Bouwman F, Mariman E, Westerterp-Plantenga MS. Associations between a single nucleotide polymorphism of the FTO Gene (rs9939609) and obesity-related characteristics over time during puberty in a Dutch children cohort. J Clin Endocrinol Metab 2011;96(6):E939-42.
14. Akinci A, Kara A, Ozgur A, Aksu S. Genomic analysis to screen potential genes and mutations in children with non-syndromic early onset severe obesity: a multicentre study in Turkey. Mol Biol Rep 2022;49(3):1883-93.
15. Agagunduz D, Gezmen-Karadag M. Association of FTO common variant (rs9939609) with body fat in Turkish individuals. Lipids Health Dis 2019;18(1):212.
16. Cole TJ, Bellizzi MC, Flegal KM, Dietz WH. Establishing a standard definition for child overweight and obesity worldwide: international survey. BMJ 2000;320(7244):1240-3.
17. Livak KJ, Schmittgen TD. Analysis of relative gene expression data using real-time quantitative PCR and the 2(-Delta Delta C(T)) Method. Methods 2001;25(4):402-8.
18. Hardy R, Wills AK, Wong A, Elks CE, Wareham NJ, Loos RJF, et al. Life course variations in the associations between FTO and MC4R gene variants and body size. Hum Mol Genet 2010;19(3):545-52.
19. Villalobos-Comparan M, Flores-Dorantes MT, Villarreal-Molina MT, Rodríguez-Cruz M, García-Ulloa AC, Robles L, et al. The FTO gene is associated with adulthood obesity in the Mexican population. Obesity (Silver Spring) 2008;16(10):2296-301.
20. Church C, Moir L, McMurray F, Girard C, Banks GT, Teboul L, Wells S, et al. Overexpression of Fto leads to increased food intake and results in obesity. Nat Genet 2010;42(12):1086-92.
21. Kloting N, Schleinitz D, Ruschke K, Berndt J, Fasshauer M, Tönjes A, Schön MR, et al. Inverse relationship between obesity and FTO gene expression in visceral adipose tissue in humans. Diabetologia 2008;51(4):641-7.
22. Landgraf K, Scholz M, Kovacs P, Kiess W, Körner A. FTO Obesity Risk Variants Are Linked to Adipocyte IRX3 Expression and BMI of Children - Relevance of FTO Variants to Defend Body Weight in Lean Children? PLoS One 2016;11(8): e0161739.
23. Bouchard C, Despres JP, Mauriege P. Genetic and nongenetic determinants of regional fat distribution. Endocr Rev 1993;14(1):72-93.
24. Finch BK, Phuong Do D, Heron M, Bird C, Seeman T, Lurie N, et al. Neighborhood effects on health: Concentrated advantage and disadvantage. Health Place 2010;16(5):1058-60.
25. Singh GK, Siahpush M, Kogan MD. Rising social inequalities in US childhood obesity, 2003-2007. Ann Epidemiol 2010;20(1): 40-52.
26. Hansen AR, Duncan DT, Tarasenko YN, Yan F, Zhang J. Generational shift in parental perceptions of overweight among school-aged children. Pediatrics 2014;134(3):481-8.
27. Powell LM, Slater S, Mirtcheva D, Bao Y, Chaloupka FJ. Food store availability and neighborhood characteristics in the United States. Prev Med 2007;44(3):189-95.
28. Kelly T, Yang W, Chen C-S, Reynolds K, He J. Global burden of obesity in 2005 and projections to 2030. Int J Obes (Lond) 2008;32(9):1431-7.

İSTANBUL UNIVERSITY PRESS

RESEARCH ARTICLE / ARAŞTIRMA MAKALESİ
Journal of Advanced Research in Health Sciences /
Sağlık Bilimlerinde İleri Araştırmalar Dergisi 2023
DOI: 10.26650/JARHS2023-1293712

SARS-COV-2 PREVALENCE IN INDIA COMPARED TO THE REST OF THE GLOBE AND ASCERTAINS EPIDEMIOLOGICAL CHARACTERISTICS ASSOCIATED WITH THE COVID-19 PANDEMIC DURING 2020 IN INDIA

HİNDİSTAN'DAKİ SARS-COV-2 PREVALANSI VE 2020 YILINDAKİ COVID-19 PANDEMİSİYLE İLİŞKİLİ EPİDEMİYOLOJİK ÖZELLİKLERİN BELİRLENMESİ

M. Rajesh Kumar RAO[1], Rabindra N. PADHY[2], Manoj Kumar DAS[1]

[1] Indian Council of Medical Research (ICMR), National Institute of Malaria Research (NIMR), IDVC Field Unit, Jharkhand, India
[2] Siksha 'O' Anusandhan Deemed to be University, Institute of Medical Sciences and Sum Hospital, Central Research Laboratory, Odisha, India

ORCID ID: M.R.K.R. 0000-0002-8217-5175; R.N.P 0000-0002-2522-9843; M.K.D. 0000-0002-7494-5969

Citation/Atıf: Rao MRK, Padhy RN, Das MK. SARS-CoV-2 prevalence in India compared to the rest of the globe and ascertains epidemiological characteristics associated with the COVID-19 pandemic during 2020 in India Journal of Advanced Research in Health Sciences 2023;6(3):250-262. https://doi.org/10.26650/JARHS2023-1293712

ABSTRACT

Objectives: SARS-CoV-2 triggers a pandemic of COVID-19. We ascertain the pandemic burden of COVID-19 disease between India and the rest of the world; monitor the burden of COVID-19 disease in Indian states and union territories compared to other countries with nearly equivalent population sizes, and study the epidemiological characteristics.

Material and Methods: A population-based comparative optimization algorithms study was conducted on all COVID positive cases reported by 31st December 2020.

Results: Confirmed cases resulted in India with a ratio of 1:7.2 to the rest of the world, with a lower mortality rate with a ratio of 1:12 (CMR per 100,000 people) than other countries. Many Indian administrative regions have lower morbidity rates (Z-values range from -2653.7369 to -11.6403) and mortality (Z-values range from -439.446 to -4.86) than the countries selected. In India, 184,728,001 tests were done, with 5.6% cases confirmed, 96.1% recovered, and 1.4% dying due to COVID-19. COVID-19 was more prevalent in males and patients aged 25–44, whereas SARS-CoV-2 killed the most people over the age of 60. Bihar had the most cases of infection, while Punjab had the most deaths.

Conclusion: SARS-CoV-2 disease led India to have a lower morbidity and mortality burden than the rest of the world. The pandemic curves of COVID-19 resulted in daily peaks most significantly, and the cumulative number of cases increased tremendously with an upward trend. Analytical, spatial, and temporal research studies will be carried out to understand the effect of climate change and indicators that correlate with the epidemiological characteristics of the emerging coronavirus.

Keywords: SARS-CoV-2, COVID-19, coronavirus, pandemic, epidemiological

ÖZ

Amaç: SARS-CoV-2, COVID-19 pandemisini tetiklemektedir. Çalışmamızda Hindistan eyaletleri ve yakın bölgelerinde COVID-19 hastalığının yükünün izlenmesi, epidemiyolojik özelliklerinin incelenmesi ve COVID-19 hastalığının pandemi yükü açısından Hindistan'ın eşdeğer nüfus büyüklüğüne sahip diğer dünya ülkeleri ile karşılaştırılması amaçlanmıştır.

Gereç ve Yöntemler: 31 Aralık 2020 tarihine kadar bildirilen tüm COVID pozitif vakaları üzerinde nüfus temelli karşılaştırmalı optimizasyon algoritmaları çalışması gerçekleştirilmiştir.

Bulgular: Doğrulanmış vakalar, Hindistan'da dünyanın geri kalanına göre 1:7,2 oranıyla sonuçlanırken, 1:12 oranıyla (100.000 kişi başına CMR) diğer ülkelere göre daha düşük bir ölüm oranı tespit edilmiştir. Hindistan'ın birçok idari bölgesinde, ekonomik durumu iyi ülkelerden daha düşük hastalık oranları (Z-değerleri -2653.7369 ile -11,6403 arasında değişmektedir) ve ölüm oranlarının (Z-değerleri -439.446 ile -4,86 arasında değişmektedir) olduğu görülmüştür. Hindistan'da 184.728.001 test yapıldığı, vakaların %5,6'sının COVID-19 tanısı yönünden doğrulandığı, %96,1'inin iyileştiği ve %1,4'ünün ise COVID-19 nedeniyle öldüğü tespit edilmiştir. COVID-19 erkeklerde ve 25-44 yaş arası hastalarda daha yaygın görülürken, SARS-CoV-2'nin ölüm oranlarının 60 yaş üstü kişilerde en yüksek olduğu saptanmıştır. En çok enfeksiyon vakasının Bihar'da, en çok ölümün ise Punjap'da olduğu bulunmuştur.

Sonuç: SARS-CoV-2 hastalığı Hindistan'da dünyanın geri kalanından daha düşük bir morbidite ve mortalite yüküne yol açmıştır. COVID-19'un pandemi eğrileri en net şekilde günlük piklerle sonuçlanmış ve kümülatif vaka sayısı yükseliş eğilimiyle muazzam bir artış göstermiştir. İklim değişikliğinin etkisi ve ortaya çıkan koronavirüsün epidemiyolojik özellikleriyle korele olan indikatörleri anlamak için analitik, mekânsal ve zamansal araştırma çalışmaları yürütülecektir.

Anahtar kelimeler: SARS-CoV-2, COVID-19, coronavirus, pandemi, epidemiyoloji

Corresponding Author/Sorumlu Yazar: M. Rajesh Kumar RAO **E-mail:** raomrajeshkumar@gmail.com

Submitted/Başvuru: 08.05.2023 • **Revision Requested/Revizyon Talebi:** 09.08.2023 • **Last Revision Received/Son Revizyon:** 10.08.2023 • **Accepted/Kabul:** 10.08.2023 • **Published Online/Online Yayın:** 13.10.2023

INTRODUCTION

Viral infection can infect humans or animals (1). Respiratory viral infection, particularly respiratory tract infections (RTIs), affects the throat, nose, bronchi, and lungs (2). Viral respiratory infections have changed the epidemiology situation, and variations occur every six to ten years and contribute severe epidemics (3). In December 2019, an aggregation of unidentified etiology acute respiratory infection cases in the lungs was reported from Wuhan City, China (4). This unspecified infection has rapidly spread from Wuhan City, China, to other countries (5). Chinese scientists identified this causative etiology as a new variant of the coronavirus strain on 7th January 2020 (4). WHO renamed this new form of coronavirus infection, i.e. known as COVID-19 (6). Coronavirus has an enormous family of viruses belonging to Coronaviridae**,** subfamily Orthocoronavirinae**,** orders Nidovirales**,** and realm Riboviria (7). Some coronaviruses, including "Middle East Respiratory Syndrome (MERS)" and "Severe Acute Respiratory Syndrome (SARS)," affect humans (8). Chinese scientists sequenced the genomes of COVID-19 (2019-nCoV) isolates from patients and have facilitated the sequencing data, including band intensities, made available on the "Global Initiative for the Sharing of All Influenza Data (GISAID)" platform as a potential source for public concern. "International Committee on Taxonomy of Viruses (ICTV)" characterized the virus subtype of COVID-19 as being "Severe Acute Respiratory Syndrome Coronavirus-2 (SARS-CoV-2)" (9).

Trevor Bedford, a bioinformatics expert, assumed coronavirus was introduced into humans in a single intro and subsequently spread among humans (10). The first coronavirus infection in a human was documented on November, 17th 2019 in China (4, 5). The initial case of COVID-19 was beginning its count in India on 30th January 2020 in Trissur, Kerala (11). ICMR-National Institute of Virology has managed to retrieve the SARS-CoV-2 strain from its contagious patients, validating that the strain from Wuhan was structurally similar to 99.9% (12). Afterward, the coronavirus disease escalates to almost every Indian province. With an exponential escalation in daily COVID-19 cases worldwide, WHO coerced this as an international health emergency and designated this epidemic as a pandemic at the end of January 2020 (13). Except for the common symptoms of fever, exhaustion, and dry toux, a few patients have issues of nasal obstruction, nasal rinsing, sore throat, myalgia, and diarrhea (14). COVID-19 incubation can occur within 1-14 days, with an average incubation time of five to seven days (15). Asymptomatic or less symptomatic patients increase the infection's transmission possibilities (16).

With a total population of about 1.3 billion people, India is a massive country with a diversified population. India has the second-highest number of people infected with COVID-19 as of the end of the year 2020. Apart from the epidemiological trends in Government databases, there is no systematic research on COVID-19 pandemic burdens among India and the rest of the world, and the pandemic COVID-19 disease trend in Indian states and Union Territories (UT) compared to other countries with a nearly equal current population size. Furthermore, the influence of COVID-19 epidemiological indicators on population density in India has yet to be revealed. Therefore, a population-based comparative optimization algorithms study was performed on all cases reported by 31st December 2020 to ascertain the pandemic burden of COVID-19 disease between India and the rest of the world. Also, monitoring the pandemic burden of COVID-19 disease in Indian states and UTs compared to other countries with populations nearly equal to the current population size. Furthermore, it studied disease prevalence and epidemiological characteristics to identify crucial indicators for the transmission of coronavirus (SARS-CoV-2) in India.

MATERIALS and METHOD

Pattern of study

A retrospective research methodology was used in this study to determine the epidemiological measures. We used to population-base comparative optimization algorithms to ascertain the pandemic burden of COVID-19 disease between India and the rest of the world.

Study period

COVID-19 cases were evaluated from 1st January 2020 to 31st December 2020, during SARS-CoV-2 infections.

Data sources

I. Worldwide data for COVID-19 was obtained from:

i. https://www.worldometers.info/coronavirus/ (U.S. Digital media company).

ii. https://www.who.int/emergencies/diseases/novel-coronavirus-2019 (World Health Organization).

II. Pandemic incidence data for COVID-19 in India was obtained from:

i. https://www.mygov.in/covid-19 (Ministry of Health & Family Welfare, Govt. of India).

ii. https://www.covid19india.org/ (Volunteer-driven, crowdsourced tracker for COVID-19 cases in India).

III. The current population of countries and union territories was obtained from:

i.https://worldpopulationreview.com/countries/ (U.S. Census Bureau).

ii. https://censusindia.gov.in/ (Office of the Registrar General & Census Commissioner, Ministry of Home Affairs, Govt. of India).

Data compilation

All population status as of 2020 and existing data for COVID-19 have been compiled in the Microsoft Excel 2007 database. The population status in 2020 of the Indian States and UTs, almost equal to the population of some countries worldwide, has been closely monitored (Figure 1). Infection cases of COVID-19 are classified as suspected (test done), confirmed (infected), recovered, and deceased. The relationship between four types of epidemiological measures, including "count, rate, proportion, ratio, prevalence, attack rate (AR), case fatality rate (CFR), the mortality rate (MR), and crude mortality rate (CMR)," was stu-

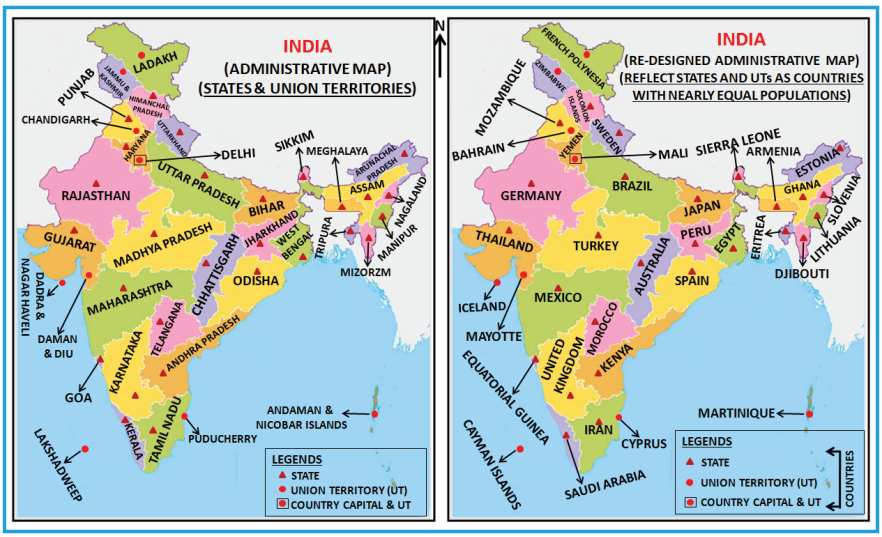

Figure 1: Map showing the Indian administrative map (states and union territories) vs. Re-designed Indian administrative map (Reflects states and UTs as selected countries around the world, in accord with nearly equal to the current population size) (9,28,37).

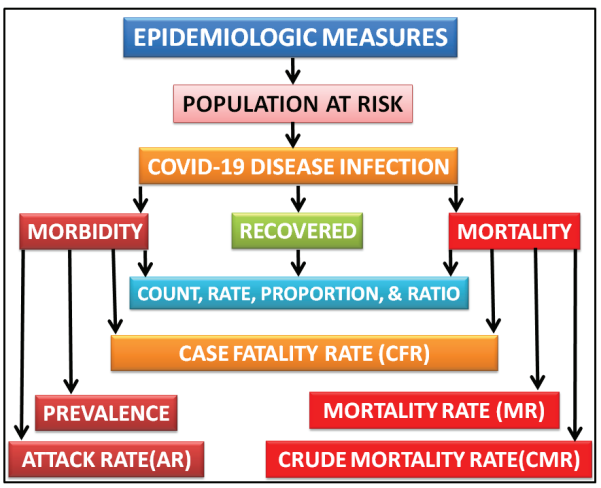

Figure 2: Flow diagram showing the epidemiological measures of disease frequency

died (Figure 2). Based on current COVID-19 data, we evaluated divergences in the COVID-19 pandemic burden and epidemiological factors between India and the rest of the world.

Population Group

The susceptible population comprises < 1 year (infants), 1–14 years (children), 15–24 years (young adults), 25–44 years (Adults), 45–60 years (middle-aged persons), and > 60 years (senior citizens).

Statistical data analysis

MS Excel version 2007 database has been used for graphics and statistical analysis. In this study, the statistics were used, which included rate, proportion, ratio, prevalence, AR, CFR, MR, and CMR, and the graph was designed using the line graph. Statistical analysis uses independent categorical variables between the two population groups. Null hypothesis (H_0) is that both proportions are almost nearly equal. The two-proportion test statistics were compared using the normal independent Z-test. The probability analysis (p-value) was performed using the statistical program, i.e., Social Science Statistics. Statistically significant was a probability value of $p<0.05$. The formula for the two-proportion test statistic is as follows:

$$z = \frac{(p_1 - p_2) - 0}{\sqrt{p(1-p)\left(\frac{1}{n_1} + \frac{1}{n_2}\right)}}$$

RESULTS

The COVID-19 pandemic burdens India compared to the rest of the world

More than 7,417 million people in 193 countries, two territories, and 22 unique islands worldwide are at risk of the COVID-19. The ratio between India and the rest of the world was 1:4.4. Of those populations, 1379.88102 million (18.6%) were Indians, and 6037.498999 million (81.4%) belonged to the rest of the world. COVID-19 affect more than 1,377 million (99.9%) of the Indian population in 36 regions of India, including 28 states and eight UTs. Suspected cases identified among the Indians were 184,728,001 (15.4%), and the remaining 1,015,773,314 (84.6%) were reported worldwide. Of those alleged cases of COVID-19, 10,280,606 (5.6%) cases had documents confirmed in India and 73,658,028 (7.3%) cases from the rest of the world. The CMR was 0.108 per thousand Indians, with the remaining 0.296 per thousand reported worldwide due to COVID-19. The prevalence of COVID-19 among Indians was 0.0075, and in the rest of the world was 0.0122. The AR was 0.75% of the Indian population, whereas the rest of the world was listed at 1.22% during the SARS-CoV-2 infection (Table 1).

Table 1: Comparison of COVID-19 pandemic burdens among India and the rest of the world during the coronavirus infections (SARS-CoV-2) as of 31st December 2020

Parameter	India	Rest of the World	Worldwide
Total states and union territories; and Total countries, territories, and unique islands	28-States, 9-UTs	192-Countries, 2-Territories, 22-Unique islands	193-Countries, 2-Territories, 22-Unique islands
Provinces at risk of Covid-19 pandemic disease	28-States, 8-UTs	192-Countries, 2-Territories, 22-Unique islands	193-Countries, 2-Territories, 22-Unique islands
Total Population	1.379,881,020	6.037,498,999	7.417.380,019
Population at risk	1.379,816,591	6.037,498,999	7.417.315,590
Population at risk (%)	99.9	100	99.9
Suspected cases	184.728,001	1.015,773,314	1.200,501,315
Suspected case rate	13.4	16.8	16.2
Proportion of suspected cases (%)	15.4	84.6	100
Suspected cases ratio	1	5	6
Confirmed cases	10.280,606	73.658,028	83.938,634
Confirmed case (Morbidity) rate	5.6	7.3	7.0
Proportion of confirmed cases (%)	12.2	87.8	100
Confirmed cases ratio	1	7	8
Prevalence	0.0075	0.0122	0.0113
Attack rate (AR)	0.75	1.22	1.13
Recovered cases	9.875,832	58.185,761	68.061,593
Recovered case rate	96.1	79.0	81.1
Proportion of recovered cases (%)	14.5	85.5	100
Recovered cases ratio	1	6	7
Active cases	404,774	15.472,267	15.877,041
Active case rate	3.9	21.0	18.9
Proportion active cases (%)	2.5	97.5	100
Active cases ratio	1	38	39
Death cases	148,981	1.786,699	1.935,680
Death case rate	1.4	2.4	2.3
Proportion of death cases (%)	7.7	92.3	100
Death cases ratio	1	12	13
Case fatality Rate (CFR)	1.4	2.4	2.3
Crude mortality rate (CMR) per 1000 populations	0.108	0.296	0.261

The COVID-19 pandemic disease scenario in Indian states and UTs compared to other countries is nearly equal to the population size

Table 2 and Table 3 show the variations in the pandemic scenario of COVID-19 disease between Indian states and UTs with population sizes similar to some countries.

Suspected cases

As a result, the suspected cases were significantly higher in 20 Indian states/UTs compared to other countries. The results were significant (Z-value ranges from 79.1123 to 3215.8398, $p<0.05$). However, the suspected cases were reported significantly lower than in other countries in the remaining 17 Indian states / UTs.

Table 2: The pandemic COVID-19 disease trend in Indian states and Union Territories compared to other countries with nearly equal to the current population size during the viral infections with corona (SARS-CoV-2) as of 31st December 2020

INDIA						Rest of the WORLD					
State/Uts	Population	Total number of cases				Country	Population	Total number of cases			
		S*	C*	D*	R*			S*	C*	D*	R*
Lakshadweep	64.429	0	0	0	0	Cayman Islands	65.623	56.819	338	2	296
Daman and Diu	242.911	33.818	1.426	0	1.414	Mayotte	271.922	51.648	5.890	55	3019
Ladakh	274.289	105.617	9.466	127	9.143	French Polynesia	280.704	23.640	16.926	114	4.956
Dadra Nagar Haveli	342.853	38.752	1.938	2	1.906	Iceland	340.964	582.761	5.754	29	5.607
Andaman and Nicobar	379.944	181.640	4.945	62	4.826	Martinique	375.301	90.932	6.091	43	141
Sikkim	658.361	68.828	5.889	127	5.139	Solomon Islands	686.884	4.043	17	0	10
Mizoram	1.091.014	177.387	4.199	8	4.091	Djibouti	986.127	80.290	5.831	61	5.789
Puducherry	1.244.464	488.451	38.132	633	37.115	Cyprus	1.206.248	2.088.108	22.651	119	10.390
Arunachal Pradesh	1.382.611	378.151	16.719	56	16.564	Estonia	1.326.425	307.336	27.989	229	18.555
Goa	1.457.723	397.386	50.981	737	49.313	Equatorial Guinea	1.396.494	76.206	5.277	86	5.222
Chandigarh	1.545.116	181.186	19.748	317	19.045	Bahrain	1.693.179	1.789.097	92.675	352	90.569
Nagaland	1.980.602	120.071	11.921	79	11.493	Slovenia	2.078.903	615.971	122.198	2.697	102.079
Manipur	2.721.756	474.524	28.139	354	26.601	Lithuania	2.726.669	1.779.426	145.277	1.802	93.263
Meghalaya	2.964.007	291.959	13.408	139	13.085	Armenia	2.960.000	776.005	159.409	2.823	145.624
Tripura	3.671.032	577.343	33.255	382	32.712	Eritrea	3.540.041	7.639	1.320	3	679
Himachal Pradesh	7.663.167	772.021	55.277	922	51.692	Sierra Leone	7.976.983	7.680.181	2.583	76	2.414
Uttaranchal	10.116.752	1.777.371	90.920	1.509	83.506	Sweden	10.091.340	4.263.118	454.758	9.707	266.747
Jammu and Kashmir	14.849.410	3.822.674	120.971	1.883	116.079	Zimbabwe	14.834.717	168.547	13.867	363	11.613
Delhi	20.188.648	8.659.830	625.369	10.536	609.322	Mali	14.834.717	147.191	7.090	269	4.919
Chhattisgarh	25.540,196	3.514,707	279.575	3.371	264.769	Australia	25.461.791	17.345.255	28.405	909	28.185
Haryana	29.808,027	4.554,156	262.325	2,905	255,853	Yemen	29.737,584	20,655	2,099	610	2,004
Assam	31.169,272	5.997,450	216.211	1,045	211,907	Ghana	30.986,096	678,726	54,771	335	53,929
Punjab	31.254,208	3.900,473	166.522	5,341	157,496	Mozambique	31.134,613	145,807	18,642	166	16,829
Jharkhand	32.966,238	4.799,240	115.113	1,030	112,424	Peru	32.912,133	6.657,725	1.015,137	37,680	990,855
Kerala	35.122,966	7.853,651	755.719	3,043	687,104	Saudi Arabia	34.742,883	15.473,708	362,741	6,223	360,076
Telangana	35.193,978	6.882,694	286.354	1,541	278,839	Morocco	36.854,173	5.504,967	439,193	7,388	414,892
Odisha	47.439,243	6.946,965	329.621	1,926	325,432	Spain	46.752,556	26.635,635	1.971,003	50,837	1.684,160
Andhra Pradesh	53.206,421	11.764,418	881.948	7,104	871,588	Kenya	53.611,938	1.023,453	96,458	1,670	50,407
Karnataka	70.462,375	14.078,158	919.496	12.090	896.116	United Kingdom	67.841.324	101.483.230	2.483.393	73.609	1.267.768
Gujarat	71.521.926	9.652.780	245.038	4.306	230.993	Thailand	69.778.286	350.029	6.884	61	4.301

INDIA						Rest of the WORLD (Continued)					
State/Uts	Population	Total number of cases				Country	Population	Total number of cases			
		S*	C*	D*	R*			S*	C*	D*	R*
Rajasthan	79.536.709	5.265.204	308.243	2.696	295.987	Germany	83.750.665	28.576.312	1.745.518	34.194	1.362.394
Tamil Nadu	82.722.262	14.191.494	818.014	12.122	797.391	Iran	83.853.830	8.384.477	1.225.143	55.23	1.044.056
Madhya Pradesh	86.044.251	4.641.648	241.791	3.606	228.831	Turkey	84.222.640	22.778.756	2.208.652	20.881	2.121.531
West Bengal	102.741.588	7.110.430	552.063	9.712	530.366	Egypt	102.078.159	1.484.602	138.062	7.631	119.736
Bihar	126.750.326	18.336.722	252.792	1.397	246.685	Japan	126.523.275	4.441.450	230.304	3.414	194.865
Maharashtra	128.466.921	12.747.633	1.932.112	49.521	1.828.546	Mexico	128.759.156	4.124.947	1.413.935	138.748	1.205.519
Uttar Pradesh	237.095.024	23.943.169	584.966	8.352	562.459	Brazil	212.368.566	22.959.582	7.675.973	194.976	6.942.041

S: Suspected cases (Test done), C: Confirmed cases (Infected), D: Death cases, R: Recovered cases

The results were significant (Z-value ranges from -20556.8045 to -48.8228, p<0.05).

Morbidity cases

Morbidity cases were significantly lower in 19 Indian states/ UTs compared to other countries. The results were significant (Z-value ranges from -2653.7369 to -11.6403, p<0.05). However, morbidity cases were reported to be significantly higher in the remaining 18 Indian states / UTs than in other countries. The results were significant (Z-value ranges from 31.7617 to 801.551, p<0.05).

Mortality cases

Mortality cases caused due to COVID-19 were reported to be significantly lower in 21 Indian states / UTs compared with the other countries. Of these, 19 Indian states / UTs compared with the other countries were lower but found significant (Z-values range from -439.446 to -4.8649, and the p<0.05). However, two Indian states/ UTs compared to the countries such as Lakshadweep vs. The Cayman Islands, and Chandigarh vs. Bahrain reported lower mortality, and the results were insignificant (Z-values=-1.4013 and -0.1708, and the p-values=0.16152 and 0.86502 were greater than 0.05, respectively).

Epidemiologic outcomes, demographic attributes, and prevalence of cases concerning COVID-19 infection persist in India

A total of 184.728,001 individuals, including 43.595,808 (23.6%) symptomatic cases and 141,132,193 (76.4%) asymptomatic cases, were suspected of coronaviral infection, and their swab samples were collected and tested in the COVID-19 laboratory, with 10,280,606 (5.6%) cases confirmed. Of the confirmed cases, 9.875,832 (96.1%) were recovered, while 148,981 (1.4%) died due to COVID-19. The maximum proportion of suspected cases tested in Andaman and Nicobar (47.8%). The highest proportion of confirmed cases found among the suspects was in Maharashtra (15.2%). The highest proportion of cases recovered in Daman and Diu (99.2%). Mortality due to COVID-19 occurred across six UTs and 28 states, with the highest mortality rates reported in Punjab (3.2%) (Table 4).

There were 10.280,606 cases confirmed as COVID-19 among whole Indians; however, only 472.164 (4.6%) of those cases had data available, and 9.808,442 (95.4%) of those cases were missing. Of these available data (N=472.164), data for the gender-based demography of COVID-19 patients were available in 119,593 (25.3%) cases. Of these (N=119,593), there were 78.363 males (65.52%), 41.212 females (35.56%), and 18 transgender individuals (0.02%). The gender ratio was 1.9:1, with men outnumbering females. Of the available data (N=472.164), data for the age group-based demographic classification in COVID-19 patients were available in 117.325 (24.8%) cases. Of these (N=117.325), the maximum cases occurred in adult age groups (41.5%). The lowest cases occurred in infant age groups (0.1%). Among the confirmed cases (10.280,606), 148,981 deaths have occurred, with a 1.4% CFR even so, only 50.183 (33.7%) of those cases had data accessible. Of these (N=50.183), data for the gender-based demography of deceased patients were available in 10.989 (21.9%) cases. Of these

Table 3: Comparison of the pandemic of COVID-19 disease scenario in Indian states and Union Territories compared to other countries with a nearly equal to the current population size during the viral infections with corona (SARS-CoV-2) as of 31st December 2020

Region		Comparison the COVID-19 disease patterns								
		Suspected case			Morbidity			Mortality		
INDIA	Rest of the WORLD	Total test done			Confirmed cases			Death cases		
State/UTs	Country	Z-Value	P-Value	Result	Z-Value	P-Value	Result	Z-Value	P-Value	Result
Lakshadweep	Cayman Islands	-314.7491	< .00001	Significant	-18.2405	< .00001	Significant	-1.4013	0.16152	Not significant
Daman and Diu	Mayotte	-48.8228	< .00001	Significant	-47.7863	< .00001	Significant	-7.0098	< .00001	Significant
Ladakh	French Polynesia	265.101	< .00001	Significant	-45.1314	< .00001	Significant	1.0171	0.30772	Not significant
Dadra Nagar Haveli	Iceland	-2293.3117	< .00001	Significant	-44.0006	< .00001	Significant	-4.8649	< .00001	Significant
Andaman and Nicobar	Martinique	213.3205	< .00001	Significant	-11.6403	< .00001	Significant	1.7914	0.07346	Not significant
Sikkim	Solomon Islands	252.7109	< .00001	Significant	78.227	< .00001	Significant	11.5115	< .00001	Significant
Mizoram	Djibouti	177.2141	< .00001	Significant	-21.4318	< .00001	Significant	-6.8087	< .00001	Significant
Puducherry	Cyprus	NaN	< .00001	Significant	59.7002	< .00001	Significant	18.3211	< .00001	Significant
Arunachal Pradesh	Estonia	79.1123	< .00001	Significant	-58.1804	< .00001	Significant	-10.6006	< .00001	Significant
Goa	Equatorial Guinea	494.9767	< .00001	Significant	189.5234	< .00001	Significant	22.0853	< .00001	Significant
Chandigarh	Bahrain	-1729.8493	< .00001	Significant	-205.9891	< .00001	Significant	-0.1708	0.86502	Not significant
Nagaland	Slovenia	-616.0483	< .00001	Significant	-297.29	< .00001	Significant	-48.4439	< .00001	Significant
Manipur	Lithuania	-1133.3517	< .00001	Significant	-285.4941	< .00001	Significant	-31.1492	< .00001	Significant
Meghalaya	Armenia	-518.1107	< .00001	Significant	356.7296	< .00001	Significant	-49.3654	< .00001	Significant
Tripura	Eritrea	762.6825	< .00001	Significant	168.8009	< .00001	Significant	18.9628	< .00001	Significant
Himachal Pradesh	Sierra Leone	-3421.2739	< .00001	Significant	224.2899	< .00001	Significant	27.4199	< .00001	Significant
Uttaranchal	Sweden	-1211.6043	< .00001	Significant	-500.268	< .00001	Significant	-77.5633	< .00001	Significant
Jammu and Kashmir	Zimbabwe	1964.9498	< .00001	Significant	292.1578	< .00001	Significant	32.0507	< .00001	Significant
Delhi	Mali	2824.2942	< .00001	Significant	684.923	< .00001	Significant	83.8799	< .00001	Significant
Chhattisgarh	Australia	-3948.174	< .00001	Significant	453.1092	< .00001	Significant	37.5338	< .00001	Significant
Haryana	Yemen	2203.3705	< .00001	Significant	506.576	< .00001	Significant	38.6407	< .00001	Significant
Assam	Ghana	2170.7518	< .00001	Significant	309.2701	< .00001	Significant	19.0034	< .00001	Significant
Punjab	Mozambique	1926.2239	< .00001	Significant	343.3474	< .00001	Significant	69.5963	< .00001	Significant
Jharkhand	Peru	-607.1615	< .00001	Significant	-854.8157	< .00001	Significant	-186.4948	< .00001	Significant
Kerala	Saudi Arabia	-1965.3115	< .00001	Significant	368.8008	< .00001	Significant	-33.5619	< .00001	Significant
Telangana	Morocco	519.4292	< .00001	Significant	-160.6584	< .00001	Significant	-59.7195	< .00001	Significant

Comparison the COVID-19 disease patterns (Continued)

Region			Suspected case			Morbidity			Mortality		
INDIA	Rest of the WORLD		Total test done			Confirmed cases			Death cases		
State/UTs	Country	Z-Value	P-Value	Result	Z-Value	P-Value	Result	Z-Value	P-Value	Result
Odisha	Spain	-4288.2013	< .00001	Significant	-1106.836	< .00001	Significant	-214.6729	< .00001	Significant
Andhra Pradesh	Kenya	3215.8398	< .00001	Significant	801.551	< .00001	Significant	58.3708	< .00001	Significant
Karnataka	United Kingdom	-20556.8045	< .00001	Significant	-893.9665	< .00001	Significant	-215.7997	< .00001	Significant
Gujarat	Thailand	3011.1041	< .00001	Significant	468.7476	< .00001	Significant	63.4275	< .00001	Significant
Rajasthan	Germany	-4333.4271	< .00001	Significant	-972.3893	< .00001	Significant	-159.1085	< .00001	Significant
Tamil Nadu	Iran	1349.2285	< .00001	Significant	-276.8263	< .00001	Significant	-164.3608	< .00001	Significant
Madhya Pradesh	Turkey	-3842.8602	< .00001	Significant	-1282.5506	< .00001	Significant	-112.0838	< .00001	Significant
West Bengal	Egypt	1950.8305	< .00001	Significant	496.5024	< .00001	Significant	15.3761	< .00001	Significant
Bihar	Japan	3047.4242	< .00001	Significant	31.7617	< .00001	Significant	29.1421	< .00001	Significant
Maharashtra	Mexico	2176.4504	< .00001	Significant	287.2302	< .00001	Significant	-205.222	< .00001	Significant
Uttar Pradesh	Brazil	-246.7233	< .00001	Significant	-2653.7369	< .00001	Significant	-439.446	< .00001	Significant

Figure 3: Pandemic curves concerning COVID-19 daily number of cases (Confirmed, recovered, and deceased) in the Indian continent during the viral infections with corona (SARS-CoV-2) as of 31st December 2020

Figure 4: Pandemic curves concerning COVID-19 cumulative number of cases (Confirmed, recovered, and deceased) in the Indian continent during the viral infections with coronavirus (SARS-CoV-2) as of 31st December 2020

(N=10.989), males (69.74%) were more vulnerable than females (30.24%). The gender ratio was 2.3:1, with men outnumbering females. Of these available data on deceased patients (N=50.183), data for the age group-based classification in COVID-19 patients were available in 11,518 (23.0%) cases. Of these (N=11.518), senior citizens (52.2%) have the maximum mortality rate among any age group. However, 4112 (0.04%) non-Indians were positive for COVID-19 (Table 5).

COVID-19 pandemic curves with the daily new epidemiological cases

The epidemiological progression of 10.280,606 patients with COVID-19 was based on the patient database. During the 337 days of the pandemic, the average number of new confirmed, recovered, and deceased cases each day was 30506, 29305, and 442, respectively. The rapid growth of newly reported confirmed and dead cases has since been reported (Figure 3).

COVID-19 pandemic curves with the cumulative number of epidemiological cases

The confirmed, recovered, and deceased cases were 10.280,606, 9.875,832, and 148.981, respectively. Only 0.001% of cases of COVID-19 exits until 1st March 2020. COVID-19 reported the first death incident on 13th March 2020. After 48 days of the first case, there was a significant increase in confirmed, recovered, and deceased cases (Figure 4).

Table 4: Epidemiological trends of COVID-19 patients included India's contour during the viral illnesses with coronavirus (SARS-CoV-2) as of 31st December 2020

State/Uts	Population	Total number of cases			
		Suspected	Confirmed	Death	Recovered
Lakshadweep	64.429	0 (0.0)	0 (0.0)	0 (0.0)	0 (0.0)
Daman and Diu	242.911	33.818 (13.9)	1.426 (4.2)	0 (0.0)	1.414 (99.2)
Ladakh	274.289	105.617 (38.5)	9.466 (9.0)	127 (1.3)	9.143 (96.6)
Dadra Nagar Haveli	342.853	38.752 (11.3)	1.938 (5.0)	2 (0.1)	1.906 (98.3)
Andaman and Nicobar	379.944	181.640 (47.8)	4.945 (2.7)	62 (1.3)	4.826 (97.6)
Sikkim	658.361	68.828 (10.5)	5.889 (8.6)	127(2.2)	5.139 (87.3)
Mizoram	1.091.014	177.387 (16.3)	4.199 (2.4)	8 (0.2)	4.091 (97.4)
Puducherry	1.244.464	488.451 (39.2)	38.132 (7.8)	633 (1.7)	37.115 (97.3)
Arunachal Pradesh	1.382.611	378.151 (27.4)	16.719 (4.4)	56 (0.3)	16.564 (99.1)
Goa	1.457.723	397.386 (27.3)	50.981 (12.8)	737 (1.4)	49.313 (96.7)
Chandigarh	1.545.116	181.186 (11.7)	19.748 (10.9)	317 (1.6)	19.045 (96.4)
Nagaland	1.980.602	120.071 (6.1)	11.921 (9.9)	79 (0.7)	11.493 (96.4)
Manipur	2.721.756	474.524 (17.4)	28.139 (5.9)	354 (1.3)	26.601 (94.5)
Meghalaya	2.964.007	291.959 (9.9)	13.408 (4.6)	139 (1.0)	13.085 (97.6)
Tripura	3.671.032	577.343 (15.7)	33.255 (5.8)	382 (1.1)	32.712 (98.4)
Himachal Pradesh	7.663.167	772.021 (10.1)	55.277 (7.2)	922 (1.7)	51.692 (93.5)
Uttaranchal	10.116.752	1.777.371 (17.6)	90.920 (5.1)	1.509 (1.7)	83.506 (91.8)
Jammu and Kashmir	14.849.410	3.822.674 (25.7)	120.971 (3.2)	1.883 (1.6)	116.079 (96.0)
Delhi	20.188.648	8.659.830 (42.9)	625.369 (7.2)	10.536 (1.7)	609.322 (97.4)
Chhattisgarh	25.540.196	3.514.707 (13.8)	279.575 (8.0)	3.371 (1.2)	264.769 (94.7)
Haryana	29.808.027	4.554.156 (15.3)	262.325 (5.8)	2.905 (1.1)	255.853 (97.5)
Assam	31.169.272	5.997.450 (19.2)	216.211 (3.6)	1.045 (0.5)	211.907 (98.0)
Punjab	31.254.208	3.900.473 (12.5)	166.522 (4.3)	5.341 (3.2)	157.496 (94.6)
Jharkhand	32.966.238	4.799.240 (14.6)	115.113 (2.4)	1.030 (0.9)	112.424 (97.7)
Kerala	35.122.966	7.853.651 (22.4)	755.719 (9.6)	3.043 (0.4)	687.104 (90.9)
Telangana	35.193.978	6.882.694 (19.6)	286.354 (4.2)	1.541 (0.5)	278.839 (97.4)
Odisha	47.439.243	6.946.965 (14.6)	329.621 (4.7)	1.926 (0.6)	325.432 (98.7)
Andhra Pradesh	53.206.421	11.764.418 (22.1)	881.948 (7.5)	7.104 (0.8)	871.588 (98.8)
Karnataka	70.462.375	14.078.158 (20.0)	919.496 (6.5)	12.090 (1.3)	896.116 (97.5)
Gujarat	71.521.926	9.652.780 (13.5)	245.038 (2.5)	4.306 (1.8)	230.993 (94.3)
Rajasthan	79.536.709	5.265.204 (6.6)	308.243 (5.9)	2.696 (0.9)	295.987 (96.0)
Tamil Nadu	82.722.262	14.191.494 (17.2)	818.014 (5.8)	12.122 (1.5)	797.391 (97.5)
Madhya Pradesh	86.044.251	4.641.648 (5.4)	241.791 (5.2)	3.606 (1.5)	228.831 (94.6)
West Bengal	102.741.588	7.110.430 (6.9)	552.063 (7.8)	9.712 (1.8)	530.366 (96.1)
Bihar	126.750.326	18.336.722 (14.5)	252.792 (1.4)	1.397 (0.6)	246.685 (97.6)
Maharashtra	128.466.921	12.747.633 (9.9)	1.932.112 (15.2)	49.521 (2.6)	1.828.546 (94.6)
Uttar Pradesh	237.095.024	23.943.169 (10.1)	584.966 (2.4)	8.352 (1.4)	562.459 (96.2)
Total	**1.379.881.020**	**184.728.001 (13.4)**	**10.280.606 (5.6)**	**148.981 (1.4)**	**9.875.832 (96.1)**

Table 5: The demographic attributes and epidemiologic outcomes concerning COVID-19 infection included in India's contour during the viral illnesses with coronavirus (SARS-CoV-2) as of 31st December 2020

Parameters	Patients (N)	Patients %
Confirmed cases	10.280.606	
Indian citizen	10276494	99.96
Non-Indian citizen	4112	0.04
Data available	472.164	4.6
Data missing*	9.808.442	95.4
Gender-based demography of confirmed cases	472.164	
Data available	119.593	25.3
Data missing*	352.571	74.7
Genders		
Male	78.363	65.52
Female	41.212	35.56
Transgender	18	0.02
Age group-based demographic classification of confirmed cases	472.164	
Data available	117.325	24.8
Data missing*	354.839	75.2
Age groups		
< 1 year (infants)	100	0.1
1–14 years (children)	7253	6.2
15–24 years (young adults)	15485	13.2
25–44 years (adults)	48723	41.5
45–60 years (middle-aged persons)	29434	25.1
> 60 years (senior citizens)	16330	13.9
Deceased cases	148.981	
Data available	50.183	33.7
Data missing*	98.798	66.3
Gender-based demographic classification of deceased cases	50.183	
Data available	10.989	21.9
Data missing*	39.194	78.1
Gender		
Male	7664	69.74
Female	3323	30.24
Transgender	2	0.02
Age group-based demographic classification of deceased cases	50.183	
Data available	11.518	23.0
Data missing*	38.665	77.0
Age group		
< 1 year (infants)	7	0.06
1–14 years (children)	41	0.34
15–24 years (young adults)	116	1.0
25–44 years (adults)	1246	10.8
45–60 years (middle-aged persons)	4101	35.6
> 60 years (senior citizens)	6007	52.2

*Data missing=Information not available in the crowd-sourced database of government information systems

DISCUSSION

Public access to a crowd-based information system is crucial in community-based public health approaches (17). The pandemic burden of COVID-19 disease between India and the rest of the world, as epidemiological factors, is assessed. We organized into groups of 37 Indian administrative regions comprising 28 states and nine UTs with 37 countries based on population sizes to determine the COVID-19 pandemic epidemiological variation between Indian states and UTs, with the selected countries.

SARS-CoV-2 infection result that, 7.417 million people at risk worldwide. COVID-19 affects 99.9% of Indians, affecting all parts of India except Lakshadweep. SARS-CoV-2 strain is typically considered unavoidable (12, 18). The disparity in confirmed cases between India and the rest of the world was 1:7.2. India had a lower mortality burden due to SARS-CoV-2 infection than the rest of the world. The COVID-19 pandemic was the most severe health hazard in the 21st century, with higher morbidity and mortality than previous global pandemics (13, 19). Our study revealed that India has 13.4% of suspected cases worldwide has 16.8. Compared to other countries, 17 Indian states/UTs reported fewer tests performed, which showed significant results. According to Reuben Abraham, the COVID-19 pandemic was spotted two months later in India than in other countries, resulting in fewer confirmed cases (20). According to print media sources, categorized persons are difficult to diagnose despite most asymptomatic cases due to their travel history (21). According to Battegay et al., due to the COVID-19 test's limited capacity, there were fewer suspects or clinically diagnosed cases (22). We concurred with these possible explanations for the suspected lower case rate than other countries in many of India's administrative regions. India had 5.6% confirmed coronavirus infections, while the global average was 7.3%. We found that morbidity in 19 Indian states/UTs was low compared to other countries. The outcomes were noteworthy, and experts had few hypotheses about why the morbidity remained low compared to other countries. According to Dr. Shahid Jameel, the early coronavirus lockdown in India contributed to minimal morbidity compared to other countries with nearly equal populations (23). According to Dr. Shiv Ayyar, the low confirmed case rate is due to limited COVID-19 testing in India (23). Ankita Sharma indicated that many cases are tested through RT-PCR and RDT (Antibody), so it is possible to perceive the exact numbers and classification of the infected cases of COVID-19 (23). According to the medical journal Lancet editor, the COVID-19 disease morbidity curve tends to flatten due to the Indian lockdown (24). We agreed with the Lancet editor's comments and shared experts' hypotheses in various newsletters. Compared to other countries, we found lower mortality due to COVID-19 in 21 Indian states/UTs. Of these, the mortality rate in 19 states/UTs was statistically significant, and two states/UTs were statistically insignificant ($p>0.05$). According to Miller et al., the Bacillus Calmette – Guérin (BCG) vaccine for tuberculosis, leprosy, Buruli ulcer, and bladder cancer is used in corona therapy in India, which reduces mortality rates (25). According to an expert, the hydroxyl chloroquine malaria vaccine was used in COVID-19, minimizing the number of deaths (26). Dr. Prabhat Jha states that over 80% of deaths in India occur at home or in rural regions without a proper medical death certificate. Such cases shall not be held liable for the fatality rates of COVID-19 (27, 28). In another expert's opinion, elderly populations are more vulnerable to corona and becoming more complicated. Furthermore, India's low COVID-19 mortality rates are due to a higher proportion of adults than other age groups (23). The findings of Miller et al. and the epidemiological hypothesis of experts on low COVID-19 mortality rates in India compared to other countries are possible facts that could be linked to our study outcomes.

In India, during the initial 337 days of the coronavirus infections, our findings, as indicated by the pandemic curves of epidemiological cases of COVID-19, 48 days after the first occurrence, the daily cases resulted in daily peaks most significantly. The cumulative number of confirmed, recovered, and deceased patients increased tremendously with an upward trend. COVID-19 spread rapidly to every corner of the Indian mainland except Lakshadweep, indicating that the strain of SARS-CoV-2 had the inherent potential to extend this epidemic (29). The suspected case rate of COVID-19 has ranged from 5.4% to 47.8%. Andaman and Nicobar reported the maximum cases of suspected individuals. SARS-CoV-2 has caused distinct illness characteristics, including 23.6% of symptomatic and 76.4% of asymptomatic patients. Our findings concurred with the previous studies undertaken by Guan et al. and Huang et al. (30, 31). Maharashtra had the most affected individuals. Daman and Diu had no reported deaths, whereas Punjab had the most. In India, the COVID-19 pandemic had a morbidity rate of about 5.6%, while the CFR was 1.4%. Indian morbidity rate remains high, and CFRs remain low compared to previous outbreaks in 2002-2003 (SARS) and 2012 (MERS) (32, 33).

Our study indicated that males outstripping females were susceptible to SARS-CoV-2, and the gender ratio was 1.9:1. According to Dr. Kyle Sue, sex hormones, including estrogen and testosterone, have a more vital role in severely affecting males than females in viral respiratory diseases (34). According to Schurz et al., the X-chromosome possesses the highest proportion of antibodies in the human genomes, which has a prominent influence in severely impacting males than females in viral respiratory problems (35). According to Voor, male blood plasma has higher angiotensin-converting enzyme 2 (ACE2) concentrations than female blood plasma, indicating a higher probability of COVID-19 (36). According to Harris and Jenkins, males are likely to spend more time engaging outside than females, which is a familiar concept and leads to higher opportunities for health-related risks (37). These studies corroborate our finding by Sue, Schurz et al., Voor, and Harris and Jenkins that infection with SARS-CoV-2 is more common in males than in females. We found that the age groups 25-44 years (adults) followed by 45-60 years (middle-aged individuals) were more susceptible to COVID-19 than the other four age groups studied. Our findings concurred with the study results of Jin Lv et al., that adults aged 25-44 and middle-aged individuals aged

45-60 are more affected by infectious diseases than other age groups (38). We found that most deaths occurred among senior citizens (> 60 years). Greenbaum et al., points out that older people with chronic deformities associated with COVID-19 have become more vulnerable, leading to death (39). According to Yi et al., senior citizens than other age groups experience health hazards and death from COVID-19 (40). Our findings corroborate Greenbaum et al. and Yi et al.'s conclusions.

Several researchers used innovative tools, i.e., mathematical models, to evaluate the trends of any ongoing epidemics and predict the spread of pandemics in the future, which can be utilized as a preventive perspective for the public (41-43). Meanwhile, the coronavirus that causes COVID-19 has mutated into new variants of the virus, resulting in the Seventh wave of a new coronavirus variant, i.e., Omicron's XBB to BA.7, will encounter in the Indian continent in recent days, as predicted by the International research organization GISIAD. According to GISIAD report, there have been around three hundred and eighty verified instances of XBB in India, with Tamil Nadu having the most recorded incidents (175 cases), followed by West Bengal (103 cases) (44).

Limitations of this study

We did not study the spatial and temporal correlations with COVID-19 in India and globally.

CONCLUSION

This prospective analytical study highlighted that the daily and cumulative number of confirmed and deceased patients increased drastically during the initial 337 days of corona in India. In India, COVID-19 was more prevalent in males and patients aged 25-44, while senior citizens mostly died due to SARS-CoV-2. Bihar had the most infections, and Punjab had the most deaths in India. India had lower confirmed cases and mortality than the rest of the world, with a ratio of 1:7.2 and 1:12, respectively. Contrasting COVID-19 trends between the Indian mainland with populations almost equal to the countries selected, many of India's administrative regions had lower morbidity and mortality rates. India's lockdown policy is gradually lifted as the new coronavirus variant weakens its havoc. Coronavirus has mutated into new variants at regular intervals. Undertake more analytical studies to understand the risk factors associated with COVID-19's epidemiological characteristics as the new coronavirus variant wave evolves. In addition, spatial and temporal-related analyses will require elucidating the role of climatic influence in coronavirus infection. Furthermore, advanced mathematical model-based studies are needed to forecast the severity and understand disease epidemiology, which would help plan and target preventive health care.

Acknowledgements: The authors are thankful to the personnel who maintained the database of a novel coronavirus (COVID-19) on government-approved web portals for public accessibility.

Ethics Committee Approval: A population-based comparative optimization algorithms study was conducted on all cases reported by 31st December 2020, during SARS-CoV-2 infections. The epidemiological data on COVID-19 disease and population status in 2020 is gathered from government-approved web portals that are freely accessible to the public. Therefore, patient consent and ethical clearances are not required. We obtained pre-approval from the Director-General Sir of the Indian Council of Medical Research to publish this original research article.

Peer Review: Externally peer-reviewed.

Author Contributions: Conception/Design of Study- M.R.K.R.; Data Acquisition- M.R.K.R.; Data Analysis/Interpretation- M.R.K.R.; Drafting Manuscript- M.R.K.R.; Critical Revision of Manuscript- M.R.K.R., R.N.P., M.K.D.; Final Approval and Accountability- M.R.K.R., R.N.P., M.K.D.; Material and Technical Support- M.R.K.R.; Supervision- M.R.K.R., R.N.P., M.K.D.

Conflict of Interest: The authors have no conflict of interest to declare.

Financial Disclosure: The authors declared that this study has received no financial support.

REFERENCES

1. Syed A. Coronavirus: a mini-review. Int J Curr Res Med Sci 2020;6(1):8-10.
2. Proenca-Modena JP, Acrani GO, Srinder CB, Arruda E. Respiratory Viral Infections. 3rd ed. Tropical Infectious Diseases: Principles, Pathogens and Practice; 2011.p.379-91.
3. Heesterbeek H, Anderson RM, Andreasen V, Bansal S, Angelis DD, Dye C, et al. Modeling infectious disease dynamics in the complex landscape of global health. Science 2015;347(6227):aaa4339.
4. Bogoch II, Watts A, Thomas-Bachli A, Huber C, Kraemer MUG, Khan K. Pneumonia of unknown aetiology in Wuhan, China: potential for international spread via commercial air travel. J Travel Med 2020;27(2):taaa008.
5. Wang C, Hornby PW, Hayden FG, Gao GF. A novel coronavirus outbreak of global health concern. Lancet 2020;395(10223):470-3.
6. World Health Organization (WHO). Naming the coronavirus disease (COVID-19) and the virus that causes it. Geneva: WHO 2020.
7. Anonymous. Coronavirus-Wikipedia. https://en.wikipedia.org/wiki/Coronavirus.
8. Paules CI, Marston HD, Fauci AS. Coronavirus infection—more than just the common cold. JAMA 2020;323(8):707-8.
9. Gorbalenya AE, Baker SC, Baric RS, Groot RJD, Drosten C, Gulyaeva AA, et al. The species severe acute respiratory syndrome-related coronavirus: classifying 2019-nCoV and naming it SARS-CoV-2. Nat Microbio 2020;5(4):536-44.
10. Cohen J, Mining coronavirus genomes for clues to the outbreak's origins. 2020. https://www.sciencemag.org/news/2020/01/mining-coronavirus-genomes-clues-outbreak-s-origins.
11. Reid D. India confirms its first coronavirus case. CNBC 2020. https://www.cnbc.com/2020/01/30/india-confirms-first-case-of-the coronavirus.html.
12. Yadav PD, Potdar VA, Choudhary ML, Nyayanit DA, Agrawal M, Jadhav SM, et al. Full-genome sequences of the first two SARS-CoV-2 viruses from India. Indian J Med Res 2020;151(2&3):200-9

13. World Health Organization. Novel Coronavirus (2019-nCoV) Situation Report-11. https://www.who.int/docs/default-source/coronaviruse/situation-reports/20200131-sitrep-11-ncov.pdf?sfvrsn=de7c0f7_4.
14. Centers for Disease Control and Prevention (CDC). Coronavirus Disease 2019 (COVID-19): Symptoms of Coronavirus. CDC 2020. https://www.cdc.gov/coronavirus/2019-ncov/symptoms-testing/symptoms.html.
15. Guo YR, Cao QD, Hong Z, Tan YY, Chen SD, Jin HJ, et al. The origin, transmission and clinical therapies on coronavirus disease 2019 (COVID-19) outbreak - an update on the status. Mil Med Res 2020;7(1):11.
16. Zou L, Ruan F, Huang M, Liang L, Huang H, Hong Z, et al. SARS-CoV-2 viral load in upper respiratory specimens of infected patients. N Engl J Med 2020;382(12) :1177-9
17. Tucker JD, Day S, Tang W, Bayus B. Crowdsourcing in medical research: concepts and applications. Peer J 2019;7:e6762.
18. Bai Y, Yao L, Wei T, Tian F, Jin DY, Chen L, Wang M. Presumed asymptomatic carrier transmission of COVID-19. JAMA 2020;323(14):1406-7.
19. Morse SS. Pandemic influenza: studying the lessons of history. Proc Natl Acad Sci USA 2007;104(18):7313-4
20. Abraham R. Why does India have so few COVID-19 cases and deaths? IDFC Institute 2020. http://www.idfcinstitute.org/knowledge/publications/op-eds/why-does-india-have-so-few-covid-19-cases-and-deaths/.
21. Anonymous. Is India running too few coronavirus tests? The Hindu business line, New Delhi; India 17.03.2020. https://www.thehindubusinessline.com/news/national/is-india-running-too-few-coronavirus-tests/article31074309.ece.
22. Battegay M, Kuehl R, Tschudin-Sutter S, Hirsch HH, Widmer AF, Neher RA. 2019-Novel coronavirus (2019-nCoV): estimating the case fatality rate: a word of caution. Swiss Med Wkly 2020;150:w20203.
23. Anonymous. What Explains India's Low COVID-19 Death Rate. Fit Connect, 04.05.2020. https://fit.thequint.com/coronavirus/explained-indias-low-covid-19-fatality-rate.
24. Editorial. India under COVID-19 lockdown. Lancet 2020;395(10233):1315.
25. Miller A, Reandelar MJ, Fasciglione K, Roumenova V, Li Y, Otazu GH. Correlation between universal BCG vaccination policy and reduced morbidity and mortality for COVID-19: an epidemiological study. MedRxiv 2020. doi: https://doi.org/10.1101/2020.03.24.20042937.
26. Anonymous. Coronavirus | Preventive drug for healthcare workers cleared. The Hindu. New Delhi. 24.03.2020. https://www.thehindu.com/sci-tech/health/coronavirus-icmr-prescribes-anti-malarial-drug-for-high-risk-covid-19-cases/article31142391.ece.
27. Anonymous. In India, most deaths go unregistered. How reliable is its COVID-19 mortality data? Scroll. in. 16.06.2020. https://scroll.in/article/961081/in-india-most-deaths-go-unregistered-how-reliable-is-its-covid-19-mortality-data.
28. Anonymous. Report on medical certification of cause of death 2017. Office of the registrar general, India. Government of India, Ministry of home affairs 2017. https://censusindia.gov.in/2011-Documents/mccd_Report1/MCCD_Report-2017.pdf.
29. Rocklov J, Sjodin H, Wilder-Smith A. COVID-19 outbreak on the Diamond Princess cruise ship: estimating the epidemic potential and effectiveness of public health countermeasures. J Trave Med 2020;18(27)(3):taaa 030.
30. Huang C, Wang Y, Li X, Ren L, Zhao J, Hu Y, et al. Clinical features of patients infected with 2019 novel coronavirus in Wuhan, China. Lancet 2020;395(10223):497-506.
31. Guan WJ, Ni ZY, Hu Y, Liang WH, Ou CQ, He JX, et al. Clinical characteristics of coronavirus disease 2019 in China. N Engl J Med 2020;382(18):1708-20.
32. Wit ED, Doremalen NV, Falzarano D, Munster VJ. SARS and MERS: recent insights into emerging coronaviruses. Na. Rev Microbio 2016;14(8):523-34.
33. Wu Z, McGoogan JM. Characteristics of and important lessons from the coronavirus disease 2019 (COVID-19) Outbreak in China: Summary of a report of 72314 cases from the Chinese Center for Disease Control and Prevention. JAMA 2020;323(13):1239-42.
34. Sue K. The science behind "man flu". BMJ 2017;359:j5560.
35. Schurz H, Salie M, Tromp G, Hoal EG, Kinnearet CJ, Moller M. The X chromosome and sex-specific effects in infectious disease susceptibility. Hum Genomics 2019;13(1):2.
36. Voor A. Men's blood contains greater concentrations of enzyme that helps COVID-19 infect cells. European Society of Cardiology 2020. https://www.sciencedaily.com/releases/2020/05/200510193241.htm.
37. Harris CR, Jenkins M, Glader D. Gender differences in risk assessment: Why do women take fewer risks than men? Judgm Decis Mak 2006;1(1):48-63.
38. Lv J, Ren ZY, Zhang YY. Study on age-dependent pre-existing 2009 pandemic influenza virus T and B cell responses from Chinese population. BMC Infect Dis 2017;17(1):136.
39. Greenbaum AH, Chen J, Reed C, Beavers S, Callahan D, Christensen D, et al. Hospitalizations for severe lower respiratory tract infections. Pediatrics 2014;134(3):546-54
40. Yi Y, Lagniton PNP, Ye S, Li E, Xu RH. COVID-19: what has been learned and to be learned about the novel coronavirus disease. Int J Biol Sci 2020;16(10):1753-66.
41. Arino J, Bauch C, Brauer F, Driedger SM, Greer AL, Moghadas SM, et al. Pandemic influenza modeling and public health perspectives. Math Biosci Eng 2011;8(1):1-20.
42. Royal Society. Infectious diseases in livestock, 2002. The Royal Society policy document 19/02. www.royalsoc.ac.uk.
43. Ray D, Salvatore M, Bhattacharyya R, Wang L, Du J, Mohammed S, et al. Predictions, role of interventions, and effects of a historic national lockdown in India's response to the COVID-19 pandemic: Data Science Call to Arms. Harv Data Sci Rev 2020;2020(Suppl 1):10.1162/99608f92.60e08ed5.
44. Anonymous. Covid-19: Omicron's XBB variant emerges as dominant in India. The India Post, India 31.10.2022. Covid-19: Omicron's XBB variant emerges as dominant in India, TN tops, India Post News Paper.

RESEARCH ARTICLE / ARAŞTIRMA MAKALESİ
Journal of Advanced Research in Health Sciences /
Sağlık Bilimlerinde İleri Araştırmalar Dergisi 2023
DOI: 10.26650/JARHS2023-1252949

COVID-19 REINFECTION: DOES IT MATTER?

COVID-19 RE-ENFEKSİYONU: ÖNEMLİ Mİ?

E. Füsun KARAŞAHİN[1], Ömer KARAŞAHİN[2], Mehtap Hülya ASLAN[3]

[1] Erzurum Provincial Health Directorate, Presidency of Publich Health, Erzurum, Turkiye
[2] University of Health Sciences, Erzurum Faculty of Medicine, Department of Infectious Diseases and Clinical Microbiology, Erzurum, Turkiye
[3] Erzurum Regional Training and Research Hospital, Medical Microbiology, Erzurum, Turkiye

ORCID ID: E.F.K. 0000-0003-4145-8117; Ö.K. 0000-0002-4245-1534; M.H.A. 0000-0002-8455-5120

Citation/Atıf: Karasahin EF, Karasahin O, Aslan MH. COVID-19 reinfection: does it matter? Journal of Advanced Research in Health Sciences 2023;6(3):263-269. https://doi.org/10.26650/JARHS2023-1252949

ABSTRACT

Objective: The aim of this study was to present the descriptive findings of 65 patients evaluated as clinical COVID-19 reinfection.

Materials and Methods: We conducted a retrospective chart review of COVID-19 reinfection cases recorded by the provincial health directorate. The time between infections (days), whether the patient was hospitalized, symptoms at the time of both positive tests, presence of risky contact, occupation, lung imaging results, laboratory findings, and RT-PCR cycle threshold (Ct) values were recorded. Results were expressed as mean (standard deviation [SD]) or median (interquartile range [IQR]), and categorical variables were expressed as frequency (percentage).

Results: The mean time between infections was 124.9 (SD 39.7) days and the median was 117 (IQR 96-143.5) days. Reinfection occurred after 45 to 89 days in 10 patients (15.4%) and after 90 days or more in 55 patients. The shortest time to reinfection was 60 days and the longest time was 272 days. The median Ct value was 24.5 (IQR 22-26.5) among patients reinfected after 45 to 89 days and 28 (IQR 25-32) among those reinfected after at least 90 days.

Conclusion: This study demonstrated that the frequency of COVID-19 reinfection is higher than predicted. The complex algorithms recommended by international health institutions make it difficult to detect these cases. However, rapid identification of these patients is essential to prevent new infections and control the pandemic.

Keywords: COVID-19, pandemics, reinfection

ÖZ

Amaç: Bu çalışmada amacımız klinik re-enfeksiyon olarak tanımlanan 65 hastanın tanımlayıcı bulgularını sunmaktır.

Gereç-Yöntem: İl sağlık müdürlüğü tarafından kaydı tutulan re-enfeksiyon vakalarının retrospektif dosya taraması yapılmıştır. İki enfeksiyon arasında geçen süre (gün), hastane yatışı olup olmadığı, vakaların her bir pozitif test sonucu dönemindeki şikayetleri, riskli temas durumları, sağlık çalışanı olup olmadıkları, varsa akciğer görüntülemesi sonuçları, laboratuvar bulguları ve RT-PCR Ct değerleri kaydedilmiştir. Bulgular ortalama±standart sapma, ortanca (çeyrekler arası değer - IQR), kategorik değişkenler frekans (yüzde) olarak sunulmuştur.

Bulgular: İki enfeksiyon arasında geçen ortalama süre 124,9±39,7 gün ve ortanca ise 117 (IQR 96 – 143,5) gündü. 10 (15,4%) kişide 45-89 gün, 55 kişide 90 gün veya daha uzun süre sonra re-enfeksiyon görüldü. Tespit edilen en kısa süre 60 gün ve en uzun süre ise 272 gündü. 45-89 gün arası sürede re-enfekte olanların ortanca Ct değeri 24,5 (22-26,5), ≥90 gün sonra re-enfekte olanların ortanca Ct değeri 28 (25-32) idi.

Sonuç: Bu çalışma ile COVID-19 re-enfeksiyon sıklığının tahmin edildiğinden daha yüksek olduğu gösterilmiştir. Uluslararası sağlık kuruluşları tarafından önerilen kompleks algoritmalar bu vakaların tespiti zorlaştırmaktadır. Ancak pandemi mücadelesi sırasında elzem olan husus vakaları çok hızlı tespit ederek yeni bulaşların olmasını önlemektir.

Anahtar kelimeler: COVID-19, pandemi, re-enfeksiyon

Corresponding Author/Sorumlu Yazar: E. Füsun KARAŞAHİN **E-mail:** karasahinfusun@gmail.com

Submitted/Başvuru: 18.02.2023 • **Accepted/Kabul:** 22.06.2023 • **Published Online/Online Yayın:** 13.10.2023

INTRODUCTION

Severe acute respiratory syndrome coronavirus 2 (SARS-CoV-2) infection was first reported in China and rapidly spread worldwide, appearing in Turkiye on March 10, 2020 (1, 2). On March 11, 2020, the World Health Organization (WHO) declared it a pandemic, and the first case in Turkiye province was reported on March 15, 2020, in a person who had returned from Umrah (3).

New information about SARS-CoV-2 infection is constantly emerging as scientists all over the world strive to elucidate the disease it causes, coronavirus disease 2019 (COVID-19). However, after the first year of the pandemic, there is still much we do not understand about COVID-19. One of these areas is reinfection.

The American Centers for Disease Control and Prevention (CDC) established research criteria for identifying cases of reinfection and recommended the use and evaluation of genomic testing of paired samples. According to their protocol, genome sequencing should be performed in patients who test positive for SARS-CoV-2 RNA again after a period of longer than 90 days (those with cycle threshold Ct value < 33 or no available Ct value). Patients who retest positive for SARS-CoV-2 RNA within 45 to 89 days must have definitive symptoms that cannot be explained by an etiology other than COVID-19 or have a history of close contact with a COVID-19 patient to be considered reinfection. Again, genomic sequencing of old and new samples (those with Ct < 33 or without a Ct value) is recommended. If genomic testing capacity is limited, the suspicion of reinfection is higher for patients with 90 days or more between two positive tests (4). In contrast, the European Centre for Disease Control and Prevention (ECDC) suggested a more complex assessment, but stated that there is still no consensus and that a case definition must be established (5). Yahav et al. referred to the difficulty of the definitions developed by the CDC and ECDC and emphasized that a simpler definition of reinfection is needed for treatment and infection control measures. In their study, they proposed categorizing reinfection as confirmed, clinical, and epidemiological. They also developed definitions for relapse/reactivation and repositivity (6).

The present study aimed to present the findings of cases of clinical reinfection, which we believe must be defined in order to prevent the disruption of treatment and infection control measures.

MATERIALS and METHODS

Patient selection

This retrospective descriptive study included 65 cases evaluated as clinical reinfection. The first case of reinfection was recorded on August 18, 2020, and the last case within the study period was detected on January 3, 2021.

Our province consists of a total of 20 districts, 3 central and 17 peripheral (the most remote district is 180 km from the center). As part of the pandemic management plan, oronasopharyngeal samples obtained in the 17 peripheral districts are transported to the public health laboratory in the central district at least three times per day using the specimen transport system established. Specimens obtained by contract tracing teams in the central districts are delivered immediately to the public health laboratory. Hospitals designated as pandemic hospitals only process specimens collected on the premises. In the last three months, the mean turnaround time from requesting a specimen to receiving the result was 7.55 hours.

The results of each specimen analyzed in the two laboratories that process SARS-CoV-2 samples were immediately shared with the Provincial Pandemic Operations Center. Based on these results, contact tracing teams were directed (number of teams, etc.). In addition, this data is recorded by the Directorate of Public Health Services, which oversees the Provincial Pandemic Operations Center, and is analyzed daily (e.g., daily new cases, daily test numbers, test positivity rate, case distribution by district/neighborhood/workplace, mortality and case-fatality rates).

As a result, each laboratory test is recorded by the Directorate of Public Health Services, and each patient's previous positive results are also followed. Unfortunately, this monitoring must be performed manually, as there is no application in the contact tracking and reporting systems implemented by the Ministry of Health that presents the previous data of people who have retested positive for SARS-CoV-2.

The Directorate of Public Health Services calls all patients who have a positive test result after an interval of 45 to 89 days to question their symptoms and reason for providing another specimen. Symptomatic patients are referred to a pandemic hospital and examined by an infectious disease specialist. If the physician concludes the patient has clinical reinfection, they arrange treatment. Immunosuppressed patients and those whose symptoms never improved are not considered reinfection.

The following diagnostic criteria for clinical reinfection were used:

i) After 90 days or more:

- Real-time polymerase chain reaction (RT-PCR) positive for SARS-Cov-2 (Ct < 35),

- Recurrence of symptoms consistent with COVID-19 after complete resolution of all symptoms of the first infection,

- High-risk contact or being in a region with an increase in cases,

- Absence of any other etiology to explain the clinical presentation.

ii) Within 45 to 89 days:

- All criteria mentioned above as well as two negative RT-PCR test results between infections (6).

The algorithms of the contact tracing software used were created according to the guidelines of the Ministry of Health. Therefore, the contact tracing process is automatically initiated for patients with another positive test result after more than 90 days but not for those with another positive test result after 45 to 89 days. Creating a new contact tracing process for reinfected patients is performed manually. Then, a contact screening is performed, and isolation and quarantine protocols are implemented.

Data collection

We conducted a retrospective chart review of the list of COVID-19 reinfection cases maintained by the provincial health directorate. The time between infections (days), whether the patient was hospitalized, symptoms experienced at the time of both positive tests, presence of risky contact, occupation, lung imaging results (if available), RT-PCR Ct values, and laboratory findings including C-reactive protein, D-dimer, ferritin, hemoglobin, white blood cell, neutrophil, and lymphocyte counts, lactate dehydrogenase, aspartate aminotransferase, alanine aminotransferase, creatinine, and albumin values were recorded. Because anti-SARS-CoV-2 antibodies are not analyzed in healthcare facilities affiliated with the Ministry of Health, antibody results were not available for these patients. After the study data were collected, the patient list was anonymized, and statistical analyses were performed. During the reinfection dates included in this study, and even at the time of writing, influenza had not yet been detected in the province.

RT-PCR

Bio-Speedy COVID-19 RT-qPCR (Bioeksen, Istanbul) kits were used to detect SARS-CoV-2 RNA in the patients' nasopharyngeal and oropharyngeal specimens. RT-PCR was performed in the C1000 Touch CFX96 (Bio-Rad, USA) device.

Statistical analyses

A statistics software package was used for all analyses. Continuous data were presented as mean (standard deviation SD) or median (interquartile range IQR), and categorical variables as frequency (percentage).

Ethics Committee Approval

This study was approved by the Clinical Research Ethical Committee of the Erzurum Regional Training and Research Hospital (Date:01.03.2021, No:2021/05-85). Due to the retrospective nature, informed consent was not obtained.

RESULTS

A total of 65 reinfection cases were included in the study. The rate of reinfection among all cases followed in our center was 0.12%. The mean (SD) age of the patients was 36.3 (14.8) years, and the median (IQR) age were 31 (24.5-47.0) years. Thirty-four patients (52.3%) were male and 29 (44.6%) were health workers. The health workers included 14 nurses, 5 doctors, and 10 support staff (health technician, security guard, secretary). Twenty-five of the health workers were working in designated

Table 1: Descriptive findings of the patients according to time to reinfection

	Reinfected within 45-89 days (n=10)		Reinfected after ≥ 90 days (n=55)	
	First infection	Reinfection	First infection	Reinfection
Age (years), mean (SD)	38.9 (15.8)	-	35.8 (14.7)	-
Sex (male), n (%)	8 (80.0)	-	26 (47.3)	-
Cycle threshold value, median (IQR)	24.5 (19-27.2)	24.5 (22-26.5)	24 (21-28)	28 (25-32)
Health worker, n (%)	6 (60.0)	-	23 (41.8)	-
Risky contact, n (%)	6 (60.0)	10 (100.0)	34 (61.8)	35 (63.6)
Hospital admission, n (%)	4 (40.0)	1 (10.0)	20 (36.4)	7 (12.7)
Length of hospital stay (days), mean (SD)	9.25 (3.1)	6	9.95 (5.8)	9.1 (3.0)
Negative test between infections, n (%)	10 (100.0)	-	42 (76.4)	-
Comorbidity, n (%)	1 (10.0)	-	17 (30.9)	-
Epilepsy	-	-	1 (1.8)	-
Chronic hepatitis B	-	-	1 (1.8)	
Asthma	-	-	6 (10.9)	-
Diabetes mellitus	1 (10.0)	-	4 (7.3)	-
Hypertension	-	-	8 (14.5)	-
Heart failure	-	-	1 (1.8)	-
Chronic kidney disease	-	-	1 (1.8)	-
History of malignancy	-	-	1 (1.8)	-
COPD	-	-	7 (12.7)	-

COPD: Chronic obstructive pulmonary disease, IQR: Interquartile range, SD: Standart deviation

Table 2: Symptoms according to time to reinfection

	Reinfected within 45-89 days (n=10)		Reinfected after ≥90 days (n=55)	
	First infection	Reinfection	First infection	Reinfection
Symptomatic, n (%)	10 (100.0)	10 (100.0)	41 (74.5)	41 (74.5)
Dyspnea, n (%)	4 (40.0)	2 (20.0)	12 (21.8)	12 (21.8)
Fatigue, n (%)	4 (40.0)	5 (50.0)	23 (41.8)	23 (41.8)
Muscle/joint pain, n (%)	6 (60.0)	7 (70.0)	20 (36.4)	24 (43.6)
Sore throat, n (%)	1 (10.0)	4 (40.0)	8 (14.5)	15 (27.3)
Loss of taste, n (%)	1 (10.0)	1 (10.0)	3 (5.5)	1 (1.8)
Loss of smell, n (%)	1 (10.0)	2 (20.0)	3 (5.5)	2 (3.6)
Hearing loss, n (%)	-	-	1 (1.8)	-
Headache, n (%)	4 (40.0)	4 (40.0)	8 (14.5)	14 (25.5)
Diarrhea, n (%)	2 (20.0)	2 (20.0)	5 (9.1)	1 (1.8)
Cough, n (%)	2 (20.0)	2 (20.0)	11 (20.0)	17 (30.9)

Table 3: Imaging and vital signs according to time to reinfection

	Reinfected within 45-89 days (n=10)		Reinfected after ≥90 days (n=55)	
	First infection	Reinfection	First infection	Reinfection
Radiological findings, n (%)				
CT findings not typical/no findings (%)	2/2 (50.0)	4/2 (66.7)	9/19 (32.1)	9/11 (45.0)
Bilateral lung involvement	2 (50.0)	3 (50.0)	4 (14.3)	5 (25.0)
Ground-glass opacities	2 (50.0)	4 (66.7)	7 (25.0)	9 (45.0)
Greater than 50% involvement	-	-	3 (10.7)	1 (5.0)
Vital findings, n (%)				
Hypoxia (saturation < 93%)	1 (10.0)	2 (20.0)	3 (5.5)	5 (9.1)
Tachycardia (pulse > 100/min)	-	-	5 (9.1)	4 (7.3)

CT: Computerized tomography

Table 4: Laboratory findings according to time to reinfection

Laboratory findings, median (IQR)	Reinfected within 45-89 days (n=10)		Reinfected after ≥90 days (n=55)	
	First infection	Reinfection	First infection	Reinfection
CRP (mg/dL)	7.5 (3.5-14.4)	5.0 (2.8-6.9)	4.3 (3-6.2)	5 (5-13.4)
D-dimer (ng/dL)	245 (190-915)	224 (190-394.5)	305 (155-407.5)	297 (190-502)
Ferritin (mg/dL)	54.6 (3-54.6)	97.1 (21.5-106.9)	34.1 (18.2-93)	33.9 (19.8-95.4)
Hemoglobin (g/dL)	15.5 (13.2-15.9)	16.0 (12.8-16.7)	14.6 (13.6-15.5)	14.3 (13.3-15.6)
White blood cell count ($x10^3$/L)	6680 (5540-7285)	6535 (4675-7902)	7170 (5350-9300)	6640 (5630-8340)
Neutrophil count ($x10^3$/L)	3270 (2705-3670)	2765 (1807-4642)	4440 (3120-5360)	4000 (2990-5365)
Lymphocyte count ($x10^3$/L)	2800 (1305-3420)	2090 (1740-2605)	2290 (1700-3160)	2210 (1505-2655)
PLT ($x10^3$/L)	229 (198.5-319.5)	228 (196.5-292.5)	245 (191-295)	247 (215-289)
LDH (U/L)	186 (166.5-213.5)	195 (187.7-231.7)	190.5 (173.5-227.7)	208 (183.5-262.7)
AST (U/L)	26 (19.5-31)	31 (17-44.7)	18 (16-26.5)	23 (17.5-26)
ALT (U/L)	32 (19-39)	36.5 (17.5-50)	20.5 (14-36.7)	23 (15-27)
Creatinine (g/dL)	0.9 (0.7-1.2)	0.9 (0.7-0.9)	0.8 (0.6-0.9)	0.7 (0.6-0.9)
Albumin (mg/dL)	45 (43-51)	47.1 (43.7-49.5)	45 (42-47)	45.5 (42.2-47)

CRP: C-reactive protein; PLT: Platelet count; LDH: Lactate dehydrogenase, AST: Aspartate aminotransferase, AST: Alanine aminotransferase, ALT: Alanine aminotransferase

pandemic hospital that only treated COVID-19 patients. Cases of reinfection were most frequent in August and November, when the province reached peak case numbers.

The mean time between infections was 124.9 (SD 39.7) days and the median was 117 (IQR 96-143.5) days. Reinfection occurred after 45 to 89 days in 10 patients (15.4%) and after 90 days or more in the other 55 patients. The shortest time to reinfection was 60 days and the longest time was 272 days. Fifty-two patients (80.0%) had at least one negative test result between infections.

Eighteen (27.7%) of the patients had at least one comorbidity. These included hypertension (n= 8;12.3%), chronic obstructive pulmonary disease (n=7;10.8%), asthma (n=6; 9.2%), diabetes mellitus (n= 5;7.7%), and one patient each with malignancy, epilepsy, chronic kidney failure, heart failure, and chronic hepatitis.

History of contact with an active COVID-19 patient was present in 40 patients (61.5%) before the first infection and 45 (69.2%) before the second infection, and 29 of these patients were health workers. Twenty-four patients (36.9%) were hospitalized during the first infection, 8 (12.3%) during the second infection, and four patients during both infections. Forty-four (67.7%) of the patients had at least one symptom in both infections. The patients' descriptive information and symptoms according to reinfection time are presented in Tables 1 and 2.

The imaging and laboratory findings of the patients according to reinfection time are presented in Tables 3 and 4. Among those reinfected within 45 to 89 days, pulmonary computed tomography (CT) was evaluated in four patients (40%) during the first infection and six (60%) during the second infection. In two of these patients (20%), lung CT findings were consistent with COVID-19 during both infections. Of those who were reinfected after 90 days or more, pulmonary CT was evaluated in 28 patients (50.9%) during the first infection and 20 patients (36.4%) during the second infection. Four (7.3%) of these patients had lung findings consistent with COVID-19 during both infections. Hypoxia was observed during both infections in only two patients (3.1%).

All patients were alive at the time of writing. One health worker developed pulmonary embolism after reinfection and is currently continuing treatment and follow-up.

DISCUSSION

Studies on SARS-CoV-2 continue at a brisk pace as scientists attempt to better understand it. However, the results vary according to the time and setting of the study. Many different durations of viral shedding have been reported. In a meta-analysis published by Cevik et al. in November 2020, the duration of SARS-CoV-2 RNA shedding was a mean of 17 days (maximum 83 days) from the upper respiratory tract and 14.6 days (maximum 59 days) from the lower respiratory tract (7). In a study published early in the pandemic, shedding occurred for a mean of 20 days after symptom onset and the longest detected shedding lasted 37 days (8). The Korean CDC published a study in which it emphasized that test positivity continued for an average of 44.9 days (range, 8-82 days) after symptom onset and 14.3 days (range, 1-37 days) after discharge (9). For this reason, some have claimed that it is most likely that repeated positive test results within 90 days are due to intermittent viral shedding and that this detected virus does not have reproductive capacity (9). Nevertheless, more and more cases of reinfection occurring within this 90-day time frame are being reported in the literature. For example, genomically confirmed reinfection has been described by Prado-Vivar et al. after 64 days, Larson et al. after 51 days, Lee et al. after 25 days, and Tillett et al. after 45 days (10-13).

In the present study, the minimum interval to retest positivity was 60 days and the maximum was 272 days. There were 10 patients evaluated as reinfected within 90 days. The classification and treatment of these patients were carried out by infectious disease and clinical microbiology specialists. While all of the patients in our study had at least two negative test results between infections, the health workers in particular had a large number of negative results (up to 12) from tests obtained both in order to return to work and during routine screenings. Especially considering the viral shedding times reported in the international literature, genomic analyses of the cases presented here would also likely demonstrate reinfection.

Cases of reinfection have also been reported in the current literature at intervals ranging from 93 to 178 days (14-16). In Turkiye, there have been two cases confirmed by genomic analysis, after 112 and 144 days (17, 18). In fact, more than 80% of these cases had an interval longer than 90 days until reinfection.

Turkiye's national guidelines are based on CDC and WHO criteria, and isolation/quarantine procedures cannot be performed in the Ministry of Health applications for people who retest positive within 90 days of a first positivity, even if they have risky contact or meet the diagnostic criteria for reinfection (19). This results in a gap in isolation/quarantine measures. Although the Korean CDC has stated that these individuals are not contagious, further studies are needed to support this information (9).

At this stage, while we are still trying to control the pandemic by preventing transmission, one of the primary goals should be to decide which cases are reinfections and prevent more risky contact through rapid contact tracing. Therefore, as stated in the Methods section, contact tracing and quarantine/isolation were implemented manually for each case evaluated as reinfection by the infectious diseases' specialist.

Criteria sought in order to be considered reinfection were the presence of characteristic symptoms after complete clinical resolution of the first infection, lack of any etiology other than COVID-19 that could explain these symptoms, and having close contact with a COVID-19 patient (6). All patients reinfected within 45 to 89 days were symptomatic and had high-risk contact. In addition, they all had at least two negative test results between the two infection episodes.

While most reinfections have been reported to be milder, cases reported from the United States and Ecuador were more severe and one reinfected patient died (10, 13, 20). Of the patients we followed, eight people required hospital admission and treatment. A 23-year-old male doctor developed pulmonary embolism and is still undergoing treatment and follow-up.

Most studies have reported seroconversion after infection. However, a few studies also documented patients who never exhibited seroconversion. It has been emphasized that in most cases neutralizing antibodies are formed, although observational studies have shown that all anti-SARS-CoV-2 antibodies decrease over time and that antibodies are even not detected in plasma donors during convalescence. Therefore, there are still gaps in our knowledge regarding the production and protection of antibodies (21-26).

Unfortunately, the main limitation of this study is the lack of genome analysis and antibody detection. However, not every province and laboratory in Turkiye is able to perform genome analysis. In fact, none of the laboratories in the province have this capacity.

Our aim in publishing this study is to report that the frequency of reinfection appears to be higher than predicted. Although international and national centers for disease control and prevention, which have an important say in the scientific community, recommend genome analysis for a definitive decision, epidemiological connections and clinical presentation are more valuable in the fight against the pandemic, especially in countries such as Turkiye that have limited capacity to perform these analyses. Therefore, regardless of confirmed or clinical reinfection, it is essential to identify these cases, organize treatment, and implement quarantine and isolation procedures in order to prevent further transmission. Accordingly, the Ministry of Health should also make its software more flexible and simplify the detection of reinfection cases. There is limited information in the literature on the contagiousness of reinfected patients. This issue should be investigated and included in the decision-making processes of governments and public health workers. Furthermore, at a time when virus variants are a major concern and the immune dynamics after previous infection remain unclear, it is predicted that the incidence of reinfection will increase. Countries should be prepared for this situation.

Ethics Committee Approval: This study was approved by the Clinical Research Ethical Committee of the Erzurum Regional Training and Research Hospital (Date:01.03.2021, No:2021/05-85).

Peer Review: Externally peer-reviewed.

Author Contributions: Conception/Design of Study- E.F.K., Ö.K.; Data Acquisition- E.F.K., Ö.K.; Data Analysis/Interpretation- E.F.K., Ö.K., M.H.A.; Drafting Manuscript- E.F.K.; Critical Revision of Manuscript- E.F.K., Ö.K., M.H.A.; Final Approval and Accountability- E.F.K.; Material and Technical Support- E.F.K.; Supervision- E.F.K., Ö.K.

Conflict of Interest: The authors have no conflict of interest to declare.

Financial Disclosure: The authors declared that this study has received no financial support.

REFERENCES

1. Demirbilek Y, Pehlivantürk G, Özgüler ZÖ, Meşe EA. COVID-19 outbreak control, example of ministry of health of Turkey. Turk J Med Sci 2020;50(SI-1):489-94.
2. World Health Organization (2020). Novel Coronavirus – China. [Online cited 14/02/2021]. https://www.who.int/csr/don/12-january-2020-novel-coronavirus-china/en/.
3. World Health Organization (2020). WHO Director-General's opening remarks at the media briefing on COVID-19. [Online cited 14/02/2021]. https://www.who.int/director-general/speeches/detail/who-director-general-s-opening-remarks-at-the-media-briefing-on-covid-19-11-March-2020.
4. Centers for Disease Control and Prevention (2020). Investigative Criteria for Suspected Cases of SARS-CoV-2 Reinfection (ICR). [Online cited 14/02/2021]. https://www.cdc.gov/coronavirus/2019-ncov/php/invest-criteria.html#:~:text=Since%20August%202020%2C%20CDC%20has,Isolation%20and%20Precautions%20for%20Adults.
5. European Centre for Disease Prevention and Control (2020). Reinfection with SARS-CoV: considerations for public health response: ECDC; 2020. [Online cited 14/02/2021]. https://www.ecdc.europa.eu/sites/default/files/documents/Re-infection-and-viral-shedding-threat-assessment-brief.pdf.
6. Yahav D, Yelin D, Eckerle I, Eberhardt CS, Wang J, Cao B, et al. Definitions for COVID-19 reinfection, relapse and PCR re-positivity. Clin Microbiol Infect 2021;27(3):315-8.
7. Cevik M, Tate M, Lloyd O, Maraolo AE, Schafers J, Ho A. SARS-CoV-2, SARS-CoV, and MERS-CoV viral load dynamics, duration of viral shedding, and infectiousness: a systematic review and meta-analysis. Lancet Microbe 2021;2(1):e13-22.
8. Zhou F, Yu T, Du R, Fan G, Liu Y, Liu Z, et al. Clinical course and risk factors for mortality of adult inpatients with COVID-19 in Wuhan, China: a retrospective cohort study. Lancet 2020;395(10229):1054-62.
9. Korean Center For Disease Control and Prevention (2020). Division of Risk assessment and International cooperation. Findings from investigation and analysis of re-positive cases. [Online cited 14/02/2021]. https:// www.cdc.go.kr/board/board.es?mid=a30402000000&bid=0030.
10. Prado-Vivar B, Becerra-Wong M, Guadalupe JJ, Márquez S, Gutierrez B, Rojas-Silva P, et al. A case of SARS-CoV-2 reinfection in Ecuador. Lancet Infect Dis 2021;21(6):e142.
11. Larson D, Brodniak SL, Voegtly LJ, Cer RZ, Glang LA, Malagon FJ, et al. A Case of Early Re-infection with SARS-CoV-2. Clin Infect Dis 73(9):e2827-8.
12. Lee J-S, Kim SY, Kim TS, Hong KH, Ryoo N-H, Lee J, et al. Evidence of severe acute respiratory syndrome coronavirus 2 reinfection after recovery from mild coronavirus disease 2019. Clin Infect Dis 2021;73(9):e3002-8.
13. Tillett RL, Sevinsky JR, Hartley PD, Kerwin H, Crawford N, Gorzalski

A, et al. Genomic evidence for reinfection with SARS-CoV-2: a case study. Lancet Infect Dis 2021;21(1):52-8.

14. Van Elslande J, Vermeersch P, Vandervoort K, Wawina-Bokalanga T, Vanmechelen B, Wollants E, et al. Symptomatic SARS-CoV-2 reinfection by a phylogenetically distinct strain. Clin Infect Dis 2021;73(2):354-6.
15. To KK-W, Hung IF-N, Ip JD, Chu AW-H, Chan W-M, Tam AR, et al. COVID-19 re-infection by a phylogenetically distinct SARS-coronavirus-2 strain confirmed by whole genome sequencing. Clin Infect Dis 2020;1-21. 2021;73(9):e2946-51
16. West J, Everden S, Nikitas N. A case of COVID-19 reinfection in the UK. Clin Med (Lond) 2021;21(1):e52-3.
17. Ozaras R, Ozdogru I, Yilmaz A. Coronavirus disease 2019 re-infection: first report from Turkey. New Microbes New Infect 2020;38:100774.
18. Türköz İ, Tüz MA, Gencer E, Aygün-Kaş FÖ, Yıldırmak T. A clinical and laboratory-defined case of COVID-19 reinfection. Klimik Derg 2020;33(3):314-6.
19. Turkish Ministry of Health (2020). Temaslı Takibi, Salgın Yönetimi, Evde Hasta İzlemi Ve Filyasyon. Contact Tracing, Pandemic Management, Outpatient Monitoring and Filiation (Online cited:14.02.2021). https://covid19.saglik.gov.tr/tr. Turkish.
20. Mulder M, van der Vegt DS, Munnink BBO, GeurtsvanKessel CH, van de Bovenkamp J, Sikkema RS, et al. Reinfection of Severe Acute Respiratory Syndrome Coronavirus 2 in an Immunocompromised Patient: A Case Report. Clin Infect Dis 2021;73(9):e2841-2.
21. Post N, Eddy D, Huntley C, van Schalkwyk MC, Shrotri M, Leeman D, et al. Antibody response to SARS-CoV-2 infection in humans: A systematic review. PloS one 2020;15(12):e0244126.
22. Schwarzkopf S, Krawczyk A, Knop D, Klump H, Heinold A, Heinemann FM, et al. Cellular Immunity in COVID-19 Convalescents with PCR-confirmed infection but with undetectable SARS-CoV-2–specific IgG. Emerg Infect Dis 2021;27(1):122-9.
23. Long Q-X, Tang X-J, Shi Q-L, Li Q, Deng H-J, Yuan J, et al. Clinical and immunological assessment of asymptomatic SARS-CoV-2 infections. Nat Med 2020;26:1200-4
24. Seow J, Graham C, Merrick B, Acors S, Pickering S, Steel KJ, et al. Longitudinal observation and decline of neutralizing antibody responses in the three months following SARS-CoV-2 infection in humans. Nat Microbiol 2020;5(12):1598-607.
25. Gudbjartsson DF, Norddahl GL, Melsted P, Gunnarsdottir K, Holm H, Eythorsson E, et al. Humoral immune response to SARS-CoV-2 in Iceland. N Engl J Med 2020;383(18):1724-34.
26. Chen S, Ren L-Z, Ouyang H-S, Liu S, Zhang L-Y. Necessary problems in re-emergence of COVID-19. World J Clin Cases 2021;9(1):1-7.

İSTANBUL UNIVERSITY PRESS

RESEARCH ARTICLE / ARAŞTIRMA MAKALESİ
Journal of Advanced Research in Health Sciences /
Sağlık Bilimlerinde İleri Araştırmalar Dergisi 2023
DOI: 10.26650/JARHS2023-1293558

SEASONAL VARIATION OF VITAMIN-D LEVELS IN THE ADULT POPULATION IN ISTANBUL/TURKEY: A POPULATION-BASED STUDY

İSTANBUL / TÜRKİYE'DE YETİŞKİN POPÜLASYONDA D VİTAMİNİ DÜZEYLERİNİN MEVSİMSEL DEĞİŞİMİ: POPÜLASYONA DAYALI BİR ÇALIŞMA

Erhan EKEN[1], Mehmet UZUNLULU[1], Osman KÖSTEK[2], Ferruh İSMAN[3], Aytekin OĞUZ[1]

[1] Istanbul Medeniyet University, Faculty of Medicine, Department of Internal Medicine, Istanbul, Turkiye
[2] Marmara University, Faculty of Medicine, Department of Oncology, Istanbul, Turkiye
[3] Istanbul Medeniyet University, Faculty of Medicine, Department of Biochemistry, Istanbul, Turkiye

ORCID ID: M.U. 0000-0001-8754-1069; O.K. 0000-0002-1901-5603; F.İ. 0000-0003-4278-4651; A.O. 0000-0002-2595-5167

Citation/Atıf: Eken E, Uzunlulu M, Kostek O, Isman F, Oguz A. Seasonal variation of vitamin-D levels in the adult population in Istanbul/Turkey: a population-based study. Journal of Advanced Research in Health Sciences 2023;6(3):270-275. https://doi.org/10.26650/JARHS2023-1293558

ABSTRACT

Objective: The current research examined if there is a variance in the frequency of vitamin D deficiency or insufficiency among adults visiting the hospital for medical problems in winter and summer, and whether comorbidities have an impact on this.

Material and Method: A total of 1155 patients (771 women, 384 men, mean age:48±15 years) who were admitted to the outpatient clinics of Istanbul Medeniyet University Goztepe Training and Research Hospital in August and February were tested for 25(OH)D levels for any reason were included. A 25(OH)D level of<20 ng/ml was stated as inadequacte, and 20–29 ng/ml was defined as insufficient. The two groups were examined in contrast in terms of vitamin D deficiency and insufficiency and the frequency of comorbidities.

Results: 25(OH)D levels were inferior in the winter compared to the summer (16.1±12.5 ng/ml versus 22.2±15.8 ng/ml, p<0.001). Vitamin D deficiency was detected in 769 (66.6%) patients, and vitamin D insufficiency was detected in 226 (19.6%). Furthermore, 51.9% and 78.6% of patients had vitamin D deficiency (p< 0.001) and 27.3% and 13.1% had vitamin D insufficiency (p<0.001) during summer and winter, respectively. Prevalence rates of diabetes (60.1% and 39.9%, respectively, p=0.04) and hypertension (62.7% and 37.3%, accordingly, p<0.01) were more common in the winter compared to the summer.

Conclusion: The findings of this research show that vitamin D insufficiency and deficiency are well-known health issues in Turkey, and although there has been some improvement, the problem persists even during the sunny seasons.

Keywords: Seasonal variation, vitamin D level, vitamin D insufficiency

ÖZ

Amaç: Vitamin D [25(OH)D] eksikliği veya yetersizliğinin mevsimsel değişiklik gösterdiği bildirilmektedir. Bu çalışmada hastaneye başvuran erişkinlerde vitamin D eksikliği veya yetersizliği sıklığının kış ve yaz aylarında farklılık gösterip göstermediği ve komorbid durumlardan etkilenip etkilenmediği araştırıldı.

Gereç ve Yöntem: Çalışmaya Ağustos 2014 (yaz grubu) ile Şubat 2015 (kış grubu) aylarında İstanbul Medeniyet Üniversitesi Göztepe Eğitim ve Araştırma Hastanesi polikliniklerine müracaat eden ve belirli bir sebeple 25(OH)D vitamini seviyelerine bakılan toplam 1155 olgu (771 kadın, 384 erkek, ortalama yaş: 48±15) dahil edildi. Vitamin D eksikliği<20 ng/ml, vitamin D yetersizligi 20-29 ng/ml olarak tanımlandı. Gruplar vitamin D ihtiyacı, yetersizliği ve komorbidite sıklıklarına göre karşılaştırıldı.

Bulgular: Tüm olgularda ortalama vitamin D düzeyi 18,9±14,4 ng/ml (kadınlarda 18,9±15,5 ng/mL, erkeklerde 18,9±12,1 ng/mL) idi. Vitamin D düzeyleri; kış grubunda yaz grubuna göre daha düşük (16,1±12,5 ng/mL'ye karşılık 22,2±15,8 ng/mL, p<0,001) bulundu. Vitamin D eksikliği 769 hastada (%66,6), vitamin D yetersizliği 226 hastada (%19,6) saptandı. Vitamin D eksikliği %51,9'u yaz aylarında, %78,6'sı kış aylarında (p<0,001), D vitamini yetersizliği % 27,3'ü yaz aylarında ve %13,1'i kış aylarında (p<0,001) idi. Kış grubunda yaz grubuna göre diyabet (sırasıyla %60,1 ve %39,9, p=0,04) ve hipertansiyon sıklığı (sırasıyla %62,7 ve %37.3, p<0,01) yüksekti.

Sonuç: Bu çalışmada güneşli yaz aylarında dahi populasyonumuzun yaklaşık yarısında, kış aylarında ise yaklaşık her 4 kişiden 3'ünde vitamin D eksikliği olduğu görülmüştür. Bu bulgular ülkemizde D vitamini eksiklik ve yetersizliğinin yaygın bir sağlık problemi olduğunu, güneşli mevsimlerde bu problemin kısmen azalsa da devam ettiğini göstermiştir.

Anahtar kelimeler: Mevsimsel değişim, vitamin D düzeyleri, vitamin D yetersizliği

Corresponding Author/Sorumlu Yazar: Erhan EKEN **E-mail:** erhan-eken@hotmail.com

Submitted/Başvuru: 06.05.2023 • **Revision Requested/Revizyon Talebi:** 12.05.2023 • **Last Revision Received/Son Revizyon:** 01.06.2023 • **Accepted/Kabul:** 12.06.2023 • **Published Online/Online Yayın:** 10.10.2023

INTRODUCTION

Vitamin D deficiency is a well-known worldwide health issue that is linked with several health problems, including bone fractures, functional limitation, diabetes, cardiovascular disease, cancer, depression, and mortality (1, 2). The risk factors for inferior levels of 25(OH)D include dark skin pigmentation, decreased vitamin D uptake, low ultraviolet light exposure, and obesity, while advanced age, female gender, low physical activity, and education levels are also related to vitamin D deficiency (3). Measuring the serum 25(OH)D concentration is the best indicator of vitamin D levels although the ideal level is still debated (4). Numerous studies have shown that vitamin D deficiency is widespread around the world, particularly in the Middle East and Asia, regardless of risk factors (5,6). The seasonal variation in serum 25 (OH)D concentration indicates that levels are at their highest in late summer and at lowest in late winter or early spring (7,8).

This study examined the prevalence of vitamin D deficiency in grown-ups visiting our outpatient clinics, evaluated whether there is an important variance in prevalence between the summer and winter, assessed the extent of cyclical variation, and investigated any links among the low vitamin D levels regarding sex, age, diabetes and hypertension.

MATERIALS and METHOD

This study included 1,155 individuals (771 females, 384 males) aged 48±15 years who visited the outpatient clinics of Istanbul Medeniyet University Goztepe Training and Research Hospital in August 2014 (the summer group) and February 2015 (the winter group) and were tested for their 25(OH)D levels for any medical purpose. The patient records were obtained retrospectively from the hospital data system while following the ethical rules outlined in the Helsinki Declaration.

Inclusion criteria: Individuals who underwent testing to specify their 25(OH)D concentrations and fell between the age sphere of 18 to 75 years old were included in the study.

Exclusion criteria: This refers to individuals who received vitamin D replacement therapy, supplementation, or related medication within the previous month, individuals with chronic renal failure characterized by a GFR of less than 60 ml/min, and pregnant women.

Study design

The study examined the age, sex, 25(OH)D levels, creatinine ranks, and GFR levels of individuals who met the criteria for inclusion. The GFR amount was found using the CKD-EPI (Chronic Kidney Disease Epidemiology Collaboration) recipe. Patient records were reviewed through the hospital information system and the Medula doctor, pharmacy, and electronic prescription system to identify comorbid diagnoses of diabetes or hypertension, and any use of vitamin D replacement therapy or related medications (9). The summer group consisted of patients who presented to the hospital in August 2014, while the winter group consisted of patients who presented in February 2015. A comparison was made between the two groups regarding the occurrence of vitamin D deficiency and insufficiency, and also the mean seasonal serum concentrations of vitamin D.

25(OH)D Levels Analysis

The chemiluminescent microparticle immunological assay (CMIA) procedure was utilized to measure the 25(OH)D levels using the Abbott ARCHITECT system 25-OH vitamin D brand kits (Abbott, USA) with Abbott ARCHITECTi 2000SR immunoanalyzers. The results were quantitatively evaluated in ng/ml, with a reference range of 10–60 ng/ml for winter and 20-100 ng/ml for summer. The levels of 25(OH)D concentration in the serum were categorized as deficient in vitamin D for measurements less than 20 ng/ml, insufficient in vitamin D for measurements between 20 and 30 ng/ml, and normal for measurements are same or more than 30 ng/ml. (4).

Statistical Analysis

The statistical analysis was conducted by utilizing IBM SPSS Statistics Version 20 software package (Copyright IBM Corporation and its Licensors 1989, 2011). The Kolmogorov-Smirnov test was utilized to assess the normality of variables. Numeric information was presented as mean and standard deviation, and categorical information was given in ratios and numbers. Qualitative data between independent groups were distinguished using the chi-square test, while Student's t-test was conducted for independent group comparisons. In cases where variables were not normally distributed or when comparing two independent groups, the Mann-Whitney U test was utilized. Statistical importance was determined as a p-value of less than 0.05 at a 95% confidence interval.

This study was approved by Istanbul Medeniyet University Goztepe Training and Research Hospital Clinical Research Ethics Committee (Date: 12.05.2015, No: 2015/0049).

RESULTS

A number of 1.155 people were considered, consisting of 771 women and 384 men with an exact age of 48±15 years. Table 1 presents the comparison of patients' analytical specifies and comorbidities, and their vitamin D levels based on seasonal variations. The mean serum 25(OH)D concentration in all patients was 18.9±14.4 ng/ml, which was inferior in the winter compared to the summer (16.1±12.5 ng/ml versus 22.2±15.8 ng/ml, $p<0.001$). Both sexes had lower serum 25(OH)D concentrations in the winter compared to the summer ($p<0.001$ for both). The frequency of diabetes and hypertension was greater during the winter season (with p-values of 0.04 and less than 0.001, respectively).

Following an adjustment for age differences among the groups, the average 25(OH)D concentration for all patients was 18.36±14.25 ng/ml, whereas the winter and summer concentrations were 15.46±12.60 ng/ml and 21.60±15.28 ng/ml, respectively (with a p-value of less than 0.001) (Table 2).

Table 1: Comparison of clinical characteristics and vitamin D levels between the studied groups according to the seasonal variation

		All population	Summer (August)	Winter	P value
Age (years)		48±15	45±14	50±15	**<0.001**[1]
Sex (n, %)					
	Female	771 (100)	397 (51.5)	374 (48.5)	
	Male	384 (100)	125 (32.6)	259 (67.4)	**<0.001**[2]
Diabetes frequency		276 (100)	110 (39.9)	166 (60.1)	**0.04**[2]
Hypertension frequency		343 (100)	128 (37.3)	215 (62.7)	**<0.001**[2]
Vitamin D (ng/mL) (Mean±SD)	All population	18.9±14.4	22.2±15.8	16.1±12.5	**<0.001**[3]
	Male	18.9±15.5	21.3±16.6	16.4±13.8	**<0.001**[3]
	Female	18.9±12.1	25.5±12.8	15.7±10.4	**<0.001**[3]

[1]Student t test, [2]Pearson Chi-Square test, [3]Mann-Whitney U test

Table 2: Comparison of clinical characteristics and vitamin D levels between the studied groups according to the seasonal variation after adjusting for age

		All population (n=952)	Summer (August) (n=448)	Winter (n=504)	P value
Age (years)		45.53±14.11	45.71±13.84	45.36±14.37	0.707[1]
Sex (n, %)					
	Female	678 (71.2)	332 (74.1)	346 (68.7)	0.063[2]
	Male	274 (28.8)	116 (25.9)	158 (31.3)	
Diabetes frequency		209 (22)	95 (21.2)	114 (22.6)	0.599[2]
Hypertension frequency		264 (27.7)	117 (26.1)	147 (29.2)	0.294[2]
Vitamin D (ng/mL) (Mean±SD, median)	All population	18.36±14.25	21.60±15.28 (18.9)	15.46±12.60 (12.3)	**<0.001**[3]
	Male	19.44±12.84 (16.5)	24.98±12.95 (22.85)	15.36±10.01 (13.15)	**<0.001**[3]
	Female	17.92±14.96 (16.85)	20.42±15.86 (16.85)	15.51±13.64 (11.30)	**<0.001**[3]

[1]Student t test, [2]Pearson Chi-Square test, [3]Mann-Whitney U test

Table 3: Comparison of the vitamin D deficiency (<20 ng/mL), insufficiency (20-30 ng/mL) and normal vitamin D levels (≥ 30 ng/mL) groups according to the seasonal variation.

25(OH)D levels	**<20 ng/mL**	**20-30 ng/mL**	**≥30 ng/mL**	**P value**[1]
Summer (August) **(n, %)**	271 (51.9)	143 (27.3)	108 (20.8)	**<0.001**
Winter (February) **(n, %)**	498 (78.6)	83 (13.1)	52 (8.5)	
p value[1]	**<0.001**	**<0.001**	**<0.001**	

[1]Pearson Chi-Square test

Table 3 shows that the prevalence of vitamin D deficiency was higher in the winter season in comparison to the summer season (78.6% versus 51.9%, with a p-value of less than 0.001).

Table 4 displays the vitamin D levels among the age groups, revealing that serum 25(OH)D concentrations were greater in males aged 51-60 compared to females in the same age range (with a p-value of 0.03). Table 5 included a comparison of patients with deficient, insufficient, and normal vitamin D ranks due to season and sex, indicating that vitamin D inadequacy was more visible during the winter for both sexes (with a p-value of less than 0.001).

Table 4: Analysis of the vitamin D levels according to the age decades

	25(OH)D levels (ng/mL)			
	Allpopulation (n=1155)	**Male (n=384)**	**Female (n=771)**	**p value[1]**
18-30 years	17.3±13.2 (14)	16.8±9.3 (13.8)	17.5±14.9 (15)	0.43
31-40 yeares	19.6±15.8 (15.9)	16.8±17.1 (15.5)	20.7±17.6 (16)	0.85
41-50 years	19.8±16.7 (15.4)	19.6±13.4 (16.1)	19.9±18.1 (14.6)	0.13
51-60 yeaers	19.6±14.2 (15.2)	21.8±16.3 (16.6)	18.5±12.9 (14.2)	**0.03**
>60 years	17.9±12.4 (13.8)	18.2±10.1 (15.2)	17.8±13.6 (13.1)	0.06

[1]Mann-Whitney U test

Table 5: Comparison of the vitamin D deficiency, insufficiency and normal vitamin D levels groups according to the seasonal variation and sex

25(OH)D levels		**<20 ng/mL**	**20-30 ng/mL**	**≥30 ng/mL**	**p value[1]**
Male		254 (66.1)	82 (21.4)	48 (12.5)	0.42
Female		515 (66.8)	144 (18.7)	112 (14.5)	
Summer					
	Male	38 (30.4)	56 (44.8)	31 (24.8)	**0.05**
	Female	233 (58.7)	87 (21.9)	77 (19.4)	
Winter					
	Male	216 (83.4)	26 (10)	17 (6.6)	**<0.001**
	Female	282 (75.4)	57 (15.2)	35 (9.4)	

[1]Pearson Chi-Square test

Table 6: Demographic characteristics and comorbidities of patients with and without vitamin D deficiency

25(OH)D vit	**<20 ng/mL**	**≥20 ng/mL**	**p value**
Age	47±15	48±14	0.41[1]
Sex (n, %)			
Female	515 (66.8)	256 (33.2)	0.84[2]
Male	254 (66.1)	130 (33.9)	
Hypertansion (n, %)	234 (68.2)	109 (31.8)	0.45[2]
Diabetes (n, %)	191 (69.2)	85 (30.8)	0.30[2]

[1]Student t test, [2]Pearson Chi Square test

Table 6 presents the demographic features and coexisting medical conditions of people with and without vitamin D deficiency. Age and sex characteristics and the prevalence of diabetes and hypertension did not change importantly among the people with and without vitamin D deficiency (with p-values greater than 0.05 for all). Furthermore, the levels of vitamin D were comparable throughout people with and without diabetes (17.4±11.9 ng/ml and 19.4±15.1 ng/ml, respectively, with a p-value of 0.12) as well as those with and without hypertension (18.1±13.1 ng/ml and 19.3±14.9 ng/ml, correspondingly, with a p-value of 0.189).

DISCUSSION

According to the current research, our patients' average vitamin D level was less than anticipated, with 51.9% of the participants suffering from vitamin D deficiency in the summer and 75% during winter. Additionally, there was considerably less serum 25(OH)D concentration (37.8%) among the winter and summer, equating to a 6.1 ng/ml difference.

The current research examined vitamin D levels in different seasons among various populations. In a study of Japanese mu-

nicipal office workers, researchers found that vitamin D levels were higher in July than in November, and vitamin D deficiency was more visible in November than in July (7). In a study from Bilecik province, Çelik et al. found that 33.47% of the patients had vitamin D deficiency and reported that there were inadequate vitamin D levels in all participants. Inferior mean values were more noticeable in spring (10). Another study of office workers found that vitamin D levels were higher in summer compared to winter, and vitamin D deficiency was more visible in winter than in summer (11). In their study, Ucar et al. found that patients' vitamin D deficiency was 51.8% and vitamin D insufficiency 20.7% (12).

In this study, the predominance of vitamin D deficiency was extreme (66.6%) in both summer and winter among the general patient population admitted to the hospital. During winter, the predominance of vitamin D deficiency was more, at 78.6%, compared to 51.9% in summer, while vitamin D insufficiency was more common during summer at 27.3% compared to 13.1% in winter. The mean serum 25(OH)D concentration was 18.9±14.4 ng/ml, and an important growth of 37.8% was observed in vitamin D levels in the time of the summer relative to winter. The results were adjusted for both sex and age, and vitamin D levels remained less in the winter group. Thus, these findings are in accordance with prior research that have demonstrated the prevalence of vitamin D deficiency and insufficiency as widespread health issues that are more prevalent during winter.

Previous studies have indicated that gender may affect vitamin D levels. For example, Heidari et al. observed that females had lower vitamin D levels than males, but there was not any important variance in terms of vitamin D deficiency (13). Burnand et al. reported that there was no significant variation in vitamin D levels between males and females (14). However, in this research, we realized that vitamin D ranks and the pervasiveness of vitamin D deficiency were similar in both sexes.

Age is a widely recognized factor that can boost the risk of vitamin D deficiency (3). Although Atlı et al. identified a significant negative correlation between age and vitamin D levels in their study Çınar et al. found no remarkable correlation among the age and vitamin D levels (11, 15). Similarly, Uçar et al. did not see any important variances in vitamin D deficiency across different age groups (12). In our review, we did not observe any important correlation between vitamin D levels and age. Furthermore, we did not find any important decrease in serum vitamin D levels with increasing age when we analyzed vitamin D levels in age groups.

The relation among the vitamin D deficiency and type 2 diabetes has been well-documented (16). The NHANES III study showed a negative correlation between among D ranks and insulin resistance and diabetes (17). Our study found that people with diabetes had lower vitamin D levels than those without diabetes, although the variance was not remarkable. Moreover, individuals with diabetes had more prevalence of vitamin D deficiency (69.2%) compared to the overall population. However, there was no significant difference among those without vitamin D deficiency.

Several debates have established a link between vitamin D deficiency and hypertension (5). For example, Bhandari et al. reported an important link among the lower 25(OH)D levels and the incidence of hypertension. They found that the incidence of hypertension was 52.4%, 40.8%, 27.2%, and 19.4% for patients with 25(OH)D levels of <15 ng/ml, 15-29ng/ml, 30-39ng/ml, and ≥40 ng/ml, respectively (18). In our study, although the variance was not remarkable, we observed lower vitamin D ranks in people with hypertension. However, the prevalence of vitamin D deficiency was more (68.2%) in people with hypertension than in the general population.

Limitations of the study

Since this study was conducted in a hospital, the findings might not be applicable to the whole Turkish community. The limitations of the study include its retrospective design, inability to assess patient anthropometric and biochemical data except for creatinine, and not investigating patients' clothing and dietary habits. However, the exclusion of patients who had undergone therapies that could affect vitamin D levels through the screening of their medical records using Medula, hospital information system, and e-prescription system enhanced the credibility of the findings.

CONCLUSION

In summary, our study shows that vitamin D deficiency and insufficiency is still a common health problem in Turkey, even during the sunny seasons, although there has been some improvement. To get the reasons better behind low vitamin D levels in a country known for its sunny weather, future studies with different approaches are necessary. Additionally, it is important to explore the symptoms and consequences of this deficiency among people having low vitamin D levels in our population, as well as to investigate any comorbidities that require treatment.

Acknowledgements: Assoc. Prof. Meryem EKEN

Ethics Committee Approval: This study was approved by Istanbul Medeniyet University Goztepe Training and Research Hospital Clinical Research Ethics Committee (Date: 12.05.2015, No: 2015/0049).

Peer Review: Externally peer-reviewed.

Author Contributions: Conception/Design of Study- E.E., A.O., M.U.; Data Acquisition- E.E., A.O., M.U., F.İ., O.K.; Data Analysis/Interpretation- O.K., M.U., E.E.; Drafting Manuscript- M.U., E.E., A.O.; Critical Revision of Manuscript- A.O., F.İ., O.K.; Final Approval and Accountability- E.E., M.U., A.O., O.K., F.İ.; Material and Technical Support- E.E., O.K., F.İ.; Supervision- A.O., M.U.

Conflict of Interest: The authors have no conflict of interest to declare.

Financial Disclosure: The authors declared that this study has received no financial support.

REFERENCES

1. Palacios C, Gonzalez L. Is vitamin D deficiency a major global public health problem? J Steroid Biochem Mol Biol 2014;144 Pt A:138-45
2. Gröber U, Reichrath J, Holick MF. Live longer with vitamin D? Nutrients 2015;7(3):1871-80.
3. LeBlanc ES, Zakher B, Daeges M, Pappas M, Chou R. Screening for vitamin D deficiency: a systematic review for the U.S. Preventive Services Task Force. Ann Intern Med 2015;162(2):109-22.
4. Holick MF. Vitamin D deficiency. N Engl J Med 2007;357(3):266-81.
5. Forests KY, Stuhidreher WL. Prevalence and correlates of vitamin D deficiency in US Adults. Nutr Res 2011;31(1):48-54
6. Mithal A, Wahl DA, Bonjour JP, Dawson-Hughes B, Eisman JA, El-Hajj Fuleihan G, et al. Global Vitamin DStatus and Determinants of Hypovitaminosis D. Osteoporos Int 2009;20(11):1807-20
7. Nanri A, Foo LH, Nakamura K, Hori A, Poudel-Tandukar K, Matsushita Y, et al. Serum 25-hydroxyvitamin d concentrations and season spesific correlates in Japanese adults. J Epidemiol 2011;21(5):346-53
8. Hyppönen E, Power C. Hypovitaminosis D in British adults at age 45y: nationwide cohort study of dietary and lifestyle predictors. Am J Clin Nutr 2007;85(3):860-8
9. SSA. Medula pharmacy system general information and medula pharmacy introduction. Social security agency (sosyal güvenlik kurumu) official web site 2014-2015. https://medeczane.sgk.gov.tr/
10. Çelik S, Çelik M, Takır M. Seasonal variability of Serum 25-Hydroxy-Vitamin D levels in the adult population living in Bilecik province: A follow-up study from Turkey. Med Med J 2018;33(4):296-9.
11. Cinar N, Harmanci A, Yildiz BO, Bayraktar M. Vitamin D status and seasonal changes in plasma concentrations of 25-hydroxyvitamin D in office workers in Ankara, Turkey. Eur J Intern Med 2014;25(2):197-201.
12. Uçar F, Taşlıpınar M, Soydaş A, Özcan N. 25-OH vitamin D levels in patients admitted to Ankara Etlik İhtisas Training and Research Hospital. Eur J Basic Med Sci 2012;2(1):12-5.
13. Heidari B, Mirghassemi MBH. Seaasonal variations in serum vitamin D according to age and sex. Caspian J Internal Med 2012;3(4):535-40
14. Burnand B, Sloutskis D, Gianoli F, Cornuz J, Rickenbach M, Paccaud F. Serum 25-hydroxyvitamin D: distribution and determinants in the Swiss population. Am J Clin Nutr 1992;56(3):537-42.
15. Atli T, Gullu S, Uysal AR, Erdogan G. The prevalence of Vitamin D deficiency and effects of ultraviolet light on Vitamin D levels in elderly Turkish population. Arch Gerontol Geriatr 2005;40(1):53-60.
16. Mezza T, Muscogiuri G, Sorice GP, Prioletta A, Salomone E, Pontecorvi A, et al. Vitamin D deficiency: a new risk factor for type 2 diabetes? Ann Nutr Metab 2012;61(4):337-48
17. Scragg R, Sowers M, Bell C. Serum 25-hydroxyvitamin D, ethnicity, and blood pressure in the Third National Health and Nutrition Examination Survey. Am J Hypertens 2007;20(7):713-9.
18. Bhandari SK, Pashayan S, Liu IL, Rasgon SA, Kujubu DA, Tom TY, et al. 25-hydroxyvitamin D levels and hypertension rates. J Clin Hypertens (Greenwich) 2011;13(3):170-7.

İSTANBUL UNIVERSITY PRESS

RESEARCH ARTICLE / ARAŞTIRMA MAKALESİ
Journal of Advanced Research in Health Sciences / Sağlık Bilimlerinde İleri Araştırmalar Dergisi 2023
DOI: 10.26650/JARHS2023-1342541

RETROSPECTIVE EVALUATION OF THE CLINICAL COURSE OF PAGET'S DISEASE OF BONE

KEMİĞİN PAGET HASTALIĞININ KLİNİK SEYRİNİN RETROSPEKTİF OLARAK DEĞERLENDİRİLMESİ

Hülya HACİŞAHİNOĞULLARI[1], Gamze BİLİK OYMAN[1], Gülşah YENİDÜNYA YALIN[1], Özlem SOYLUK SELÇUKBİRİCİK[1], Nurdan GÜL[1], Ferihan ARAL[1], Refik TANAKOL[1,2], Ayşe KUBAT ÜZÜM[1]

[1] Istanbul University, Istanbul Faculty of Medicine, Department of Internal Medicine, Division of Endocrinology and Metabolism, Istanbul, Turkiye
[2] American Hospital, Internal Medicine Clinic, Division of Endocrinology and Metabolism, Istanbul, Turkiye

ORCID ID: H.H. 0000-0001-9989-6473; G.B.O. 0000-0001-8636-8700; G.Y.Y. 0000-0002-9013-5237; Ö.S.S. 0000-0003-0732-4764; N.G. 0000-0002-1187-944X; F.A. 0000-0002-4429-187X; R.T. 0000-0003-1636-1444; A.K.Ü. 0000-0003-0478-1193

Citation/Atıf: Hacisahinogullari H, Bilik Oyman G, Yenidunya Yalin G, Soyluk Selcukbiricik O, Gul N, Aral F, et al. Retrospective evaluation of the clinical course of Paget's disease of bone. Journal of Advanced Research in Health Sciences 2023;6(3):276-280. https://doi.org/10.26650/JARHS2023-1342541

ABSTRACT

Objective: Paget's disease of bone (PDB) is a focal, chronic, metabolic disorder of bones and causes complications such as bone deformity, fractures, and heart failure. This study aimed to evaluate the clinical characteristics of patients with PDB and patients' responses to antiresorptive treatments.

Material and Methods: In the study, we retrospectively evaluated the medical records of patients who were followed up with PDB at the Istanbul Faculty of Medicine and treated with antiresorptive therapy.

Results: A total of 26 patients (12 females/14 males) with PDB were evaluated. The mean age at diagnosis was 62.9±13.5 years. The median time from the onset of symptoms to diagnosis was 17.5 months (range 1-480). The symptoms were as follows: pain in 16, swelling in 3, rubor in 2, bone fracture in 1, nephrolithiasis in 1, and hearing loss in 1 patient. Laboratory tests revealed the following results (mean±SD); Alkaline phosphatase (ALP) 512±557 U/L, bone-specific ALP 81.2±51.4 µg/L, and the mean ALP was 4.12±4 times of upper limit of the normal range. The distribution of the disease was as follows: pelvis in 58%, vertebra in 46%, skull in 35%, femur in 23%, tibia in 11.5%, humerus in 3.8% of the patients. Of 26 patients, 21 were treated with zoledronic acid alone. Relapse occurred in four patients; the mean duration from therapy to relapse was 72.25±28.7 months.

Conclusion: Zoledronic acid is a very potent antiresorptive drug and provides long-term remission of the disease even with a single dose of therapy.

Keywords: Paget's disease of bone, zoledronic acid, alkaline phosphatase

ÖZ

Amaç: Kemiğin Paget hastalığı (KPH), fokal, kronik, metabolik bir kemik hastalığıdır ve kemik deformitesi, kırıklar ve kalp yetmezliği gibi komplikasyonlara neden olur. Bu çalışma, KPH hastalarının klinik özelliklerini ve hastaların antiresorptif tedavilere yanıtlarını değerlendirmeyi amaçladı.

Gereç ve Yöntemler: Bu çalışmada İstanbul Tıp Fakültesi'nde KPH tanısı ile takip edilen ve antirezorptif tedavi uygulanan hastaların tıbbi kayıtları retrospektif olarak değerlendirildi.

Bulgular: KPH olan toplam 26 hasta (12 kadın/14 erkek) değerlendirildi. Ortalama tanı yaşı 62.9±13.5 idi. Semptomların başlangıcından tanıya kadar geçen medyan süre 17.5 aydı (1-480 arası). Belirtilerden ağrı 16 hastada, şişlik 3 hastada, kızarıklık 2 hastada, kırık 1 hastada, nefrolitiazis 1 hastada, işitme kaybı 1 hastada mevcuttu. Laboratuvar incelemesinde ortalama alkalen fosfataz (ALP) 512±557 U/L, kemiğe özgü ALP 81.2±51.4 µg/L ve ALP üst limitin 4.12±4 katı idi. Hastalığın tutulum yerleri %58 pelvis, %46 vertebra, %35 kafatası, %23 femur, %11.5 tibia, %3.8 humerus şeklinde idi. Toplam 26 hastanın 21'i tek başına zoledronik asit ile tedavi edilmişti. Dört hastada nüks meydana geldi ve tedaviden nükse kadar geçen ortalama süre 72.25±28.7 aydı.

Sonuç: Zoledronik asit çok güçlü bir antirezorptif ilaçtır ve tek doz tedavi ile bile hastalığın uzun süreli remisyonunu sağlar.

Anahtar Kelimeler: Kemiğin Paget hastalığı, zoledronik asit, alkalen fosfataz

Corresponding Author/Sorumlu Yazar: Hülya HACİŞAHİNOĞULLARI **E-mail:** mercandogru@hotmail.com

Submitted/Başvuru: 13.08.2023 • **Revision Requested/Revizyon Talebi:** 18.08.2023 • **Last Revision Received/Son Revizyon:** 18.08.2023 • **Accepted/Kabul:** 18.08.2023 • **Published Online/Online Yayın:** 10.10.2023

INTRODUCTION

Paget's disease of bone (PDB) is a focal and chronic disorder of bones. It is characterized by increased bone resorption by osteoclast and followed by accelerated osteoblast activity, bone remodeling, and overgrowth (1). The disease may occur in a single site (monostotic) or multiple sites (polyostotic). The most affected sites include the pelvis, spine, femur, tibia, and skull. The prevalence of the disease is higher in the UK and in countries where the British population has migrated, such as the United States. The prevalence is 1-2% in the United States, but it is declining (2,3). It is rare for Paget's disease of bone to present before the age of 50, and it is seen equally in men and women however, some studies have reported that it is more common in men (4-6).

Although the exact cause is not known, genetic factors and environmental factors such as a slow virus infection are involved in the development of the Paget disease The majority of patients are sporadic (7). The most important gene responsible for the disease is the SQSTM1 (8,9).

Most of the patients are asymptomatic and they are diagnosed during the evaluation of incidentally detected lesions or elevated serum alkaline phosphatase (ALP) levels. Pain and deformity are two important clinical manifestations. Complications related to Paget's disease include heart failure, deformity, hearing loss, bone fracture, nerve compression, and sarcoma.

The diagnosis of PDB is made by clinical features, and typical findings of the disease in radiological and scintigraphic examination. In laboratory analysis bone turnover markers including ALP, bone-specific ALP (BALP), procollagen type 1 N-terminal propeptide (P1NP), serum C-telopeptide (CTx), and urinary N-telopeptide (NTx) are frequently elevated. If there are typical findings in radiographs, scintigraphy is taken to evaluate the extent of the disease. Computerized tomography (CT) or magnetic resonance imaging (MRI) is used to evaluate suspicious lesions. Treatment options for PDB include calcitonin, bisphosphonates, and denosumab. Current guidelines recommend a single dose of 5 mg intravenous zoledronic acid if there is no contraindication for use (10,11). Although the response to treatment is different, it was shown that a single dose of zoledronic acid provided remission for 5-6 years (12).

This study aimed to evaluate the clinical characteristics of patients with PDB and patients' responses to the treatments.

MATERIAL and METHODS

In the study, we retrospectively evaluated medical records of patients who were followed up with the diagnosis of PDB and treated with antiresorptive therapy in the Department of Endocrinology and Metabolic Diseases of Istanbul Faculty of Medicine between 1980 and 2023.

Clinical and demographic features of patients, age, gender, family history, symptoms, duration from symptom onset to diagnosis, disease involvement, distribution of disease on bone scintigraphy, and additional imaging methods for diagnosis were evaluated. Before the treatment serum levels of creatinine, adjusted calcium, phosphorus, albumin, magnesium, parathyroid hormone (PTH), 25 OH vitamin D, total serum ALP, and BALP were analyzed. ALP level was expressed as the upper limit of the normal range (ULNR).

Patients' responses to treatment, duration of remission and time to relapse, and major side effects related to treatment were assessed in patients who were treated with only zoledronic acid for PDB.

Remission was defined as the normalization of ALP or BALP. If ALP was normal before the therapy, BALP was monitored to assess the patient's responses to therapy. Relapse was defined as the elevation of ALP (or BALP) above the normal range or increased by more than 25% from the nadir ALP value in patients who did not achieve ALP normalization.

The study protocol was approved by the Clinical Ethics Committee of Istanbul University, Istanbul Faculty of Medicine (Date: 21.07.2023, No: 15). Written informed consent was waived due to the nature of this retrospective study. Statistical analyses were performed using SPSS version 21.0. Categorical variables were presented as percentage and frequency, whereas numerical variables were presented as mean±standard deviation (SD).

RESULTS

In this study, a total of 26 patients with Paget's disease of bone were evaluated. There were 12 females and 14 males, male/female ratio was 1.17. The mean age at diagnosis was 62.9±13.5 years (median 65.5, range 33-84). The mean age of the females was 70±10.9 years (median 71.5, range 53-84), and the mean age of the males was 56.6±12.6 years (median 58.5 range 33-72).

The median duration from the onset of symptoms to diagnosis was 17.5 months (range 1-480). The symptoms were as follows: pain in 16 (61.5%), swelling in 3 (11.5%), rubor in 2 (7.7%), bone fracture in 1 (3.8%), nephrolithiasis in 1 (3.8%), and hearing loss in 1 (3.8%) patient. The diagnosis of PDB was made during the evaluation of elevated ALP levels in 3 asymptomatic patients. In one patient, pagetic lesions were detected in cranial computed tomography performed to evaluate post-accident head trauma. Two patients had similarly affected siblings and both of them were involved in this study. These two patients were diagnosed by family screening for PDB.

Laboratory tests revealed the following results (mean±SD): Plasma creatinine 0.89±0.24 mg/dL (normal range 0.7-1.4), GFR 82.1±19.4, phosphorus 3.6±0.45 mg/dl (normal range 2.7- 4.5), adjusted calcium 9.3±0.45 mg/dL (normal range 8.5-10.5), PTH 55.6±24 pg/ml (normal range 15-65), 25 OH D 34±30 ng/mL (normal range 30-80), ALP 512±557 U/L (median 296, range 70-2339) (normal range 40-120), BALP 81.2±51.4 µg/L (median 63, normal range 4-22). The mean ALP was 4.12±4 ULNR (median 2.6 range 1.01-16.5).

Table 1: Distribution of bone involvement of Paget's disease on scintigraphy imaging

Localization	Number of patients
Skull	9
Vertebra	12
Servical	1
Dorsal	7
Lomber	9
Sacrum	5
Humerus	1
Right	1
Scapula	2
Right	1
Left	1
Pelvis	15
Right	6
Left	12
Femur	6
Right	4
Left	5
Tibia	3
Right	1
Left	2

Bone scintigraphy was performed to determine the extent of the disease in all patients at initial evaluation. The distribution of the disease was; pelvis in 15 patients (15/26, 58%), vertebra in 12 patients (12/26, 46%), skull in 9 patients (9/26, 35%), femur in 6 patients (6/26, 23%), tibia in 3 patients (3/26, 11.5%), scapula in 2 patients (2/26, 7.7%), humerus in 1 patient (1/26, 3.8%). The distribution of PDB is summarized in Table 1. Eleven patients (42.3%) had polyostotic disease (7 females, 4 males). We performed bone biopsies on 3 patients to confirm the diagnosis due to suspicious lesions.

Of 26 patients, 21 were treated with zoledronic acid alone, and 3 patients were treated with pamidronate followed by zoledronic acid. The remaining two patients were treated with pamidronate or ibandronate. The patients treated with only zoledronic acid for PDB were evaluated for the efficiency of therapy. The mean duration from therapy to normalization of ALP was 4.37±3.6 months (range 1-13). The nadir ALP level was 64.76±19.21 and achieved after 17.3±12.9 months (median 13). The mean duration of follow-up was 53.4±38.3 months after zoledronic acid therapy. Fourteen patients were in remission after a single dose of zoledronic acid and the mean duration of follow-up was 51.3±30.6 months. We could not assess remission because of the short follow-up time in Case 5 and Case 20 (Table 2). In 1 patient (Case 6), the ALP value decreased

Table 2: Baseline characteristics and treatment responses of patients treated with zoledronic acid

	Gender	Age at diagnosis	ALP	ALP (ULNR)	BALP	Distribution of disease	Duration of followed up (month)	Presence of remission/relapse
Case 1	M	62	107	*	25	Monostotic	69	Remission
Case 2	F	73	338	2.75	123	Polyostotic	24	Remission
Case 3	F	54	292	2.78	75	Monostotic	66	Relapse
Case 4	M	67	245	1.88	163	Monostotic	60	Remission
Case 5	M	72	459	3.53	51	Monostotic	3	**
Case 6	F	70	1740	16.5	>90	Polyostotic	12	***
Case 7	F	64	202	1.94	46.9	Polyostotic	43	Remission
Case 8	M	52	403	3.1	>90	Monostotic	33	Remission
Case 9	F	58	183	1.74	56	Monostotic	54	Remission
Case 10	M	33	131	1.01	32	Monostotic	14	Remission
Case 11	M	58	337	2.59	84	Polyostotic	64	Remission
Case 12	F	84	70	*	20	Monostotic	36	Remission
Case 13	F	53	667	5.13	>90	Polyostotic	104	Remission
Case 14	F	75	613	5.8	NA	Polyostotic	93	Relapse
Case 15	M	59	504	3.87	>90	Polyostotic	93	Relapse
Case 16	M	47	296	2.27	>90	Monostotic	108	Remission
Case 17	M	41	195	1.5	59,9	Polyostotic	8	Remission
Case 18	F	68	281	2.18	178	Monostotic	133	Relapse
Case 19	M	46	139	1.1	37	Monostotic	50	Remission
Case 20	F	84	1232	11.7	>90	Polyostotic	1	**
Case 21	M	71	213	1.63	68	Monostotic	18	Remission

NA: Not available, ALP: Alkaline phosphatase (normal range 40-120 U/L), ULNR: Upper limit of the normal range, BALP: Bone specific Alkaline phosphatase (normal range 4-22 µg/L), * It was not calculated because of ALP value was normal, **Short follow-up time limited to assess remission, ***The decline of ALP was not enough to define remission.

significantly from 1740 to 169 U/L in the first year after zoledronic acid therapy, although it was above the upper limit of normal. Relapse occurred in four patients; the mean duration from therapy to relapse was 72.25±28.7 months (range 30-94). The characteristics of the patients and patient's responses to zoledronic acid therapy were summarized in Table 2.

Bisphosphonate-related major side effects were not present in the patients treated with zoledronic acid. However, osteonecrosis of the jaws occurred in 1 patient who was treated with ibandronate. PDB-related complications were as follows: hearing loss in 6 patients, nerve compression in 3 patients, and bone fracture in 1 patient. Bone malignancy did not occur in any of the patients.

DISCUSSION

In this study, we reviewed patients' demographic and clinical features and also assessed the effect of a single dose of zoledronic acid in the treatment of PDB. PDB is more common in people over the age of 55 years, it rarely presents before age 40. The mean age of our study group is compatible with the literature, however, seven patients were younger than 55 years at diagnosis and one of them was 33 years old. The male/female ratio was 1.17, and as in similar studies, there was a small male predominance (2).

Most patients with PDB are asymptomatic, but in our study, the majority of patients were symptomatic, and only five patients were asymptomatic (10). Bone pain is one of the most common clinical manifestations. In the study of Tan et al., it was reported in 73.8% of patients. Similarly, the most common symptom in our study was pain and it was present in 61.5% of the patients (13).

The pelvis is reported to be the most common site of involvement in PDB. In the study of Guyer et al., pelvis involvement was present in 74-76% of the patients and there was a tendency to the involvement of the right side. Similarly, the most common site of involvement was the pelvis in our study. However, left-side involvement was more common than right (14).

Multiple genetic loci associated with PDB have been identified and the inheritance of the disease seems to be autosomal dominant. The most important gen is SQSTM1. It encodes a protein which is called p62 and has a role in the activation of the transcription factor NF-κB (15,16). There were siblings from two different families in the present study, but the genetic analysis could not be performed.

Treatment is recommended in patients with active PDB to prevent the development of complications. Treatment options include three antiresorptive groups: bisphosphonates, denosumab, and calcitonin. Recommended bisphosphonates are zoledronic acid, pamidronate, and oral bisphosphonates such as alendronate, and risedronate. First-choice treatment is zoledronic acid because it is the most potent agent (10,11). It was reported that a single dose provided biochemical remission in 96% of patients with PDB and the duration of remission was longer than 5 years (12,17). Relapse developed in 4 of 21 patients treated with a single dose of zoledronic acid. Similar to the studies in the literature, the time from zoledronic acid treatment to relapse was longer than 5 years in our study.

CONCLUSION

PDB is a common metabolic bone disorder that causes complications and has a negative long-term physical impact. Zoledronic acid improves symptoms and prevents complications. It is a potent antiresorptive agent and provides long-term remission as shown in our study

Ethics Committee Approval: This study was approved by Istanbul Faculty of Medicine Clinical Research Ethics Committee (Date: 21.07.2023, No: 15).

Peer Review: Externally peer-reviewed.

Author Contributions: Conception/Design of Study- A.K.Ü., R.T., F.A., N.G., Ö.S.S., G.Y.Y., H.H., G.B.O; Data Acquisition- G.B.O., H.H., N.G., A.K.Ü.; Data Analysis/Interpretation- H.H., G.B.O., N.G., A.K.Ü.; Drafting Manuscript- A.K.Ü., R.T., F.A., N.G., Ö.S.S., G.Y.Y., H.H., G.B.O; Critical Revision of Manuscript- H.H., A.K.Ü., G.B.O.; Final Approval and Accountability- A.K.Ü., R.T., F.A., N.G., Ö.S.S., G.Y.Y., H.H., G.B.O; Material and Technical Support- A.K.Ü., R.T., F.A., N.G., Ö.S.S., G.Y.Y., H.H., G.B.O; Supervision- G.B.O., H.H., N.G., A.K.Ü., Ö.S.S.

Conflict of Interest: The authors have no conflict of interest to declare.

Financial Disclosure: The authors declared that this study has received no financial support.

REFERENCES

1- Meunier PJ, Coindre JM, Edouard CM, Arlot ME. Bone histomorphometry in Paget's disease. Quantitative and dynamic analysis of pagetic and nonpagetic bone tissue. Arthritis Rheum 1980;23(10):1095-103.

2- Altman RD, Bloch DA, Hochberg MC, Murphy WA. Prevalence of pelvic Paget's disease of bone in the United States. J Bone Miner Res 2000;15(3):461-5.

3- Husseini JS, Oganesyan R, Staffa SJ, Huang E, Habibollahi S, Hemke R, et al. Prevalence of Paget's disease of bone: review of consecutive abdominopelvic CT scans and literature. Acta Radiol 2023;64(3):1086-92.

4- Cook MJ, Pye SR, Lunt M, Dixon WG, Ashcroft DM, O'Neill TW. Incidence of Paget's disease of bone in the UK: evidence of a continuing decline. Rheumatology (Oxford) 2021;60(12):5668-76.

5- Mays S. Archaeological skeletons support a northwest European origin for Paget's disease of bone. J Bone Miner Res 2010;25(8):1839-41.

6- Guañabens N, Garrido J, Gobbo M, Piga AM, del Pino J, Torrijos A, et al. Prevalence of Paget's disease of bone in Spain. Bone 2008;43(6):1006-9.

7- Reddy SV, Singer FR, Roodman GD. Bone marrow mononuclear cells from patients with Paget's disease contain measles virus nucleocapsid messenger ribonucleic acid that has mutations in a specific region of the sequence. J Clin Endocrinol Metab 1995;80(7):2108-11.

8- Hocking LJ, Herbert CA, Nicholls RK, Williams F, Bennett ST, Cundy T, et al. Genomewide search in familial Paget disease of bone shows evidence of genetic heterogeneity with candidate loci on chromosomes 2q36, 10p13, and 5q35. Am J Hum Genet 2001;69(5):1055-61.

9- Cronin O, Subedi D, Forsyth L, Goodman K, Lewis SC, Keerie C, et al. Characteristics of early Paget's disease in SQSTM1 mutation carriers: Baseline analysis of the ZiPP study cohort. J Bone Miner Res 2020;35(7):1246-52.

10- Singer FR, Bone HG 3rd, Hosking DJ, Lyles KW, Murad MH, Reid IR et al. Endocrine Society. Paget's disease of bone: an endocrine society clinical practice guideline. J Clin Endocrinol Metab 2014;99(12):4408-22.

11- Ralston SH, Corral-Gudino L, Cooper C, Francis RM, Fraser WD, Gennari L, et al. Diagnosis and Management of Paget's Disease of Bone in Adults: A Clinical Guideline. J Bone Miner Res 2019;34(4):579-604.

12- Reid IR, Lyles K, Su G, Brown JP, Walsh JP, del Pino-Montes J, el al. A single infusion of zoledronic acid produces sustained remissions in Paget disease: Data to 6.5 years. J Bone Miner Res 2011;26(9):2261-70.

13- Tan A, Ralston SH. Clinical presentation of Paget's disease: evaluation of a contemporary cohort and systematic review. Calcif Tissue Int 2014;95(5):385-92.

14- Guyer PB. Paget's disease of bone: the anatomical distribution. Metab Bone Dis Relat Res 1981;3(4-5):239-41.

15- Hocking LJ, Lucas GJ, Daroszewska A, Mangion J, Olavesen M, Cundy T, et al. Domain specific mutations in Sequestosome 1 (SQSTM1) cause familial and sporadic Paget's disease. Hum Mol Genet 2002;11(22):2735-9.

16- Moscat J, Diaz-Meco MT. p62 at the crossroads of autophagy, apoptosis, and cancer. Cell 2009;137(6):1001-4.

17- Reid IR, Miller P, Lyles K, Fraser W, Brown JP, Saidi Y, et al. Comparison of a single infusion of zoledronic acid with risedronate for Paget's disease. N Engl J Med 2005;353(9):898-908.

İSTANBUL UNIVERSITY PRESS

RESEARCH ARTICLE / ARAŞTIRMA MAKALESİ
Journal of Advanced Research in Health Sciences /
Sağlık Bilimlerinde İleri Araştırmalar Dergisi 2023
DOI: 10.26650/JARHS2023-1283136

ARE ONLINE STREAMING VIDEOS ON TRACHEOSTOMY CARE APPROPRIATE FOR MEDICAL EDUCATION?

TRAKEOSTOMİ BAKIMIYLA İLGİLİ ÇEVRİMİÇİ VİDEO AKIŞ SİTELERİNDE YAYINLANAN VİDEOLAR TIP EĞİTİMİNDE KULLANILMAK İÇİN UYGUN MUDUR?

Murat TANYILDIZ[1], Furkan YAVUZ[2], Sinem OĞUZ[2], Aslı Ece YAKICI[1], Ömer ÖZDEN[1], Ozan GÖKLER[3]

[1] Koc University, School of Medicine, Department of Pediatric Critical Care, Istanbul, Turkiye
[2] Koc University, School of Medicine, Istanbul Turkiye
[3] Koc University, School of Medicine, Department of Otolaryngology, Istanbul, Turkiye

ORCID ID: M.T. 0000-0001-8804-032X; F.Y. 0000-0001-7151-4007; S.O. 0000-0002-5796-3890 A.E.Y. 0000-0002-8490-4749; Ö.Ö. 0000-0003-0297-5250; O.G. 0000-0003-1621-3687

Citation/Atıf: Tanyildiz M, Yavuz F, Oguz S, Yakici AE, Ozden O, Gokler O. Are online streaming videos on tracheostomy care appropriate for medical education? Journal of Advanced Research in Health Sciences 2023;6(3):281-288. https://doi.org/10.26650/JARHS2023-1283136

ABSTRACT

Objective: We aimed to analyze the quality of videos about tracheostomy care on an online video streaming site for teaching healthcare staff and medical students.

Material and Methods: In this cross-sectional, quantitative and exploratory study, firstly an online YouTube search was performed using the keywords "tracheostomy care" and "pediatric tracheostomy care". The total view counts, video duration and video source were recorded. The educational quality and accuracy of the video content were evaluated using the DISCERN, Global Quality Score (GQS), and Journal of the American Medical Association (JAMA) scores. Secondly, a pre-test comprising questions about tracheostomy care was administered to medical faculty students and intensive care nurses. Participants watched the three videos with the highest DISCERN, JAMA, and GQS scores before taking a post-test. The pre- and post-test scores were then compared.

Results: From the initial 339 videos, duplicated, non-English, and low sound quality videos were excluded, and 122 videos were analyzed. The mean DISCERN score was 39.4±8.7 (fair), the mean JAMA score 2.1±0.8 (fair), and the mean GQS 3.3±1.1 (fair). Sixty-one (50%) videos were related to medical education and 57 (46.7%) to patient education. Most of the videos were uploaded by non-physician healthcare staff. The pre- and post-test results showed that the videos uploaded by medical education websites and academic institutions had higher educational quality and may be utilized for online education.

Conclusions: Tracheostomy care videos on YouTube with the highest DISCERN, JAMA and GQS scores could be used for online learning by medical students and nurses in resource-limiting centers.

Keywords: Tracheostomy care, online and digital learning, YouTube video quality.

ÖZ

Amaç : Sağlık personeli ve tıp öğrencilerine yönelik eğitim veren çevrimiçi bir video akışı sitesindeki trakeostomi bakımıyla ilgili videoların kalitesini analiz etmeyi amaçladık.

Gereç ve Yöntem: YouTube araması "trakeostomi bakımı" ve "pediatrik trakeostomi bakımı" anahtar kelimeleri kullanılarak yapıldı. Toplam görüntüleme sayısı, video süresi ve video kaynağı kaydedildi. Video içeriğinin eğitim kalitesi ve doğruluğu DISCERN, Global Quality Score (GQS) ve Journal of the American Medical Association (JAMA) puanları kullanılarak değerlendirildi.

İkinci olarak tıp fakültesi öğrencilerine ve yoğun bakım hemşirelerine trakeostomi bakımına ilişkin soruları içeren bir ön test uygulandı. Katılımcılar son teste girmeden önce DISCERN, JAMA ve GQS puanları en yüksek olan üç videoyu izlediler. Daha sonra ön ve son test puanları karşılaştırıldı. Katılımcılar son teste girmeden önce DISCERN, JAMA ve GQS puanları en yüksek olan üç videoyu izlediler. Daha sonra ön ve son test puanları karşılaştırıldı.

Bulgular: İlk 339 videodan kopya, İngilizce olmayan ve düşük ses kalitesine sahip videolar hariç tutuldu ve 122 video analiz edildi. Ortalama DISCERN puanı 39,4±8,7 (orta), ortalama JAMA puanı 2,1±0,8 (orta), GQS ortalaması 3,3±1,1 (orta) idi. Videoların 61'i (%50) tıp eğitimi, 57 m'si (%46,7) hasta eğitimi ile ilgiliydi.

Videoların çoğu doktor dışı sağlık personeli tarafından yüklendi. Ön ve son test sonuçları, tıp eğitimi veren siteler ve akademik kurumlar tarafından yüklenen videoların eğitim kalitesinin daha yüksek olduğunu ve çevrimiçi eğitim için kullanılabileceğini gösterdi.

Sonuçlar: YouTube'daki en yüksek DISCERN, JAMA ve GQS puanlarına sahip trakeostomi bakım videoları, kaynak kısıtlı merkezlerdeki tıp öğrencileri ve hemşireler tarafından çevrimiçi öğrenim için kullanılabilir.

Anahtar Kelimeler: Trakeostomi bakımı, çevrimiçi ve dijital öğrenme, YouTube video kalitesi.

Corresponding Author/Sorumlu Yazar: Murat TANYILDIZ **E-mail:** murattanyildiz@gmail.com

Submitted/Başvuru: 14.04.2023 • **Revision Requested/Revizyon Talebi:** 23.06.2023 • **Last Revision Received/Son Revizyon:** 28.06.2023 • **Accepted/Kabul:** 06.07.2023 • **Published Online/Online Yayın:** 10.10.2023

INTRODUCTION

According to US data, more than 50.000 patients receive tracheostomies annually (1). As the number of tracheostomies continues to rise, appropriate care for patients with tracheostomies is gaining further importance. Proper care prolongs life expectancy, increases quality of life, reduces morbidity, restores physiological functions, ensures normal growth and development and reduces the frequency/duration of hospitalizations, thus reducing health costs. However, if health personnel lack the necessary training and experience, patients with tracheostomies may receive suboptimal treatment and encounter serious complications, even death (2). Multidisciplinary teams are assembled to improve the care of patients with tracheostomy in some institutions (3). Educating the responsible staff on tracheostomy care is critical, and various methods can be applied to provide such education and achieve the best patient outcomes. Specialized teams and standardized training protocols using various simulations as well as written and visual materials for healthcare professionals and families can shorten the length of hospital stays and reduce costs (3). However, it is not feasible for every institution to access such simulation education or assemble multidisciplinary teams. Accordingly, online education with digital learning can play a major role, especially in centers with limited resources, and YouTube may be a video-based education tool for such centers (4).

YouTube is one of the most utilized social media platforms in the world and has developed into an exceptionally quick-growing visual library that surpasses 2.6 billion visitors per month and with five billion videos watched per day (5). Given its boundless data, YouTube offers a resource from which people can seek answers, gain information and obtain education (6). Since the videos on YouTube are quick, easy to access and free, they can also be used by medical students and healthcare workers (7,8). However, due to insufficient fact-checking and monitoring of the videos, YouTube may contain false and misleading health-related content. As a result, publishers and viewers of health-related videos need to be careful about the reliability and validity of the presented medical information (9). Even though different studies from a range of medical fields have assessed YouTube videos to our knowledge, no prior studies have analysed YouTube videos on tracheostomy care and their educational value (9,10). We therefore aimed to evaluate the quality and value of YouTube videos on tracheostomy care and to determine whether these videos could be used to educate medical students and intensive care (ICU) nurses.

MATERIALS and METHODS

Aim and study design

This study was a cross-sectional, quantitative, and exploratory study. The first part of the study included data collection and the evaluation of videos using DISCERN, Journal of the American Medical Association (JAMA) scores, and the Global Quality Score (GQS) to assess the academic and educational competences, and reliability of the video content. In the second part, we used pre- and post-tests to determine whether the videos with the highest scores had educational value. This study received approval from an institutional ethical committee (Date: 11.08.2022, No: 2022.278.IRB3.117).

Data collection

We conducted an online video search of YouTube on 18 April 2022 using the terms 'tracheostomy care' and 'pediatric tracheostomy care'. One experienced otolaryngologist (OG) and one pediatric intensivist (OO) assessed the videos. The default search settings were 'order videos by view count'. To prevent biased recommendations, all the video searches were conducted after completely clearing the browser search history and erasing all account log-ins.

Videos in any language other than English, soundless videos, duplicate videos and videos unrelated to tracheostomy care were excluded. Each video's total views count, title, duration (in seconds), time since upload (days), views per day, number of comments, number of likes and dislikes and like ratios (like×100/(like+dislike) were noted. The video's source was categorized into the following: physician (created by an individual physician, not an institution), healthcare staff (nurse, physiotherapist, etc.), hospital, organization, university, medical education website (professional healthcare video-sharing and digital learning websites), patient/patient-caregiver and other (advertising for trading company, private hospital). The videos were also grouped according to whether they provided medical education, patient education, or a patient's experience of tracheostomy.

DISCERN, JAMA, and GQS scores

DISCERN, GQS and JAMA are scoring systems used to assess the academic, educational competence and reliability of educational content. Oxford University developed the DISCERN grading system, which assesses the accuracy and instructional value of information, particularly concerning medical care. It comprises three sections, 16 questions, with each question having scores ranging from 1 to 5. The first segment (questions 1-8) assesses the validity of a publication. The following segment (questions 9-15) centers around information on treatment-related topics, and the last section analyses the overall calibre of the educational content. The evaluation is based on 15 questions, and the final question in the third segment is not scored. According to the 15-75 point rating scale, an item is either excellent (63-75 points), good (51-62 points), fair (39-50 points), poor (27-38 points), or very poor (15-26 points) (Supplementary Data 1) (11).

A video source's publishing and privacy details can be evaluated using the well-known JAMA rating system. Authorship, attribution, disclosure and currency are the four criteria, with each graded from 0 to 1. Four points denote the highest level of quality (12). Even though the DISCERN and JAMA scores were originally created for written information, these scores have been widely applied in various studies (13-15). The GQS scale can be utilized by users to assess video content via a five-point scoring system, with each response scoring 1-5 for a maximum achievable score of 5 points (see Supplementary Data 2 for the GQS and JAMA instruments) (16).

Video evaluation

The mean GQS, JAMA, and DISCERN scores of the investigators were recorded. To determine the inter-rater reliability, Kappa consistency analysis was used. The Kappa coefficient lies between 0 and 1, with values between 0.93 and 1.00 indicating perfect consistency, 0.81-0.92 very good consistency, 0.61-0.80 good consistency, 0.41-0.60 moderate consistency, 0.21-0.40 below moderate level consistency and 0.20-0.01 weak consistency. At the end of the evaluation, the three videos with the highest scores for all three scoring systems were selected as training videos to test their educational value.

Statistics

We used SPSS software version 23.0 (SPSS Inc., Chicago, IL) for all the statistical analyses. The descriptive statistics of the tracheostomy videos are shown as means and standard deviations. The frequency and percentages are presented for the categorical variables. To determine the normal distribution of the data, the Kolmogorov–Smirnov test was initially performed. The Kruskal–Wallis test was used to confirm the differences between the continuous variables among the groups. The significance of the pairwise differences with Bonferroni adjustment was examined using the Mann–Whitney *U* test. The correlation statistics were computed using Spearman's test. P values less than 0.05 were considered statistically significant.

Evaluation and statistical analysis of the pre-and post-tests

The second part of the study involved administering a pre-test to the medical faculty students (n=20), and ICU nurses (n=20). While the medical faculty students had no previous experience with tracheostomy care, the ICU nurses knew how to monitor and care for patients with tracheostomies. The pre-test was developed by an experienced pediatric intensivist (MT) who works as an instructor in an institutional simulation education center and within a multidisciplinary tracheostomy team. The pre-test comprised questions about tracheostomy care and an emergency condition in a patient with a tracheostomy. The test contained 10 multiple choice questions each scoring 10 points. The lowest total score in the test was 0 and the highest 100. Informed consent was obtained from all the participants before the pre-test. The participants watched the three YouTube videos (Supplementary Data 3) and then completed the post-test, which was the same as the pre-test (Supplementary Data 4). The pre- and post-tests were evaluated by the same researcher who scored each question equally. The total scores for each individual and the medical student and ICU nurse groups from the pre- and post-tests were compared.

The pre- and post-test results of the groups were compared using the Wilcoxon test. The pre- and post-test results of the groups were examined independently using the Mann–Whitney *U* test. Given a 5% first-type error (α), 0.95 standardized effect size, distribution ratio of 1:1 between the groups and 80% power (β is 0.20), the required minimum sample size was 38 participants in total with 19 participants for each group. G-Power was used for the power analysis. Twenty participants were included in each group to avoid the possibility of missing erroneous observations.

RESULTS

Descriptive characteristics

Of the 339 evaluated videos, 122 met the inclusion criteria (Table 1). Videos in any language other than English (n=10), soundless videos (n=16), duplicate videos (n=118), and videos unrelated to tracheostomy care (n=73) were excluded (Figure 1). Among the 122 videos, 41 (33.6%) were related to pediatric tracheostomy care and 81 (66.3%) to adult tracheostomy care. Thirty-nine (31.9%) videos were uploaded by non-physician healthcare-staff, 28 (22.9%) by hospitals, 26 (21.3%) by organizations, eight (6.5%) by universities, eight (6.5%) by medical education websites, four (3.2%) by physicians, and four (3.2%) by patient caregivers. In terms of content, 61 (50%) videos presented medical education content, 57 (46.7%) patient education content and four (3.2%) patient caregiver experience of patients with tracheostomies. The majority of the videos were posted in the United States (75%) and the UK (13.9%), with 4.9% in China and 2.4% in India.

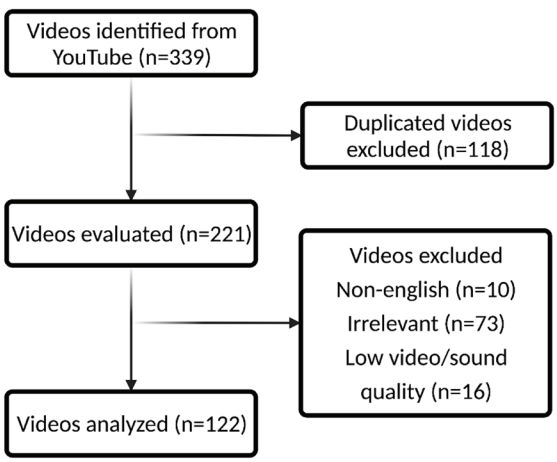

Figure 1: Flow chart of tracheostomy videos that were evaluated

Table 1: Descriptive statistics of tracheostomy videos

Descriptive statistics	Mean±SD	Range
View count, (n)	88185.8±185970.4	39-1403098
Duration of video (second)	404±336.8	42-1420
Time since upload date (day)	1921.2±1103.3	243-4916
View ratio (Daily views)	46.2±79.6	0.1-637.7
Likes, (n)	430.8±793.4	0-5000
Dislikes, (n)	28.3±76.9	0-677
Comments, (n)	13.2±26.2	0-182
Like ratio	93.9±6.3	66.3-100
DISCERN score	39.4±8.7	21-59
GQS score	3.3±1.1	1-5
JAMA score	2.1±0.8	0-4

GQS: Global Quality Score, JAMA: Journal of American Medical Association, SD: Standard deviation

Table 2: The mean DISCERN score, GQS score, and JAMA score according to categories of tracheostomy videos

Categories	n	DISCERN	GQS	JAMA
Medical education	61	38.6±7.1	3.2±0.9	1.9±0.8
Patient education	57	40.3±10.1	3.6±1.3	2.3±0.7
Patient/care giver experience	4	38.5±13.1	3.0±0.8	1.0±0.1
Total	122	39.4±8.7	3.3±1.1	2.1±0.8
p value		0.61	0.097	0.001

GQS: Global Quality Score, JAMA: Journal of American Medical Association, SD: Standard deviation,

Table 3: The mean DISCERN score, GQS score, and JAMA score according to categories of publishers

Publishers	n	DISCERN	GQS	JAMA
Non-Physician Health Personal	39	39.0±6.5	3.3±0.7	1.7±0.7
Hospital	28	43.2±8.7	4.1±0.9	2.2±0.6
Organization	26	35.1±7.5	2.7±1.2	2.3±0.6
University	8	43.5±6.9	3.6±0.9	2.6 ±0.7
Medical education website	8	51.1±6.4	4.6±0.5	3.1±0.6
Physician	4	34.0±7.8	2.2 ±1.2	1.7±0.9
Patient caregiver	4	30.0±9.4	2.6±0.9	1.0±0.1
Others	5	33.2±12.4	2.4±0.9	1.8±1.1
Total	122	39.4±8.7	3.3±1.1	2.1±0.8

GQS: Global Quality Score, JAMA: Journal of American Medical Association, SD: Standard deviationv

Interrater reliability analysis

The interrater reliability of two investigators' Kappa consistency analysis revealed that the DISCERN, GQS and JAMA scores had very good consistency. The Kappa coefficients of the DISCERN, GQS, JAMA scores were 0.84, 0.82 and 0.91, respectively (p<0.001). The highest consistency was evident in the JAMA scores. Since there was consistency between the scores given by the two researchers, the scores were calculated using the average of the two investigators.

DISCERN evaluation

The mean DISCERN score for all the videos was 39.4±8.7 (fair). Based on the video categories, the mean DISCERN scores of the medical education, patient education and patient/caregiver experience videos were 38.6±7.1, 40.3±10.1 and 38.5±13.1 respectively. The differences were not statistically significant (p=0.61) (Table 2). For the video publisher categories, the DISCERN score of the medical education websites was highest at 51.1±6.4 (good), while university, hospital, and healthcare-staff's videos scored 43.5±6.9, 43.2±8.7, 39.0±6.5, respectively (Table 3).

JAMA evaluation

The mean JAMA score of all the videos was 2.1±0.8. For the video categories, the JAMA scores were 2.3±0.7, 1.9±0.8 and 1.0±0.1, for the patient education, medical education and patient/caregiver experience videos, respectively (Table 2). For the video publisher categories, the mean JAMA score for the medical education website was highest (3.1±0.6), followed the videos by universities (2.6±0.7), organizations (2.3±0.6) and hospitals (2.2±0.6; p<0.001) (Table 3).

GQS evaluation

The mean GQS of all the videos was 3.31.1, while in the individual categories, the patient education videos scored 3.6±1.3, the medical education videos 3.2±0.9 and the patient/caregiver experience videos 3.0±0.8 (Table 2). For the video publisher categories, the mean GQS score of medical education website was highest at 4.6±0.5, with the hospital and university videos scoring 4.1±0.9 and 3.6±0.9, respectively (Table 3).

Comparison of the DISCERN, JAMA, and GQS scores

The mean values of the DISCERN, GQS and JAMA scores were 39.4±8.7 (poor), 3.3±1.1 (fair), and 2.1±0.8 (fair), respectively. No statistically significant differences were found for the DISCERN, and GQS scores for the patient education, medical education and patient/caregiver experience video categories (p=0.60, p=0.097, p=0.67 respectively). In contrast, the mean JAMA scores were significantly different among the video categories (p<0.001), with the patient educational videos receiving the highest JAMA score (Table 2). The patient education and medical educational videos had significantly higher JAMA scores than those of the patient/caregiver experience videos (patient education videos vs. patient/caregiver experience vi-

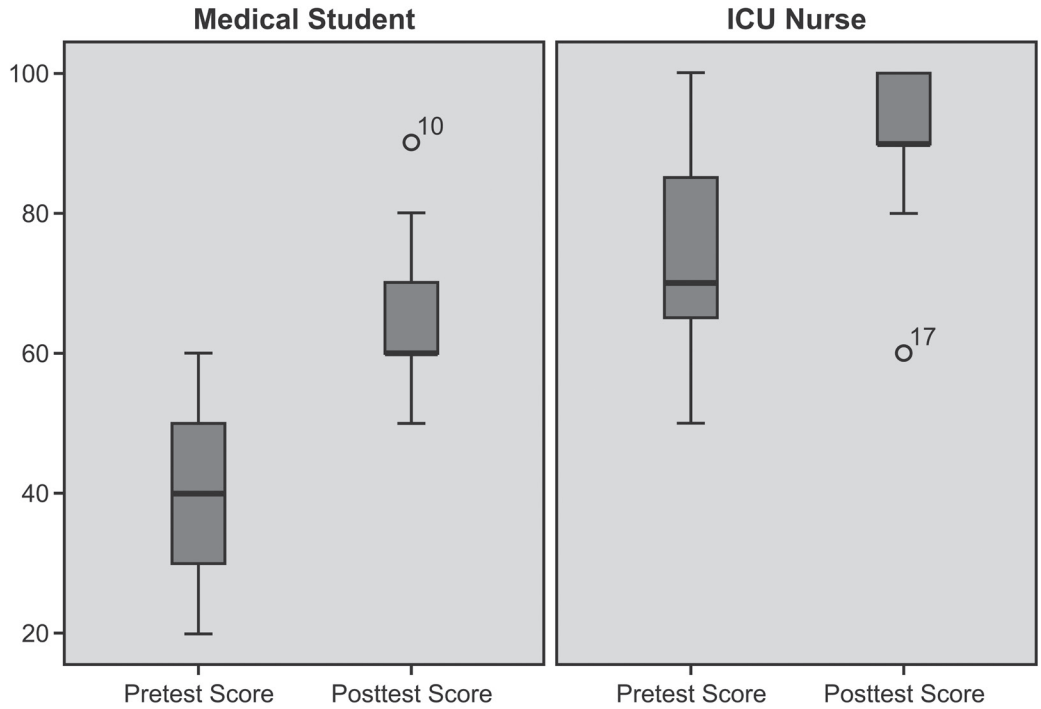

Figure 2: The pre-test and post-test scores of the medical student and ICU nurse are shown with Boxplot chart. On the left side of the figure medical student pre-test and post-test scores, and on the right side, the ICU nurse pre-test and post-test scores are shown. Accordingly, for medical students the pre-test minimum score was 20, the post-test minimum score was 50. For the ICU nurse, the pre-test minimum score was 50, the post-test minimum score was 60. In the box plot, the upper lines show the max value in the data set. While the maximum score was 60 for the pre-test for the medical group, this value is 90 for the post-test. For the nurse group, the maximum score is 100 for the pre-test, the maximum score is 100 for the post-test. The difference between these values (min-max) is the range value and shows the distribution. The length of the post-test score box is two times shorter than in the pre-test score box. This shows that the distribution of the post-test score is narrower than the pre-test. The bold lines in the boxes in the figure show the median values. For the medical student group, the median value of the pre-test is 40, while the median value of the post-test is 60. For the ICU nurse group, the median value of the pre-test was 70, while the median value of the post-test was 90. When the pre and post-test results were compared, it was seen that there was a significant increase in scores for each participant individually and for a group average (p<.001).

deos p<0.001, medical education videos vs. patient/caregiver experience videos p<0.01, patient education vs. medical education p<0.01) (Table 2). In terms of publishers, the medical education website videos had the highest DISCERN (51.1±6.4), GQS (4.6±0.5), and JAMA scores (3.1±0.6) (p< 0.01) (Table 3). The videos uploaded by the medical education websites, hospitals and universities had higher DISCERN, GQS, and JAMA scores than physicians' videos (individually uploaded by a physician, not an institution), the non-physician healthcare staff videos, the patient videos and other advertising-sourced videos (p<0.01, p< 0.01, p< 0.001, respectively).

Selection of the videos that used for tracheostomy care education

Since the JAMA score had highest reliability and consistency among the 122 videos, the seven videos with the highest JAMA scores were chosen (4). Of these, the three videos with the highest DISCERN and GBS scores were selected (the DISCERN and GBS scores of the first, second and third videos were 55, 54, 55 and 5, 5, 5 respectively). After the first pre-test, the participants watched these three videos, and the post-test was then administered.

Figure 2 shows the participants' pre- and post-test scores. The minimum pre-test scores for the medical students and ICU nurses were 20 and 40, and the minimum post-test scores 50 and 70, respectively. Although the maximum pre-test score was 60 for the for the medical student group, this value was 90 in the post-test. The maximum pre- and post-test scores were 90 and 100, respectively for the ICU nurse group. The median values of the pre-tests were 40 and 70 for the medical student and ICU nurse groups and 60 and 90 for the post-tests, respectively.

When the pre- and post-test results were compared, a significant increase was noted in the scores for each participant individually and the group average ($p<0.001$).

DISCUSSION

Technology and internet usage is increasing every day and YouTube has become one of the most important education modalities, especially in nursing, teaching technical skills and promoting self-confidence of patient care in medicine (17-21). Although healthcare professionals may prefer YouTube as a platform to access educational videos on tracheostomy care, our results demonstrated that most of these videos provided inadequate information. In our study regarding the video categories, medical education videos were the highest per category; however, the scores of the medical education videos were not on par. Nonetheless, the 'medical educational videos' had higher and statistically significant scores compared to the videos within the 'patient' and 'patient-caregiver experience' categories. Fisher et al analyzed educational value of arthrocentesis videos showed similar results that the majority of YouTube videos related with arthrocentesis were of moderate quality (22). However, Katz et al suggested in their review study that the COVID-19 pandemic brought online web-based learning to the foreground of medical education and institutions should use social media platform for rapid information dissemination in medical education (23). Tackett et al explained the advantages of the online videos over traditional education modalities in that they can reach learners all over the world free of charge; however, the content and quality of videos are the main issues to be discussed (24). In our study, interestingly, the average DISCERN, GQS, and JAMA scores of the eight videos under the 'medical education website' category had statistically higher scores than all the other groups (DISCERN score=51.1±6.4 [good], GQS=4.6±0.5 [good], and JAMA score=3.1±0.6 [good], $p<0.01$). All eight videos were uploaded via the medical education website OPEN pediatrics (www.openpediatrics.org), which is a free, open-access and peer-reviewed online network for healthcare professionals that is supported by hospitals and research institutions such as Boston Children's Hospital. These videos were better than the others in terms of the video quality, and reliability and currency of the information. Therefore, such global formations, universities, research centers, and associations can collaborate to produce high-quality educational videos to be used by healthcare professionals especially in resource-limiting centers. During our analysis, the absence of key expressions in titles, such as 'for healthcare professionals' or 'for patients' were noted for most of the videos. Therefore, content creators responsible for uploading videos with the intention of training healthcare personnel should be aware that patients may have access to the content. To enable a better understanding by viewers, it would be beneficial to clearly identify or create a specific submission option for videos aimed at patients vs. healthcare professionals. Kucuk et al. similarly stressed the significance of identifying videos' intended audience in the video title (19). Sterling et al. reviewed twenty-nine studies to examine the effect of social media platform in graduate medical education and they showed that most of the studies were moderate in quality and most of those studies could not measure the knowledge of the residents that obtained from watched videos (25). The most striking feature of this study, compared to other studies, is that the top three videos with the highest scores from all three scoring systems were evaluated by pre- and post-tests. When the pre- and post-test results were compared, a significant increase in scores was noted for each individual participant and the group average. The study participants included medical students who had not yet received any tuition on tracheostomy care. In contrast, the ICU nurses would have received in-service training on tracheostomy care in addition to providing care for tracheostomy patients. This could explain the nurses' higher pre-tests results. Nevertheless, despite having no previous training, the medical student group, with as well as the nurse group with adequate training, scored significantly higher in the post-test, demonstrating that appropriate videos could be used both to educate students and provide continuing professional development for healthcare staff.

The DISCERN, JAMA, and GQS scores positively correlated with one another which is a considerably important discovery of the present study. Kucuk et al. and Yildiz et al. yielded similar findings by their studies that DISCERN, JAMA, and GQS scoring largely produced equidistant results with respect to the educational quality and video accuracy of the videos (19, 20). On the contrary, according to Azer, neither the DISCERN nor JAMA scoring systems were appropriate for analyzing videos because they were created for written information long before the YouTube era, and the included items are not capable of assessing videos (26). However, these scores have been widely applied in numerous similar studies (13-15). Moreover, Chen et al., demonstrated a positive correlation between DISCERN and GQS scores, and the latter have been used to assess the quality of the videos (13). Nonetheless, while these scoring systems are not perfect for evaluating videos, they can be used as quality and value indicators for videos. The length of the videos also had a statistically significant and positively correlated relationship with the DISCERN, JAMA, and GQS scores. We observed that the DISCERN, JAMA, and GQS scoring systems had a positive correlation with the duration of the videos. As the duration of the videos increases, the extent of educationally valuable, quality information expanded in a parallel manner. Meanwhile, according to Gill et al, online streaming well-established popular videos typically have a duration far less than the allotted ten minutes, which may be considerably important for healthcare professionals due to their very limited time (27). During the video preparation, it is therefore essential that the videos present adequate information within an appropriate time to prevent a loss of concentration among viewers (28).

A limitation of our study is that the pre and post-tests were only administered to one group (n=20) of medical students and one group (n=20) of ICU members. Although the actual sample size surpassed the calculated number, an increase in the sample size and bigger groups could be constructive in future studies. Furthermore, even though the pre- and post-test were

prepared and evaluated by a single person, the higher post-test scores demonstrate that the students and nurses increased their knowledge easily within a short period of time. In addition, although the post-test results showed an increase in scores for both groups, and it can be deduced that those who scored higher provide better care, we could not establish a direct link between the groups knowledge. However, by watching the videos several times, nurses and medical students could improve their knowledge and provide better care.

The inclusion of only English language videos in our study caused language barriers and was a significant constraint. The lack of proper subtitles and the translation of high-quality educational videos disadvantages participants from non-English speaking countries. A possible solution is for each country's relevant association (s) to collaborate with global associations to create videos in the national languages. Lastly, it should be noted that the analyzed videos were retrieved on 18 April 2022, so videos uploaded after that time were not included in this analysis.

Notwithstanding the aforesaid limitations, to decrease the subjectivity of the video evaluation process, the videos in our study were watched and analyzed separately by two researchers (OG; an otolaryngologist, and OO; a pediatric intensivist) who work in the multidisciplinary tracheostomy care team at our center. The calculated average of the DISCERN, GQS, and JAMA scores given by the researchers were included in the analysis. To avoid bias, a different researcher (MT) prepared and scored the participants' pre- and post-tests rather than the researchers who evaluated the videos.

Finally, the results of our study show that free online training can be provided for healthcare professionals and medical school students using well-prepared, high-quality and reliable videos. Online training may thus be an excellent alternative to improve the time and cost of student and healthcare staff training at centers with limited resources, inadequate capacity and/or simulation tools and lack of time and staffing to allocate to education. Nonetheless, several other studies with a higher number of participants and more videos of higher quality are needed to confirm and expand our findings. Likewise, cooperation between academic institutions, associations, and centers is necessary to prepare higher quality and reliable videos in the future.

CONCLUSION

Most of the videos on YouTube that provide education on tracheostomy care are sub-standard. Consequently, physicians and healthcare workers need to be aware of such restrictions when using this online platform to ensure they are receiving accurate medical information. Notwithstanding, videos that have the highest education scores can be utilized for online and digital learning purposes and continuing medical education. If global entities can collaborate to produce high-quality educational videos, they will appeal to large audiences, and free online training on YouTube could be organized for healthcare professionals working in resource-limited centers.

Acknowledgements: Special thanks to the medical students and intensive care nurses who voluntarily participated in this study. We also thank to Koc University Hospital Aerodigestive Team for their valuable insight.

Ethics Committee Approval: This study was approved by Koc University Ethics Committee for Social Sciences (Date: 11.08.2022, No: 2022.278.IRB3.117).

Peer Review: Externally peer-reviewed.

Author Contributions: Conception/Design of Study- M.T., O.G.; Data Acquisition- Ö.Ö., F.Y., S.O., A.E.Y.; Data Analysis/Interpretation- M.T.; Drafting Manuscript- M.T., F.Y., S.O., A.E.Y.; Critical Revision of Manuscript- Ö.Ö., O.G.; Final Approval and Accountability- M.T., F.Y., S.O., A.E.Y., Ö.Ö., O.G.

Conflict of Interest: The authors have no conflict of interest to declare.

Financial Disclosure: The authors declared that this study has received no financial support.

REFERENCES

1. Abril MK, Berkowitz DM, Chen Y, Waller LA, Martin GS, Kempker JA. The epidemiology of adult tracheostomy in the United States 2002-2017:A serial cross-sectional study. Crit Care Explor 2021;3(9):e0523.
2. Muller RG, Mamidala MP, Smith SH, Smith A, Sheyn A. Incidence, epidemiology, and outcomes of pediatric tracheostomy in the United States from 2000 to 2012. Otolaryngol Head Neck Surg 2019;160(2):332-8.
3. Garrubba M, Turner T, Grieveson C. Multidisciplinary care for tracheostomy patients: a systematic review. Crit Care 2009;13(6):R177.
4. Seymour-Walsh AE, Bell A, Weber A, Smith T. Adapting to a new reality: COVID-19 coronavirus and online education in the health professions. Rural Remote Health 2020;20(2):6000.
5. Blogger G. YouTube user statistics 2022. https://www.globalmediainsight.com/blog/youtube-users-statistics/.
6. Drozd B, Couvillon E, Suarez A. Medical YouTube videos and methods of evaluation: Literature review. JMIR Med Educ 2018;4(1):e3.
7. Hasamnis AA, Patil SS. YouTube as a tool for health education. J Educ Health Promot 2019;8:241.
8. Özsaban A, Bayram A, Durgun H. Youtube videos as an educational resource for ventrogluteal injection: A content, reliability and quality analysis. Nurse Educ Today 2021;107:105107.
9. Tanyıldız B, Oklar M. Evaluating the quality, utility, and reliability of the information in uveitis videos shared on YouTube. Int Ophthalmol 2023;43(2):549-55.
10. Enver N, Doruk C, Kara H, Gürol E, Incaz S, Mamadova U. YouTube™ as an information source for larynx cancer: a systematic review of video content. Eur Arch Otorhinolaryngol 2020;277(7):2061-9.
11. Charnock D, Shepperd S, Needham G, Gann R. DISCERN: an instrument for judging the quality of written consumer health

information on treatment choices. J Epidemiol Community Health 1999;53(2):105-11.
12. Silberg WM, Lundberg GD, Musacchio RA. Assessing, controlling, and assuring the quality of medical information on the Internet: Caveant lector et viewor--Let the reader and viewer beware. JAMA 1997;277(15):1244-5.
13. Chen Z, Pan S, Zuo S. TikTok and YouTube as sources of information on anal fissure: A comparative analysis. Front Public Health 2022;10:1000338.
14. Jung MJ, Seo MS. Assessment of reliability and information quality of YouTube videos about root canal treatment after 2016. BMC Oral Health 2022;22(1):494.
15. Sasse M, Ohrndorf S, Palmowski A, Wagner AD, Burmester GR, Pankow A, et al. Digital health information on autoinflammatory diseases: a YouTube quality analysis. Rheumatol Int 2023;43(1):163-71.
16. Bernard A, Langille M, Hughes S, Rose C, Leddin D, Veldhuyzen van Zanten S. A systematic review of patient inflammatory bowel disease information resources on the world wide web. Am J Gastroenterol 2007;102(9):2070-7.
17. Erdem MN, Karaca S. Evaluating the accuracy and quality of the information in kyphosis videos shared on YouTube. Spine (Phila Pa 1976). 2018;43(22):E1334-E9.
18. Gause G, Mokgaola IO, Rakhudu MA. Technology usage for teaching and learning in nursing education: An integrative review. Curationis 2022;45(1):e1-e9.
19. Kuçuk B, Sirakaya E. An Analysis of YouTube videos as educational resources for patients about refractive surgery. Cornea 2020;39(4):491-4.
20. Yildiz MB, Yildiz E, Balci S, Özçelik Köse A. Evaluation of the quality, reliability, and educational content of YouTube videos as an information source for soft contact lenses. Eye Contact Lens 2021;47(11):617-21.
21. Ozdemir Zeydanli E, Alkan AA. Era of "Dr. YouTube":Evaluation of YouTube videos as a valid source for patient education on keratoconus. Eye Contact Lens 2021;47(9):526-32.
22. Fisher J, Geurts J, Valderrabano V, Hügle T. Educational quality of YouTube videos on knee arthrocentesis. J Clin Rheumatol 2013;19(7):373-6.
23. Kartz M, Nandi N. Social media and medical education in the context of the COVID-19 Pandemic: Scoping review. JMIR Med Educ 2021;7(2):e25892.
24. Tackett S. Medical education videos for the world: an analysis of viewing patterns for a YouTube channel. Acad Med 2018;93(8):1150-6.
25. Sterling M, Leung P, Wright D, Bishop TF. The use of social media in graduate medical education: A systematic review. Acad Med 2017;92(7):1043-56.
26. Azer SA. Are DISCERN and JAMA suitable instruments for assessing YouTube videos on thyroid cancer? Methodological Concerns. J Cancer Educ 2020;35(6):1267-77.
27. Gill P, Arlitt M, Li Z, Mahanti A. YouTube traffic characterization: A view from the edge. IMC '07: Proceedings of the 7th ACM SIGCOMM conference on internet measurement Association for Computing Machinery, New York, NY, USA, 2007. p.15-28.
28. Gross RT, Ghaltakhchyan N, Nanney EM, Jackson TH, Wiesen CA, Mihas P et al. Evaluating video-based lectures on YouTube for dental education. Orthod Craniofac Res 2023. doi: 10.1111/ocr.12669.

İSTANBUL UNIVERSITY PRESS

RESEARCH ARTICLE / ARAŞTIRMA MAKALESİ
Journal of Advanced Research in Health Sciences / Sağlık Bilimlerinde İleri Araştırmalar Dergisi 2023
DOI: 10.26650/JARHS2023-1323336

ASSOCIATION OF SERUM AMH WITH LABORATORY AND PHENOTYPE IN WOMEN WITH POLYCYSTIC OVARY SYNDROME: A RETROSPECTIVE STUDY

POLİKİSTİK OVER SENDROMLU KADINLARDA SERUM AMH İLE LABORATUVAR VE FENOTİP İLİŞKİSİ: RETROSPEKTİF ÇALIŞMA

Özlem KARABAY AKGÜL[1], **Nurşen KURTOĞLU AKSOY**[1]

[1] University of Health Sciences, Bağcılar Training and Research Hospital, Gynecology and Obstetrics Clinic, Istanbul, Turkiye

ORCID ID: Ö.K.A. 0000-0003-0313-1893; N.K.A. 0000-0002-8609-4487

Citation/Atıf: Karabay Akgul O, Kurtoglu Aksoy N. Association of serum Amh with laboratory and phenotype in women with polycystic ovary syndrome: a retrospective study. Journal of Advanced Research in Health Sciences 2023;6(3):289-294. https://doi.org/10.26650/JARHS2023-1323336

ABSTRACT

Objective: The aim of this study was to compare the endocrine and phenotypic characteristics of women with polycystic ovary syndrome (PCOS) with serum Anti-Mullerian Hormone (AMH) levels of 4-10 ng/mL and >10 ng/mL, and to investigate the importance of high AMH levels in the diagnosis of PCOS.

Materials and Methods: In this retrospective cohort study, the laboratory and demographic characteristics of women with serum AMH ≥4 ng/mL whose follow-up was initiated at the infertility outpatient clinic of a tertiary health care institution were investigated. Fasting levels of Homeostasis Model Assessment (HOMA), Luteinizan hormon (LH), Follkül stimulan hormon (FSH), estradiol, androstenedione, total testosterone, prolactin, 17- hydroxyprogesterone (17OHP), dehydroepiandrosterone sulphate (DHEAS), and AMH were recorded from hospital records. Age, gravidity, BMI, infertility status, hirsutism, menstrual cycle and ultrasonographic ovarian morphology were recorded. Patients were divided into two groups, as those with serum AMH values of 4-10 ng/mL and those with serum AMH values of >10 ng/mL. Women with AMH >10 ng/mL were defined as the "high AMH group" and those with AMH >14 ng/mL were defined as the "very high AMH group." Women on hormone-containing drugs, metformin, and/or chronic medication, as well as women with endocrine organ tumors and/or who have had ovarian surgery were excluded.

Results: The patients were between 21 and 38 years of age. Fifty-four women with AMH values of 4-10 ng/mL, 12 women with 10-14 ng/mL and 16 women with >14 ng/mL were included in the study. Forty-four patients were primary infertile, and 28 patients had clinical hirsutism. Women with high AMH values had more primary infertility and hirsutism. Thirty-four patients had menstrual irregularities, and there was no statistically significant difference between the two groups in terms of menstrual irregularities. Among laboratory values, total testosterone, androstenedione, and the LH/FSH ratio were significantly associated with high AMH. Primary infertility and hirsutism were more common in women with high AMH. PCOM was seen in all the women with AMH >10 ng/mL. There was no difference between the two groups in terms of HOMA and BMI criteria. Other endocrine values were not associated with AMH levels.

Conclusion: There is a positive correlation between androgens and AMH in women with high AMH values, with the possibility of high AMH being an additional marker for the diagnosis of PCOS. We believe that women with hirsutism and high amounts of androgens and especially women with PCOM may have high AMH, and infertility treatments should be organized by taking into account the related drug resistance.

Keywords: Anti-mullerien hormone, hirsutism, PCOS, androgens

ÖZ

Amaç: Bu çalışmanın amacı serum Anti Müllerien Hormon (AMH) değeri 4-10 ng/ml ve >10 ng/ml olan polikistik over sendromlu kadınlardaki endokrin ve fenotipik özellikleri karşılaştırmak ve polikistik over sendrom (PCOS) tanısında yüksek AMH seviyesinin önemini araştırmaktır.

Gereç ve Yöntem: Bu retrospektif cohort çalışmada tersiyer sağlık kuruluşunda infertilite polikliniğinde takipleri başlatılan, serum AMH değeri ≥4 ng/ml kadınların laboratuar, demografik özellikleri araştırıldı. Hastane kayıtlarından kadınların foliküler fazda açlık Homeostasis Model Assessment (HOMA), Luteinizan hormon (LH), Folikül stimulan hormon (FSH), östradiol, androstenedion, total testosteron, prolaktin, 17 hidroksiprogesteron (17OHP), dehidroepiandrosteron sülfat (DHEAS) ve AMH düzey sonuçları kaydedildi. Hastaların yaşı, gravidası, BMI, infertilite durumu, hirsutizm, adet düzeni ve ultrasonografik over morfolojisi kaydedildi. Hastalar serum AMH değeri 4-10 ng/ml ve >10 ng/ml olanlar olarak 2 gruba ayrıldı. AMH'ı 10 ng/ml'dan yüksek olan kadınlar '' yüksek AMH grubu'', AMH > 14 ng/ml olanlar da ''çok yüksek AMH grubu'' olarak adlandırıldı. Hormon içeren ilaç kullanan kadınlar, metformin kullanan kadınlar, kronik bir ilaç kullanan kadınlar, endokrin organ tümörü tanısı olanlar ve over cerrahisi geçirmiş kadınlar çalışmaya alınmadı.

Bulgular: Hastalar 21- 38 yaş aralığındaydı. AMH değeri 4-10 ng/ml olan 54, 10-14 ng/ml arası 12 ve >14 ng/ml 16 kadın çalışmaya alınmıştı. 44 hasta primer infertildi; 28 hastada klinik hirsutizm şikayeti vardı. Yüksek AMH değeri olan kadınlarda daha çok primer infertilite ve hirsutizm vardı. 34 hastada adet düzensizliği vardı ve iki grup arasında adet düzensizliği açısından fark yoktu. Laboratuar değerlerinden total testosteron, androstenedion, LH/FSH oranı ile yüksek AMH arasında anlamlı ilişkili bulundu. Yüksek AMH olan kadınlarda daha çok primer infertilite ve hirsutizm vardı. Tüm >10 ng/ml AMH değeri olan kadınlarda PCOM görülmüştü. Adet düzensizliği açısından iki grup benzerdi. 2 grup arasında HOMA ve BMI kriterleri açısından fark yoktu. Diğer endokrin değerler AMH düzeyi ile ilişkili değildi.

Sonuç: Yüksek AMH değeri olan kadınlarda androjenler ile AMH arasında pozitif korelasyon vardır, AMH yüksekliği PCOS tanısı konulmasına ek bir marker olabilir. Hirsutizm ve yüksek androjen olan kadınlarda ve özellikle PCOM olan kadınlarda yüksek AMH olabileceği ve infertilite tedavilerinde buna bağlı ilaç dirençlerinin dikkate alınarak tedavinin düzenlenmesi gerektiğini düşünüyoruz.

Anahtar Kelimeler: Antimüllerien hormon, hirsutizm, PCOS, androjenler

Corresponding Author/Sorumlu Yazar: Özlem KARABAY AKGÜL **E-mail:** ozlem74akgul@hotmail.com

Submitted/Başvuru: 05.07.2023 • **Revision Requested/Revizyon Talebi:** 06.07.2023 • **Last Revision Received/Son Revizyon:** 06.07.2023 • **Accepted/Kabul:** 26.07.2023 • **Published Online/Online Yayın:** 13.10.2023

INTRODUCTION

Apart from the infertile patient population, the laboratory and clinical effects of AMH in women have received little attention. AMH is a biomarker indicating ovarian reserve (1). There are few studies describing which value of AMH leads to which results. Studies mostly focus on polycystic ovary syndrome (PCOS), responses to assisted reproductive technology (ART) treatments and the relationship between AMH levels and menopause prediction.

AMH is a glycoprotein produced in primary follicles and antral follicles prior to FSH-dependent follicle selection. It functions as an autocrine and paracrine regulator of follicular maturation. Since the size of the residual follicular pool depends on the number of small antral follicles and decreases over time, the serum AMH level in women reaches its highest value at the age of 25, plateaus for a while, and starts to decline. This decline accelerates in menopause and becomes undetectable shortly after menopause (2).

Ovarian folliculogenesis is mediated by the joint interactions of FSH, AMH, estradiol and androgens. AMH inhibits follicle recruitment and development and promotes follicle atresia. In fact, AMH is an inhibitory factor that prevents folliculogenesis from reaching a point of being difficult to impossible to control. This inhibition may explain the anovulation that accompanies the increased number of antral follicles in PCOS. In women with PCOS, AMH increases ambient androgen and insulin resistance by inhibiting FSH-induced aromatase. Therefore, weight loss becomes difficult in these women and the response to ovulation induction decreases. Patients' clinical course recovered with the lowering of AMH. This allows us to see that AMH has an active role in PCOS, which is an example of exaggerated folliculogenesis (3). Nevertheless, a number of studies show that weight loss does not decrease AMH in obese women with or without PCOS (4).

The two opposite poles in the clinical reflection of folliculogenesis are polycystic ovary syndrome and menopause. The normal range for AMH is not clear; however, serum AMH levels are high in women with PCOS and unmeasurable in menopause.

In women with PCOS, both the number of pre-antral and the number of antral follicles increase and serum AMH is high because of the increased production per follicle (due to increased granulosa cells) (5). Different results can be found in the literature related to AMH-secreting cell sizes (4, 6, 8 and 9 mm) (6). In the literature, abnormalities secondary to increased AMH are variable. We still therefore cannot predict which hormones are affected in women, the development of clinical abnormalities independent of hormone levels, and the phenotype changes of women based on the AMH level. Conversely, we do not know what changes occur in problems such as menstrual irregularity and hirsutism that should, but cannot, be measured in the laboratory and whether AMH changes can explain this abnormality despite normal hormone levels.

The main aim of this study was to investigate the association of AMH with PCOS phenotypes and laboratory tests in addition to discussing the role of AMH in the diagnosis of PCOS.

MATERIALS and METHODS

The study was initiated after obtaining detailed verbal and written consent from all participants following the approval of the ethics committee. Non-interventional clinical trials were approved by the ethics committee (Date: 10.11.2022, No: 950). This study was conducted in full accordance with the guidelines of the Declaration of Helsinki. The data of women who applied to the infertility clinic of a tertiary health institution between January 2019 and May 2023 were reviewed from hospital records and files by obtaining the verbal and written consent from the patients.

Age, menstrual cycle, hirsutism (Ferriman-Gallwey score >8 points), primary or secondary infertility status, BMI, and the presence of polycystic morphology in the ovaries were recorded in 81 women aged 20 to 40 years who applied at the infertility outpatient clinic and did not receive any treatment. Homeostasis Model Assessment (HOMA), (fasting glucose x fasting insulin ÷405), Luteinizan hormone (LH), Follicle stimulating hormone (FSH), prolactin, AMH, androgens (androstenedione, 17- hydroxyprogesterone (17OHP), total testosterone, dehydroepiandrosterone sulphate (DHEAS**)** measured in the morning blood on the second, third, and fourth day of menstruation were recorded.

Serum AMH levels were measured using the Elica technique (Roche E411, USA).

Every patient underwent morning transvaginal ultrasonography (TVUSG) on the second, third and fourth days of menstruation. Polycystic ovarian morphology (PCOM) was defined as ≥ 12 follicles in either ovary, measuring 2-9 mm in diameter and/or increased ovarian volume for each ovary >10 mL on the ultrasound scan (7).

Women who were taking hormone-containing drugs for any reason, women with known ovarian mass and disease, and women with a history of adnexal surgery were excluded. Women with congenital adrenal hyperplasia, thyroid dysfunction and diabetes mellitus were also excluded.

Statistical analysis

Mean, Standard Deviation and Median IQR values were given in the descriptive statistics for the continuous data, and the number and percentage values were given in the discrete data. The Shapiro-Wilk test was used to examine the conformity of continuous data to the normal distribution.

An independent samples t test was used to compare patient ages in the AMH groups, and the Mann Whitney U test was used to compare the laboratory values.

The relationships between the AMH values and ages and laboratory values were analyzed using Spearman's correlation

Table 1: Patient characteristics

	(n= 81)
Age Mean±SD (Min-Max)	28.89±3.88; (21-38)
BMI n (%)	
18-25	39 (48.1%)
25-30	16 (19.8%)
≥ 30	26 (32.1%)
Menstruation n (%) (n=78)	
Irregular	34 (42.0%)
Regular	47 (58.0%)
Infertility n (%)	
Primary	44 (54.3%)
Secondary	37 (45.7%)
PCOM	
No	13 (16%)
Yes	68 (84%)
Hirsutism (n=78)	
No	53 (65.4%)
Yes	28 (34.6%)
HOMA index	
<2.5	44 (54.3%)
≥2.5	37 (45.7%)

BMI: Body mass index, PCOM: Polycystic ovarian morphology, HOMA: Homeostasis Model Assessment

coefficient.

Chi-Square and Fisher's Exact test were used for comparisons of nominal variables between the AMH groups (in cross-tabulations).

The IBM SPSS version 20 (Chicago, IL, USA) program was used in the evaluations, and p<0.05 was accepted as the limit of statistical significance.

In the study including 54 patients with AMH values ≤10 ng/mL and 27 patients with AMH values >10 ng/mL, and comparing the presence of hirsutism as the primary outcome, the power of the test was found to be power=0.88 (88%) with Type I error=0.05.

In the study examining the relationship between AMH values and LH/FSH values as the primary outcome in 81 patients included in the study, the power of the test with Type I error=0.05, power=0.99 (99%).

The calculation was performed using the 'GPower 3.1.9.2' program.

Table 2: Laboratory findings of the patients

		Mean±SD	Median (IQR)
Estradiol	81	46.83±17.55	43 (34-55)
LH/FSH	81	1.39±0.67	1.26 (0.96-1.80)
Androstenedione	81	2.47±1.33	2.19 (1.35-3.50)
Testosterone	81	0.50±0.27	0.41 (0.32-0.64)
17OHP	81	1.40±1.52	0.85 (0.63-1.50)
DHEAS	81	248.53±104.90	229 (161.30-317.0)
AMH	81	10.11±8.48	7.52 (4.97-11.88)
Prolactin	81	19.17±8.59	18 (6.5-48)

IQR:Inter quantile range, LH: Luteinizan hormone, FSH: Follicle stimulating hormone, DHEAS: dehydroepiandrosterone sulphate, AMH: Anti-Mullerian Hormone, 17OHP: 17 hydroxyprogesterone

Table 3: AMH distribution (ng/mL)

AMH *n* (%)	
≤10	54 (66.7%)
>10	27 (33.3%)

AMH: Anti-Mullerian Hormone

RESULTS

A total of 81 infertility patients with AMH levels of 4 ng/mL and above were included in the study. The mean age of the patients was 28.89±3.88 years (minimum 21 and maximum 38 years). Patients with serum AMH>10 ng/mL were younger than patients with AMH≤10 ng/mL (p<0.01) (Table 1).

AMH values were found to be >10 ng/mL in 33.3% of the patients (Table 3).

Approximately half of the patients (48%) had a normal body mass index (BMI 18-25 kg/m^2), and there was no significant difference in the BMI levels between the two groups (p>0.05) (Table 1).

Primary infertility was found in 54.3% of the patients and secondary infertility in 45.7%. Primary infertility was found more frequently in patients with AMH >10 ng/mL (p<0.05) (Table 1).

Menses were regular in the majority of the patients (58%), and

Table 4: Comparison of the characteristics of patients with an AMH value ≤10 ng/mL and patients with an AMH value >10 ng/mL

	AMH ≤10		AMH >10		p value
Age (year) Mean±SD	29.80±3.92		27.07±3.16		**0.002[a]**
BMI n (%)					
18-25	29	53.7	10	37.0	
25-30	11	20.4	5	18.5	0.224[c]
≥ 30	14	25.9	12	44.4	
Menstruation n (%)					
Irregular	19	35.2	15	55.6	0.080[c]
Regular	35	64.8	12	44.4	
Infertility n (%)					
Primary	24	44.4	20	74.1	**0.012**[c]
Secondary	30	55.6	7	25.9	
PCOM n (%)					
No	13	24.1	0	0	**0.004**[c]
Yes	41	75.9	27	100	
Hirsutism n (%)					
No	42	77.8	11	40.7	**0.001**[c]
Yes	12	22.2	16	59.3	
HOMA n (%)					
<2.5	28	51.9	16	59.3	0.528[c]
≥2.5	26	48.1	11	40.7	

AMH: Anti müller hormone, a: Independent samples t test, c: Chi-square Test/Fisher's Exact test, BMI: Body mass index, PCOM: Polycystic ovarian morphology, HOMA: Homeostasis Model Assessment

there was no statistically significant difference between the two groups in terms of menstrual irregularity (p>0.05). Polycystic ovarian morphology was seen in 84% and all the patients with an AMH value >10 ng/mL had PCOM (p<0.01) (Table 1).

Approximately one-third of the patients (34.6%) had hirsutism, which was significantly more common in patients with AMH values >10 ng/mL (p<0.01) (Table 1).

It was found that 45.7% of the patients had HOMA values ³2.5 (Table 1). However, there was no statistically significant difference between the two groups in terms of HOMA elevation (p>0.05) (Table 1).

Table 5: Comparison of laboratory values of patients with AMH ≤10 ng/mL and patients with AMH >10 ng/mL

Median (IQR)	AMH ≤10	AMH >10	p value
Estradiol	40 (34-53.2)	44.3 (35-59)	0.300[b]
LH/FSH	0.52 (0.81-1.57)	1.54 (1.24-2.20)	**<0.001**[b]
Androstenedione	2.0 (1.19-3.09)	2.98 (1.88-3.86)	**0.020**[b]
Testosterone	0.36 (0.29-0.52)	0.68 (0.46-0.86)	**<0.001**[b]
17OHP	0.88 (0.67-1.43)	0.78 (0.45-1.83)	0.227[b]
DHEAS	251.5 (158.7-317.0)	216.0 (162.6-323.0)	0.648[b]
Prolactin	18.5 (11.8-24.0)	18.0 (12.2-26.0)	0.722[b]

IQR: Inter quantile range, AMH: Anti müller hormone, b: Mann Whitney U test, DHEAS: dehydroepiandrosterone sulphate, 17OHP: 17-hydroxyprogesterone

Table 6: Correlations between AMH, age and laboratory parameters

	AMH	
	r*	p
Age (year)	**−0.453**	**<0.001**
Estradiol	0.128	0.255
LH/FSH	**0.471**	**<0.001**
Androstenedione	0.140	0.212
Testosterone	**0.458**	**<0.001**
17OHProgesterone	−0.156	0.166
DHEAS	−0.090	0.422
Prolactin	0.068	0.548

AMH: Anti müller hormone, *Spearman's correlation coefficient, LH: Luteinizan hormone, FSH: Follicle stimulating hormone, 17OHP: 17-hydroxyprogesterone, DHEAS: dehydroepiandrosterone sulphate

LH/FSH, androstenedione and testosterone values were higher in patients with AMH>10 ng/mL (p<0.001) (Table 2).

There was a negative correlation between the ages of the patients and AMH values (r=−0.453 p<0.001) (Table 6).

Positive correlations were found between LH/FSH values, testosterone values and AMH (r=0.471 and r=0.458, respectively, p<0.001) (Table 6).

No difference could be seen between the E2, 17OHP, DHEAS, and PRL values of the patients with AMH ≤10 ng/mL and pati-

ents with AMH >10 ng/mL (p>0.05) (Table 5).

DISCUSSION

According to the results of our study, we found androgenic effects correlated with AMH, therefore making AMH possibly one of the diagnostic markers of PCOS.

Unlike the publications showing that AMH does not change intra- and inter-cyclically, the lowest level of AMH is measured in the luteal phase immediately after ovulation (8). Considering these differences, we included women in the study in whom AMH was measured in the follicular phase. In this study, a serum AMH level >4 ng/mL was accepted as the optimal cut-off for the diagnosis of PCOS (9).

In a study conducted on IVF patients, relationships were found between AMH>5.7 ng/mL and hyperandrogenism, PCOM, menstrual irregularity and high LH/FSH. Accordingly, the LH/FSH ratio may increase in women with high AMH because in PCOS, FSH is secreted normally, while LH is secreted at normal or increased levels. However, it would not be correct to diagnose PCOS only by looking at this ratio. In the same study, a correlation between menstrual irregularity and the LH/FSH ratio was also reported (10). We also found a higher LH/FSH ratio in the high AMH group (>10 ng/mL).

In our study, no correlation was found between AMH and insulin resistance (HOMA) in accordance with a number of studies in the literature (11).

In a study conducted with a small group of cases in the literature, it was reported that women with high AMH levels were thinner, had higher androgen levels and suffered more from amenorrhea. According to the results of our study, testosterone is positively correlated with AMH levels (12). Although we did not find a correlation between androstenedione and AMH, we did find a correlation between androstenedione levels of <10 ng/mL and >10 ng/mL (see Tables 5 and 6). These two androgens are expected to cause clinical hyperandrogenism and changes in body fat distribution. In a study conducted on a small number of patients, the garnered data reported that there was no correlation between BMI and LH/FSH (13). Although the BMI of the patients was similar in our study, we were not able to compare the waist/hip ratio with fat distribution, so we cannot comment on the fat distribution.

It is natural that high AMH and accompanying androgen levels make some changes in the phenotype. Although obesity is common in women with PCOS, women with very high AMH have been shown to be leaner. In a study conducted by dividing 134 patients into three groups according to AMH value, Tal et al. reported that PCOS was present in a large proportion of women at AMH >10 ng/mL. These women were thinner with AMH levels and PCOS severity being correlated (14). Among the women in our study, being overweight was more common in those with high AMH (about half of the patients). However, in those with AMH ≤10 ng/mL, half of the patients were of normal weight. As a result, we did not find a relationship between elevated AMH levels and BMI.

A positive correlation between serum AMH levels and androgens has been previously reported. It has been reported that hyperandrogenism is an intrinsic defect of thecal cells in women with PCOS and is positively associated with testosterone levels and ovarian volume (15). In our study, a relationship was found between hirsutism and AMH, but we observed that the frequency of menstrual cycle abnormalities did not increase with high AMH (Table 4). This is directly related to serum AMH levels in patients with oligo-/amenorrhea and increased AFC (PCOM) (16). Although menstrual irregularity is common in women with PCOS, menstrual irregularity in women in our two groups was seen in half of the patients with AMH>10 ng/mL.

In our study, PCOM was observed in all of our patients with AMH>10 ng/mL. We also detected 2/3 PCOM in women with an AMH of 4-10 ng/mL. Patients with accepted PCOS also have PCOM or increased ovarian volume. In our study, we compared the clinical changes associated with AMH by comparing women with high AMH levels and two groups with far higher AMH (such as 63 ng/mL and 34 ng/mL).

In this study, we grouped not according to the presence of PCOS but according to the AMH level. We accepted a limit of 4 ng/mL, which is believed to mark the onset of PCOS pathology, and thus included all women with normal and abnormal conditions. We believe that our classification of clinical and laboratory features with AMH in a mixed group similar to that in the general population is the strength of our study and will provide more information than working with a selected group with PCOS. However, the most important limitation is that it was not performed with a higher number of age groups and patients. The absence of a control group was a limitation, but it is very difficult to find similarities in AMH <4 ng/mL in and of itself and between different age groups. There will already be a known and incomparable difference between women with high AMH and those without.

It should not be forgotten that the phenotypic appearance in PCOS does not change only with measurable values. The age, activity status and diet of the woman are also having effects. In this study, data are limited due to the fact that, with the exception of age, we do not have any information about these factors. Moreover, there are a small number of patients and they are not age-matched.

As a result, we believe that high AMH can be used in the diagnosis of PCOS in accordance with ovarian appearance on ultrasonography and clinical and/or laboratory hyperandrogenism.

Ethics Committee Approval: This study was approved by Istanbul Medipol University Non-Interventional Clinical Research Ethics Committee (Date: 10.11.2022, No: 950).

Peer Review: Externally peer-reviewed.

Author Contributions: Conception/Design of Study- Ö.K.A., N.K.A.; Data Acquisition- Ö.K.A., N.K.A.; Data Analysis/Interpretation- Ö.K.A., N.K.A.; Drafting Manuscript- Ö.K.A., N.K.A.; Critical Revision of Manuscript- Ö.K.A., N.K.A.; Final Approval and Accountability- Ö.K.A., N.K.A.; Material and Technical Support- Ö.K.A., N.K.A.; Supervision- Ö.K.A., N.K.A.

Conflict of Interest: The authors have no conflict of interest to declare.

Financial Disclosure: The authors declared that this study has received no financial support.

REFERENCES

1. Tal R, Seifer DB. Ovarian reserve testing: a user's guide. Am J Obstet Gynecol 2017;217(2):129-40.
2. Shrikhande L, Shrikhande B, Shrikhande A. AMH and Its Clinical Implications. J Obstet Gynaecol India 2020;70(5):337-41.
3. Garg D, Tal R. The role of AMH in the pathophysiology of polycystic ovarian syndrome. Reprod Biomed Online 2016;33(1):15-28.
4. Kataoka J, Larsson I, Lindgren E, Kindstrand LO, Schmidt J, Stener-Victorin E. Circulating Anti-Müllerian hormone in a cohort-study of women with severe obesity with and without polycystic ovary syndrome and the effect of a one-year weight loss intervention. Reprod Biol Endocrinol 2022;20(1):153.
5. Alebić MŠ, Stojanović N, Duhamel A, Dewailly D. The phenotypic diversity in per-follicle anti-Müllerian hormone production in polycystic ovary syndrome. Hum Reprod 2015;30(8):1927-33.
6. Bedenk J, Vrtačnik-Bokal E, Virant-Klun I. The role of anti-Müllerian hormone (AMH) in ovarian disease and infertility. J Assist Reprod Genet 2020;37(1):89-100.
7. Balen AH, Laven JS, Tan SL, Dewailly D. Ultrasound assessment of the polycystic ovary: international consensus definitions. Hum Reprod Update 2003;9(6):505-14.
8. Russell N, Gilmore A, Roudebush WE. Clinical Utilities of Anti-Müllerian Hormone. J Clin Med 2022;11(23):7209.
9. Tzeng CR, Huang Z, Asada Y, Zhang C, Ho MT, Li RHW, et al. Factors affecting the distribution of serum anti-müllerian hormone levels among infertile Asian women: a multi-nation, multi-centre, and multi-ethnicity prospective cohort study. Hum Reprod 2023;38(7):1368-78.
10. Laven JS, Imani B, Eijkemans MJ, Fauser BC. New approach to polycystic ovary syndrome and other forms of anovulatory infertility. Obstet Gynecol Surv 2002;57(11):755-67.
11. Liu S, Hong L, Mo M, Xiao S, Wang X, Fan X, et al. Association of anti-müllerian hormone with polycystic ovarian syndrome phenotypes and pregnancy outcomes of in vitro fertilization cycles with fresh embryo transfer. BMC Pregnancy Childbirth 2022;22(1):171.
12. Tal R, Seifer CM, Khanimov M, Seifer DB, Tal O. High serum Antimullerian hormone levels are associated with lower live birth rates in women with polycystic ovarian syndrome undergoing assisted reproductive technology. Reprod Biol Endocrinol 2020;18(1):20.
13. Saadia Z. Follicle Stimulating Hormone (LH: FSH) Ratio in Polycystic Ovary Syndrome (PCOS) - Obese vs. Non-Obese Women. Med Arch 2020;74(4):289-93.
14. Tal R, Seifer DB, Khanimov M, Malter HE, Grazi RV, Leader B. Characterization of women with elevated antimüllerian hormone levels (AMH): correlation of AMH with polycystic ovarian syndrome phenotypes and assisted reproductive technology outcomes. Am J Obstet Gynecol 2014;211(1):e1-8.
15. Carlsen SM, Vanky E, Fleming R. Anti-Müllerian hormone concentrations in androgen-suppressed women with polycystic ovary syndrome. Hum Reprod 2009;24(7):1732-8.
16. Butt MS, Saleem J, Aiman S, Zakar R, Sadique I, Fischer F. Serum anti-Müllerian hormone as a predictor of polycystic ovarian syndrome among women of reproductive age. BMC Women's Health 2022;22(1):199.

RESEARCH ARTICLE / ARAŞTIRMA MAKALESİ
Journal of Advanced Research in Health Sciences /
Sağlık Bilimlerinde İleri Araştırmalar Dergisi 2023
DOI: 10.26650/JARHS2023-1268235

COGNITIVE VERSUS MOTOR DUAL TASK BALANCE PERFORMANCE AND FALLS IN MIDDLE-AGED AND ELDERLY ADULTS

ORTA YAŞLI VE YAŞLI YETİŞKİNLERDE BİLİŞSEL VE MOTOR ÇİFT GÖREV DENGE PERFORMANSI VE DÜŞMELER

Senem DEMİRDEL[1], Gözde TEKİN[2], Derya ÇAĞLAR[3], Buse KILINÇ[4], Büşra Nur FINDIK[5], Betül ERBAY[6]

[1] University of Health Sciences, Gülhane Faculty of Physiotherapy and Rehabilitation, Ankara, Turkiye
[2] Muş Alparslan University, Vocational School of Health Services, Healthcare Services Department, Mus, Turkiye
[3] Recep Tayyip Erdogan University, Guneysu Vocational School of Physical Therapy and Rehabilitation, Rize, Turkiye
[4] University of Health Sciences, Gulhane Institute of Health Sciences, Ankara, Turkiye
[5] Nevşehir Hacı Bektaş Veli University, Kozaklı Vocational School, Therapy and Rehabilitation Department, Nevsehir, Turkiye
[6] Bartın University, Health Services Vocational School, Department of Therapy and Rehabilitation, Bartin, Turkiye

ORCID ID: S.D. 0000-0001-7395-8859; G.T. 0000-0002-1049-111X; D.Ç. 0000-0003-4167-3212; B.K. 0000-0001-9822-0965; B.N.F. 0000-0002-1811-3164; B.E. 0000-0002-7130-0129

Citation/Atıf: Demirdel S, Tekin G, Caglar D, Kilinc B, Findik BN, Erbay B. Cognitive versus motor dual task balance performance and falls in middle-aged and elderly adults. Journal of Advanced Research in Health Sciences 2023;6(3):295-301. https://doi.org/10.26650/JARHS2023-1268235

ABSTRACT

Objective: This study investigated the cognitive and motor dual-task performance and falls in middle-aged and elderly adults.

Materials and Method: This cross-sectional study included 84 adults, separated into two age groups of middle-aged adults (50-64 years) and elderly adults (65 years and older). The descriptive characteristics of the participants and the fall rate in the last year were recorded. The timed up-and-go test, four square step test and one leg step test performances were evaluated under single task, cognitive dual task (verbal fluency) and motor dual task (tray-carrying) conditions.

Results: The fall rate was 16.7% in middle-aged adults and 33.3% in elderly adults. The performance of elderly adults in the timed up-and-go test, four square step test and one leg stance test was lower than those of middle-aged adults under single task, cognitive dual task and motor dual task conditions ($p<0.05$). Performance was lower under cognitive dual task conditions for all tests in middle-aged and elderly adults ($p<0.05$). The timed up and go test and four square step test performances of non-faller elderly adults were better than those who fell ($p<0.05$).

Conclusion: The results of this study showed that single-task and dual-task balance performance in older adults is lower than in middle-aged adults, and lower in elderly adults who have a history of falls than in non-fallers. Efforts such as dual-task balance training to improve dual-task performance from middle age may be beneficial in reducing the risk of falls.

Keywords: Aging, dual task, balance, fall

ÖZ

Amaç: Bu çalışmanın amacı, orta yaşlı ve yaşlı yetişkinlerde bilişsel ve motor ikili görev performansını ve düşmeyi araştırmaktır.

Gereç ve Yöntem: Bu kesitsel çalışmaya seksen dört yetişkin dâhil edildi. Katılımcılar yaşa göre orta yaşlı yetişkinler (50-64 yaş) ve yaşlı yetişkinler (65 yaş ve üstü) olarak iki gruba ayrıldı. Katılımcıların tanımlayıcı özellikleri ve son bir yıldaki düşme oranları kaydedildi. Tekli görev, bilişsel ikili görev (sözel akıcılık) ve motor ikili görev (tepsi taşıma) koşullarında süreli kalk ve yürü testi, dört kare adım testi ve tek ayak üzerinde durma testi performansları değerlendirildi.

Bulgular: Düşme oranı orta yaşlı erişkinlerde %16,7 ve yaşlı erişkinlerde %33,3 idi. Tek görev, bilişsel ikili görev ve motor ikili görev koşullarında yaşlı yetişkinlerin süreli kalk ve yürü testi, dört kare adım testi ve tek ayak üzerinde durma testi performansları orta yaşlı yetişkinlere göre daha düşüktü ($p<0,05$). Performans, orta yaşlı ve yaşlı erişkinlerde tüm testler için bilişsel ikili görev koşullarında daha düşüktü ($p<0,05$). Düşen ve düşmeyen yaşlı yetişkinler arasında zamanlı kalk ve yürü testi ile dört kare adım testi performanslarında anlamlı fark bulundu ($p<0,05$).

Sonuç: Bu çalışmanın sonuçları, yaşlı yetişkinlerde tek görev ve ikili görev denge performansının orta yaşlı erişkinlere göre daha düşük olduğunu ve düşen yaşlı yetişkinlerde düşmeyenlere göre daha düşük olduğunu göstermektedir. Orta yaştan itibaren ikili görev performansını geliştirmeye yönelik ikili görev denge eğitimi gibi çalışmalar düşme riskini azaltmak açısından faydalı olabilir.

Anahtar Kelimeler: Yaşlanma, ikili görev, denge, düşme

Corresponding Author/Sorumlu Yazar: Senem DEMİRDEL **E-mail:** senem.demirdel@sbu.edu.tr

Submitted/Başvuru: 20.03.2023 • **Revision Requested/Revizyon Talebi:** 15.06.2023 • **Last Revision Received/Son Revizyon:** 11.07.2023 • **Accepted/Kabul:** 14.07.2023 • **Published Online/Online Yayın:** 10.10.2023

INTRODUCTION

Balance deteriorates due to functional losses caused by natural physiological processes such as loss of strength and flexibility and cognitive disorders seen with aging. Maintaining balance in the elderly population is an important factor for maintaining functional independence (1). Balance disorders have been identified as one of the strongest predictors of falls (2). Impaired balance and gait, and a history of falls are major risk factors for falls in elderly individuals (3). Considering the role of balance in maintaining postural balance, improving balance capability in the elderly is often a goal of fall prevention interventions (4).

Activities of daily living are complex tasks, as they require individuals to perform multiple tasks at the same time and falls often occur during activities that require multitasking. Therefore, dual task (DT) ability indicates the individual's real daily life activity performance (5). Successful dual-task performance is necessary for elderly individuals to remain independent and can be difficult due to the decrease in cognitive and physical functions during the aging process (6).

Deterioration in both motor and cognitive performances may occur in individuals because of the decreased ability to divide attention resources and the degeneration of neural pathways in the aging process (7). Due to task complexity and decreased sensory feedback, balance disorders can be detected in the pre-elderly period (8). There is emerging evidence that midlife may represent an important period for balance related interventions. It has been reported that the prevalence of falls is significant in middle-aged adults, at a rate of 8.7%-31.1% (9).

Static and dynamic balance are important indicators of physical function and mobility in the elderly (10). It is important to evaluate balance and mobility in different dual-task conditions, as dual-task ability is critical to the safe performance of many activities of daily living (7). With current increases in the elderly population, it is of great importance to evaluate balance and mobility performance in different age groups so that preventive interventions related to physical function can be developed to reduce adverse events. The hypothesis of this study was that motor and cognitive dual-task performance would be worse in elderly adults and fallers. Therefore, the aim of this study was to evaluate cognitive and motor dual-task performance in middle-aged and elderly adults and to compare them according to age and fall history.

MATERIAL and METHODS

Study design and participants

This cross-sectional study was conducted at the University of Health Sciences Turkey, Faculty of Physiotherapy and Rehabilitation. Community-dwelling middle-aged and elderly individuals aged 50-82 years were included in the study. The inclusion criteria were; 1) age between 50-82 years, 2) ability to walk at least ten meters without using a walking aid, 3) Standardized Mini Mental Test score of ≥24 points. The exclusion criteria were; 1) diagnosis of any orthopedic, cognitive or neurological illness, 2) polypharmacy (>5 medication)

Ethical approval

The study was approved by the University of Health Sciences Turkey, Gülhane Scientific Research Ethics Committee in accordance with the declaration of Helsinki (Date/No:2022,147). Written consent was obtained from the participants who volunteered for the study.

Procedure

All the participants were questioned about age, height, weight, education level, marital status, living environment, number of falls in the last year, physical exercise habits, and number of medications. A fall was defined as an event that resulted in inadvertently landing on the ground (3). For those who reported falling, the place of fall and the reason for falling were questioned. Those who had one or more fall history in the last year were classified as "fallers", and those without a fall history were classified as "non-fallers". The Standardized Mini Mental State (MMS) examination was used to assess cognitive level. The timed up-and-go test, four square step test and one leg stance test were used to evaluate mobility and balance. The order of the tests was decided randomly. Balance and mobility performance were evaluated in single task (ST), motor dual task (DT) and cognitive DT conditions. As a cognitive concurrent task, individuals counted words beginning with a specific letter (K, E or A letters) while performing balance or mobility tasks. As a motor concurrent task, individuals carried a tray with a glass of water on it. The order of single task, motor DT and cognitive DT tests was chosen randomly. Verbal fluency and tray carrying are frequently used tasks to evaluate dual-task performance in the elderly (11, 12). The following formula was used to calculate the dual task cost (DTC):"DTC=((single task performance-dual task performance)/single task performance)×100". According to this formula, negative values indicate that the DT performance value is greater (13).

Outcome measures

The Standardized Mini Mental State test is a standardized method used to evaluate cognitive status. This test consists of 11 items. The highest possible score is 30 points. As a result of the evaluation, 23/24 points and above are considered as normal cognitive function. The Turkish version of the Standardized Mini Mental Test is proven to be valid and reliable (14, 15).

The timed up-and-go (TUG) test is a test often used to evaluate functional mobility. The test measures speed during many functional maneuvers such as standing up, walking, turning, and sitting. It is a test frequently used in elderly individuals to determine the risk of falling (16, 17).

The Four Square Step (FSS) test was used to evaluate dynamic balance. In this test, individuals are asked to step into four squares as quickly as possible. The ability to step to the right, left, front and back is evaluated. It is a valid and reliable test in elderly individuals (18,19).

The one-leg stance (OLS) test is a commonly used balance test in the evaluation of static balance (20). The duration of standing on the preferred leg with the eyes open was recorded. The test is terminated when the position of the arms and the raised foot deteriorates or the foot in contact with the ground moves to maintain balance, or at the completion of 45 seconds. A longer test time indicates better balance ability (21,22).

Statistical analysis

Data were analyzed using the SPSS version 25.0 statistical software (SPSS Inc., Chicago, IL, USA). The conformity of the data to normal distribution was examined using visual and analytical methods. Continuous variables were presented as mean and standard deviation or median and interquartile range values, and categorical variables as frequency and percentage. The Mann-Whitney U test was used to compare the single task and DT functional performance of middle-aged and elderly individuals. The Mann-Whitney U test was used to compare the single task and DT functional performance of fallers and non-fallers in elderly individuals. Effect size (ES) was calculated with the formula "ES = z / √N" using the z score of the Mann-Whitney U test. An ES value of 0.1-0.3 indicates a small effect size, 0.3-0.5 indicates medium, and >0.5 indicates a large effect size. Wilcoxon Paired Samples tests were used to compare single task performance-cognitive DT performance and single task performance-motor DT performance. The level of statistical significance was accepted as $p<0.05$.

GPower 3.1.9.4 software (Heinrich-Heine-Universität Düsseldorf) was used to determine the required sample size. When

Table 1: Descriptive characteristics of the participants

		Middle-aged adults (n=42)		Elderly adults (n=42)	
		Mean	**Standard deviation**	**Mean**	**Standard deviation**
Age (years)		56.19	4.46	71.59	4.62
Height (cm)		160.23	7.35	158.33	9.11
Weight (kg)		73.04	10.77	70.94	11.14
Body mass index (kg/m^2)		28.47	4.01	28.35	4.22
Mini mental status examination score		27.54	2.19	26.52	2.56
		n	**%**	**n**	**%**
Gender	Female	33	78.6	31	73.8
	Male	9	11.9	11	26.2
Marital status	Single	3	7.1	3	7.1
	Married	33	78.6	25	59.5
	Widow	6	14.3	14	33.4
Educational status	≤ 5 years	33	78.6	31	73.8
	>5 years	9	11.9	11	26.2
Living environment	Alone at home	2	4.8	11	26.2
	With a spouse at home	13	31	22	52.4
	With spouse and children at home	20	47.6	2	4.8
	With children/relatives at home	7	16.6	7	16.6
Physical exercise habit	No exercise	36	85.7	35	83.3
	Less than 2 hours per week	3	7.1	4	9.5
	More than 2 hours per week	3	7.1	3	7.1
Fall history	No	35	83.3	28	66.7
	1-2 in the last year	6	14.3	9	21.5
	3-4 in the last year	0	0	2	4.8
	More than 5 in the last year	1	2.4	3	7.1
Number of medications	0	29	69	6	14.3
	1	8	19	18	42.8
	2	4	9.5	7	16.7
	More than 3	1	2.4	11	26.2

the timed up-and-go test was accepted as the primary outcome measure, it was calculated that there should be 40 people in each group for 0.843 ES, 0.05 alpha and 0.98 power (1). The study was completed with 84 participants.

RESULTS

Evaluation was made of 84 middle-aged and elderly individuals. Most of the participants were female (76.5%), married (68.2%), and had a sedentary lifestyle (84.7%). The descriptive characteristics of all the participants are presented in Table 1.

Tripping was seen to be the most common cause of falls in elderly fallers (50%). Other causes of falls include slipping, dizziness, ankle sprains, and lifting heavy objects. In middle-aged individuals, the causes of falls were reported as slipping, tripping and loss of balance. It was noted that most falls (85.7%) in middle-aged adults occurred outdoors, while in older adults most (57.1%) falls occurred at home.

The TUG test, FSS test and OLS test performance under single task, motor DT and cognitive DT conditions were significantly different in middle-aged and elderly adults (p≤0.001), and effect sizes were medium or large (Table 2). In the middle-aged group, the TUG test duration under cognitive DT condition was greater than its single task value (p<0.001), the FSS test duration under cognitive DT condition was greater than its single task value (p<0.001), the OLS test duration under cognitive DT condition was lower than its single task value (p=0.037), and the OLS test duration under motor DT condition was lower than its single task value (p=0.013). In the elderly group, the TUG test duration under cognitive DT condition was greater than its single task value (p<0.001), the FSS test duration under cognitive DT condition was greater than its single task value (p<0.001),

Table 2: Functional performance results under single task, cognitive dual task and motor dual task conditions in middle aged and elderly adults

	Middle-aged adults (N=42)		Elderly adults (N=42)			
Single task	**Median**	**IQR**	**Median**	**IQR**	**P**	**ES**
Timed up and go test (s)	8.64	2.63	11.28	2.87	<0.001	0.48
Four square step test (s)	10.43	3.47	14.88	4.37	<0.001	0.63
One leg stance test (s)	45	18.37	11.01	21.48	<0.001	0.58
Cognitive dual task						
Timed up and go test (s)	10.65*	3.48	14.15*	6.5	<0.001	0.42
Four square step test (s)	15.19*	5.75	18.14*	10.4	0.001	0.36
One leg stance test (s)	40*	24.43	9*	3.25	<0.001	0.55
Motor dual task						
Timed up and go test (s)	8.58	2.32	11.27	3.89	<0.001	0.50
Four square step test (s)	10.69	3.35	14.4	4.43	<0.001	0.57
One leg stance test (s)	37.5*	26.84	12.5	20.8	<0.001	0.49

IQR: Interquartile range, ES: Effect size, *Wilcoxon Paired sample test, significantly different from its value in single task condition (p<0.05)

Table 3: Dual-Task Costs of functional performance tests under cognitive dual task and motor dual task conditions in middle-aged and elderly adults.

	Middle-aged adults (N=42)		Elderly adults (N=42)		
	Median	**IQR**	**Median**	**IQR**	**P**
Cognitive dual task cost					
Timed up and go test (%)	-24.99	22.47	-23.06	26.9	0.795
Four square step test (%)	-37.49	31.78	-29.4	31.13	0.074
One leg stance test (%)	0	25.18	16.44	57.94	0.148
Motor dual task cost					
Timed up and go test (%)	0.58	10.63	0.86	7.53	0.823
Four square step test (%)	-2.03	11.48	1.33	9.35	**0.019**
One leg stance test (%)	0	29.82	0	46.54	0.124

IQR: Interquartile range

Table 4: Comparison of single task and dual task performances of faller and non-faller elderly

	Fallers (N=14)		Non-fallers (N=28)			
Single task	**Median**	**IQR**	**Median**	**IQR**	**P**	**ES**
Timed up and go test (s)	13.82	4.93	10.59	3.06	**0.016**	0.37
Four square step test (s)	16.15	5.74	13.64	3.36	**0.035**	0.32
One leg stance test (s)	9.45	19.83	13.79	22.85	0.321	0.15
Cognitive dual task						
Timed up and go test (s)	19.65*	9.63	12.8*	4.53	**0.043**	0.31
Four square step test (s)	21.66*	16.85	17.23*	8.86	0.107	0.25
One leg stance test (s)	8.31	14.5	9.67	21.86	0.321	0.15
Motor dual task						
Timed up and go test (s)	14.78	4.94	10.65	2.47	**0.01**	0.39
Four square step test (s)	16.15	5.59	13.46	3.25	**0.043**	0.31
One leg stance test (s)	12.25	17.3	12.66	29.3	0.376	0.13

IQR: Interquartile range, ES: Effect size, *Wilcoxon Paired sample test, significantly different from its value in single task condition (p<0.05)

Table 5: Dual-Task Costs of functional performance tests under cognitive dual task and motor dual task conditions in faller and non-faller elderly.

	Fallers (N=14)		Non-fallers (N=28)		
	Median	**IQR**	**Median**	**IQR**	**P**
Cognitive dual task cost					
Timed up and go test (%)	-32	48.2	-21.03	21.88	0.947
Four square step test (%)	-27.45	35.32	-29.54	35.64	0.722
One leg stance test (%)	14.26	74.36	21.12	56.47	0.793
Motor dual task cost					
Timed up and go test (%)	1.21	7.47	-0.78	7.25	0.420
Four square step test (%)	2.51	9.09	0.96	8.99	0.626
One leg stance test (%)	0	46.72	-1.85	50.95	0.709

IQR: Interquartile range

and the OLS test duration under cognitive DT condition was lower than its single task value (p=0.043).

There was no significant difference between the cognitive or motor DTCs of the TUG test (p=0.795, p=0.823 respectively) and OLS test (p=0.148, p=0.124 respectively) in middle-aged and elderly individuals. The motor DTC of the four square step test was significantly different in middle-aged and elderly adults (p=0.019) (Table 3).

As the rate of middle-aged participants with a history of falls was low, no analysis could be performed. The TUG test times of the faller elderly under single task, cognitive DT and motor DT conditions were higher than those of the non-faller elderly (p=0.016, p=0.043, p=0.01 respectively). The FSS test times under single task and motor DT conditions of faller elderly individuals were longer than those of elderly individuals who did not fall (p=0.035, p=0.043 respectively), (Table 4). The TUG test duration under cognitive DT condition was greater than its single task value (p=0.001), the FSS test duration under cognitive DT condition was greater than its single task value (p=0.002) in the faller elderly group. The TUG test duration under cognitive DT condition was greater than its single task value and the FSS test duration under cognitive DT condition was greater than its single task value (p<0.001) in the non-faller elderly group.

There was no significant difference between the faller and non-faller elderly individuals in respect of the cognitive or motor DTCs of the functional performance tests (p>0.05) (Table 5).

DISCUSSION

This study was planned to evaluate dual-task balance and mobility performance in middle-aged and elderly individuals, and the results showed that single task, DT balance and mobility performance were worse in elderly individuals, but no significant difference was found between the age groups in terms of DTC. Performance was worse under cognitive DT conditions in both age groups. Although it was observed that balance and mobility

were worse under single task and cognitive DT conditions in faller elderly individuals than in non-faller elderly individuals, no difference was found in terms of DTC.

Cognitive DT performance is adversely affected in older individuals due to the decline in executive function over time and age-related neurodegenerative conditions (7). Considering the studies that evaluated balance performance under dual task conditions, it is thought that this is the reason why the cognitive task is used more frequently as a secondary task. However, performing a simultaneous motor task while walking increases demands for dynamic balance, and the effort not to spill water from the glass also increases attention demands (23). Mobility performance is multidimensional and requires high levels of motor control and cognitive load to pay attention to various external stimuli (6). Therefore, in the current study, balance performance was evaluated under both motor DT and cognitive DT conditions.

In the pre-elderly period, when balance ability and physical functions begin to decline, it is a critical period for early interventions to prevent falls (9). Single task and DT mobility and balance performance are reported to worsen with aging (1, 6, 13). In the current study, balance and mobility performance was found to be better in middle-aged individuals under single task, motor DT and cognitive DT conditions. Efforts to protect these performances of middle-aged adults would be beneficial in order to prevent adverse events that could occur in the future.

It is reported that DTCs related to gait parameters do not change with age or are higher in young individuals than in older individuals (24, 25). Research found that the postural DTCs of younger adults and older adults are similar in stable standing conditions (26). No age-related change was detected in the cost of the TUG test under motor DT conditions, and the cost of cognitive DT is reported to be higher in elderly individuals (13). The current study results demonstrated no difference between middle-aged and elderly adults with respect to DTCs. One reason for this could be that the middle-aged group was in the immediate pre-elderly age range. The fact that DTCs in functional performance tests are similar between age groups suggested that DT assessments should be considered in individuals aged 50-64 years, also called the pre-elderly period, as well as in elderly individuals (27).

Li et al. reported that the rate of outdoor falls is higher in middle-aged individuals than in elderly individuals, tripping is the most common cause of falls and poor health is an important risk factor, especially for indoor falls (28). In the current study, the rates of falling at home were higher in the elderly, partly because the elderly spent less time outside and partly because the elderly were in poorer health. In the current study, individuals who fell had worse performance in both single task and cognitive DT conditions, although the DTCs were similar. Muhaidat et al. found that the test performances were different and DTCs were similar in faller and non-faller adults (29). Asai et al. reported that DTCs were lower in faller elderly adults (30). This could be due to the inclusion of community-dwelling elderly individuals with good cognitive status. The results of the current study suggested that in community-dwelling elderly people with good cognitive status, fallers could manage dual-task conditions similarly to non-fallers and that assessments of falls should focus on single task and cognitive DT performance rather than DTC.

This is the first study that examined the effects of motor and cognitive simultaneous tasks on functional mobility, static and dynamic balance in middle-aged and older adults in Turkey. The results of this study provide important information about the change and decline in cognitive DT and motor DT performance during the aging process. However, the fact that most of the participants were female and sedentary individuals limits the generalizability of the results. In addition, the use of only one type of cognitive and motor task could be considered a limitation. It is suggested that in future studies, cognitive and motor simultaneous task performance of varying degrees of difficulty be evaluated in middle-aged and elderly individuals.

CONCLUSION

The results of this study suggested that balance and mobility performance deteriorates with aging in single task, motor DT and cognitive DT conditions and a simultaneous cognitive task significantly reduced balance and mobility performance. It also showed that balance and mobility performance in single task and cognitive DT conditions were worse in elderly individuals with a history of falls than in non-fallers. In order to prevent future adverse events, the evaluation of single task and DT performances in middle-aged and elderly individuals should be considered.

Ethics Committee Approval: This study was approved by University of Health Sciences Gulhane Scientific Research Ethics Committee (Date: 26.05.2022, No: 2022-147).

Peer Review: Externally peer-reviewed.

Author Contributions: Conception/Design of Study- S.D., G.T., D.Ç., B.K., B.N.F., B.E.; Data Acquisition- G.T., D.Ç., B.K., B.N.F., B.E.; Data Analysis/Interpretation- S.D., G.T., D.Ç., B.K., B.N.F., B.E.; Drafting Manuscript- S.D., G.T., D.Ç., B.K., B.N.F., B.E.; Critical Revision of Manuscript- S.D., G.T., D.Ç., B.K., B.N.F., B.E.; Final Approval and Accountability- S.D., G.T., D.Ç., B.K., B.N.F., B.E.; Material and Technical Support- S.D., D.Ç., B.K., B.N.F., B.E.; Supervision- S.D.

Conflict of Interest: The authors have no conflict of interest to declare.

Financial Disclosure: The authors declared that this study has received no financial support.

REFERENCES

1. Aslan UB, Cavlak U, Yagci N, Akdag B. Balance performance, aging and falling: a comparative study based on a Turkish sample. Arch Gerontol Geriatr 2008;46(3):283-92.

2. Ganz DA, Bao Y, Shekelle PG, Rubenstein LZ. Will my patient fall? JAMA 2007;297(1):77-86.
3. Ambrose AF, Paul G, Hausdorff JM. Risk factors for falls among older adults: a review of the literature. Maturitas 2013;75(1):51-61.
4. Sherrington C, Fairhall NJ, Wallbank GK, Tiedemann A, Michaleff ZA, Howard K, et al. Exercise for preventing falls in older people living in the community: an abridged Cochrane Sysytematic Review. Br J Sports Med 2020;54(15):885-91.
5. Brustio PR, Magistro D, Zecca M, Liubicich ME, Rabaglietti E. Fear of falling and activities of daily living function: mediation effect of dual-task ability. Aging Ment Health 2018;22(6):856-61.
6. Brustio PR, Magistro D, Zecca M, Rabaglietti E, Liubicich ME. Age-related decrements in dual-task performance: Comparison of different mobility and cognitive tasks. A cross sectional study. PloS one 2017;12(7):e0181698.
7. Kahya M, Moon S, Ranchet M, Vukas RR, Lyons KE, Pahwa R, et al. Brain activity during dual task gait and balance in aging and age-related neurodegenerative conditions: a systematic review. Exp Gerontol 2019;128:110756.
8. Osoba MY, Rao AK, Agrawal SK, Lalwani AK. Balance and gait in the elderly: A contemporary review. Laryngoscope Investig Otolaryngol 2019;4(1):143-53.
9. Peeters G, van Schoor NM, Cooper R, Tooth L, Kenny RA. Should prevention of falls start earlier? Co-ordinated analyses of harmonised data on falls in middle-aged adults across four population-based cohort studies. PLoS one 2018;13(8):e0201989.
10. Shubert TE, Schrodt LA, Mercer VS, Busby-Whitehead J, Giuliani CA. Are scores on balance screening tests associated with mobility in older adults? J Geriatr Phys Ther 2006;29(1):33-9.
11. Bayot M, Dujardin K, Dissaux L, Tard C, Defebvre L, Bonnet CT, et al. Can dual-task paradigms predict falls better than single task?–a systematic literature review. Neurophysiol Clin 2020;50(6):401-40.
12. Muir-Hunter S, Wittwer J. Dual-task testing to predict falls in community-dwelling older adults: a systematic review. Physiotherapy 2016;102(1):29-40.
13. Brustio PR, Magistro D, Rabaglietti E, Liubicich ME. Age-related differences in dual task performance: A cross-sectional study on women. Geriatr Gerontol Int 2017;17(2):315-21.
14. McCollum L, Karlawish J. Cognitive impairment evaluation and management. Med Clin 2020;104(5):807-25.
15. Gungen C. Standardize Mini Mental Test'in Turk toplumunda hafif demans tanisinda gecerlik ve guvenilirligi. Turk Psikiyatri Derg 2002;13(4):273-81.
16. Alexandre TS, Meira DM, Rico NC, Mizuta SK. Accuracy of Timed Up and Go Test for screening risk of falls among community-dwelling elderly. Braz J Phys Ther 2012;16(5):381-8.
17. Beauchet O, Fantino B, Allali G, Muir S, Montero-Odasso M, Annweiler C. Timed Up and Go test and risk of falls in older adults: a systematic review. J Nutr Health Aging 2011;15(10):933-8.
18. Dite W, Temple VA. A clinical test of stepping and change of direction to identify multiple falling older adults. Arch Phys Med Rehabil 2002;83(11):1566-71.
19. Isık E, Altug F, Cavlak U. Relıabılıty And Valıdıty Of Four Step Square Test In Older Adults. Turk Geriatri Derg 2015;18(2):151-5.
20. Michikawa T, Nishiwaki Y, Takebayashi T, Toyama Y. One-leg standing test for elderly populations. J Orthop Sci 2009;14(5):675-85.
21. Springer BA, Marin R, Cyhan T, Roberts H, Gill NW. Normative values for the unipedal stance test with eyes open and closed. J Geriatr Phys Ther 2007;30(1):8-15.
22. Lin MR, Hwang HF, Hu MH, Wu HDI, Wang YW, Huang FC. Psychometric comparisons of the timed up and go, one-leg stand, functional reach, and Tinetti balance measures in community-dwelling older people. J Am Geriatr Soc 2004;52(8):1343-8.
23. Lundin-Olsson L, Nyberg L, Gustafson Y. Attention, frailty, and falls: the effect of a manual task on basic mobility. J Am Geriatr Soc 1998;46(6):758-61.
24. Holtzer R, Mahoney JR, Izzetoglu M, Izzetoglu K, Onaral B, Verghese J. fNIRS study of walking and walking while talking in young and old individuals. J Gerontol- Biomed Sci Med Sci 2011;66(8):879-87.
25. Malcolm BR, Foxe JJ, Butler JS, De Sanctis P. The aging brain shows less flexible reallocation of cognitive resources during dual-task walking: a mobile brain/body imaging (MoBI) study. Neuroimage 2015;117:230-42.
26. Boisgontier MP, Beets IA, Duysens J, Nieuwboer A, Krampe RT, Swinnen SP. Age-related differences in attentional cost associated with postural dual tasks: increased recruitment of generic cognitive resources in older adults. Neurosci Biobehav Rev 2013;37(8):1824-37.
27. Carmona-Torres JM, Cobo-Cuenca AI, Pozuelo-Carrascosa DP, Latorre-Román PÁ, Párraga-Montilla JA, Laredo-Aguilera JA. Physical activity, mental health and consumption of medications in pre-elderly people: the National Health Survey 2017. Int J environmental research and public health 2021;18(3):1100.
28. Li W, Keegan TH, Sternfeld B, Sidney S, Quesenberry Jr CP, Kelsey JL. Outdoor falls among middle-aged and older adults: a neglected public health problem. Am J Public Health 2006;96(7):1192-200.
29. Muhaidat J, Kerr A, Evans JJ, Skelton DA. Exploring gait-related dual task tests in community-dwelling fallers and non-faller: a pilot study. Physiother Theory Pract 2013;29(5):351-70.
30. Asai T, Oshima K, Fukumoto Y, Yonezawa Y, Matsuo A, Misu S. Association of fall history with the Timed Up and Go test score and the dual task cost: A cross-sectional study among independent community-dwelling older adults. Geriatr Gerontol Int 2018;18(8):1189-93.

İSTANBUL UNIVERSITY PRESS

RESEARCH ARTICLE / ARAŞTIRMA MAKALESİ
Journal of Advanced Research in Health Sciences / Sağlık Bilimlerinde İleri Araştırmalar Dergisi 2023
DOI: 10.26650/JARHS2023-1221034

DETERMINATION OF METASTATIC CAPACITY IN PRIMARY LUNG CANCER CELLS: REFLECTION OF PATIENT PROFILE IN THE CLINIC USING *IN VITRO* METHODS

PRİMER AKCİĞER KANSER HÜCRELERİNDE METASTATİK KAPASİTENİN BELİRLENMESİ: KLİNİKTEKİ HASTA PROFİLİNİN *İN VİTRO* YÖNTEMLERLE YANSITILMASI

Seçil YILMAZ[1], Medine DOĞAN SARIKAYA[1], Elif YAŞAR[1], Burcu ŞEN BAĞCI[1], Özlem CANÖZ[2], Ömer ÖNAL[3]

[1] Erciyes University, Genome and Stem Cell Center, Kayseri, Turkiye
[2] Erciyes University, Faculty of Medicine, Department of Pathology, Kayseri, Turkiye
[3] Erciyes University, Faculty of Medicine, Department of Thoracic Surgery, Kayseri, Turkiye

ORCID ID: S.Y. 0000-0001-9381-828X; M.D.S. 0000-0003-0435-6066; E.Y. 0000-0001-5974-4176; B.Ş.B. 0000-0002-4526-5198; Ö.C. 0000-0002-0200-6970; Ö.Ö. 0000-0002-9971-7401

Citation/Atıf: Yilmaz S, Dogan Sarikaya M, Yasar E, Sen Burcu B, Canoz O, Onal O. determination of metastatic capacity in primary lung cancer cells: reflection of patient profile in the clinic using *in vitro* methods. Journal of Advanced Research in Health Sciences 2023;6(3):302-311. https://doi.org/10.26650/JARHS2023-1221034

ABSTRACT

Objective: There is a scarcity of *in vivo* models that accurately reflect tumor growth and metastasis in cancer research. Research using cell lines with increasing passage numbers may give misleading results because the tumor loses its characteristic feature. Primary culture is the best method to represent the cellular profile of cancer patients in the laboratory environment. Therefore, we worked with patient-derived primary culture. The most common subtype of the most diagnosed lung cancer worldwide is Non-Small Cell Lung Cancer (NSCLC). Therefore, we aimed to determine patient-specific metastatic capacities by comparatively examining the migration abilities of primary cancer cells of NSCLC patients on the same platform.

Materials and methods: The migration abilities of primary cancer cells of NSCLC patients were demonstrated through wound healing assays on cisplatin and non-cisplatin groups, and measurements were made with Image J software.

Results: In the results of the wound healing assays performed on the cancer cells of five patients, it was observed that there was correlation between the wound widths, wound areas, wound closure percentages, and metastasis in the groups with and without cisplatin in Patient 3, Patient 4, and Patient 5.

Conclusion: To reflect the profile of patients visiting the clinic using patient-derived primary tumor cells, the wound healing assay can be used as a tool to demonstrate tumor behaviors, such as the patients' responses to treatment and their metastasis-forming capacity. Detailed studies are needed in a larger population so that the physician can use in vitro tools in the decision support mechanism.

Keywords: Lung cancer, primary culture, migration, wound healing assay

ÖZ

Amaç: Kanser çalışmalarında tümöre dair büyüme ve metastaz durumunu birebir yansıtan *in vivo* modellerin azlığı söz konusudur. Hücre hatları kullanılan çalışmalarda ise pasaj sayıları ilerledikçe tümörün karakteristik özelliğini kaybetmesinden dolayı yanıltıcı sonuçlar verebilmektedir. Kanser hastalarının hücresel profilini laboratuvar ortamına taşıyabilmek için en iyi yöntem primer kültürdür. Bu nedenle çalışmamızda hasta kaynaklı primer kültür ile çalıştık. Dünya çapında en çok tanı konulan akciğer kanserinin en sık görülen alt tipi Küçük Hücreli-Dışı Akciğer Kanseri (KHDAK)'dir. Bu nedenle çalışmamızda KHDAK tanısı alan hastalardan elde edilen primer kanser hücrelerinin migrasyon yeteneklerinin tek bir platformda karşılaştırmalı olarak incelenerek hastaya özgü metastatik kapasitelerinin belirlenmesi amaçlanmıştır.

Gereç ve Yöntem: KHDAK hastalarına ait primer kanser hücrelerinin migrasyon yetenekleri yara iyileştirmesi deneyiyle cisplatin içeren ve içermeyen grup üzerinde gösterilmiştir ve ölçümler Image J yazılımıyla yapılmıştır.

Bulgular: Beş hastanın kanser hücresine ait yapılan yara iyileşmesi deneyi sonuçlarında; Hasta 3, Hasta 4 ve Hasta 5'e ait cisplatin içeren ve içermeyen gruplarda yara genişlikleri, yara alanları ve yara bölgesini kapatma yüzdeleri ile metastaz arasında ilişki olduğu gözlendi.

Sonuç: Kliniğe başvuran hasta profilinin *in vitro* ortama en iyi şekilde yansıması için hasta kaynaklı primer tümör hücreleri kullanılarak hastaların tedaviye karşı vermiş oldukları yanıtların çeşitliliği ve metastaz oluşturma kapasiteleri gibi birçok tümör davranışının gösterilmesinde yara iyileşmesi deneyi bir araç olarak kullanılabilir. Hekimin karar destek mekanizmasında *in vitro* araç olarak kullanılabilmesi için daha geniş popülasyonda detaylı çalışmalara ihtiyaç duyulmaktadır.

Anahtar Kelimeler: Akciğer Kanseri, primer kültür, migrasyon, yara iyileşmesi deneyi

Corresponding Author/Sorumlu Yazar: Seçil YILMAZ **E-mail:** siyilmaz@erciyes.edu.tr

Submitted/Başvuru: 19.12.2022 • **Revision Requested/Revizyon Talebi:** 07.02.2023 • **Last Revision Received/Son Revizyon:** 18.04.2023 • **Accepted/Kabul:** 28.04.2023 • **Published Online/Online Yayın:** 10.10.2023

INTRODUCTION

Lung cancer is one of the most common cancers in the world, with approximately 2 million new cases and 1.76 million deaths per year, and is the leading cause of cancer-related death (1). Lung cancer consists of molecular and histologically heterogeneous subtypes. Two of these are non-small cell lung cancer (NSCLC) and small cell lung cancer (SCLC) (2). NSCLC accounts for 85% of all lung cancer diagnoses (3). Despite significant advances in treatment, NSCLC after surgical resection has a poor prognosis. Lung carcinomas are mostly in metastatic stage IV when diagnosed, and there are targeted organs for metastasis, such as the brain, bones, and adrenal glands (4,5). Lung carcinomas metastasize to lymphatic as well as blood vessels (6). When resected lung carcinomas are carefully evaluated, vascular invasion is often observed in low-stage tumors, which often leads to an increased incidence of recurrence and reduced patient survival (5). Therefore, identifying the molecular mechanisms underlying lung cancer progression may aid in the development of potential biomarkers and new therapeutic targets for malignancy (7).

For years, it has been suggested that collective cell migration plays important roles in the invasion and metastasis of malignant tumors (8). Collective cell migration is a fundamental process, a coordinated movement of grouped cells connected via cell-cell connections (9). Various in vitro techniques have been developed to study the dynamic process of collective cell migration. Among these techniques, the wound-healing assay is one of the most fundamental and commonly used methods to study collective cell migration because of its potential to visualize cells during migration (10). It is also commonly used in drug trials to test the effectiveness of potential therapeutic drugs and similar approaches (11,12).

In vivo and in vitro studies are frequently applied in cancer research. However, the development and preclinical testing of new cancer treatments is limited due to the scarcity of *in vivo* models that demonstrate tumor growth and metastatic progression (13). In addition, *in vivo* models are insufficient to demonstrate essential aspects of human malignancies such as invasion and metastasis; they are not predictive of clinical outcomes and are expensive, as well as time-consuming (14,15). However, *in vitro* models allow quantitative analysis and control of most experimental variables in the tumor microenvironment (16). In studies with cell lines, cell lines lose the characteristics of the primary tumor and may produce different results, since increasing passage numbers of cell lines can cause genotypic and phenotypic differences (17,18). Furthermore, understanding the genetic and epigenetic diversity of millions of patients from a small number of cell lines is difficult because there is wide variation in response to treatment between patients. This is the driving force behind personalized medicine and the development of methods for obtaining and culturing primary tumor cells from patients (19).

In addition to measuring the migration capacities of primary cells obtained from NSCLC patients, the aim of this study was to determine the treatment resistance profiles of patients by demonstrating the effect of cisplatin, one of the "first choice" drugs to treat lung cancer, on cell migration with the wound healing assay.

MATERIAL AND METHODS

The experiments carried out within the scope of this project are briefly schematized in Figure 1.

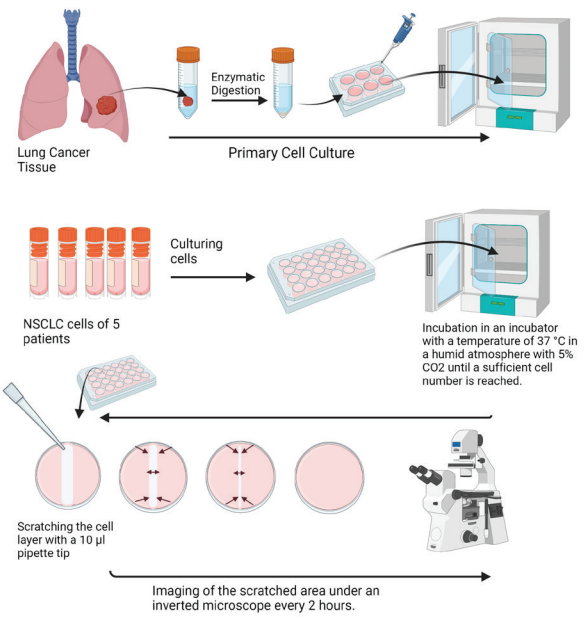

Figure 1: Summary of the experiments carried out within the scope of the project. Lung cancer cells isolated within the scope of the previous project and stocked at -80°C were re-cultured and incubated until sufficient cell number was reached. After reaching a sufficient number, a vertical scratch was created on the cell layer with a 10 µl pipette tip. Images of the scratched area were taken every 2 hours under an inverted microscope.

Collection of samples and primary cell culture

Patients who were diagnosed with definite NSCLC as a result of pathological examinations after surgical resection at Erciyes University Thoracic Surgery Department were included in the study. An informed consent form was signed from the patients before the samples were collected. The cells used in this study were obtained from the TUBITAK 1001 project "Genomic Profiling of Cancer Stem Cells in Lung Cancer Patients," numbered 215S849. This study was approved by the clinical research ethics committee of the Erciyes University Faculty of Medicine under decision number 2015/372, dated 26.08.2015, and was carried out according to the Declaration of Helsinki Principles (www.wma.net/e/policy/b3.htm). For primary culture of patient-derived lung cancer cells, cancer tissues were brought to the Genome and Stem Cell Center from Erciyes University Medical Pathology Department in a cold transport medium (Dulbecco's Modified Eagle medium (DMEM; Gibco, Grand Island, NY, USA, Cat. No. 41966029)) with 1% penicillin-streptomycin (Thermo Fisher Scientific Waltham, Massachusetts, USA, Cat. No. 15070063) within 30 minutes. Cells isolated from

the tumor tissue after mechanical and enzymatic digestion in the cabinet, with 1% penicillin-streptomycin (Thermo Fisher Scientific Waltham, Massachusetts, USA, Cat. No. 15070063), 1% Amphotericin (Thermo Fisher Scientific Waltham, Massachusetts, USA, Cat. No. 15290026) and 1% L-Glutamine (STEMCELL Technologies Inc., Vancouver, Canada, Cat. No. 7100) contained in the DMEM (Gibco, Grand Island, NY, USA, Cat. No. 41966029), were cultured at 37°C incubator with 5% CO_2 atmosphere.

Wound healing assay for determination of patient-specific migration ability 4-8

For the wound healing experiment, which was designed with 3 repetitive groups, cells with passage numbers in the range 4-8 were cultured in a 24-well plate with cell densities of $2x10^4$ cells/well. A total of $12x10^4$ NSCLC cells were used. When the cells were at 80% confluence in the 24-well plate, a wound was created by scratching using a sterile 10 µl micropipette tip, which created a cell-free gap. Images were recorded with the microscope every two hours for 24 hours to measure the wound size.

Drug preparation and administration in wound healing experiment

For the wound healing experiment, which was carried out in 3 repetitive drug groups 5 µM cisplatin and 3 repetitive control groups, the cells with passage numbers in the range 4-8 were cultured in a 24-well plate with $2x10^4$ cells/well. A total of $12x10^4$ NSCLC cells were used. 5 µM cisplatin was prepared, while the cells were expected to coat the 24-well plate.

Cisplatin preparation

cis-Diamineplatinum (II) dichloride (Sigma, Cat No: 479306) was prepared in accordance with the protocol for making stock solution from powder form. The protocol is explained below in brief:

-Stock cisplatin was prepared with 1 mg of cisplatin in 1 ml of medium.

-Since 5 µM cisplatin would be used within the scope of this study, 5 µl of stock cisplatin was taken and 995 µl of falcon with medium was taken. After pipetting to ensure heterogeneous distribution in the solution, the 5 µM cisplatin dose was kept at 4°C, ready to use. It was added to the culture dishes by pipetting before use.

When the cells covered the culture dishes, the wound was created by scratching the cell layer with a 10 µl pipette tip and was then washed with DPBS to eliminate the raised cells from the culture dishes. Then, 5 µM cisplatin was added to the drug group, while only the medium was added to the control group. Wound closure was observed every two hours with an inverted light microscope (DMi1, Leica, Germany). Images of the created wound were recorded using the Leica application package V4 software.

Analysis

The wound area was measured using Java's Image J software (http://rsb.info.nih.gov). The migration of cells towards wounds is expressed as percent wound closure. Wound closure percentages were calculated according to the formula % wound closure= [(At=0h- At=Δh)/At=0h] X 100% (20). The correlation of the migration in the patients' cells between the hours was analyzed by calculating their mean and standard deviation.

RESULTS

Clinical information of lung cancer patients

Tumor diameter, metastasis status, survival, and adjuvant treatment options for patient-derived NSCLC cells used in this study are given in Table 1. According to the information obtained from the Erciyes University Thoracic Surgery Department, it was seen that Patient 1 and Patient 3 had brain and lymph node metastases.

Wound healing assay of patient-derived lung cancer cells

Images of the wounds created with a 10 µl pipette tip in the wound healing assay are shown in Figure 2. When cells cultured in 24-well plates were scratched after covering the culture dish, it was considered the 0th hour of the wound healing assay. Cell images were recorded every two hours for 24 hours.

Table 1: Clinical information of patients with non-small cell lung cancer

Patient Numbers	Age	Tumor Diameter	Stage	Metastasis	Survival	Adjuvant treatment
Patient 1	52	6*4*4	III	Brain-Lymph node	Ex	-
Patient 2	58	1.2*0.8*0.*8	I	-	Living without disease	-
Patient 3	67	6*4*4	III	Brain-Lymph node	Living with disease	-
Patient 4	72	4*3*3	I	-	Ex	Chemotherapy
Patient 5	52	5.5*4.5*4	II	-	Living without disease	Chemotherapy

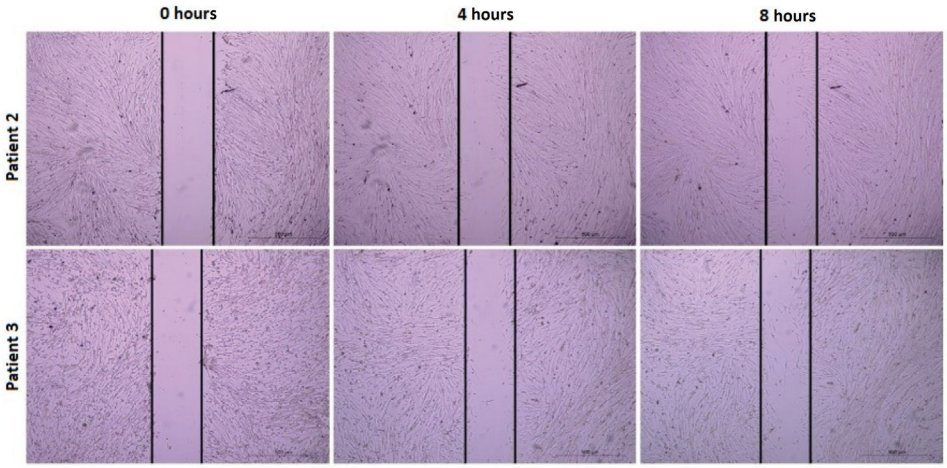

Figure 2: Wound healing assay images of cancer cells of Patient 2 and Patient 3. The wound area is indicated by lines. Images of the wound area at 0, 4, and 8 hours were recorded with a 4X objective. (Three repetitions)

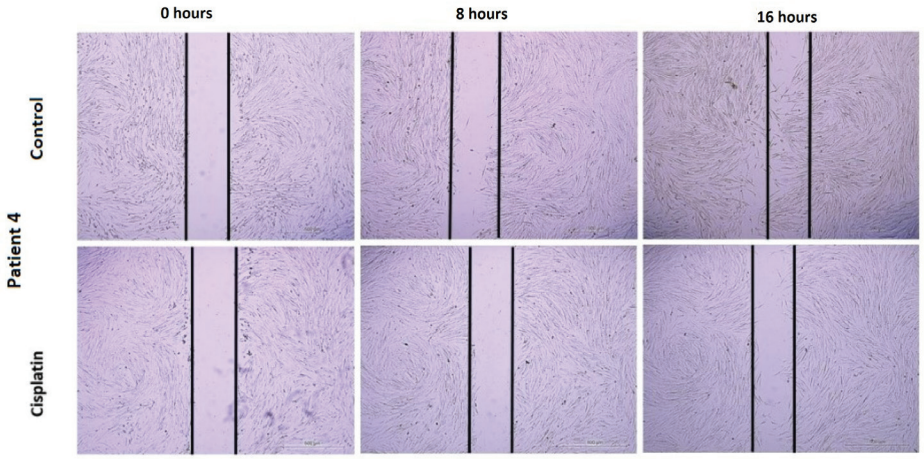

Figure 3: Wound healing assay images of Patient 4, which was performed by creating an experimental group containing 5 µM cisplatin and a control group without cisplatin in cancer cells of NSCLC patients. 0, 8 and 16 hours are shown. Cell images with a scratch area were recorded with a 4X objective. (Three repetitions)

Wound healing assay of patient-derived lung cancer cells (cisplatin)

Within the scope of this study, cell images of two different groups, the experimental group containing 5 µM cisplatin and the control group without cisplatin, were recorded every two hours for 24 hours. Likewise, images of wounds created with a 10 µl pipette tip are shown in Figure 5 for both groups. When cells cultured in 24-well culture dishes were scratched after covering the culture dish, it was considered the 0th hour of the wound healing experiment. Width (Figure 4A-B) and area measurements were made on the recorded cell images with the ImageJ program (Figure 4C-D).

Comparison of wound widths in patient-derived primary lung cancer cells

The findings of the comparison of wound widths of both groups with and without cisplatin are shown in Figure 5. In order to show the differences between the patients more clearly, the graph of each patient is shown separately.

Comparison of wound areas in patient-derived primary lung cancer cells

The findings of the comparison of the wound areas of both groups with and without cisplatin are shown in Figure 6.

Comparison of wound closure percentages in patient-originated primary lung cancer cells

Wound closure percentages were calculated according to the formula % wound closure= [(At=0h- At=Δh) /At=0h] X 100% in order to compare the clinical data and CSC rates of the patients according to the closure between the experimental and control groups (Figure 10).

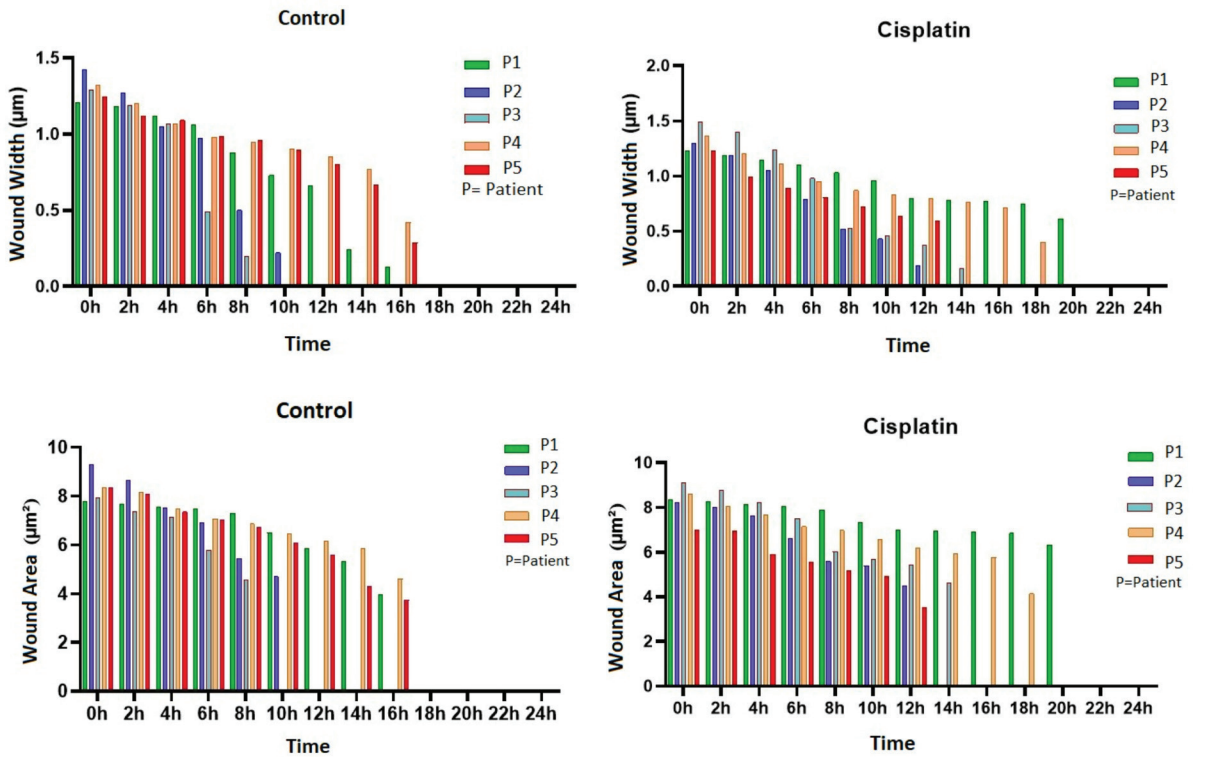

Figure 4: Measurements of the experimental and control groups obtained as a result of the 24-hour follow-up of the wound widths and wound areas created as a result of the wound healing assay of NSCLC patients. (A-B) Measurements of wound widths every two hours for 24 hours in the drug and control groups in the wound healing assay of NSCLC patients. (C-D) Measurements of wound areas every two hours for 24 hours as a result of the wound healing assay of NSCLC patients. All experiments were repeated three times.

DISCUSSION

NSCLC migration is the most prevalent subtype of lung cancer, with a five-year survival rate of roughly 15% (21). At the time of diagnosis, the majority of NSCLC patients are in the metastatic stage (22). 90% of all cancer-related deaths are thought to be caused by tumor metastases (23). Studies both *in vivo* and *in vitro* demonstrate that metastatic cancer cells spread one at a time (24). For a better understanding of metastasis, it is essential to comprehend the methods through which these tumor cells migration and penetrate (25). The molecular underpinnings of lung cancer and studies on metastasis must be further investigated because lung cancer is already metastatic when it is diagnosed. Therefore, our study compared the migration capabilities of patient-derived primary cells with different profiles in NSCLC, the most common subtype of lung cancer. Table 1 displays the patients' clinical profiles. It is seen that Patient 1 (P1) and Patient 3 (P3) have metastases, and Patient 4 (P4) and Patient 5 (P5) receive chemotherapy.

Although cell migration has an important role in cancer and metastasis, approaches to studying cell migration are very important in oncology, since cell migration is related to the effects of new therapeutic drugs and chemoattractants in the metastatic process. (26,11). Particularly, collective cell migration is a common type of migration seen during wound healing and metastasis of epithelial cancers (27,28). In addition, cell migration, which plays a role in re-epithelialization, is a mediator of angiogenesis and tumor invasion (29-31). Therefore, cell migration may also mediate cancer. Cell migration is an essential component of pathological and physiological processes encompassing all these (10). It is possible to monitor the metastasis potential of cancer cells with the wound healing assay, which is a common in vitro biological assay used to investigate cancer cell migration and to test drugs with therapeutic efficacy. In the study by Bahar et al. on four ovarian cancer cell lines, it was shown that the cell lines have different migration capacities (11). In the study by Pijuan and colleagues, the migration capacity of melanoma cells was demonstrated by a wound healing experiment (32). In another study by Jonkman and colleagues, the migratory capacity of breast cancer cells was demonstrated with a wound healing experiment in MCF7, a breast cancer cell line (33). In addition, in the study by Sullivan et al., it was shown that the wound area decreased three times faster in MDA-MB-231 cells compared to the less invasive MDA-MB-468 cells (34).

Wound healing assay is frequently used in the literature to measure the migration ability of cells. Although the wound healing assay is widely used, there are some limitations to the traditional wound healing experiment. First, the scratch rate

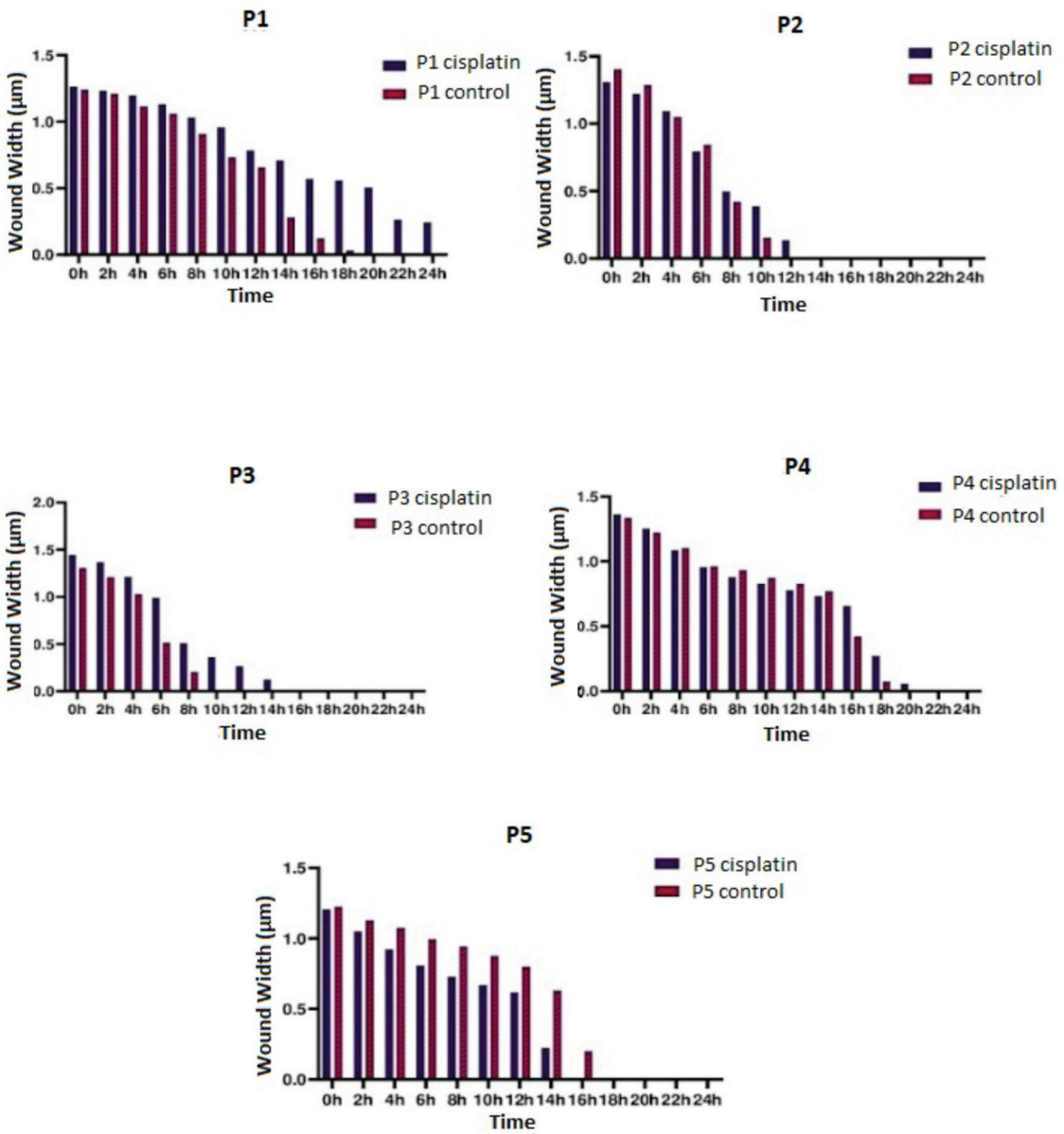

Figure 5: Comparison of wound widths in cisplatin and control groups of NSCLC patients (Three repetitions)

and shape of the injured area may vary between different experiments. Second, scraping involves mechanical damage to cells and cellular contents may be released into the environment. The extent of cell damage is difficult to control and can complicate the process of cell migration (10). These limitations can make comparisons between experiments difficult. For this reason, the optimization of the experiment was performed and the images of the cells were taken at intervals of two hours, as the experiments were repeated in triplicate. Two-way verification was provided by calculating the area as well as the wound width. The Image J program was used to avoid manual errors in the measurements. As a result of measuring the wound width according to a fixed area determined, at the 10th hour of the cancer cells of P3 and the 12th hour of the cancer cells of P2 the cancer cells completely covered the wound width it was observed that the cancer cells of P1, P4, and P5 completely covered the wound width at the 18th hour (Figure 4A). Consistent with these data, cancer cells were detected in the entire wound area belonging to P3 at the 10th hour and cancer cells of P2 at 12th hour. It was observed that the cancer cells of P1, P4, and P5 completely closed at 18 hours (Figure 4B). Although they closed the wound area at the same time, it was observed that the cancer cells with the slowest rate of closing the wound area belonged to P4, followed by P5 and P1, respectively. It was observed that the cancer cells that closed the wound area the fastest belonged to P3. These results show that cells from different patients exhibit different profiles. Images of the wound healing experiment in the cancer cells of P2

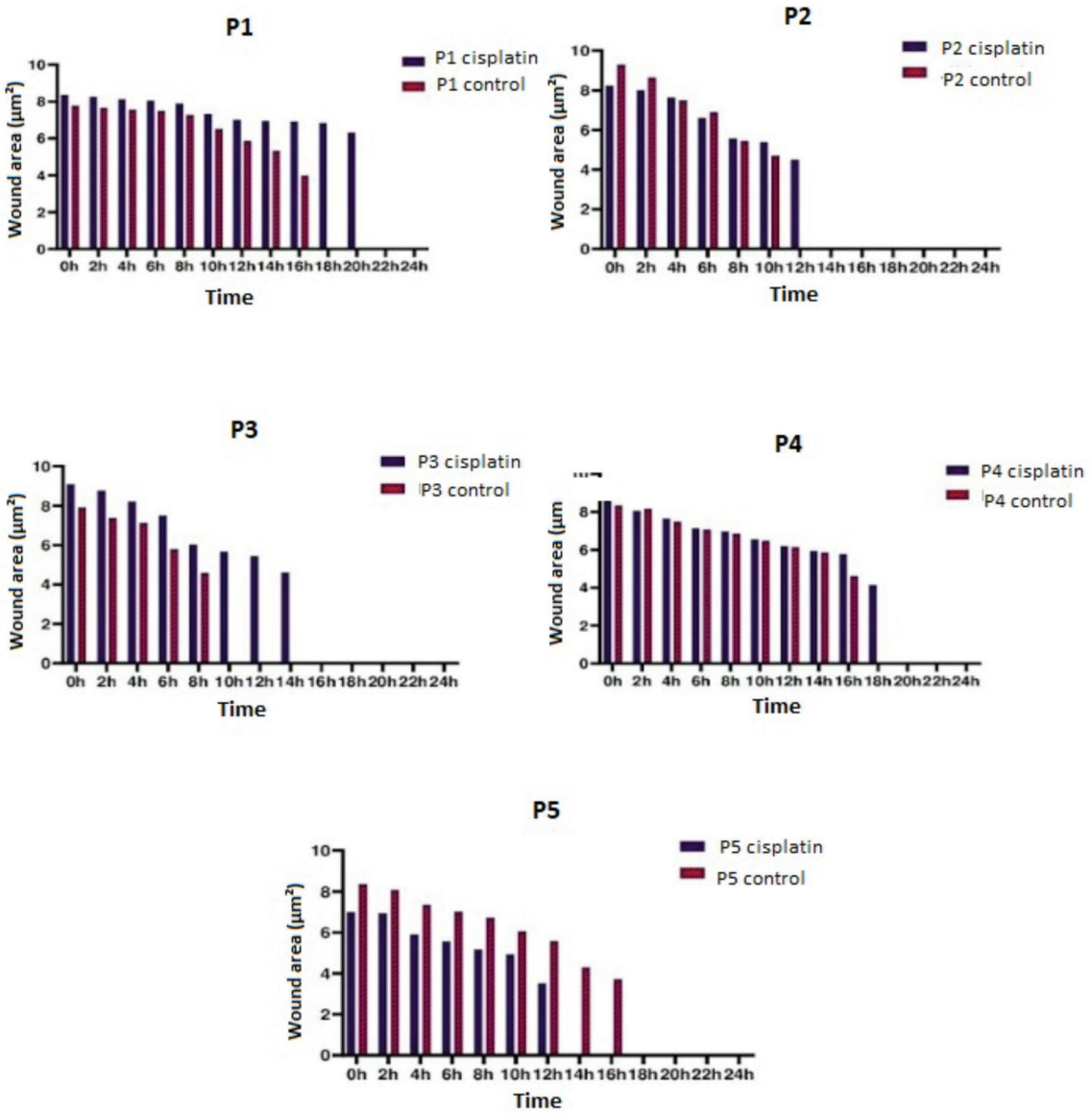

Figure 6: Comparison of the wound area in the cisplatin and control groups of NSCLC patients (Three repetitions)

and P3 (both NSCLC patients) are given in Figure 2. When we look at the images of the wound area at 0 hours, 4 hours, and 8 hours in patients whose wound area is indicated by lines, it is seen that P3's cells migrated to the injured area more quickly compared to P2. In these images of both patients, it is seen that the migration abilities of the cancer cells of the two patients are different. Considering the clinical information of the patient in Table 1, which confirms this finding, it is seen that P3 has brain-lymph node metastasis. It can be said that this migration ability of P3's cells is related to metastasis.

Adjuvant cisplatin-based chemotherapy is the standard of care in patients with completely resected NSCLC stage II-III and in patients with stage I NSCLC (35). Cisplatin interacts with DNA double strands by formation of interstrand and intrastrand adducts, and thereby induces apoptosis in cancer cells through the interference with DNA replication and gene transcription. Similar to other chemotherapeutic agents, the effect of cisplatin is commonly limited by the resistance of cancer cells. Cisplatin resistance can be intrinsic or acquired (36). Manguinhas and colleagues investigated cancer cell migration and invasion with the chemotherapeutic agent cisplatin and the cytotoxicity E3330 using the NSCLC cell line H1975 with a wound healing assay used to assess collective cell migration, maintenance of functional cell-cell junctions, and movement of cells across a horizontal surface (37). To investigate the effect of cisplatin on human lung cancer epithelial H460 cells migration, Maiuthed and colleagues performed wound healing assays (38). In this

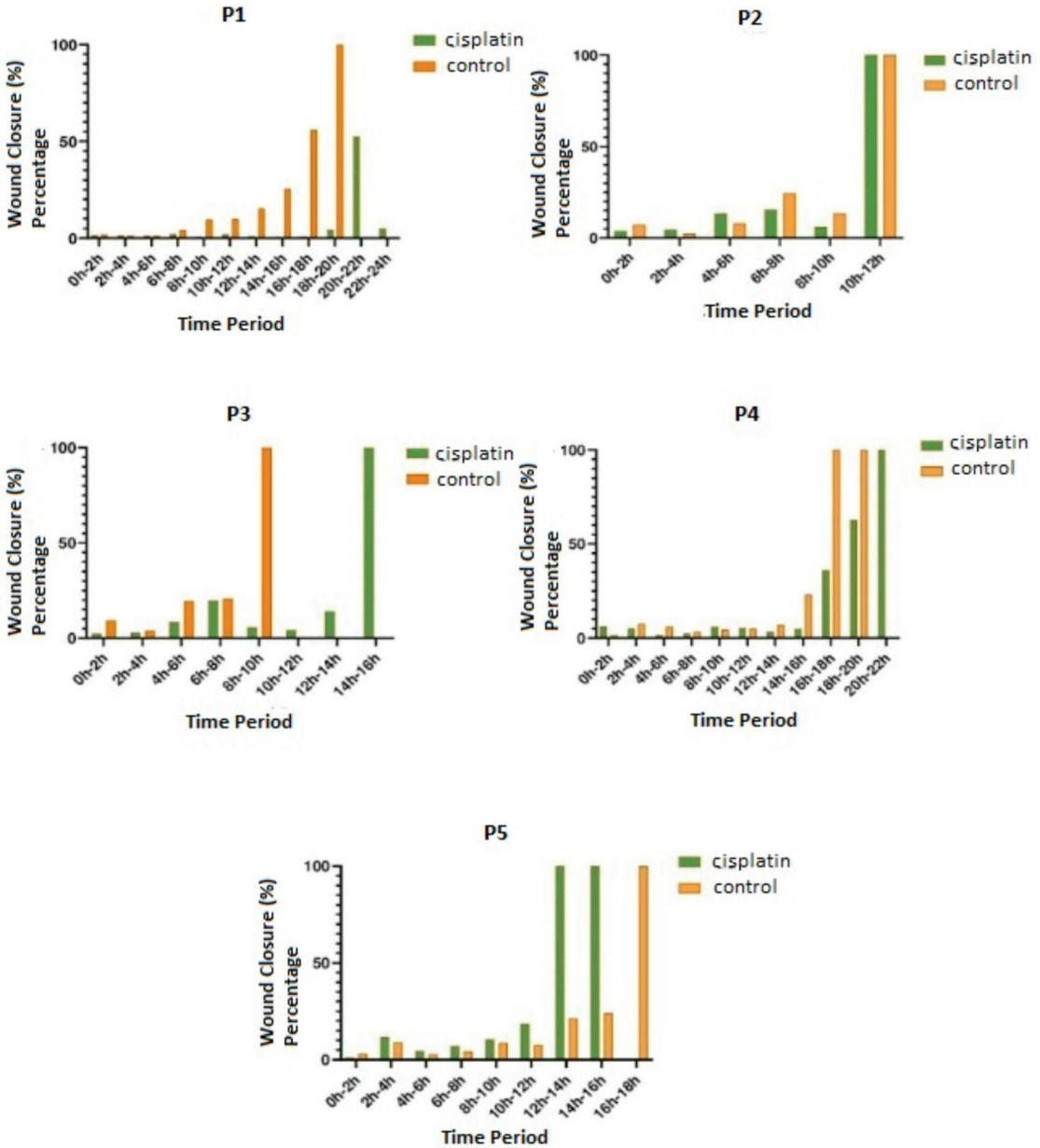

Figure 7: Comparison of the percentage of wound closure in the cisplatin and control groups of NSCLC patients (Three repetitions)

project, cisplatin, as the most widely used drug in NSCLC patients, was chosen for migration profiling of patient-derived cells in cell migration, since it blocks cell division. As a result of the experiments, the cell images of both the control and drug groups of P4, one of the cisplatin-administered groups, are given in Figure 3. It was observed that the wound areas were completely closed as follows. According to a fixed region determined in the groups, the wound width was determined by the cancer cells of P2 and P5 at the 12th hour, the cancer cells of P3 at the 16th hour, the cancer cells of P4 at the 20th hour, and the cancer cells of P1 at the 20th hour. (Figure 4B). Consistent with these data, in the cisplatin administered groups, it was observed that the wound area was completely closed at the 12th hour in the cancer cells of P2 and P5, at the 16th hour in the cancer cells of P3, at the 20th hour in the cancer cells of P4, and at the 22nd hour in the cancer cells of P1 (Figure 4D). When the closure rate was compared among the patients, it was observed that although P2 and P5 closed the wound area at the same time, the cancer cells with the fastest rate of closing the wound area belonged to P2. P3, P4, and P1 followed the rate of closure of the wound area by the cancer cells from high to low (Figure 4). The fact that both wound widths and wound areas, which were formed from triplicate groups according to the patient, supported each other, and that similar quantitative values showed the standardization of the study, provided support for the differences between

patients with more data (Figure 5,6). When the graph obtained is matched with the patients' clinical information, the absence of metastases in P2 and P5 can be interpreted as reduced aggressiveness and being more affected by the chemotherapeutic agent cisplatin. The closure of P1 in the cisplatin-containing group at the 22nd hour was examined. This patient's clinical data includes metastasis information, which does not reflect the aggressiveness and invasiveness of P1's cancer cells.

Wound closure percentages were calculated according to the formula in the literature in Figure 7 (20). When these graphs are examined, (i) as expected, the control group of Patient 1 was found to close earlier than the cisplatin group. It is found in the clinical data that this patient has metastasis. Although there is metastasis, delayed closure of the wound area compared to other patients may also be the result of heterogeneity between patients. (ii) P2 does not seem to have a history of metastasis or chemotherapy. In the wound healing experiment created from the cancer cells of this patient, it was observed that both the control group and the drug group containing cisplatin were closed very quickly at the 12th hour. When compared with the clinical picture of other patients, there was no correlation between metastasis and closure rate. (iii) It was observed that the wound area created in P3 closed faster than the cisplatin-containing drug group, as expected in the control group. Considering that cancer cells belonging to P3 are the fastest closure group compared to other patients and they have metastases in their clinical information, there may be a relationship between the ability to migrate and metastasize. (iv) In the wound healing experiment of P4, who was known to have received chemotherapy and had no metastases, it was observed that the control group had closed before, as expected. Compared to the closure time of the wound created in other patients, P4 closed later and the slower migration ability compared to other patients may be associated with metastasis. (v) The clinical picture of P5 shows that the patient received chemotherapy and has no metastases. In the areas where wound damage was created, closure occurred in both groups at close hours. In another study, it was shown that cisplatin-resistant cancer cells migrated more than non-resistant cells in a wound healing assay (39). The reason for this may be that cancer cells develop resistance to chemotherapy and therefore close at similar times between the drug group and the control group. In addition, considering that the control group closed later than other patients, slow migration abilities compared to other patients may be associated with metastasis.

Wound healing assay can be used as a tool in demonstrating the patient-specific migration ability of patients applying to the clinic *in vitro*, measuring differences in response to treatment and differences in drug resistance between patients. Detailed studies should be carried out by analyzing more patients and different parameters in order to be used as support in clinical decisions, such as the treatment to be given by the physician in the clinic according to the patient profile.

The authors' contributions to the study were equal and they did not receive any support for the study. The authors do not declare any conflict of interest.

Acknowledgements: We would like to thank Nilhan Mutlu for her help in this study, and the Erciyes University BAP unit and TUBITAK for their financial support.

Ethics Committee Approval: This study was approved by Erciyes University Faculty of Medicine Clinical Research Ethics Committee (Date: 26.08.2015 No: 2015/372).

Peer Review: Externally peer-reviewed.

Author Contributions: Conception/Design of Study- S.Y.; Data Acquisition- S.Y., Ö.Ö., Ö.C., M.D.S., B.Ş.B., E.Y.; Data Analysis/Interpretation- S.Y., Ö.D.S., E.Y.; Drafting Manuscript- S.Y., Ö.D.S., E.Y.; Critical Revision of Manuscript- S.Y., Ö.Ö., Ö.C., M.D.S., B.Ş.B., E.Y.; Final Approval and Accountability- S.Y., Ö.Ö., Ö.C.; Material and Technical Support- S.Y., Ö.Ö., Ö.C., M.D.S., B.Ş.B., E.Y.; Supervision- S.Y., Ö.Ö.

Conflict of Interest: The authors have no conflict of interest to declare.

Financial Disclosure: The study was supported by the Erciyes University Scientific Research Projects Unit (Project Number: THD_2021_11187) and the Scientific and Technological Research Council of Turkey (TÜBİTAK) 1001 project (Project Number: 215S849).

REFERENCES

1. Siegel RL, Miller KD, Fuchs HE, Jemal A. Cancer statistics, 2022. CA Cancer J Clin 2022;72(1):7-33.
2. Howlader N, Forjaz G, Mooradian MJ, Meza R, Kong CY, Cronin KA, et al. The effect of advances in lung-cancer treatment on population mortality. N Engl J Med 2020;383(7):640-9.
3. Cengiz H, Demirci A, Varım C, Mandel NM, Turna Z. Küçük hücreli dışı akciğer kanserinde neoadjuvan ve adjuvan tedavi sonuçları. Sakarya Tıp Dergisi 2020;10(3):450-8.
4. Riihimäki M, Hemminki A, Fallah M, Thomsen H, Sundquist K, Sundquist J, et al. Metastatic sites and survival in lung cancer. Lung Cancer 2014;86(1):78-84.
5. Popper HH. Progression and metastasis of lung cancer. Cancer Metastasis Rev 2016;35(1):75-91.
6. Achen MG, Stacker SA. Molecular control of lymphatic metastasis. Ann N Y Acad Sci 2008;1131:225-34.
7. Wu Q, Zhang B, Li B, Cao X, Chen X, Xue Q. PTBP3 promotes migration of non-small cell lung cancer through regulating E-cadherin in EMT signaling pathway. Cancer Cell Int 2020;20:172.
8. Deisboeck TS, Couzin ID. Collective behavior in cancer cell populations. Bioessays 2009;31(2):190-7.
9. Friedl P, Gilmour D. Collective cell migration in morphogenesis, regeneration and cancer. Nat Rev Mol Cell Biol 2009;10(7):445-57.
10. Riahi R, Yang Y, Zhang DD, Wong PK. Advances in wound-healing assays for probing collective cell migration. J Lab Autom 2012;17(1):59-65.
11. Bahar E, Yoon H. Modeling and predicting the cell migration

properties from scratch wound healing assay on cisplatin-resistant ovarian cancer cell lines using artificial neural network. Healthcare (Basel) 2021;9(7):911.

12. Kauanova S, Urazbayev A, Vorobjev I. The Frequent sampling of wound scratch assay reveals the "opportunity" window for quantitative evaluation of cell motility-impeding drugs. Front Cell Dev Biol 2021;9:640972.
13. DeRose YS, Wang G, Lin YC, Bernard PS, Buys SS, Ebbert MT, et al. Tumor grafts derived from women with breast cancer authentically reflect tumor pathology, growth, metastasis and disease outcomes. Nat Med 2011;17(11):1514-20.
14. Kondo J, Inoue M. Application of cancer organoid model for drug screening and personalized therapy. Cells 2019;8(5):470.
15. Hait WN. Anticancer drug development: the grand challenges. Nat Rev Drug Discov 2010;9(4):253-4.
16. Katt ME, Placone AL, Wong AD, Xu ZS, Searson PC. In vitro tumor models: Advantages, disadvantages, variables, and selecting the right platform. Front Bioeng Biotechnol 2016;4:12.
17. Kaur G, Dufour JM. Cell lines: Valuable tools or useless artifacts. Spermatogenesis 2012;2(1):1-5.
18. Fallahi P, Ferrari SM, Elia G, Ragusa F, Patrizio A, Paparo SR, et al. Primary cell cultures for the personalized therapy in aggressive thyroid cancer of follicular origin. Semin Cancer Biol 2022;79:203-16.
19. Mitra A, Mishra L, Li S. Technologies for deriving primary tumor cells for use in personalized cancer therapy. Trends Biotechnol 2013;31(6):347-54.
20. Grada A, Otero-Vinas M, Prieto-Castrillo F, Obagi Z, Falanga V. Research techniques made aimple: Analysis of collective cell migration using the wound healing assay. J Invest Dermatol 2017;137(2):e11-6.
21. Fangjun L, Zhijia Y. Tumor suppressive roles of eugenol in human lung cancer cells. Thorac Cancer 2018;9(1):25-9.
22. Schettino C, Bareschino MA, Rossi A, Maione P, Sacco PC, Colantuoni G, et al. Targeting angiogenesis for treatment of NSCLC brain metastases. Curr Cancer Drug Targets 2012;12(3):289-99.
23. Spano D, Heck C, De Antonellis P, Christofori G, Zollo M. Molecular networks that regulate cancer metastasis. Semin Cancer Biol 2012;22(3):234-49.
24. Fares J, Fares MY, Khachfe HH, Salhab HA, Fares Y. Molecular principles of metastasis: a hallmark of cancer revisited. Signal Transduct Target Ther 2020;5(1):28.
25. Bravo-Cordero JJ, Hodgson L, Condeelis J. Directed cell invasion and migration during metastasis. Curr Opin Cell Biol 2012;24(2):277-83.
26. Simpson KJ, Selfors LM, Bui J, Reynolds A, Leake D, Khvorova A, et al. Identification of genes that regulate epithelial cell migration using an siRNA screening approach. Nat Cell Biol 2008;10(9):1027-38.
27. Friedl P, Wolf K. Tumour-cell invasion and migration: Diversity and escape mechanisms. Nat Rev Cancer 2003;3(5):362-74.
28. Wang X, Decker CC, Zechner L et al. In vitro wound healing of tumor cells: inhibition of cell migration by selected cytotoxic alkaloids. BMC Pharmacol Toxicol 2019;20:4.
29. Tonnesen MG, Feng X, Clark RA. Angiogenesis in wound healing. J Invest Derm Symp Proc 2000;5(1):40-6.
30. Small JV, Geiger B, Kaverina I, Bershadsky A. How do microtubules guide migrating cells? Nat Rev Mol Cell Bio 2002;3(12):957-64.
31. Ridley AJ, Schwartz MA, Burridge K, Firtel RA, Ginsberg MH, Borisy G, Parsons JT, Horwitz AR. Cell migration: integrating signals from front to back. Science. 2003;302(5651):1704–9.
32. Pijuan J, Barceló C, Moreno DF, Maiques O, Sisó P, Marti RM, et al. In vitro cell migration, invasion, and adhesion assays: From Cell Imaging to Data Analysis. Front Cell Dev Biol 2019;7:107.
33. Jonkman JE, Cathcart JA, Xu F, Bartolini ME, Amon JE, Stevens KM et al. An introduction to the wound healing assay using live-cell microscopy. Cell Adh Migr 2014;8(5):440-51.
34. Sullivan R, Holden T, Tremberger G, Jr J, Cheung E, Branch C, et al. Fractal dimension of breast cancer cell migration in a wound healing assay. Int J Biomed Biol Engine 2008; 2(8):186-91.
35. Pirker R. Adjuvant chemotherapy of non-small cell lung cancer. Tanaffos 2012;11(1):12-7.
36. Han XJ, Yang ZJ, Jiang LP, Wei YF, Liao MF, Qian Y, Li Y, Huang X, Wang JB, Xin HB, Wan YY. Mitochondrial dynamics regulates hypoxia-induced migration and antineoplastic activity of cisplatin in breast cancer cells. Int J Oncol 2015;46(2):691-700.
37. Manguinhas R, Fernandes AS, Costa JG, Saraiva N, Camões SP, Gil N, et al. Impact of the APE1 redox function inhibitor E3330 in non-small cell lung cancer cells exposed to cisplatin: increased cytotoxicity and impairment of cell migration and invasion. Antioxidants 2020;9(6): 550.
38. Maiuthed A, Chanvorachote P. Cisplatin at sub-toxic levels mediates integrin switch in lung cancer cells. Anticancer Res 2014;34(12):7111-7.
39. Wang H, Zhang G, Zhang H, Zhang F, Zhou B, Ning F, et al. Acquisition of epithelial-mesenchymal transition phenotype and cancer stem cell-like properties in cisplatin-resistant lung cancer cells through AKT/β-catenin/Snail signaling pathway. Eur J Pharmacol 2014;723:156-66.

RESEARCH ARTICLE / ARAŞTIRMA MAKALESİ
Journal of Advanced Research in Health Sciences / Sağlık Bilimlerinde İleri Araştırmalar Dergisi 2023
DOI: 10.26650/JARHS2023-1277768

EFFECT OF SILVER DIAMINE FLUORIDE ON FRACTURE RESISTANCE OF CLASS I COMPOSITE RESTORATIONS

GÜMÜŞ DİAMİN FLORÜRÜN SINIF I KOMPOZİT RESTORASYONLARIN KIRILMA DİRENCİNE ETKİSİ

Sevgi ZORLU[1], Aslı TOPALOĞLU AK[1], Polen NİSA BULUT[2]

[1]Istanbul Aydın University, Faculty of Dentistry, Department of Pedodontics, Istanbul, Turkiye
[2]Istanbul Aydın University, Faculty of Dentistry, Istanbul, Turkiye

ORCID ID: S.Z. 0000-0003-3435-6833; A.T.A. 0000-0003-4572-1875; P.N.A. 0000-0001-5428-1635

Citation/Atıf: Zorlu S, Topaloglu Ak A, Nisa Bulut P. Effect of silver diamine fluoride on fracture resistance of class I composite restorations. Journal of Advanced Research in Health Sciences 2023;6(3):312-316. https://doi.org/10.26650/JARHS2023-1277768

ABSTRACT

Objective: This study investigated the effect of silver diamine fluoride (SDF) pretreatment on the fracture resistance of Class I composite restorations in molars.

Materials and Methods: Twenty non-carious human third molars were extracted for orthodontic needs and pericoronitis were used. The teeth were randomly divided into control (n=10), and study (n=10) groups, and occlusal cavities were prepared. In the study group, 38% SDF solution was applied to the cavity and dried for 1 minute. The cavity was treated with Gluma (Heraeus Kulzer, Dormagen, Germany), a self-etch adhesive, for 20 seconds and light-cured for 20 seconds. Filtek Z250 composite resin (3M ESPE, Seefeld, Germany) was inserted and light-cured for 40 seconds. The control group underwent the same procedure without SDF pretreatment. Both groups experienced thermocycling for 5000 cycles between 5 and 55°C. Samples were embedded in acrylic cylindrical pipes and tested for fracture resistance using a fracture resistance test device. The continuously increasing compressive load was applied at a 0.5 mm/min crosshead speed until specimen fracture. The values at the moment of fracture were recorded in Newtons (N). Data were analyzed using an independent samples t-test, with p-values <0.05 considered significant.

Results: The mean fracture resistance for the group treated with 38% SDF was 1568 ± 461.8 N, while the group without SDF treatment showed 1192 ± 307.6 N. No statistically significant difference was found between the groups p>0.05.

Conclusion: SDF pretreatment did not enhance the fracture resistance of Class I composite restorations in molars.

Keywords: Composite resin, fracture resistance, silver diamine fluoride

ÖZ

Amaç: Bu çalışma, gümüş diamin florür (GDF) ön işlem uygulamasının molar dişlerdeki sınıf I kompozit restorasyonların kırılma direnci üzerindeki etkisini araştırmayı amaçlamaktadır.

Gereç ve Yöntem: Ortodontik gereksinimler ve perikoronit nedeniyle çekilmiş 20 adet çürüksüz insan üçüncü azı dişi kullanıldı. Dişler rastgele kontrol (n=10) ve çalışma (n=10) gruplarına ayrıldıktan sonra oklüzal kaviteler açıldı. Çalışma grubunda, %38 GDF solüsyonu kaviteye uygulanarak 1 dakika kurumaya bırakıldı. Kavite, 20 saniye boyunca Gluma (Heraeus Kulzer, Dormagen, Almanya), kendinden asitli adezivle işleme tabi tutuldu ve 20 saniye ışıkla polimerize edildi. Filtek Z250 kompozit reçine (3M ESPE, Seefeld, Almanya) yerleştirildi ve 40 saniye ışıkla polimerize edildi. Kontrol grubu, GDF ön işlemi yapılmadan aynı restorasyon işlemine tabi tutuldu. Her iki grup da 5 ve 55°C arasında 5000 döngü termosiklus işlemine tabi tutuldu. Örnekler akrilik silindirik borulara yerleştirildi ve kırılma direnci test cihazı kullanılarak kırılma direnci için test edildi. Sürekli artan sıkıştırma yükü, numune kırılıncaya kadar 0,5 mm/dk çapraz kafa hızında uygulandı. Kırılma anındaki değerler Newton (N) cinsinden kaydedildi. Veriler bağımsız örneklem t-testi ile analiz edildi ve p değerleri <0,05 olanlar istatistiksel olarak anlamlı kabul edildi.

Bulgular: %38 GDF ile işlem gören grup için ortalama kırılma direnci 1568±461,8 N iken, GDF işlemi yapılmayan grup 1192±307,6 N gösterdi. Gruplar arasında istatistiksel olarak anlamlı bir fark bulunmamıştır p>0.05.

Sonuç: GDF ön işlem uygulaması, molar dişlerdeki sınıf I kompozit restorasyonların kırılma direncini artırmamıştır.

Anahtar Kelimeler: Kompozit rezin, kırılma direnci, gümüş diamin florür

Corresponding Author/Sorumlu Yazar: Sevgi ZORLU **E-mail:** sevgizorlu@aydin.edu.tr

Submitted/Başvuru: 07.04.2023 • **Revision Requested/Revizyon Talebi:** 08.05.2023 • **Last Revision Received/Son Revizyon:** 25.07.2023 • **Accepted/Kabul:** 31.07.2023 • **Published Online/Online Yayın:** 13.10.2023

INTRODUCTION

Dental caries is the most prevailing health problem experienced among children early in life. Moreover, its incidence has been reported to have increased in recent years. Consequently, the quality of life is adversely affected due to the rapid progression of carious lesions leading to pain and tooth loss unless an appropriate treatment protocol is applied (1).

In recent years minimally invasive dentistry has become the preferred treatment option by clinicians, as it meanwhile preserving healthy tissues. One of the crucial principles of the minimally invasive approach is minimizing the risk of recurrent disease. There is unequivocal evidence that secondary caries are the most common cause of restoration failure (2). To prevent secondary caries formation, creating a pathogenic bacteria-free cavity is essential before restoration (3). Silver diamine fluoride (SDF) has been recommended since it arrests and prevents new caries formation, either as a standalone treatment or under restorations (3-9).

SDF is an alkaline, colorless, topically applicable solution containing fluoride and silver ions. Silver compounds are used in medicine and dentistry because they can provide an antimicrobial effect. On the other hand, fluoride is routinely used in various forms and ratios to prevent and stop caries as a gold standard. It has been suggested that the synergistic effects of silver and fluoride can halt the caries process and prevent the development of new caries (8, 9).

It has been shown that following the application of SDF, demineralized enamel and dentin undergo remineralization, resulting in a mineral-rich surface containing calcium and phosphate within the carious lesions and subsequently reducing mineral loss (10).

When applied to dentin cavities, silver has the ability to inhibit bacterial growth by interacting with bacterial cell membranes and enzymes. Furthermore, silver is also a potent cathepsin inhibitor and prevents dentin collagen degradation (11-13). However, integrating silver particles into dentinal tubules might affect the mechanical characteristics of restorations adversely (4).

It is claimed that SDF helps to eradicate cariogenic bacteria and promotes remineralization when applied in the same appointment prior to either under glass ionomer or composite resin restorations (7, 14).

The effects of SDF under restorations on avoidance of recurrent caries and the quality of bond strength are well documented (3-9). However, it remains unclear whether SDF affects fracture resistance, because the use of SDF has increased, particularly in permanent teeth, during the pandemic. Therefore the aim of this in vitro study was to investigate the effect of silver diamine fluoride (SDF) pretreatment on the fracture resistance of Class I composite restorations in molars. The null hypothesis of this study is that SDF pretreatment of Class 1 cavities in non-carious molar teeth has no effect on fracture resistance of composite restorations

MATERIALS and METHODS

Twenty non-carious human third molars extracted due to orthodontic needs and pericoronitis were used in the study. Before the commencement of the study, signed written consent from the participants and ethical approval from the Istanbul Aydin University Ethical Committee (Date/No: 2021/373) was taken.

All teeth were examined under a magnifying glass to exclude cracked samples from the study. Mesiodistal and buccolingual widths of the teeth were measured by a digital caliper (Mitutoyo Corp, Tokyo, Japan). In order to standardize the cavity

Table 1: The force values at which fracture occurred of each sample in the study and control groups and statistical analysis of the data

	Study group (n=10) (Newton)	Control group (n=10) (Newton)	p
	2148.0	349.2	
	2234.9	621.9	
	2199.6	1534.4	
	1350.9	1514.4	
	1319.8	1055.8	
	861.0	1383.0	
	1289.0	1462.6	
	1075.7	1803.3	
	1687.1	1231.0	
	1514.0	964.4	
Mean±SD (Newton)	1192±307.6	1568±461.8	0.09

SD: Standard deviations

dimensions, teeth with a mesiodistal width of 12.0±0.5mm and buccolingual widths of 10±0.5mm were included in the study. The teeth were randomly divided into control (n=10) and study (n=10) groups. All cavity preparations and restorations were performed by one operator (PNB). Class I cavities with a depth of 2mm, buccolingual width of 2mm, and a mesiodistal width of 8mm were prepared using round and fissure diamond burs. Cavity dimensions were checked by a millimeter-tipped periodontal probe. In the control group, after preparing the cavities, the self-etch adhesive system Gluma (Heraeus Kulzer, Dormagen, Germany) was applied to the cavity using a micro brush and massaged for 20 seconds. The adhesive was then air-thinned and light-cured for 20 seconds with a high-intensity LED curing unit operating at 1470 mW/cm^2 and 430-480nm wavelength (Elipar™ Deepcure-S, 3M ESPE, St. Paul, MN, USA). Subsequently, a composite resin, Filtek Z 250 in A2 shade (3M ESPE, Seefeld, Germany), was inserted in the cavity and was light-cured for 40s. Finally, the restoration was polished using extra-fine diamond finishing burs and alumina-oxide-containing discs (Soflex; 3M ESPE, Seefeld, Germany).

In the study group, 38% SDF solution (Saforide™, Toyo Seiyaku Kasei Co. Ltd., Osaka, JP) was applied in cavities prior to composite resin restorations. One drop of SDF was taken into the bond brush and rubbed on the cavity floor, and it remained there for one minute. The excess was removed with the help of cotton pellets and air-dried. Then, restorations were completed as described for the control group.

The restored teeth underwent thermocycling for 5000 cycles between 5 and 55°C with a dwell time of 30s and a transfer time of 15s. Following the thermocycling procedure, all samples were embedded in acrylic cylindrical pipes up to the enamel-cement junctions and were connected to a fracture resistance test device (Modental, Esetron, Ankara, Turkey). The compressive load was subjected to the point corresponding to the central fossa of the sample teeth. The fracture resistance strength test was performed by applying a force parallel to the long axis of the tooth at a speed of 5 mm/min with a continuously increasing rate. Values were recorded in Newton (N) when the fracture was observed.

Ultimately, fracture type was individually determined by two blinded examiners (ATA, PNB) under a stereo-microscope (SFC-11A N2GG Motic, Motic Group Co. Ltd., Hong Kong, China).

The following classification was used to determine the fracture type:

Type I: Adhesive fracture between dentin and adhesive

Type II: Cohesive fracture in dentin

Type III: Cohesive fracture in material

Type IV: Mix fracture; in both the restorative material and dentin (15).

Statistical analyses

All analyses were performed using SPSS 19 (IBM SPSS Statistics 19, SPSS Inc., an IBM Co., Somers, NY, USA). Data were analyzed by using an independent sample t-test. Values of p <0.05 were considered significant.

RESULTS

The fracture resistance (N) for each sample for SDF and control groups are shown in Table 1. The mean fracture resistance values and standard deviations for Class I composite restorations were 1568±461.8 for the study group and 1192±307.6 for the control group (Table 1). There was no statistically significant difference between the two groups according to the independent samples t-test result (p=0.09). Upon examining the fractured specimens to determine the fracture type, it was found that all the restorations displayed adhesive failures (Type I).

DISCUSSION

A restorative material not only repairs lost tooth structure but also enhances the fracture resistance of the tooth and provides effective marginal sealing (16). However, secondary caries and fractures are the primary reasons for composite restoration failure (17). The resistance of the cavity wall and margins must be increased to inhibit the recurrence of secondary caries. SDF application can potentially address this issue (9). In the present study, the mean fracture resistance values and standard deviations for Class I composite restorations were 1568±461.8 for the study group and 1192±307.6 for the control group (Table 1). There was no statistically significant difference between the two groups according to the independent samples t-test result (p=0.09). Therefore, the null hypothesis was confirmed that SDF pretreatment of Class 1 cavities in non-carious molar teeth has no effect on fracture resistance of composite restorations.

Thermal cycling is an ageing process that simulates thermal stresses typically occurring in the mouth by exposing samples to extreme temperatures (16). According to ISO TR 11450 (1994) standards, although immersing the specimens in water baths for at least 20s at 5 and 55°C for 500 times and the transfer time between baths 5s-10s is a suitable accelerated ageing method, this cycle number is insufficient to imitate the tooth bonding efficiency of the restoration (18). Therefore, in the present study, the specimens were undergone 5000 thermo-cycles between 5 and 55°C with a dwell time of 30s and a transfer time of 15s.

In an effort to prevent secondary caries formation under restorations, various antibacterial and remineralizing agents are recommended to inhibit and remineralize affected dentin lesions. Some are integrated into adhesive systems and restorations, whereas others are applied directly to cavities as a base/liner. These agents have been reported to inactivate residual bacteria and condition dentine to achieve a better restoration bonding (3, 19). Likewise, SDF has also been effective in preventing new caries formation and promoting remineralization of enamel and dentin (20). Shimizu and Kawagoe reported no recurrent caries development after 26 months in SDF-pretreated primary teeth restored with

amalgam (21). Mei et al. observed a reduction in secondary caries under composite resin and glass ionomer cement restorations following SDF conditioning (7).

Considering its potential use under restorations intrigued the researchers to assess its possible effect on the bonding of restorations (3, 15). However, studies on enamel bond strength are limited and reveal different results (15, 22). SDF application on enamel has shown no significant impact on orthodontic bracket bonding strength, but it reduced the bond stability of self-etch universal adhesives (15, 22). Such deviations could be attributed to different study designs and adhesive systems. A systematic review of the effects of SDF application on the bond strength of dentin to adhesives and glass ionomer cement could not reach a definitive conclusion, as the results revealed inconsistent outcomes (23). Danaeifar et al. reported that dentin pretreatment with SDF did not affect the shear bond strength of the tested bulk-fill materials in human permanent premolars (24). While this study did not specifically investigate the impact of SDF on restoration bond strength, both the experimental and control groups exhibited adhesive failures.

To date, there is not a study that has investigated the application of SDF on fracture resistance of composite restorations. In the present study, both groups showed higher mean fracture resistance values compared to the maximum human physiological masticatory and biting loads, reported to be 880N and 900N, respectively (25, 26). Although the group treated with SDF had higher fracture resistance than the control group, the difference was insignificant. This in-vitro study mimics intraoral conditions; however, it is well known that in-vivo studies are required for realistic results. On the other hand, it would be beneficial to test shear-bond strength on carious teeth to support our results. Within the limitations of the present study, the use of SDF in non-carious Class I cavities had no beneficial effect on the fracture resistance of composite restorations.

CONCLUSION

The present study demonstrated that the application of SDF in Class I cavities of non-carious permanent molars did not csignificantly alter the fracture resistance of the restorations. However, various mechanical tests and further clinical studies are required to expand its clinical use as a remineralizing and caries-inhibiting agent under restorations. Further studies, both in-vitro and in-vivo, with larger sample sizes and varied experimental conditions, are recommended to evaluate fracture resistance.

Ethics Committee Approval: This study was approved by Istanbul Aydin University Non-Interventional Clinical Research Ethics Committee (Date: 03.02.2021, No: 2021/373).

Peer Review: Externally peer-reviewed.

Author Contributions: Conception/Design of Study- S.Z., A.T.A.; Data Acquisition- P.N.B.; Data Analysis/Interpretation- S.Z., A.T.A.; Drafting Manuscript- S.Z., P.N.B.; Critical Revision of Manuscript- A.T.A.; Final Approval and Accountability- S.Z., A.T.A., P.N.B.; Material and Technical Support- S.Z., A.T.A., P.N.B.; Supervision- S.Z., A.T.A.

Conflict of Interest: The authors have no conflict of interest to declare.

Financial Disclosure: The authors declared that this study has received no financial support.

REFERENCES

1. FDI World Dental Federation. The challenge of oral disease: a call for global action. In: the oral health atlas, 2nd ed; FDI World Dental Association: Geneva, Switzerland, 2015. p.12-5.
2. Mackenzie L, Banerjee A. Minimally invasive direct restorations: a practical guide. Br Dent J 2017;223(3):163-71.
3. Gupta J, Thomas MS, Radhakrishna M, Srikant N, Ginjupalli K. Effect of silver diamine fluoride-potassium iodide and 2% chlorhexidine gluconate cavity cleansers on the bond strength and microleakage of resin-modified glass ionomer cement. J Conserv Dent 2019;22(2):201-6.
4. Burgess JO, Vaghela PM. Silver diamine fluoride: a successful anticarious solution with limits. Adv Dent Res 2018;29(1):131-4.
5. Sorkhdini P, Crystal YO, Tang Q, Lippert F. The effect of silver diamine fluoride in preventing in vitro primary coronal caries under pH-cycling conditions. Arch Oral Biol 2021;121:104950.
6. Jabin Z, Nasim I, Priya V V, Agarwal N. Comparative evaluation of salivary fluoride concentration after topical application of silver diamine fluoride and sodium fluoride: a randomized controlled trial. Int J Clin Pediatr Dent 2022;15(3):371-5.
7. Mei ML, Zhao IS, Ito L, Lo EC, Chu CH. Prevention of secondary caries by silver diamine fluoride. Int Dent J 2016;66(2):71-7.
8. Greenwall-Cohen J, Greenwall L, Barry S. Silver diamine fluoride - an overview of the literature and current clinical techniques. Br Dent J 2020;228(11):831-8.
9. Contractor IA, Girish MS, Indira MD. Silver diamine fluoride: extending the spectrum of preventive dentistry, a literature review. Ped Dent J 2021;31(1):17-24.
10. Zhao IS, Gao SS, Hiraishi N, Burrow MF, Duangthip D, Mei ML et. al. Mechanisms of silver diamine fluoride on arresting caries: a literature review. Int Dent J 2018;68(2):67-76.
11. Mei ML, Ito L, Cao Y, Li QL, Lo EC, Chu CH. Inhibitory effect of silver diamine fluoride on dentine demineralisation and collagen degradation. J Dent 2013;41(9):809-17.
12. Mei ML, Li QL, Chu CH, Lo EC, Samaranayake LP. Antibacterial effects of silver diamine fluoride on multi-species cariogenic biofilm on caries. Ann Clin Microbiol Antimicrob 2013;12:4.
13. Chu CH, Lo EC. Microhardness of dentine in primary teeth after topical fluoride applications. J Dent 2008;36(6):387-91.
14. Alvear Fa B, Jew JA, Wong A, Young D. Silver modified atraumatic restorative technique (smart): an alternative caries prevention tool. Stoma Edu J 2016;3(2):243-9.
15. Markham MD, Tsujimoto A, Barkmeier WW, Jurado CA, Fischer NG, Watanabe H et. al. Influence of 38% silver diamine fluoride application on bond stability to enamel and dentin using universal

adhesives in self-etch mode. Eur J Oral Sci 2020;128(4):354-60.
16. de V Habekost L, Camacho GB, Azevedo EC, Demarco FF. Fracture resistance of thermal cycled and endodontically treated premolars with adhesive restorations. J Prosthet Dent 2007;98(3):186-92.
17. Demarco FF, Collares K, Correa MB, Cenci MS, Moraes RR, Opdam NJ. Should my composite restorations last forever? Why are they failing? Braz Oral Res 2017;31(suppl 1):e56.
18. International Standardization Organization. Dental materials guidance on testing of adhesion to tooth structure, technical report 11405. 1st ed. Geneva, Switzerland; 1994.p.1-14.
19. Boutsiouki C, Frankenberger R, Lücker S, Krämer N. Inhibition of secondary caries in vitro by addition of chlorhexidine to adhesive components. Dent Mater 2019;35(3):422-33.
20. Oliveira BH, Rajendra A, Veitz-Keenan A, Niederman R. The effect of silver diamine fluoride in preventing caries in the primary dentition: a systematic review and meta analysis. Caries Res 2019;53(1):24-32.
21. Shimizu A, Kawagoe M. A clinical study of diamine silver fluoride on recurrent caries. J Osaka Univ Dent Sch 1976;16:103-9.
22. Camacho KJ, English JD, Jacob HB, Harris LM, Kasper FK, Bussa HI et. al. Silver diamine fluoride and bond strength to enamel in vitro: A pilot study. Am J Dent 2018;31(6):317-9.
23. Jiang M, Mei ML, Wong MCM, Chu CH, Lo ECM. Effect of silver diamine fluoride solution application on the bond strength of dentine to adhesives and to glass ionomer cements: a systematic review. BMC Oral Health 2020;20(1):40.
24. Danaeifar N, Nejat AH, Cehreli Z, Ballard RW, Johnson JT. The effect of silver diamine fluoride on bond strength of three types of bulk-fill restorative materials to dentin. Pediatr Dent 2022;44(4):290-5.
25. Bates JF, Stafford GD, Harrison A. Masticatory function - a review of the literature. III. Masticatory performance and efficiency. J Oral Rehabil 1976;3(1):57-67.
26. Waltimo A, Könönen M. Maximal bite force and its association with signs and symptoms of craniomandibular disorders in young Finnish non-patients. Acta Odontol Scand 1995;53(4):254-8.

İSTANBUL UNIVERSITY PRESS

RESEARCH ARTICLE / ARAŞTIRMA MAKALESİ
Journal of Advanced Research in Health Sciences /
Sağlık Bilimlerinde İleri Araştırmalar Dergisi 2023
DOI: 10.26650/JARHS2023-1253456

THE EFFECT OF FINISHING AND POLISHING SYSTEMS ON THE SURFACE ROUGHNESS OF INDIRECT COMPOSITE RESINS

BİTİRME VE CİLA SİSTEMLERİNİN İNDİREKT KOMPOZİT REÇİNELERİN YÜZEY PÜRÜZLÜLÜĞÜNE ETKİSİ

Hasibe Sevilay BAHADIR[1], İrem ÇETİNBAK[2], Selin POLATOĞLU[3], Çiğdem ÇELİK[4]

[1] Ankara Yıldırım Beyazıt University, Faculty of Dentistry, Department of Restorative Dentistry, Ankara, Turkiye
[2] Dental Health Center, Sakarya, Turkiye
[3] Private Clinic, Ankara, Turkiye
[4] Kırıkkale University, Faculty of Dentistry, Department of Restorative Dentistry, Kırıkkale, Turkiye

ORCID ID: H.S.B. 0000-0001-8577-4408; İ.Ç. 0000-0002-7295-1855; S.P. 0000-0001-8368-277X; Ç.Ç. 0000-0002-5936-0196

Citation/Atıf: Bahadir HS, Cetinbak I, Polatoglu S, Celik C. The effect of finishing and polishing systems on the surface roughness of indirect composite resins. Journal of Advanced Research in Health Sciences 2023;6(3):317-322. https://doi.org/10.26650/JARHS2023-1253456

ABSTRACT

Objective: The aim of this study was to evaluate the effects of different types of finishing and polishing systems on the surface roughness of indirect composite resins.

Materials and Methods: In this study, 2 indirect composite resins (Gradia Plus (GC Inc., Kyoto, Japan, and Ceramage, SHOFU Inc., Kyoto, Japan) and 2 direct composite resins (FiltekZ250, 3M ESPE, St. Paul, USA and GradioSO, VOCO GmbH, Cuxhaven, Germany) were used. A total of 144 discs specimens were prepared. The specimens were randomly divided into 3 subgroups (n=12). Group K: Mylar Strip Band (Control), Group L: Silicone Polisher (Nais, Sofia, Bulgaria), Group D: Super Snap disc (SHOFU, Kyoto, Japan) polishing systems were used. The surface roughness of the specimens was measured using a profilometer (Surftest-211, Kanagawa, Japan). The data were analyzed statistically ($p<0.05$).

Results: The Mylar strip band surface (control) was measured as the smoothest surface in all groups. While the roughest surface measured was polishing with silicone polishers. ($p<0.05$). While there is no significant statistical difference between the Mylar strip band and yellow rubber polishing system in all materials, a significant difference was found in the Super Snap polishing disc system between Filtek Z250 and Ceramage material ($p=0.002$).

Conclusions: In this study, both the polishing systems used and the materials used had an effect on the surface roughness of indirect resin composites.

Keywords: Indirect composite resin, polishing systems, surface roughness

ÖZ

Amaç: Bu çalışmanın amacı; farklı tipteki bitirme ve cila sistemlerinin indirekt kompozit reçinelerin yüzey pürüzlülüğüne etkisini incelemektir.

Gereç ve Yöntem: Bu çalışmada 2 indirekt kompozit rezin (Gradia Plus, GC Inc., Kyoto, Japonya) ve Ceramage (SHOFU Inc., Kyoto, Japonya) ve 2direkt kompozit rezin (FiltekZ250 (3M ESPE, St. Paul, ABD) ve GradioSO (VOCO GmbH, Cuxhaven, Almanya) kullanılmıştır. Toplam 144 adet disk şeklinde örnek hazırlandı. Örnekler rastgele 3 alt gruba ayrıldı (n=12). Grup K: Mylar Strip Band (Kontrol), Grup L: Silikon Parlatma Lastiği (Nais, Sofia, Bulgaristan), Grup D: Super Snap disk (SHOFU, Kyoto, Japonya) polisaj sistemi kullanıldı. Örneklerin yüzey pürüzlülük ölçümü profilometre (Surftest-211, Kanagava, Japonya) kullanılarak ölçüldü. Elde edilen veriler istatistiksel olarak analiz edildi ($p<0,05$).

Bulgular: Bütün gruplarda istatistiksel olarak anlamlı şekilde Mylar strip band altı yüzey (kontrol) en pürüzsüz yüzey olarak ölçülürken; en pürüzlü yüzey silikon parlatma lastiğiyle yapılan cilada ölçülmüştür. ($p<0,05$). Bütün materyallerde Mylar strip band ve silikon lastik cila sistemi arasında istatistiksel olarak anlamlı bir fark görülmezken; Filtek Z250 ve Ceramage materyali arasında Super Snap cila disk sisteminde anlamlı fark bulunmuştur ($p=0,002$).

Sonuçlar: Bu çalışmada, indirekt kompozit reçinelerin yüzey pürüzlülüğüne hem kullanılan polisaj sistemlerinin hem de materyallerin etkisi olmuştur.

Anahtar Kelimeler: İndirekt kompozit reçine, cila sistemleri, yüzey pürüzlülüğü

Corresponding Author/Sorumlu Yazar: Hasibe Sevilay BAHADIR **E-mail:** sevilay.bahadir@hotmail.com

Submitted/Başvuru: 20.02.2023 • **Revision Requested/Revizyon Talebi:** 01.05.2023 • **Last Revision Received/Son Revizyon:** 01.05.2023 • **Accepted/Kabul:** 01.05.2023 • **Published Online/Online Yayın:** 10.10.2023

INTRODUCTION

Nowadays, the demand for tooth-colored restorations continues to increase in direct proportion to the aesthetic expectations of the patients. Composite resins are the first-choice materials for direct restorations by clinicians (1). Indirect composite resin restorations are also used in restorative dentistry to overcome some of the disadvantages seen in direct composite restorations, such as polymerization shrinkage and difficulties in obtaining an ideal proximal contact and anatomical form (2-4). Indirect composite resins (inlay, onlay, overlay, etc.) are composite restorations prepared in laboratories. The indirect composite inlay technique was introduced in the early 1980s and first-generation indirect composites were produced thanks to this technique. First-generation indirect composites have advantages such as ease of fabrication, adequate marginal adaptation, reduced polymerization shrinkage, and adequate proximal contact. Despite these advantages, first-generation composites have microfill filler content and have been shown to have disadvantages such as marginal and isthmus fractures under heavy occlusal loads, occlusal wear, and poor color stability. In the mid-1990s, a second generation of indirect composites was produced by Touati (3-5). The clinical performance of second-generation indirect composite resins was found to be better than first-generation composites, as they have improved mechanical properties with a high filler content of 60-70% (3-5). For the polymerization of indirect composites used in laboratories, special devices containing light, heat, pressure, or a combination of these have been produced. This method of polymerization increases the durability and longevity of composites (5).

For a good composite restoration, in addition to the composite resin properties, finishing and polishing processes are also of great importance (6). Proper finishing and polishing of restorative materials are very important procedures that increase the aesthetic properties and the clinical life of restorations. The composite resin's organic matrix and inorganic filler types, particle sizes and amounts, technique and the tools used affects the surface structure of the restoration and determine its polishability. The difference in hardness between inorganic filler particles and organic matrices causes the surface to remain rough after polishing. Inorganic filler particles are harder and have less wear than organic matrix (6-8). The surface of a rough restoration increases plaque accumulation which results in gingival inflammation, surface discoloration, and discoloration in the restoration. In addition, an increase in friction coefficient and wear rate is observed on rough surfaces. Therefore, a smooth surface is a crucial factor for the long-term clinical performance of restorations (7). Also, a smooth surface contributes to patient comfort, as a 0.2-0.3 µm change in surface roughness can be detected with the tip of the tongue (8).

While finishing means removing the irregularities at the finishing border of the restoration and creating anatomical contours in order to obtain the desired anatomy, polishing means reducing the roughness created by the finishing tools and removing the scratches (6). Composite resins polymerized against clear tape will have the smoothest possible surface, although not devoid of surface imperfections. Although this surface is rich in an organic matrix, this layer must be removed by finishing and polishing operations. At the same time, with these finishing and polishing processes, excess materials are removed and restorations are reshaped (7).

One of the most important purposes of restorative dentistry practices is to make restorations with the closest physical properties to the tooth tissue. It is the aim of well-finished and polished restorations to have a surface similar to the enamel tissue. In order to obtain a smooth surface, there are carbide and diamond burs, white stones, polishing rubbers and discs, tapes, aluminum oxide, or diamond-containing rubber and pads on the market. However, properties such as the structure, filler content, and type of composite resins affect the success of the finishing and polishing processes (9).

According to the literature, there are many studies examining the effects of polishing systems on the surface roughness of composite resins (7,10-14). However, there are a limited number of studies examining the surface roughness of structurally developed indirect composite resins, the usage areas of which are gradually expanding (15,16).

The aim of this in-vitro study was to evaluate the effects of different polishing systems on the surface roughness of indirect composite resins. The null hypothesis of this study was different polishing systems do not affect the surface roughness of indirect composites.

MATERIALS and METHODS

In this study, 2 different indirect composite resins, Gradia Plus (GC Inc., Kyoto, Japan) and Ceramage (SHOFU Inc., Kyoto, Japan), and two different direct composite resins FiltekZ250 (3M ESPE, St. Paul, USA) and GradioSO (VOCO GmbH, Cuxhaven, Germany) were used. Table 1 shows the manufacturer and material contents.

The required minimum number of specimens for the study was calculated using G*Power v.3.1 software (Heinrich, Düsseldorf, Germany), based on an alpha level of 0.05 (type I error), effect size of 0.4, and beta power of 0.90 (1 - type II error). The estimated minimum number of specimens for each group was determined to be 12. In this study, a total of 144 specimens of 2 mm height and 6 mm diameter were prepared, 36 specimens of each restorative material. After the composite resin was placed on the plastic molds, the upper surface was covered with Mylar strip tape and compressed with a glass plate to obtain a smooth surface. Then, the direct composite resins were light-cured for 20 seconds using an LED light device (Elipar S10, 3M ESPE, St. Paul, USA). To complete the polymerization of the indirect composite resins, the specimens were placed in a laboratory light-curing device (GC LABOLIGHT LV-III, GC, Tokyo, Japan) for 3 minutes according to the manufacturer's instructions. After polymerization, all samples were removed from the

Table 1: Materials, ingredients and manufacturers used in the study

Material	Manufacturer	Material type	Ingredients	Lot number
Gradia Plus, (Indirect composite)	GC Inc., Kyoto, Japan	Microhybrid	UDMA, EDMA (weight 75% filler: Ceramic, Prepolymer, SiO2)	1901151
Ceramage (Indirect Composite)	SHOFU Inc., Kyoto, Japan	Microhybrid	UDMA, UDA, zirconium silicate (weight 73% filler), Pigments and others.	121828
GradioSO (Direct Composite)	VOCO GmbH, Cuxhaven, Germany	Nanohybrid	Resin matrix: bis-GMA, TEGDMA, bis-EMA Filler: 1 µ glass ceramic fillers with 20–40 nm silicon dioxide nanoparticles. 89% filler by weight.	1921607
Filtekz250 (Direct Composite)	3M ESPE, St. Paul, MN, ABD	Microhybrid	Organic matrix: TEGDMA < 1–5%; Bis-GMA < 1–5%; Bis-EMA 5–10%; UDMA 5–10% Filler: Zirconium/silica; 60% volume inorganic filler	NA14156
Super Snap Disc Set (Aluminum oxide coated discs)	SHOFU Inc., Kyoto, Japan	Polishing disc	Aluminum oxide	0321017
Silicon Rubber	Nais Ltd, Sofia, Bulgaria	Polishing rubber	Fine grain silicon particle	1002F082017563

BisGMA: Bisphenol A diglycidyl ether dimethacrylate, BisEMA: Bisphenol A Polyethylene Glycol Diether Dimethacrylate, TEGDMA: Triethylene Glycol Dimethacrylate, UDMA: Diurethane Dimethacrylate, SiO2: Silicon diooxide, EDMA: Ethyleneglycoldimethacrylate

plastic mold and kept in distilled water at 37 °C for 24 hours. All specimens were then divided into 3 different groups (n=12) according to finishing polishing procedures. All specimens except for the control group (Mylar strip) were ground-finished, respectively, with 400, 800, and1200 grit silicon carbide abrasive paper (English Abrasives, UK) on a sanding machine (Phoenix Beta, Buehler, Illinois, USA) and subjected to water cooling (300 revs/min, during 5 s) before polishing. A low-speed handpiece at a maximum of 12000 rpm was used with a continuous repetitive tapping motion. The polishing disc system was used in 4 stages coarse, medium, fine, and extra-fine-grained, with 6 strokes at each stage [12]. After each polishing disc stage, the specimens were thoroughly rinsed with water for 10 seconds to remove any residue on them and air-dried for 5 seconds. The polishing discs were renewed after every 5 samples. All operations were performed by a single operatör (Hasibe Sevilay BAHADIR) to reduce variability.

The groups were divided for each composite resin as follows:

Group K: (Control) (Mylar strip)

Group L: Silicone rubber

Group D: Super-Snap Polishing Disc

The polished composite resin samples were washed, left to dry, and kept at 100% humidity for 24 hours before measuring the average surface roughness values (Ra). The surface roughness test was performed using a contact profilometer (Surftest-211, Mitutoyo; Kanagawa, Japan) moved at a constant speed of 0.05 mm/s with a cut-off value of 0.25 mm. Three random measurements were made on each surface and the average Ra was calculated.

Statistical Package for Social Sciences (SPSS, Chicago, IL, USA) version 18 was used for data analysis. Whether the data were normally distributed or not was determined by the Shapiro-Wilk test. Also, the data were controlled with a Levene's Test for equality of variances. Data were statistically analyzed with a two-way analysis of variance (ANOVA), multiple comparisons were made with the Tukey post hoc, and pairwise comparisons were made with the Bonferroni test at a significance level of 0.05.

RESULTS

Table 2 shows the average surface roughness values (Ra) of composite resins after polishing. In all groups, the surface under the mylar strip (control) was measured as the smoothest surface. Following this, the Super Snap polishing system was measured to be rougher than the mylar strip and finally, the roughest surface measured was polishing made with silicone rubber ($p<0.05$). While there was no significant statistical difference between the materials, Mylar strip, and silicone rubber system. A significant difference was found in the Super Snap polishing disc system between Filtek Z250 and Ceramage material ($p=0.002$), (Table 2).

DISCUSSION

Finishing and polishing processes are an important step that directly affects the aesthetic properties and life of composite resins, and finishing and polishing using a minimum amount of time and tools is clinically important (7). In this study, it was investigated whether polishing systems with different properties would affect the surface roughness (Ra) of different types of composite resins, and the null hypothesis examined based on the results of the study were rejected.

Table 2: Average surface roughness(Ra) + standard deviation values of groups

Restorative Materials	Mylar (Control Group)	Silicon Rubber	Super Snap Disc	p
Ceramage	0.163±0.028[a]	0.612±0.028[b]	0.561±0.028[c#]	.000
Gradia Plus	0.110±0.028[a]	0.658±0.028[b]	0.474±0.028[c]	.000
GrandioSO	0.093±0.028[a]	0.595±0.028[b]	0.453±0.028[c]	.000
Filtek Z250	0.102±0.028[a]	0.730±0.028[b]	0.388±0.028[c#]	.000

While statistical differences in the groups on the same line are shown with different letters ([a, b, c]), statistical differences in the same column are indicated by the symbol ([c] and [c#]) ($p<0.05$).

In this study, different types of indirect and direct composites were used. In order to ensure clinical standardization, all groups except the Mylar strip surface (control group) were sanded under water with 1200 grid silicon carbide papers before the finishing process (9,13). The findings were found to be compatible with the results of many studies. In the studies conducted by Tuncer et al., Antonson et al., Korkmaz et al., Duraes et al., and Baseren; The polymerized composite surface under the Mylar strip band was determined as the smoothest surface (9, 10, 13, 15, 17). Even though, a low roughness surface is obtained in composite resins made with Mylar strip; this surface is rich in organic matrix. Therefore, this layer must be removed by finishing and polishing operations. This will result in a harder, wear-resistant surface (18).

When polishing systems are compared with each other; In all materials, surfaces polished with the Super Snap disc system were statistically significantly smoother than surfaces polished with silicone rubber. Even though there was no significant statistical difference Ceramage indirect composite material polished with a super snap disc system was found to be rougher than Gradia Plus, and even though there was no significant statistical difference ($p>0.05$). Ceramage indirect composite material polished with silicone rubber polishers was found to be smoother than Gradia Plus. GradioSO direct composite material Filtek Z250 polished with Super Snap disc system has a rougher surface, although there is no statistical difference compared to direct composites; GradioSO direct composite material, which was polished with silicone rubber, was found to have a less rough surface, although there was no statistical difference compared to Filtek Z250 direct composite. The roughness of the surfaces obtained by polishing depends on the efficiency, geometry, flexibility, applied pressure, application time, and particle hardness of the systems used for polishing (18).

In order for the polishing systems to be effective on the composite resin surface; the abrasive particles must be harder than the fillers of composite resins. If the abrasive particles in the polishing system are softer than the fillers in composite resins, only the soft resin matrix of the composites will disappear, causing the filler particles to break off from the surface (11, 18). Discs impregnated with aluminum oxide particles, one of the polishing systems, have the same lifting capacity as filler particles and resin matrix. However, this polishing system has limitations due to its geometry. It can be difficult to anatomically finish and polish restorations in the posterior region, especially on contoured surfaces (19). Bilgili et al., Lu et al., and Venturini et al., concluded in their studies that aluminum oxide discs are the best material to provide smoother surfaces in composite resins (18, 20, 21). In our study, a Super Snap disc system containing aluminum oxide was found to be the best polishing method. At the same time, the highest surface roughness was found in silicone rubber containing silicon particles. This is because silicon particles do not have harder abrasives than filler particles of composite resins such as diamond or aluminum oxide particles. Therefore, silicone rubbers are not sufficient for effective finishing and polishing (11). Although there is no statistical difference, polishing with a Super Snap disc may be clinically preferable for Filtek Z250 and Gradia Plus materials. Likewise, polishing with silicone rubber may be clinically preferable for Ceramage and GradioSO materials, although there is no statistical difference.

In recent years, single or two-stage polishing systems have been developed to reduce both the application phase and the application time clinically. In addition to these advantages of single-stage systems, minimizing the risk of cross-infection also makes them more clinically preferred (9,12). Different results have been obtained in studies on single or multi-stage polishing systems. While Yap et al., and St- Georges et al., found similar surface roughness values obtained with single or multi-stage systems in their studies; Tuncer et al., Aytac et al., Bilgili et al., and Uctasli et al., found that multi-stage polishing systems have lower surface roughness values than single-stage polishing systems (9, 11, 18, 22, 23, 24). In our study, single-stage silicone polishing rubber and multi-stage Super Snap Disk systems were compared, and the multi-stage polishing system was found to be more successful.

For composite resins, the roughness value after polishing is required to be below 0.2 µm. It has been observed that the adhesion of bacterial species and the risk of secondary caries are reduced on restorations with a value of less than 0.2 µm (11). In a clinical study conducted by Aytac et al., it was determined that the patients were able to notice an average roughness value of 0.3 µm. (11). The surface roughness value for all composite resin types was found to be higher than 0.3 µm for the finishing and polishing systems used in this study.

In this study, when composite resin types were compared, a statistical difference was observed between the surface roughness of Filtek Z250 and Ceramage composite resin types polished only with Super Snap. Filtek Z250 composite material was found to be smoother. Duraes et al., in a study they carried out, they examined the effect of different polishing systems on the surface roughness of Ceramage indirect composite resin and they found the highest surface roughness in the silicone rubber polishing system (15). Korkmaz et al., in a study they conducted, investigated the effect of different polishing systems on the surface roughness of direct composite resins Grandio and Filtek Z250 and found that Filtek Z250, which was polished with an aluminum oxide-containing polishing system, was statistically smoother than Grandio (13).

Ersöz et al., in another study they conducted, they examined the effect of a polishing system containing diamond particles on the surface roughness of GrandioSO and Gradia Plus materials and found the surface roughness of both materials to be similar (16). The surface roughness of composite resin materials depends on the structure of the composite material as well as the finishing and polishing systems used (14,25). One of the many factors affecting the surface properties of composite resins is the filler size. At the same time, the type, shape, amount, and bonding of the filler particles to the resin matrix affect the clinical performance of composite resins (11). Composites with harder and larger filler particles show higher Ra values after finishing and polishing (9). While the filler particle ratio of Ceramage, the indirect composite used in this study, was 73%; Filtek Z250, which is a direct composite, has a filler particle ratio of 60%. While a higher filler ratio provides a better mechanical property; it can damage the aesthetics of the material and make it difficult to polish (15). When we examine the literature, while Endo et al., reported that the polishing system had an effect on the surface roughness in their study, Bashetty et al., reported that the material had an effect on the surface roughness in their study (12, 26). In their study, Marghalani et al., reported that both the material and the polishing system had an effect on surface roughness (27). In this study, in accordance with the study of Marghalani et al., both the polishing systems used and the materials had an effect on the surface roughness.

This study has several limitations. Profilometer is used to measure surface roughness in in-vitro studies. However, two-dimensional data is obtained with the profilometer; Three-dimensional information is not available. Obtaining surface roughness with only a profilometer is one of the limitations of this study. Another limitation is that polishing systems with different abrasive content are not used. There is also a need for long follow-up clinical studies that mimic the oral environment.

CONCLUSION

Within the limitations of this study, the following conclusions were reached:

The lowest surface roughness was found in the Super Snap polishing system in all materials except the control group.

Filtek Z250 group, in which a Super Snap polishing system is used, has a lower surface roughness than the Ceramage group.

The results of this study present different options for dentists in choosing the appropriate finishing and polishing techniques for clinical application.

Ethics Committee Approval: Ethics Committee approval is not required for this study.

Peer Review: Externally peer-reviewed.

Author Contributions: Conception/Design of Study- H.S.B., S.P., İ.Ç., Ç.Ç.; Data Acquisition- H.S.B., S.P., İ.Ç., Ç.Ç.; Data Analysis/Interpretation- H.S.B., S.P., İ.Ç., Ç.Ç.; Drafting Manuscript- H.S.B., S.P., C.Ç.; Critical Revision of Manuscript- H.S.B., C.Ç., İ.Ç.; Final Approval and Accountability- H.S.B., S.P., İ.Ç., Ç.Ç.; Material and Technical Support- H.S.B., C.Ç.; Supervision- H.S.B., C.Ç.

Conflict of Interest: The authors have no conflict of interest to declare.

Financial Disclosure: The authors declared that this study has received no financial support.

REFERENCES

1. Kirmali O, Barutcugil C, Harorli O, Kapdan A, Er Kursat. Resin cement to indirect composite resin bonding: Effect of various surface treatments. Scanning 2015;37(2):89-94.
2. Visuttiwattanakorn P, Suputtamongkol K, Angkoonsit D, Kaewthong S, Charoonanan P. Microtensile bond strength of repaired indirect resin composite. J Adv Prosthodont 2017;9(1):38-44.
3. Souza EM, Francischone CE, Powers JM, Rached RN, Vieira S. Effect of different surface treatments on the repair bond strength of indirect composites. Am J Dent 2008;21(2):93-6.
4. Kimyai S, Oskoee SS, Mohammadi N, Rikhtegaran S, Bahari M, Oskoee PA, et al. Effect of different mechanical and chemical surface treatments on the repaired bond strength of an indirect composite resin. Lasers Med Sci 2015;30(2):653-9.
5. Karaarslan ES, Ertas E, Bulucu B. Clinical evaluation of direct composite restorations and inlays: Results at 12 months. J Rest Dent 2014;2(2):70-77.
6. Ölmez A, Kisbet S. Kompozit rezin restorasyonlarda bitirme ve polisaj işlemlerindeki yeni gelişmeler. Acta Odontol Turc 2012;30(2):115-22.
7. Choi M-S, Lee Y-K, Lim B-S, Rhee S-H, Yang H-C. Changes in surface characteristics of dental resin composites after polishing. J Mater Sci 2005;16(4):347-53.
8. Ergücü Z, Türkün L. Surface roughness of novel resin composites polished with one-step systems. Oper Dent 2007;32(2):185-92.
9. Tuncer D, Halaçoğlu DM, Çelik Ç, Arhun N. Bitirme ve Parlatma Sistemlerinin Farklı Tipteki Kompozit Rezinlerin Yüzey Pürüzlülüğüne Etkisi. 7tepe Klinik Dergisi 2016;12(2):25-30.
10. Antonson SA, Yazici AR, Kilinc E, Antonson DE, Hardigan PC.

Comparison of different finishing/polishing systems on surface roughness and gloss of resin composites. Int J Dent 2011;39(Suppl 1):e9-17.

11. Aytac F, Karaarslan ES, Agaccioglu M, Tastan E, Buldur M, Kuyucu E. Effects of novel finishing and polishing systems on surface roughness and morphology of nanocomposites. J Esthet Restor Dent 2016;28(4):247-61.
12. Bashetty K, Joshi S. The effect of one-step and multi-step polishing systems on surface texture of two different resin composites. J Conserv Dent 2010;13(1):34-8.
13. Korkmaz Y, Ozel E, Attar N, Aksoy G. The influence of one-step polishing systems on the surface roughness and microhardness of nanocomposites. Oper Dent 2008;33(1):44-50.
14. Ozel E, Korkmaz Y, Attar N, Karabulut E. Effect of one-step polishing systems on surface roughness of different flowable restorative materials. Dent Mater J 2008;27(6):755-64.
15. Durães I, Macêdo GL, Carvalho CF, Oliveira VMB, Lima EMCX. Effects of different polishing systems on the surface roughness of two ceromers. Bra Dent Sci 2016;19(2):56-63.
16. Ersöz B, Karaoğlanoğlu S, Oktay EA, Aydın N. Color stability and surface roughness of resin based direct and indirect restorative materials. E An Dent Sci 2021;48(1):1-6.
17. Baseren M. Surface roughness of nanofill and nanohybrid composite resin and ormocer-based tooth-colored restorative materials after several finishing and polishing procedures. J Biomater Appl 2004;19(2):121-34.
18. Bilgili D, Dündar A, Barutçugil Ç, Öcal İB. Farkli cila sistemlerinin kompozit rezinlerin yüzey pürüzlülükleri üzerine etkisi. 7tepe Klinik Dergisi 2020;16(2):147-53.
19. Turkun L, Turkun M. The effect of one-step polishing system on the surface roughness of three esthetic resin composite materials. Oper Dent 2004;29(2):203-11.
20. Lu H, Roeder LB, Powers JM. Effect of polishing systems on the surface roughness of microhybrid composites. J Esthet Restor Dent 2003;15(5):297-304.
21. Venturini D, Cenci MS, Demarco FF, Camacho GB, Powers JM. Effect of polishing techniques and time on surface roughness, hardness and microleakage of resin composite restorations. Oper Dent 2006;31(1):11-7.
22. Yap AU, Yap S, Teo C, Ng J. Finishing/polishing of composite and compomer restoratives: effectiveness of one-step systems. Oper Dent 2004;29(3):275-9.
23. St-Georges AJ, Bolla M, Fortin D, Muller-Bolla M, Thompson JY, Stamatiades PJ. Surface finish produced on three resin composites by new polishing systems. Oper Dent 2005;30(5):593-7.
24. Uctasli M, Arisu HD, Omurlu H, Eliguzeloglu E, Ozcan S, Ergun G. The effect of different finishing and polishing systems on the surface roughness of different composite restorative materials. J Contemp Dent Pract 2007;8(2):89-96.
25. Erdemir U, Yildiz E, Eren MM, Ozsoy A, Topcu FT. Effects of polishing systems on the surface roughness of tooth-colored materials. J Dent Sci 2013;8(2):160-9.
26. Endo T, Finger WJ, Kanehira M, Utterodt A, Komatsu M. Surface texture and roughness of polished nanofill and nanohybrid resin composites. Dent Mater J 2010;29(2):213-23.
27. Marghalani HY. Effect of finishing/polishing systems on the surface roughness of novel posterior composites. J Esthet Restor Dent 2010;22(2):127-38.

İSTANBUL UNIVERSITY PRESS

RESEARCH ARTICLE / ARAŞTIRMA MAKALESİ
Journal of Advanced Research in Health Sciences /
Sağlık Bilimlerinde İleri Araştırmalar Dergisi 2023
DOI: 10.26650/JARHS2023-1221508

CONE BEAM COMPUTED TOMOGRAPHY IMAGING CHARACTERISTICS OF MANDIBULAR DENTIGEROUS CYSTS AND POSSIBLE IMAGING FEATURES ASSOCIATED WITH BONE EXPANSION

MANDİBULAR DENTİJERÖZ KİSTLERİN KONİK IŞINLI BİLGİSAYARLI TOMOGRAFİ GÖRÜNTÜLEME ÖZELLİKLERİ VE KEMİK EKSPANSİYONU İLE İLİŞKİLİ OLABİLECEK GÖRÜNTÜLEME ÖZELLİKLERİ

Gökçen AKÇİÇEK[1], Leyla Berna ÇAĞIRANKAYA[1], Nursel AKKAYA[1], Hatice Yağmur ZENGİN[2]

[1] Hacettepe University, Faculty of Dentistry, Department of Dentomaxillofacial Radiology, Ankara, Turkiye
[2] Hacettepe University, Faculty of Medicine, Department of Biostatistics, Ankara, Turkiye

ORCID ID: G.A. 0000-0002-3734-0098; L.B.Ç. 0000-0003-0761-5166; N.A. 0000-0002-2854-1138; H.Y.Z. 0000-0002-9855-2449

Citation/Atıf: Akcicek G, Cagirankaya LB, Akkaya N, Zengin HY. Cone beam computed tomography imaging characteristics of mandibular dentigerous cysts and possible imaging features associated with bone expansion. Journal of Advanced Research in Health Sciences 2023;6(3):323-331. https://doi.org/10.26650/JARHS2023-1221508

ABSTRACT

Objective: Dentigerous cysts (DC) are one of the most common cysts in the jaw, and radiographic features are important for diagnosis. This study aims to evaluate the radiographic features of mandibular DCs on cone beam computed tomography (CBCT) images and investigate the possible associations between the imaging features and bone expansion.

Material and Methods: Patients who had CBCT images with pathologically proven DC within the mandible were included the study. On CBCT images, besides lesion radiographic features, the position of the impacted tooth and cyst-to-crown relationship were also recorded.

Results: Among 36 DCs, 69.4% affected the impacted tooth (61.1% were displaced, 5.6% were resorbed and 2.8% were both displaced and resorbed), 80.6% expanded, 100% had cortical involvement (perforation and thinning), 80.6% affected the inferior alveolar canal (%13.9 resorption, %11.1 displacement, 55.6% resorption and displacement), 65.7% affected the adjacent teeth (27.8% resorption, 30.6% lamina dura loss, 5.6% displacement and lamina dura loss), 25% of impacted tooth position were in buccal/lingual obliquity, and 55.5% had a lateral type cyst-to-crown relationship. There was a statistically significant relationship between the expansion rate and effect on the impacted tooth (p=0.023), between the expansion rate and effect on the adjacent tooth (p=0.011), and between the cyst-to-crown relationship and impacted tooth buccolingual position (p=0.031).

Conclusion: Resorption and displacement of the impacted tooth and resorption, displacement and lamina dura loss of the adjacent tooth were common and statistically related with DCs expansion rates. These imaging features could be a sign of expansion and should be carefully examined.

Keywords: Cone beam computed tomography, dentigerous cyst, mandible

ÖZ

Amaç: Dentijeröz kist (DK), çenelerde sık görülen kistlerden biri olup teşhis edilmesinde radyografik özellikleri önem taşımaktadır. Bu çalışmanın amacı mandibular DK'lerin konik ışınlı bilgisayarlı tomografi (KIBT) görüntüleme özelliklerini incelemek ve kemik ekspansiyonu ile görüntüleme özellikleri arasındaki olası ilişkileri değerlendirmektir.

Gereç ve Yöntem: Çalışmaya KIBT görüntüsü olan ve patoloji raporu ile tanısı doğrulanan hastalar dahil edilmiştir. KIBT görüntülerinde lezyonun radyografik özelliklerinin yanı sıra, gömülü dişin pozisyonu ve kist-kron ilişkisi de değerlendirilmiştir.

Bulgular: 36 DK'nin %69,4'ünün gömülü dişi etkilediği (%61,1 yer değişikliği, %5,6 rezorpsiyon ve %2,8 yer değişikliği ve rezorpsiyon), %80,6'sının ekspansiyona neden olduğu, %100'ünün kortikal tabakalarda tutuluma neden olduğu (perforasyon ve incelme), %80,6'sının inferior alveolar kanalı etkilediği (%13,9 rezorpsiyon, %11,1 yer değişikliği, %55,6 rezorpsiyon ve yer değişikliği), %65,7'sinin komşu dişi etkilediği (%27,8 rezorpsiyon, %30,6 lamina dura kaybı, %5,6 yer değişikliği ve lamina dura kaybı), gömülü dişlerin %25'inin bukkal/lingual oblik pozisyonda olduğu ve %55,5'inde lateral tip kist-kron ilişkisi olduğu tespit edildi. Ekspansiyon oranı ile gömülü dişe etki (p=0,023) ve komşu dişe etki (p=0,011) arasında istatistiksel olarak anlamlı ilişki saptandı. Ayrıca kist-kron ilişkisi ile gömülü dişin bukkolingual konumu arasında da istatistiksel olarak anlamlı ilişki gözlendi (p=0,031).

Sonuç: Bu çalışmada gömülü dişte rezorpsiyon ve yer değişikliği ile komşu dişte yer değişikliği ve lamina dura kaybının sık olduğu ve bunların DK'lerin ekspansiyon oranı ile istatistiksel olarak ilişkili olduğu bulundu. Bu bulgular ekspansiyonun belirtisi olabileceğinden dikkatlice değerlendirilmelidir.

Anahtar Kelimeler: Konik ışınlı bilgisayarlı tomografi, dentijeröz kist, mandibula

Corresponding Author/Sorumlu Yazar: Gökçen AKÇİÇEK **E-mail:** gokcenturkak81@gmail.com

Submitted/Başvuru: 19.12.2022 • **Revision Requested/Revizyon Talebi:** 28.03.2023 • **Last Revision Received/Son Revizyon:** 12.07.2023 • **Accepted/Kabul:** 04.07.2023 • **Published Online/Online Yayın:** 13.10.2023

INTRODUCTION

Dentigerous cysts (DC) are one of the most common cysts in the jaw and represent 17.1-30% of jaw cysts (1-3). Although in previous studies an inflammatory etiology was suggested, in 2022 World Health Organization Classification DC was classified as an odontogenic developmental cyst (1). In clinical features there is usually no pain or discomfort, but hard swelling and facial asymmetry are possible (4). Typically, DC presents as an asymptomatic unilocular radiolucency enclosing the crown of an unerupted or impacted tooth, mostly mandibular third molar (2,4). Radiographic features of DCs on panoramic radiographs have been well defined by various studies (5,6). However, there were limited studies about the radiographic features of DCs on cone beam computed tomography (CBCT) images. Although the recent studies demonstrated different imaging characteristics of intraosseous jaw lesions, including DCs, between the panoramic and CBCT images, the possible associations between the imaging features have not been evaluated (7-9).

CBCT is widely accepted and used in different fields of dentistry (10-13). However, the radiation dose and cost are important factors that should be considered when making a CBCT imaging decision (14). Also, CBCT has some disadvantages, including susceptibility to various artefacts from metallic restorations, patient motion, inadequate scanner calibration and undersampling (4,10). Thereby CBCT images are not always used for surgical treatment planning of DCs and, in some cases, treatment planning could be made only on panoramic images. However, the ability to enable three-dimensional imaging promotes CBCT preference in the evaluation of intraosseous pathologies in the oral and maxillofacial region (15). CBCT provides unobstructed views of both anatomic structures and intraosseous lesions in their precise locations (7). Also, it plays an important role in the delineation of maxillofacial cystic lesions and their impact on the adjacent tissues (15). Because of its three-dimensional nature, CBCT demonstrates lesion expansion, cortical involvement and the effect on surrounding structures of intraosseous jaw lesions better than panoramic imaging (7,8).

As DC is a common developmental cyst and bone expansion is usually the only clinical sign, its imaging features and possible associations between the imaging features, especially lesion expansion, is critical. Therefore, this study aims to evaluate the imaging characteristics of mandibular DCs on CBCT images and investigate the possible associations between the imaging features, especially lesion expansion, which is difficult to evaluate on panoramic images.

MATERIAL and METHODS

This retrospective study was reviewed and approved by the Non-Interventional Non-Invasive Clinical Studies Ethics Board of Hacettepe University (Date:06.11.2018, No: GO 18/1051) and all procedures followed were in accordance with the ethical standards of the responsible committee on human experimentation (institutional and national) and with the Helsinki Declaration of 1975, as revised in 2008. For this type of study, formal consent is not required. CBCT images were obtained from the CBCT image archives in the Department of Oral and Maxillofacial Radiology, Faculty of Dentistry, Hacettepe University. The CBCT scans were acquired with an i-CAT Next Generation (Imaging Sciences International, Hatfield, PA, USA) unit. A tube voltage of 120 kVp was used for all acquisitions, with variation in the field of view, acquisition voxel size (0.200-0.250 mm), tube current (3-7 mA), and exposure time.

A total of 5974 CBCT scans obtained for various reasons between January 2016 and October 2018 were evaluated and 502 images that showed cyst-like lesions were detected. Among these images, patients with inconclusive pathology results and CBCT images of poor diagnostic quality were excluded from the study. Patients who had CBCT images with pathologically proven DC within the mandible were included in the study. The final sample consisted of 34 patients. The images were viewed with i-CAT Vision software (version 1.9.3.14, Imaging Science International, Hatfield, PA, USA). All images were evaluated by two oral and maxillofacial radiologists (28 and 17 years of experience, respectively). In the event of disagreement, a final diagnosis was reached by consensus reading.

Evaluation of CBCT images

The following imaging features of DCs were analyzed:

Location and Size: Locations of the lesions were classified as inter-canine region, posterior (premolar-molar) region, and ramus region. Lesion size was measured at its maximum length on axial, sagittal and coronal planes. The measurements were recorded and repeated by the same observer at an interval of 2 weeks and the mean value was used for analysis.

Shape: The outline of an entire lesion was classified as circular (Figure 1), oval (Figure 2), and scalloped.

Internal structure: DCs were classified as radiolucent, mixed density (radiolucent lesion with radiopaque foci) (Figure 2), or multilocular.

Borders: Lesion borders were divided between corticated and non-corticated.

Effects on surrounding structures: Lesion expansion, cortical involvement and its effect on the impacted tooth, inferior alveolar canal and adjacent teeth were evaluated.

Figure 1: Sagittal CBCT image showing a circular-shaped, central-type dentigerous cyst. Note the root resorption at the distal root of the adjacent second molar

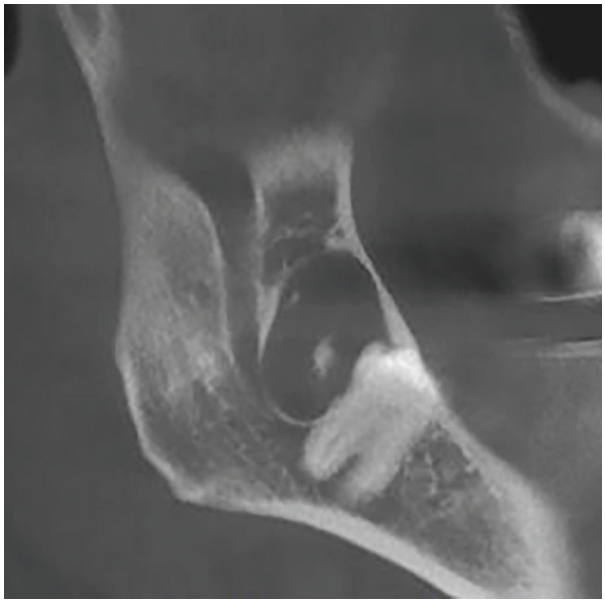

Figure 2: Sagittal CBCT image showing an oval-shaped, lateral-type dentigerous cyst. Note the radiopaque foci inside the radiolucent lesion

Expansion: Expansion rate was categorized as absent, mild and severe. Lesions with expansion were noted and the maximum length of expansion was measured. In the same image section, the healthy opposite side was measured and the ratio of expanded lesion side/healthy opposite side was calculated. Ratios ≤ 1.5 were recorded as mild and ratios > 1.5 were recorded as severe expansion. Also, expansion direction (buccal, lingual, alveolar crest, etc.) was recorded.

Cortical involvement: Cortical plates were evaluated for existence of perforation and thinning.

Effect on impacted tooth: DC's effect on the impacted tooth was recorded as resorption and/or displacement.

Effect on the inferior alveolar canal: DC's effect on the inferior alveolar canal was recorded as absent, resorption, displacement, and resorption and displacement.

Effect on the adjacent teeth: Adjacent teeth were evaluated for resorption (Figure 1), displacement, and loss of lamina dura.

Position of impacted tooth: Impacted tooth position was recorded using Winter Classification as mesioangular, distoangular, horizontal, vertical, buccal/lingual obliquity, transverse or inverse. Also the impacted tooth's buccolingual position in bone was recorded using the modified Khojastepour method as lingual position (epicenter of the crown located in the lingual one third of the buccolingual distance), buccal position (epicenter of the crown located in the buccal one third of the buccolingual distance) and central position (epicenter of the crown located in the center of the buccolingual distance) (16).

Cyst-to-crown relationship: Tooth-DC relationship was classified as central (Figure 1), lateral (Figure 2) and circumferential (Figure 3). In the central type the cyst surrounds the crown of the tooth and the enveloped tooth is positioned at the center of the cyst. In this type the cyst is attached to tooth at the region of cementoenamel junction. In the lateral type the radiographic appearance results from dilatation of the follicle on one aspect of the crown and cyst grows laterally along the root surface and attaches to the middle or apical region of the root. Lateral type DC is commonly seen with a partially erupted tooth that its superior aspect is exposed. In the circumferential type, the entire tooth appears to be enveloped by the cyst (3,17).

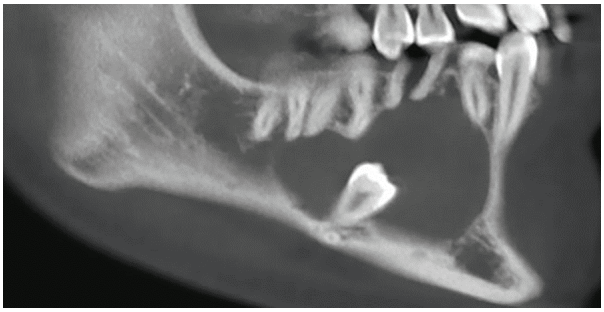

Figure 3: Sagittal CBCT image showing a circumferential type dentigerous cyst. The entire tooth is enveloped by the cyst

Statistics

Mean±Standard Deviation was used as descriptive statistics for normally distributed numerical variables such as age. Otherwise, median, minimum and maximum values were used. The normality of the numerical variables was assessed by using Shapiro-Wilk Normality test. Independent groups were compared using the Independent samples t-test where the parametric test assumptions were satisfied and there are two independent groups. In addition to the evaluating normality assumption, the Levene test was used for assessing homogeneity of group variances. When the parametric test assumptions were violated, the Mann-Whitney U test was used to compare two independent groups. One-way Analysis of Variance test was used where the parametric test assumptions were satisfied and there are more than two independent groups. Otherwise, the Kruskal-Wallis test was used.

Categorical data were presented by frequencies and percentages as n (%). Depending on the dimension of the contingency table, Fisher's Exact test or the Fisher-Freeman-Halton Exact test were used for evaluating dependency between categorical variables.

Significance level was set at 0.05. All analysis was carried out using IBM SPSS Statistics v23.0 for Windows OS.

RESULTS

This study included 34 patients with a mean age of 38.12±19.01 years who had both CBCT images and pathology reports. Among 34 patients, 11 (32.4%) were females with a mean age of 26.64±19.55 years and 23 (67.6%) were males with a mean age of 43.61±16.47 years. The age distribution of males was significantly different from females (p=0.013). Two patients

Table 1: CBCT imaging characteristics of 36 dentigerous cysts

Imaging Feature		Frequency (%)
Localization		
	Posterior region	32 (88.9)
	Ramus region	3 (8.3)
	Inter-canine region	1 (2.8)
Impacted tooth		
	Right third molar	16 (44.4)
	Left third molar	11 (30.6)
	Right second molar	1 (2.8)
	Right second premolar	3 (8.3)
	Left second premolar	3 (8.3)
	Right canine	1 (2.8)
	Left second deciduous molar	1 (2.8)
Shape		
	Oval	26 (72.2)
	Circular	9 (25)
	Scalloped	1 (2.8)
Internal structure		
	Lucent	33 (91.6)
	Mixed	2 (5.6)
	Multilocular	1 (2.8)
Borders		
	Corticated	32 (88.9)
	Non-corticated	4 (11.1)
Effect on surrounding structures		
	Effect on the impacted tooth	25 (69.4)
	Displaced	22 (61.1)
	Resorbed	2 (5.6)
	Displaced and resorbed	1 (2.8)
	Expansion	29 (80.6)
	Buccal	2 (5.6)
	Lingual	14 (38.9)
	Buccal and lingual	10 (27.8)
	Coronal	3 (8.3)
	Cortical involvement	36 (100)
	Effect on the inferior alveolar canal	29 (80.6)
	Resorption	5 (13.9)
	Displacement	4 (11.1)
	Resorption and displacement	20 (55.6)
	Effect on adjacent teeth	23 (65.7)
	Resorption	10 (27.8)
	LLD	11 (30.6)
	Displacement and LLD	2 (5.6)
Cyst-to-crown relationship		
	Lateral	20 (55.5)
	Central	15 (41.7)
	Circumferential	1 (2.8)
Impacted tooth position Winter Classification	Vertical	8 (22.2)
	Horizontal	8 (22.2)
	Buccal/lingual obliquity	9 (25)
	Inverse	6 (16.7)
	Mesioangular	2 (5.6)
	Distoangular	2 (5.6)
	Transverse	1 (2.8)
Impacted tooth position Modified Khojastepour Classification	Central	23 (63.9)
	Lingual	10 (27.8)
	Buccal	3 (8.3)
Lesions dimensions		Mean Values
	Mesio-distal direction	23.08±9.80 mm
	Bucco-lingual direction	13.50±2.71 mm
	Apico-incisal direction	20.42±7.33 mm

LLD: Loss of lamina dura

Table 2: Detailed distribution of the relation between the expansion and effect on impacted tooth and adjacent tooth

Expansion	Effect on impacted tooth				
	Absent	**Present**		**Total**	
Absent	5 (71.4%)	2 (28.6%)	0 (0%) Resorption 2 (28.6%) Displacement 0 (0%) Resorption and displacement	7 (100%)	p=0.023*
Mild	1 (9.1%)	10 (90.9%)	0 (0%) Resorption 10 (90.9%) Displacement 0 (0%) Resorption and displacement	11 (100%)	
Severe	5 (27.8%)	13 (72.2%)	2 (11.1%) Resorption 10 (55.6%) Displacement 1 (5.6%) Resorption and displacement	18 (100%)	
	Effect on adjacent tooth				
	Absent	**Present**		**Total**	
Absent	4 (57.1%)	3 (42.9%)	2 (28.6%) Resorption 1 (14.3%) LLD 0 (0%) Displacement and LLD*	7 (100%)	
Mild	6 (60%)	4 (40%)	0 (0%) Resorption 2 (20%) LLD 2 (20%) Displacement and LLD	10 (100%)	p=0.011*
Severe	2 (11.1%)	16 (88.9%)	8 (44.4%) Resorption 8 (44.4%) LLD 0 (0%) Displacement and LLD	18 (100%)	

One dentigerous cyst was excluded from this evaluation because although the adjacent tooth had resorption it also had periapical lesion, which could be the reason of the root resorption, *p<0.005 statistically significant relation, LLD: Loss of lamina dura

(15-year-old female and 67-year-old male) had bilateral DCs, thus 36 DCs were evaluated. Table 1 shows CBCT imaging features of 36 DCs.

The median age of patients whose DCs associated with primary teeth, permanent canine and premolars (12 years (6-75)) were younger than patients whose DCs associated with permanent molars (42.50 years (15-67)) (p=0.017). Although the median age of the lateral type DC (42.45 years) was higher than the central type (34.20 years) this wasn't statistically significant.

There were 7 (19.4%) no expansion, 11 (30.6%) mild, and 18 (50%) severe expansion rates. The expansion rate and the other imaging features relations were examined and there was a statistically significant relationship between the expansion rate and its effect on the impacted tooth (p=0.023). The relationship was statistically significant between the expansion rate and the effect on the adjacent tooth (p=0.011). DCs with expansion showed significantly more impacted teeth with displacement and/or resorption and more adjacent tooth with lamina dura loss than the DCs without expansion (Table 2). Also, there were significant relationships between the expansion rate and mesio-distal and apico-incisal dimensions of the lesion (p=0.017 and p=0.001 respectively), however, there was no relationship between expansion and the bucco-lingual dimension (p=0.07) of the lesion. There was no relation between age and expansion rate and mean ages were statistically similar among expansion groups (no expansion 40.86±21.043 years, mild expansion 33.55±17.688 years, severe expansion 40.17±20.523 years) (p=0.638). Similarly, there was no relationship between age and lesion dimensions. Table 3 shows the detailed characteristics of expansion.

Among 15 central type DCs, the most common bucco-lingual position was central (13 (86.7%)), while 1 (6.7%) was in the buccal, and 1 was (6.7%) in the lingual position. Twenty lateral type DCs' bucco-lingual positions were 10 (50%) central, 2 (10%) buccal and 8 (40%) lingual. There was only 1 circumferential type DC and it was in the lingual position. There was a statistically significant relationship between the cyst-to-crown relationship, the impacted tooth's bucco-lingual position, and central type DCs were commonly central in the bucco-lingual position (p=0.031).

DISCUSSION

Dental professionals must be knowledgeable about jaw cysts as they are common, and DCs are one of the most common cysts of the jaw. Many jaw cysts have no clinical symptoms or have similar symptoms like jaw expansion and missing teeth. Radiographs provide useful diagnostic information about cysts that influence the treatment plan (3, 4, 18). Usually, panoramic imaging is the first imaging choice in the surgical treatment planning of DC as it is easy to access and has low radiation dose (19, 20). However, differential diagnosis of DC and odontogenic keratocyst (OKC) on panoramic images is difficult as their radiographic features are similar. Expansion is a common radiographic finding of DC and is widely used for differential diagnosis of DC with OKC (4, 21). However, because of pano-

Table 3: Detailed characteristics of expansion

		Expansion			p-value
		Absent	Mild	Severe	
Gender					
	Female	2 (28.6%)	3 (27.3%)	7 (38.9%)	p=0.897
	Male	5 (71.4%)	8 (72.7%)	11 (61.1%)	
	Total	7 (100%)	11 (100%)	18 (100%)	
Localization					
	Ramus	3 (42.9%)	0 (0%)	0 (0%)	p=0.005*
	Posterior	4 (57.1%)	11 (100%)	17 (94.4%)	
	Inter-canine	0 (0%)	0 (0%)	1 (5.6%)	
	Total	7 (100%)	11 (100%)	18 (100%)	
Shape					
	Circular	3 (42.9%)	4 (36.4%)	2 (11.1%)	p=0.270
	Oval	4 (57.1%)	7 (63.6%)	15 (83.3%)	
	Scalloped	0 (0%)	0 (0%)	1 (5.6%)	
	Total	7 (100%)	11 (100%)	18 (100%)	
Perforation					
	Absent	2 (28.6%)	1 (9.1%)	4 (22.2%)	p=0.633
	Present	5 (71.4%)	10 (90.9%)	14 (77.8%)	
	Total	7 (100%)	11 (100%)	18 (100%)	
Thinning					
	Absent	2 (28.6%)	0 (0%)	1 (5.6%)	p=0.113
	Present	5 (71.4%)	11 (100%)	17 (94.4%)	
	Total	7 (100%)	11 (100%)	18 (100%)	
Effect on inferior alveolar canal					
	Absent	3 (42.9%)	2 (18.2%)	2 (11.1%)	p=0.209
	Present	4 (57.1%)	9 (81.8%)	16 (88.9%)	
	Total	7 (100%)	11 (100%)	18 (100%)	
Bucco-lingual position					
	Central	7 (100%)	5 (45.5%)	11 (61.1%)	p=0.051
	Buccal	0 (0%)	0 (0%)	3 (16.7%)	
	Lingual	0 (0%)	6 (54.5%)	4 (22.2%)	
	Total	7 (100%)	11 (100%)	18 (100%)	
Cyst-to-crown relationship					
	Central	4 (57.1%)	3 (27.3%)	8 (44.4%)	p=0.620
	Lateral	3 (42.9%)	8 (72.7%)	9 (50%)	
	Circumferential	0 (0%)	0 (0%)	1 (5.6%)	
	Total	7 (100%)	11 (100%)	18 (100%)	

*p=0.005 statistically significant relation

ramic imaging, two-dimensional nature lesion expansion and cortical involvement, its effect on surrounding structures could not be properly evaluated. These radiographic features could be more accurately evaluated with CBCT images (7, 8, 10). In this study, besides DCs radiographic features on CBCT images, relations among these features, especially lesion expansion, were investigated. As jaw expansion could be the only clinical symptom of DC and is critical for differential diagnosis of DC, this study aims to evaluate the relation between lesion expansion and other radiographic features.

In this study, 34 patients with 36 DCs (2 patients had bilateral DCs) were evaluated and their mean age (38.12±19.01 years) and gender distribution (female 32.4%, male 67.6%) was similar with the literature (2, 5, 20, 22). Females (26.64±19,556) were at a younger age compared to males (43,61±16,470 (p=0.013). Also, the localization of legions, (88.9% posterior region), involved tooth (75% third molar), and shape (97.2% oval or circular) were compatible with the literature (2, 15, 18). Previous studies reported that DC is associated with permanent teeth (2, 23). However, in this study, one DC was associated with a deciduous tooth (Figure 4). The median age of patients whose DCs were

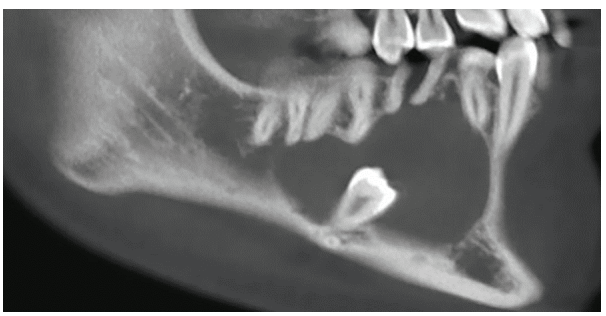

Figure 4: Cropped reconstructed panoramic image demonstrating a DC with deciduous tooth

associated with primary tooth, permanent canine and premolars (12 years) were younger than patients whose DCs were associated with permanent molars (42.50 years) (p=0.017). As permanent third molars are the last teeth that develop in the oral cavity, DCs associated with these teeth were seen in older age groups. When age and cyst-to-crown relationships were evaluated, it was seen that the median age of the lateral type DC (42.45 years) was higher than the central type (34.20 years). However, this wasn't statistically significant.

Terauchi et al. and Main analyzed DCs around the mandibular third molar and reported that there was no relationship between the lesion size and age (5, 24). Similarly, Akçiçek et al. analyzed 25 DCs, 5 in the maxilla and 20 in the mandible and found no relation between lesion size and age (25). The present study found similar results suggesting that lesion enlargement is independent from age.

DCs are usually defined as unilocular radiolucent lesions around the crown of an impacted or unerupted tooth with no septa or loculation within the cyst (4, 21). In this study, most of the DCs fit this definition. However, the internal structure of 2 (5.6%) DCs were radiolucent with radiopaque foci and 1 (2.8%) was multilocular. Although mixed internal structure is unexpected in DCs, there are reports of DCs containing radiopaque foci (calcifications) in radiolucent lesions, as in this study (21, 23, 26, 27). Another unexpected radiographic feature is septa formation within the cyst and in this study, this feature was observed in 1 (2.8%) patient. There have been some studies that reported multilocular appearance of DCs (5, 28, 29). Terauchi et al. investigated panoramic images of 257 DCs and there were 229 (89.1%) unilocular and 28 (10.9%) multilocular cysts (5). Occasionally, trabeculations may be seen in DCs and this may cause multilocular internal structure with an erroneous impression (3, 28). In this study, DCs were evaluated with CBCT images, while Terauchi et al. used panoramic images (5). Therefore, it is possible that they classified trabeculations in DCs as multilocularity on panoramic images. Similarly, Martinelli-Klay et al. reported a DC that showed multilocular radiographic features on a panoramic image. However, multi-slice computed tomography revealed a unilocular lesion without septations (28).

As previously mentioned, expansion is a common radiographic finding of DCs and is widely used for differential diagnosis of DC with OKC (4, 21). A unilocular radiolucent OKC with an impacted tooth has similar radiographic findings with DC except for cortical expansion (4, 15). However cortical expansion could not be adequately evaluated with panoramic images, the most widely used dental imaging method, and could be properly determined with CBCT images (7, 10). Meng et al. investigated DCs in the maxilla and found 78.5% buccal expansion and 36.7% lingual expansion (15). The present study investigated 36 DCs in the mandible and found 33.3% buccal expansion and 69.4% lingual expansion. The different results between Meng et al. and the present study are because of different jawbones (15). As the external oblique ridge is located on the buccal surface, the buccal side of the mandible is denser than the lingual side and this may restrict the expansion.

Expansion and the other radiographic features' relations were examined and there was a statistically significant relationship between the expansion and its effect on the adjacent tooth (resorption and loss of lamina dura) (p=0.011). The effect on the adjacent tooth was seen on 23 (64%) DCs and this was higher than the other studies (Meng et al. 10.1%, Açıkgöz et al. 13.1%) (15,18). Among these studies, different imaging methods used and different effects were evaluated and these could cause differences in the results too.

Also, there was a statistically significant relationship between the expansion and the effect on the impacted tooth (p=0.023). Among 25 (69.4%) impacted teeth the most seen alteration was tooth displacement (22, 61.1%). Displaced teeth can affect surrounding structures, can perforate the cortical plates or inferior alveolar canal, as in this study, and consequently complicate treatment. In this study, resorption of the impacted tooth was only seen in DCs with severe expansion. However, it is not possible to conclude that resorption of the impacted tooth occurs only in DCs with severe expansion because of our limited study sample. Further studies with larger samples are needed. Nevertheless, in the cases with a displacement of the impacted tooth, resorption and/or loss of lamina dura at the adjacent tooth in panoramic images the thought that there may be expansion should be considered.

DC expands the cortical boundary of the involved jaw as it grows (4, 17). This property was obviously observed in the present study; cortical expansion was seen in 29 (80.6%) cases. There was a statistically significant relationship between the expansion and lesion dimensions, especially the mesio-distal and apico-insical dimensions (p=0.017 and p=0.001 respectively). This feature is important for differential diagnosis of DC and OKC, as growing along the internal aspect of the jaws and causing minimal expansion is characteristic of OKC (4, 17).

Impacted tooth displacement was 61.1% (22/36) in this study and this was higher than in other studies (Açıkgöz et al. 9.9%, Lee et al. 19.15%) (18, 30). Similarly, expansion (80.6%) and cortical perforation (80.6%) rates were higher than in other studies (Lee et al. 67.3% expansion, 36.7% cortical perforation) (30). Lee et al. used computed tomography imaging to identify expansion and cortical perforation while in the present study, CBCT imaging is used (30). Different imaging methods have different resolutions and interval sections that could influence the results, especially cortical perforation.

Many lesions in the mandible can affect the inferior alveolar canal and DC is one of them (3, 4, 31). In the present study, this effect was found in 29 (80.6%) of DCs and was higher from Kauke et al. results (31). This may be due to our study only included mandibular DCs and also most of them localized at the posterior region.

Some lesions with unerupted teeth can have similar radiographic images to DC (22). In some studies, the cyst-to-crown

relationship is used for differential diagnosis and it was stated that DC attaches to the tooth at the cementoenamel junction and this feature is important for differential diagnosis (4, 31). Ikeshima and Tamura investigated the attachment point of lesions to the impacted tooth and reported that DCs' attachment points to the root were closer to the cementoenamel junction than benign tumors (22). However, it was also reported that, as in our former study, the cyst-to-crown relationship of DCs shows several radiographic variations (15, 25). In this study only 15 (41.7%) DCs were central type, 20 (55.5%) were lateral and 1 (2.8%) was circumferential type. This was similar to our previous study that DCs cyst-to-crown relationship was categorized as an attachment at the cementoenamel junction (40%) and attachment the at root surface (60%) (25). Meng et al. reported similar central type DC (44.3%), however, their lateral (38%) and circumferential (11.4%) types were different (15).

In this study, Khojastepour classification is modified and the epicenter of the crown is used for the impacted tooth buccolingual position (16). There was a statistically significant relationship between impacted tooth buccolingual position and cyst-to-crown relationship (p=0.031) and centrally positioned DCs' cyst-to-crown relationship was the most common central type. This finding has critical importance while surgical treatment is planned with panoramic images.

The biggest limitation of this study is the small sample size. Although a total of 5974 CBCT scans were evaluated, only 34 patients were included in the study. Despite this limited sample size DCs displayed varying imaging characteristics than expected. For a better understanding of these variations, future studies with larger sample groups are needed.

CONCLUSIONS

In this study, resorption and displacement of impacted tooth and resorption, displacement, and lamina dura loss of adjacent tooth are related to DCs expansion rates. Therefore, these radiographic features could be a sign of expansion and should be carefully examined.

Ethics Committee Approval: This study was approved by Hacettepe University Non-Invasive Clinical Studies Ethics Board (Date: 06.11.2018, No: GO 18/1051).

Peer Review: Externally peer-reviewed.

Author Contributions: Conception/Design of Study- G.A., L.B.Ç., N.A.; Data Acquisition- G.A., L.B.Ç.; Data Analysis/Interpretation- G.A., L.B.Ç., N.A., H.Y.Z.; Drafting Manuscript- G.A., H.Y.Z.; Critical Revision of Manuscript- G.A., L.B.Ç., N.A.; Final Approval and Accountability- G.A., L.B.Ç., N.A., H.Y.Z.

Conflict of Interest: The authors have no conflict of interest to declare.

Financial Disclosure: The authors declared that this study has received no financial support.

REFERENCES

1. World Health Organization. Classification of Tumours Editorial Board. Head and neck tumours. Lyon (France): International Agency for Research on Cancer; 2022. WHO classification of tumours series, 5th ed.; vol. 9. https://publications.iarc.fr/Book-And-Report-Series/Who-Classification-Of-Tumours/WHO-Classification-Of-Head-And-Neck-Tumours-2017
2. Zhang LL, Yang R, Zhang L, Li W, MacDonald-Jankowski D, Poh CF. Dentigerous cyst: a retrospective clinicopathological analysis of 2082 dentigerous cysts in British Columbia, Canada. Int J Oral Maxillofac Surg 2010;39(9):878-82.
3. Shear M, Speight P. Cysts of the oral and maxillofacial regions. 4th ed. Munksgaard: Blackwell; 2007. pp.59-78.
4. White SC, Pharoah MJ.Oral radiology; principles and interpretation. 5th ed. St. Louis (MO):Mosby;2004. pp.721-974.
5. Terauchi M, Akiya S, Kumagai J, Ohyama Y, Yamaguchi S. An analysis of dentigerous cyst developed around a mandibular third molar by panoramic radiographs. Dent J Basel 2019;7(1):13.
6. Shibata Y, Asaumi J, Yanagi Y, Kawai N, Hisatomi M, Matsuzaki H, et al. Radiographic examination of dentigerous cysts in the transitional dentition. Dentomaxillofac Radiol 2004;33(1):17-20.
7. Lim LZ, Padilla RJ, Reside GJ, Tyndall DA. Comparing panoramic radiographs and cone beam computed tomography: Impact on radiographic features and differential diagnoses. Oral Surg Oral Med Oral Pathol Oral Radiol 2018;17:(18)30888-5.
8. Mao W, Lei J, Lim LZ, Gao Y, Tyndall DA, Fu K. Comparison of radiographical characteristics and diagnostic accuracy of intraosseous jaw lesions on panoramic radiographs and CBCT. Dentomaxillofac Radiol 2021;50(2):20200165.
9. Cardoso LB, Lopes IA, Ikuta CRS, Capelozza ALA. Study between panoramic radiography and cone beam-computed tomography in the diagnosis of ameloblastoma, odontogenic keratocyst, and dentigerous cyst. Craniofac Surg 2020;31(6):1747-52.
10. Suomalainen A, Esmaeili EP, Robinson S. Dentomaxillofacial imaging with panoramic views and cone beam CT. Insights Imaging 2015;6(1):1-16.
11. Kapila SD, Nervina JM. CBCT in orthodontics: assessment of treatment outcomes and indications for its use. Dentomaxillofac Radiol 2015;44(1):20140282.
12. Patel S, Durack C, Abella F, Shemesh H, Roig M, Lemberg K. Cone beam computed tomography in Endodontics - a review. Int Endod J 2015;48(1):3-15.
13. Matzen LH, Schropp L, Spin-Neto R, Wenzel A. Radiographic signs of pathology determining removal of an impacted mandibular third molar assessed in a panoramic image or CBCT. Dentomaxillofac Radiol 2017;46(1):20160330.
14. Suomalainen A, Kiljunen T, Käser Y, Peltola J, Kortesniemi M. Dosimetry and image quality of four dental cone beam computed tomography scanners compared with multislice computed tomography scanners. Dentomaxillofac Radiol 2009;38(6):367-78.
15. Meng Y, Zhao YN, Zhang YQ, Liu DG, Gao Y. Three-dimensional radiographic features of ameloblastoma and cystic lesions in the maxilla. Dentomaxillofac Radiol 2019;48(6):20190066.
16. Khojastepour L, Khaghaninejad MS, Hasanshahi R, Forghani M, Ahrari F. Does the Winter or Pell and Gregory classification system indicate the apical position of impacted mandibular third molars?

J Oral Maxillofac Surg 2019;77(11):2222.e1-9.

17. Neville BW, Damm DD, Allen CM, Bouquot JE. Odontogenic cysts and tumors. In: Oral and maxillofacial pathology. 3rd ed. China: Elsevier; 2009.p.678-740.
18. Açıkgöz A, Uzun-Bulut E, Özden B, Güngüz K. Prevalence and distribution of odontogenic and nonodontogenic cysts in a Turkish Population. Med Oral Pathol Oral Cir Bucal 2012;17(1):e108-15.
19. Henien M, Sproat C, Kwok J, Beneng K, Patel V. Coronectomy and dentigerous cysts: a review of 68 patients. Oral Surg Oral Med Oral Pathol Oral Radiol 2017;123(6):670-4.
20. Avril L, Lombardi T, Ailianou A, Burkhardt K, Varoquaux A, Scolozzi P, et al. Radiolucent lesions of the mandible: a pattern-based approach to diagnosis. Insights Imaging 2014;5(1):85-101.
21. Borghesi A, Nardi C, Giannitto C, Tironi A, Maroldi R, Di Bartolomeo F, et al. Odontogenic keratocyst: imaging features of a benign lesion with an aggressive behavior. Insights Imaging 2018;9(5):883-97.
22. Ikeshima A, Tamura Y. Differential diagnosis between dentigerous cyst and benign tumor with an embedded tooth. J Oral Sci 2002;44(1):13-7.
23. Lin HP, Wang YP, Chen HM, Cheng SJ, Sun A, Chiang CP. A clinicopathological study of 338 dentigerous cysts. J Oral Pathol Med 2013;42(6):462-7.
24. Main DM. Follicular cysts of mandibular third molar teeth: radiological evaluation of enlargement. Dentomaxillofac Radiol 1989;18(4):156-9.
25. Akçiçek G, Çağirankaya LB, Akkaya N. Dentigerous Cyst: Evaluation of the cyst-to-crown relationship and other imaging features on cone beam computed tomography images [in Turkish]. Selcuk Dent J 2019;6(4):135-40.
26. Borras-Ferreres J, Sanchez-Torres A, Aguirre-Urizar JM, Gay-Escoda C. Dentigerous cyst with parietal and intracystic calcifications: a case report and literature review. J Clin Exp Dent 2018;10(3):e296-9.
27. Shimizu M, Ogawa D, Okamura K, Kawazu T, Chikui T, Yoshiura K. Dentigerous cysts with calcification mimicking odontogenic tumors: differential diagnosis by CT. Oral Radiol 2015;31(1):14-22.
28. Martinelli-Kläy CP, Martinelli CR, Martinelli C, Macedo HR, Lombardi T. Unusual imaging features of dentigerous cyst: A case report. Dent J (Basel) 2019;7(3):76.
29. Perez A, Lenoir V, Lombardi T. Dentigerous cysts with diverse radiological presentation highlighting diagnostic challenges. Diagnostics (Basel) 2022;12(8):2006.
30. Lee JH, Kim SM, Kim HJ, Jeon KJ, Park KH, Huh JK. Characteristics of bony changes and tooth displacement in the mandibular cystic lesion involving the impacted third molar. J Korean Assoc Oral Maxillofac Surg 2014;40(5):225-32.
31. Kauke M, Safi AF, Grandoch A, Nickenig HJ, Zoller J, Kreppel M. Volemtric analysis of keratocystic odontogenic tumors and non-neoplastic jaw cysts-comparison and its clinical relevance. J Craniomaxillofac Surg 2018;46(2):257-63.
32. Apajalahti S, Hagström J, Lindqvist C, Suomalainen A. Computerized tomography findings and recurrence of keratocystic odontogenic tumor of the mandible and maxillofacial region in a series of 46 patients. Oral Surg Oral Med Oral Pathol Oral Radiol Endod 2011;111(3):e29-37.

RESEARCH ARTICLE / ARAŞTIRMA MAKALESİ
Journal of Advanced Research in Health Sciences /
Sağlık Bilimlerinde İleri Araştırmalar Dergisi 2023
DOI: 10.26650/JARHS2023-1325701

ARTIFICIAL INTELLIGENCE EVALUATION OF RELEASE PROPERTIES OF TABLET FORMULATION CONTAINING FLURBIPROFEN

FLURBİPROFEN İÇEREN TABLET FORMÜLASYONUNUN SALIM ÖZELLİKLERİNİN YAPAY ZEKÂ İLE DEĞERLENDİRİLMESİ

Burcu MESUT[1], **Yavuz Selim ÇELİK**[2]

[1] Istanbul University, Faculty of Pharmacy, Department of Pharmaceutical Technology, Istanbul Turkiye
[2] Istanbul University, Institute of Graduate Studies in Health Sciences, Pharmaceutical Technology Program, Istanbul, Turkiye

ORCID ID: B.M. 0000-0003-2838-1688; Y.S.Ç. 0000-0001-9601-4615

Citation/Atıf: Mesut B, Celik YS. Artificial intelligence evaluation of release properties of tablet formulation containing flurbiprofen. Journal of Advanced Research in Health Sciences 2023;6(3):332-336. https://doi.org/10.26650/JARHS2023-1325701

ABSTRACT

Objective: The aim of this study was to examine the behavior of two different modified release polymers at different concentrations in terms of their similarity to a commercial product in the market, and to perform optimization studies with these polymers using artificial intelligence to find the most suitable formulation.

Materials and Methods: Hydroxypropyl methyl cellulose K100M and sodium alginate polymers were compressed at three different concentrations with the same pressing force. Tests for tablet weights, tablet hardness, diameter/ thickness values and dissolution rate were conducted. The results were evaluated with Minitab19™.

Results: Tablet weights were found to be between 0.2142 mg±0.039 mg and 0.2974 mg±0.001 mg. Tablet thickness varied between 3.80 mm±0.00 mm and 5.00 mm±0.00 mm. Hardness values of formulations containing the 20 mg polymer could not be measured. For other polymer concentrations, they were between 22.6 N±10.11 N and 111.4 N±9.50 N. The dissolution results of formulations prepared with HPMC were lower than those of sodium alginate at the same concentration. The obtained data was evaluated with Minitab19™, which suggested a 41% sodium alginate concentration as the closest formulation to the reference product.

Conclusion: The advantages of artificial intelligence applications are not to be underestimated, and researchers are able to find and obtain results of experiments that they might not be able to conduct. In the light of all these findings, it would not be wrong to say that artificial intelligence will become even more preferable in the coming years.

Keywords: Flurbiprofen, modified release, artificial intelligence, Minitab, optimization

ÖZ

Amaç: Çalışmada iki farklı uzatılmış salım polimerinin farklı konsantrasyonlarda ki davranışının piyasada bulunan bir ticari ürüne benzerliği yönünden incelenmesi ve yapay zeka uygulaması olan Minitab19™ kullanılarak bu polimerlerle optimizasyon çalışması yapılması ve en uygun formülasyonun bulunması amaçlanmıştır.

Gereç ve Yöntem: Hidroksipropil metil selüloz K100 M ve sodyum aljinat polimerleri üç farklı konsantrasyonda, her tablette 20 mg, 60 mg ve 100 mg polimer içerecek şekilde aynı baskı kuvveti, 1000 psi'da basılmıştır ve basılan tabletlerin tablet ağırlıkları, sertlik testleri, çap/yükseklik değerleri ve çözünme hızı testleri gerçekleştirilmiştir. Orijinal ürüne benzer bir salım profili gösterecek bir formülasyon yapay zeka programı olan Minitab19™ ile sonuçlar değerlendirilmiş ve optimizasyon çalışması yapılmıştır.

Bulgular: Hazırlanan tabletlerin tablet ağırlıkları 0,2142 mg±0,039 mg ile 0,2974 mg±0,001 mg arasında bulunmuştur. Tablet çapları 3,80mm±0,00mm ile 5,00 mm±0,00 mm arasında değişkenlik göstermektedir. 20 mg polimer içeren formülasyonların tablet sertlik değerleri ölçülememişken, diğer polimer konsantrasyonları için 22,6 N±10,11 N ile 111,4 N±9,50 N arasında bulunmuştur. HPMC K100M ile hazırlanan formülasyonların çözünme hızı testi sonuçları aynı konsantrasyonda ki sodyum Aljinat sonuçlarına göre daha düşük bulunmuştur. Yapılan çalışmalar sonucunda elde edilen veriler Minitab19™ ile değerlendirilmiş ve yapay zeka programı %41 oranında sodyum aljinat konsantrasyonunu referans ürüne en yakın formülasyon olarak önermiştir.

Sonuç: Yapay zeka uygulamalarının sağladıkları avantajlar azımsanamayacak düzeydedir ve bilim insanlarının belki de deneme şansı olamayacak sonuçları datalar arasından bulup çıkartabilmektedirler. Tüm bu veriler ışığında önümüzdeki süreçlerde daha da tercih edilir hale geleceğini söylemek yanlış olmayacaktır.

Anahtar kelimeler: Flurbiprofen, modifiye salım, yapay zeka, Minitab, optimizasyon

Corresponding Author/Sorumlu Yazar: Burcu MESUT **E-mail:** bmesut@istanbul.edu.tr

Submitted/Başvuru: 11.07.2023 • **Revision Requested/Revizyon Talebi:** 16.08.2023 • **Last Revision Received/Son Revizyon:** 17.08.2023 • **Accepted/Kabul:** 17.08.2023

INTRODUCTION

Modified release (MR) formulations have been developed as an alternative option, since multiple drug administration and the need for repeated doses are a disadvantage in terms of patient compliance. Thus, the frequency of dosing and fluctuations in plasma levels are reduced and controlled (1). One of the groups of excipients used to develop a modified release formulation is hydrophilic polymers. By preparing matrix tablets with these polymers, it is possible to develop a formulation that will allow drug intake at the desired frequency (2). Among the polymers that can be used for this purpose are cross-linked hydrophilic polymers; sodium carboxymethylcellulose (CMC-Na), poly (ethylene glycol) (PEG), hyaluronic acid, hydrophilic matrices (such as hydroxypropyl methylcellulose (HPMC), hydroxypropyl cellulose (HPC)), alginates, poly (hydroxyethyl methacrylate) or poly (HEMA) , and poly(vinyl alcohol) (PVA) (3). These polymers swell when they come into contact with water, and the drug begins to dissolve with the water that enters between the polymer chains that swell and move away (4). Although they show similar behavior in general, the specific behavior of each polymer differs.

HPMC is one of the most preferred polymers in modified release tablets (5). Likewise, another polymer used as a release retarder in modified release tablets is sodium alginate (6).

The disease groups in which modified-release drugs are most preferred are chronic diseases or painkillers that require the patient to take drugs several times a day (7). Flurbiprofen (FLB) is a Non-Steroidal pain reliever that is a derivative of phenyl propionic acid. Its solubility in water is low, therefore it shows low bioavailability. It can be used up to 400 mg per day (8). FLB is a pain-relieving agent preferred in acute musculoskeletal diseases with the treatment of rheumatoid arthritis, osteoarthritis and ankylosing spondylitis signs and symptoms (9).

Today, artificial intelligence applications are used for a wide variety of formulation studies (10, 11). It has also been determined in different studies that it is very useful in the development of modified-release tablets and saves time, cost and labor (12, 13).

This study aimed to evaluate the release properties of different polymers with artificial intelligence in the development of a modified release tablet of low solubility FLB, which is preferred in the treatment of chronic pain, and to compare the health effects of different types of polymers and concentrations.

MATERIALS and METHOD

Flurbiprofen was gifted from Santa Farma İlaç San. A.Ş., Türkiye, and Pronatal pH 6160 (IMCD, Türkiye), hydroxypropyl methyl cellulose (HPMC) K100 M (Colorcon, ABD), magnesium sterate (Parteck LUB, Merck, Sweden) were also gifted. All other reagents were analytical grade.

Analytical method

The analyses of FLB tablets were performed using a UV spectrophotometer (Shimadzu UV-1280, Japan) at a wavelength of 248 nm (14). Accuracy, LOD and LOQ values were calculated.

Preparation of tablets

In order to evaluate the properties of HPMC and sodium alginate, 200 mg of FLB was kept constant in each formulation. Additionally, in order to compare the release properties of the polymers, the amounts of the lubricant Parteck LUB that was added to the formulation was also fixed at 3 mg in each formulation. The amount of polymer added for each tablet in the formulation and the formulation codes are given in Table 1.

Table 1: Formulation codes and polymer content ratios

Formulations	Polymer ratio		
	20 mg (-1)	60 mg (0)	100 mg (+1)
HPMC K100M	F1	F2	F3
Sodium alginate	F4	F5	F6

HPMC: Hydroxypropyl methylcellulose

The active substance and excipients were weighed precisely (Sartorius, France). The weighed powders were mixed in a cubic mixer (Aymes, Turkiye) for 10 minutes by adding FLB and polymers, then magnesium stearate for 5 minutes. The mixed powders were printed on a manual tablet pressing machine (Yener, Turkiye) with a 9.0 mm punch that has a pressing force of 1000 psi.

Physicochemical properties

Diameter, height, hardness and weight deviations of the tablets in each printed tablet formulation were checked (n=10). Mean and SD values were calculated. Diameter and height measurements were carried out with the help of a caliper (Werka, Switzerland), weight deviation control was made with a precision balance (Sartorius, France) and hardness test was done with Sotax HT (Switzerland).

Dissolution studies

Dissolution rate test of the pressed tablets in phosphate buffer (pH=6.8) was performed (Sotax AT7 Smart, Switzerland). 900 mL of dissolution medium was filled into each vessel and set to 37°C±0.5°C. After 30 min., 1h, 2 h, 3 h, 4 h, 5 h, 6 h, 8 h, 10 h and 12 h, samples were taken and filtered through a 0.45 µm nylon filter (GVS, USA) in the Shimadzu UV-1280 spectrophotometer (Shimadzu, Japan) were analyzed (n=3, mean, SD).

Evaluation by artificial intelligence

Analysis results of the analyzed tablets were evaluated with Minitab19™ (Minitab Inc., USA) program, and the $p<0.05$ significance values of Pareto charts, R^2 and models were examined. In addition, an optimization study was carried out for the selection of the polymer and the concentration that would allow to obtain the physicochemical properties and the release profile closest to the reference product.

RESULTS

Analytical method

The correct equation of the analytical method developed

for the dissolution study of FLB tablets was calculated as y=0.0783x+0.0015 and R^2=0.9993. The LOD and LOQ values were 0.7485 µg/mL and 2.2684 µg/mL, respectively.

At the end of the study, an analytical method meeting the ICH Q2 (A) requirements and criteria was developed and used in FLB analysis studies.

Physicochemical properties

The data obtained at the end of the physicochemical test analyses are given in Table 2.

Table 2: Physicochemical test results of the tablets (n=10)

Formulation Code	Tablet Weight (g) (mean, ±SD)	Thickness (mm) (mean, ±SD)	Diameter (mm) (mean, ±SD)	Crushing Force (N) (mean, ±SD)
F1	0.2142±0.039	3.85±0.00	8.8±0.00	-
F2	0.2564±0.002	4.39±0.03	8.8±0.00	73.6±10.11
F3	0.2974±0.001	5.00±0.00	8.8±0.00	111.4±9.50
F4	0.2177±0.002	3.80±0.00	8.8±0.00	-
F5	0.2551±0.002	4.30±0.00	8.8±0.00	22.6±10.11
F6	0.2953±0.001	4.80±0.00	8.8±0.00	32.0±5.44

SD: Standard deviation

Dissolution studies

The findings of the reference product and formulation studies as a result of the dissolution rate test performed in pH 6.8 phosphate buffer are given in Figure 1.

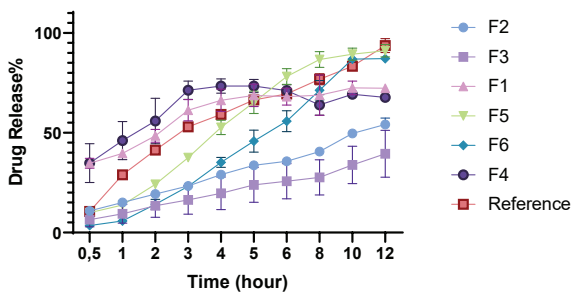

Figure 1: Formulation studies and dissolution rate data graph of reference product

Evaluation by artificial intelligence

The findings obtained as a result of evaluating the obtained data with Minitab19™ are given in Table 3.

These data of significance were also supported by Pareto Charts. Pareto charts are one of the methods used to determine the input that most influences the findings (15). Pareto graphs of these findings are given in Figure 2.

Matrix plots are used to see the relationships between several pairs of inputs and outputs at once. A matrix plot is an array of scatterplots. When you have many input and output variables a matrix of plot becomes very effective to see relationships among pairs of variables. In the Figure 3, the relationship of each input with each other can be seen with the matrix plot (Figure 3).

Table 3: Model R^2 values and p-value data of the outputs

	R^2 value (%)	Model p-value (<0.05)
Tablet weight	99.98	0.019
Crushing Force	99.57	0.099
Diss. 30 minutes	99.99	0.014
Diss. 1h	99.83	0.063
Diss. 2h	99.99	0.016
Diss. 3h	99.56	0.099
Diss. 4h	97.80	0.221
Diss. 5h	94.63	0.341
Diss. 6h	89.81	0.463
Diss. 8h	89.86	0.462
Diss. 10h	96.89	0.262
Diss. 12h	95.89	0.300

R^2: Coefficient of determination, Diss: Dissolution

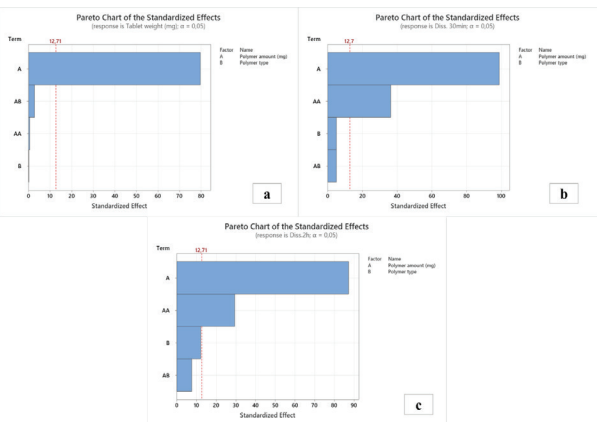

Figure 2: Pareto charts. a: Tablet weight; b: 30-minute dissolution; c: 2 hours dissolution

In the matrix plot, the effects of different polymer types and concentrations on the % release at different time points in the dissolution rate test are seen.

After all these evaluations, an optimization study was carried out and Minitab19™ recommended to prepare a formulation using 41% sodium alginate as the most suitable option. Dissolution rate test findings of the prepared formulation are given in Figure 4.

In the developed optimum formulation, the R^2 value for zero order release kinetics was 0.9836, and 0.9342 for the reference product.

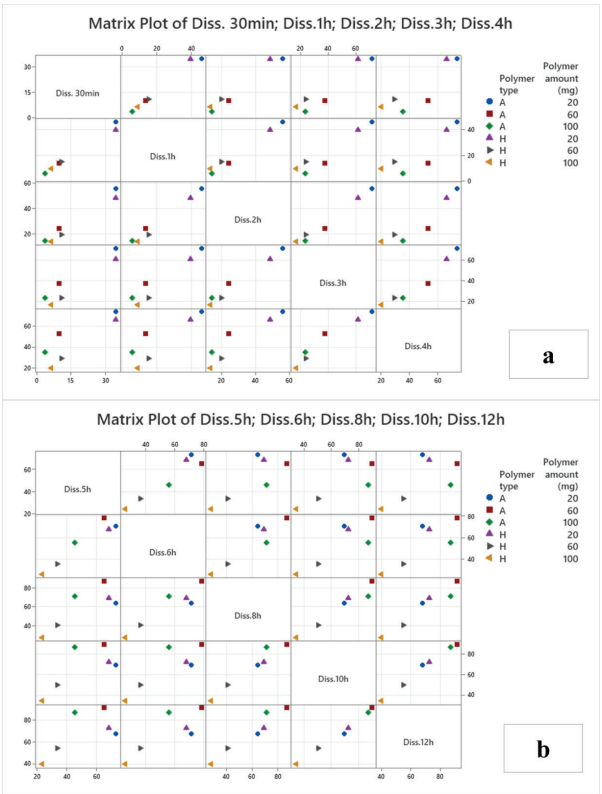

Figure 3: Matrix plot graph. a: Dissolution 30 min to 4h; b: Dissolution 5h to 12h.

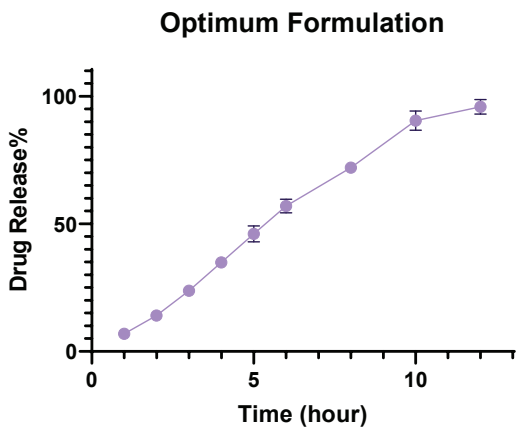

Figure 4: Dissolution rate data graph of the Optimum Formulation and reference product

DISCUSSION

As a result of the physicochemical tests, the tablet weight and thickness value increased due to the increased polymer amount, but there was no change in the tablet diameter despite the different weights with different polymers. The crushing force (N) values increased in proportion with the increase in the amount of polymer in the tablets, but the tablet properties of the two polymers differ at the same hardness values. In the formulations, polymer concentrations varied while the FLB and lubricant ratios were kept constant. The strength of tablets prepared with 20 mgs of polymer were found to be insufficient after tablet compression and thus could not provide sufficient compressibility of the tablet. In addition, the thickness values of the tablets prepared with HPMC K100M were higher than the thickness values of the tablets containing sodium alginate. However, this is not due to the looser binding of the tablet granules because the hardness test results of the tablets are also greater for formulations containing HPMC K100M. This finding is thought to be due to the different powder properties of the two polymers. Further evaluations were made on Minitab19™.

It is a known fact that different polymers and their different concentrations affect drug release and a parallel result was obtained from the findings we obtained (16). When the two polymers were compared, it was observed that HPMC further reduced the release rate with increasing concentration compared to sodium alginate. The viscosity value of HPMC K100M (Colorcon, USA) used here is approximately 100,000 cp at 20 rpm, although it gives different results when measured at different speed and rpm for its 2% solution (17). The viscosity value given for sodium alginate was determined as approximately 1000-1500 mPa for its 1% solution (18). It is possible to say that these differences obtained in the dissolution profile depend on the polymer viscosities.

After the evaluation by artificial intelligence program Minitab$^{19™}$, the R^2 value being above 85% means that the interaction of the inputs and the outputs in the models is highly significant. In addition, p-values below 0.05 indicate the usefulness of the models (19). In the study, it is shown that the R^2 values of all models were found to be high and that it was beneficial. Tablet weight, p-value results of 30-minute dissolution and 2 hours dissolution were found below 0.05, and it was revealed that the polymer type and concentration were effective especially at these points.

According to the Pareto charts, it has been found that the amount of polymer used in the input formulation has the most effect on the output.

It is seen that the optimum formulation for a matrix structured formulation shows a more favorable release kinetics (20). Artificial intelligence was used in formulation optimization in an alternative formulation study of the market product by comparing HPMC and sodium alginate, two different polymers that are used quite frequently, and a similar dissolution rate to the reference product was obtained, in which an ammonium methacrylate copolymer mixture was used as the polymer (9).

The mean crushing force of the formulation was found to be 44 N. When all these findings are evaluated, the closest ratio to the original product is the previously untested 41% sodium alginate value. When the general values are examined, HPMC has a slower release rate, sodium alginate has a faster release, and the release rate in formulations prepared with sodium alginate has shown a more similar profile to the reference product.

CONCLUSION

Interest in artificial intelligence applications is increasing day by day and these algorithms are used for many different purposes. In this study, artificial intelligence was used in formulation optimization studies and a value that was not studied as a formulation was proposed by the program. As can be seen, these applications provide data to researchers, who cannot obtain said data by conducting experiments one-by-one with their estimations, thus saving time. In addition to that, they also help reduce expenses, as the cost advantages they bring are at a level that cannot be ignored.

In this study, a formulation that provides similar release characteristics to the market product containing FLB was developed. The polymer ratio at the concentration recommended by artificial intelligence was not one of the ratios that were originally tested in the experimental design. The program successfully evaluated the dataset, filtered it and suggested the most appropriate ratio.

Ethics Committee Approval: Authors declared that ethics committee approval is not required for this study.

Peer Review: Externally peer-reviewed.

Author Contributions: Conception/Design of Study- B.M., Y.S.Ç.; Data Acquisition- Y.S.Ç., B.M.; Data Analysis/Interpretation- B.M., Y.S.Ç.; Drafting Manuscript- B.M., Y.S.Ç; Critical Revision of Manuscript- B.M., Y.S.Ç; Final Approval and Accountability- B.M., Y.S.Ç.; Material and Technical Support- B.M., Y.S.Ç.; Supervision- B.M., Y.S.Ç.

Conflict of Interest: The authors have no conflict of interest to declare.

Financial Disclosure: The authors declared that this study has received no financial support.

REFERENCES

1. Hedaya MA, El-Masry SM, Helmy SA. Physiologically relevant model to establish the in vivo-in vitro correlation for etamsylate controlled release matrix tablets. J Drug Deliv Sci Technol 2021;1(66):102864.
2. Moussa E, Siepmann F, Flament MP, Benzine Y, Penz F, Siepmann J, et al. Controlled release tablets based on HPMC: lactose blends. J Drug Deliv Sci Technol 2019;1(52):607-17.
3. Paolini MS, Fenton OS, Bhattacharya C, Andresen JL, Langer R. Polymers for extended-release administration. Biomed Microdevices 2019;21(2):45.
4. Cascone S, Lamberti G, Titomanlio G, d'Amore M, Barba AA. Measurements of non-uniform water content in hydroxypropyl-methyl-cellulose based matrices via texture analysis. Carbohydr Polym 2014;103:348-54.
5. Rogers TL, Hewlett KO, Theuerkauf J, Balwinski KM. Assessing how the physical properties of enhanced powder flow of HPMC affect process control during direct compression of matrix tablets. Tablets Capsule (October) 2013;14-22.
6. Mandal S, Basu SK, Sa B. Sustained release of a water-soluble drug from alginate matrix tablets prepared by wet granulation method. AAPS PharmSciTech 2009;10(4):1348-56.
7. Geraili A, Xing M, Mequanint K. Design and fabrication of drug-delivery systems toward adjustable release profiles for personalized treatment. View 2021;2(5):20200126.
8. Shaheen N, Shahiq uz Zaman. Development of fast dissolving tablets of flurbiprofen by sublimation method and its in vitro evaluation. Braz J Pharm Sci 2018;54(4):e17061.
9. RxMedia, 2023, Majezik 200 mg SR Kapsül, Accessed date: 01.05.2023. https://www.eczanet.com/rxmediapharma/.
10. Almotairi N, Mahrous GM, Al-Suwayeh S, Kazi M. Design and optimization of lornoxicam dispersible tablets using Quality by Design (QbD) Approach. Pharmaceuticals 2022;25:15(12):1463.
11. Mehanna MM, Abla KK. Recent advances in freeze-drying: variables, cycle optimization, and innovative techniques. Pharm Dev Technol 2022;14:27(8):904-23.
12. Mesut B, Aksu N, Ozsoy Y. Design of sustained release tablet formulations of alfuzosin HCl by means of neuro-fuzzy logic. Lat Am J Pharm 2013;32(9):1288-97.
13. Özçelik E, Mesut B, Buket AK, Özsoy Y. Quetiapine fumarate extended-release tablet formulation design using artificial neural networks. Turk J Pharm Sci 2017;14(3):213-21.
14. Aswaissi H, Acar ET. Simultaneous determination of flurbiprofen and thiocolchicoside in pharmaceutical preparations by a validated HPLC method. J Res Pharm (online) 2022;26(3):663-74.
15. Manwar J, Kumbhar DD, Bakal R, Baviskar S, Manmode R. Response surface based co-optimization of release kinetics and mucoadhesive strength for an oral mucoadhesive tablet of cefixime trihydrate. Bull Fac Pharm Cairo Univ 2016;54(2):227-35.
16. Galata DL, Zsiros B, Knyihár G, Péterfi O, Mészáros LA, Ronkay F, et al. Convolutional neural network-based evaluation of chemical maps obtained by fast Raman imaging for prediction of tablet dissolution profiles. Int J Pharm 2023;640:123001.
17. Sally A, Kassem AA, El-Kamel AH. Design and evaluation of gastroretentive levofloxacin floating mini-tablets-in-capsule system. Saudi Pharmaceutical Journal 2014;22(6):570-9.
18. Dupont, Kelcosol Pronatal pH 6160, https://www.pharmaexcipients.com/product/protanal-ph-6160kelcosol-nf/.
19. Mesut B, Tok YP, Alkan B, Vefai MK, Al-Mohaya M, Özsoy Y. Effect of mannitol particle size on melatonin dissolution and tablet properties using a Quality by Design Framework. Risk Manag 2023;2:12-21.
20. Charoenying T, Opanasopit P, Ngawhirunpat T, Rojanarata T, Akkaramongkolporn P, Patrojanasophon P. Development of a novel tablet-shaped floating 3D-printed device with adjustable floating time as floating drug delivery systems provided zero-order release kinetics. J Drug Deliv Sci Technol 2023;1(84):104506.

Aims and Scope

Journal of Advanced Research in Health Sciences (JARHS) is an international, scientific, open access periodical published in accordance with independent, unbiased, and double-blinded peer-review principles. The journal is the official publication of Institute of Health Sciences of İstanbul University and it is published every 4 months on February, June, and October. The publication language of the journal is English as of June 2023.

Journal of Advanced Research in Health Sciences (JARHS) aims to contribute to the literature by publishing manuscripts at the highest scientific level on all fields of medicine. The journal publishes original experimental and clinical research articles, reports of rare cases, reviews that contain sufficient amount of source data conveying the experiences of experts in a particular field, and letters to the editors as well as brief reports on a recently established method or technique or preliminary results of original studies related to all disciplines of medicine from all countries.

Editorial Policies and Peer Review Process

The editorial and publication processes of the journal are shaped in accordance with the guidelines of the International Council of Medical Journal Editors (ICMJE), the World Association of Medical Editors (WAME), the Council of Science Editors (CSE), the Committee on Publication Ethics (COPE), the European Association of Science Editors (EASE), and National Information Standards Organization (NISO). The journal conforms to the Principles of Transparency and Best Practice in Scholarly Publishing (doaj.org/bestpractice).

Originality, high scientific quality, and citation potential are the most important criteria for a manuscript to be accepted for publication. Manuscripts submitted for evaluation should not have been previously presented or already published in an electronic or printed medium. The journal should be informed of manuscripts that have been submitted to another journal for evaluation and rejected for publication. The submission of previous reviewer reports will expedite the evaluation process. Manuscripts that have been presented in a meeting should be submitted with detailed information on the organization, including the name, date, and location of the organization.

Manuscripts submitted to Journal of Advanced Research in Health Sciences will go through a double-blind peer-review process. Each submission will be reviewed by at least two external, independent peer reviewers who are experts in their fields in order to ensure an unbiased evaluation process. The editorial board will invite an external and independent editor to manage the evaluation processes of manuscripts submitted by editors or by the editorial board members of the journal. The Editor in Chief is the final authority in the decision-making process for all submissions.

An approval of research protocols by the Ethics Committee in accordance with international agreements (World Medical Association Declaration of Helsinki "Ethical Principles for Medical Research Involving Human Subjects," amended in October 2013, www.wma.net) is required for experimental, clinical, and drug studies and for some case reports. If required, ethics committee reports or an equivalent official document will be requested from the author(s). For manuscripts concerning experimental research on humans, a statement should be included that shows that written informed consent of patients and volunteers was obtained following a detailed explanation of the procedures that they may undergo. For studies carried out on animals, the measures taken to prevent pain and suffering of the animals should be stated clearly. Information on patient consent, the name of the ethics committee, and the ethics committee approval number should also be stated in the Materials and Methods section of the manuscript. It is the author(s)' responsibility to carefully protect the patients' anonymity. For photographs that may reveal the identity of the patients, signed releases of the patient or of their legal representative should be enclosed.

All submissions are screened by a similarity detection software (iThenticate by CrossCheck).

In the event of alleged or suspected research misconduct, e.g., plagiarism, citation manipulation, and data falsification/fabrication, the Editorial Board will follow and act in accordance with COPE guidelines.

Each individual listed as an author should fulfill the authorship criteria recommended by the International Committee of Medical Journal Editors

(ICMJE - www.icmje.org). The ICMJE recommends that authorship be based on the following 4 criteria:

1. Substantial contributions to the conception or

design of the work; or the acquisition, analysis, or interpretation of data for the work; AND

2. Drafting the work or revising it critically for important intellectual content; AND
3. Final approval of the version to be published; AND
4. Agreement to be accountable for all aspects of the work in ensuring that questions related to the accuracy or integrity of any part of the work are appropriately investigated and resolved.

In addition to being accountable for the parts of the work he/she has done, an author should be able to identify which co-authors are responsible for specific other parts of the work. In addition, authors should have confidence in the integrity of the contributions of their co-authors.

All those designated as authors should meet all four criteria for authorship, and all who meet the four criteria should be identified as authors. Those who do not meet all four criteria should be acknowledged in the title page of the manuscript.

The Editorial Board of the journal handles all appeal and complaint cases within the scope of COPE guidelines. In such cases, authors should get in direct contact with the editorial office regarding their appeals and complaints. When needed, an ombudsperson may be assigned to resolve cases that cannot be resolved internally. The Editor in Chief is the final authority in the decision-making process for all appeals and complaints.

Journal of Advanced Research in Health Sciences requires each submission to be accompanied by a Copyright Agreement Form (available for download at https://dergipark.org.tr/en/pub/sabiad). When using previously published content, including figures, tables, or any other material in both print and electronic formats, authors must obtain permission from the copyright holder. Legal, financial and criminal liabilities in this regard belong to the author(s).

Statements or opinions expressed in the manuscripts published in Journal of Advanced Research in Health Sciences reflect the views of the author(s) and not the opinions of the editors, the editorial board, or the publisher; the editors, the editorial board, and the publisher disclaim any responsibility or liability for such materials. The final responsibility in regard to the published content rests with the authors.

Publication Policy

The journal is committed to upholding the highest standards of publication ethics and pays regard to Principles of Transparency and Best Practice in Scholarly Publishing published by the Committee on Publication Ethics (COPE), the Directory of Open Access Journals (DOAJ), the Open Access Scholarly Publishers Association (OASPA), and the World Association of Medical Editors (WAME) on https://publicationethics.org/resources/guidelines-new/principles-transparency-and-best-practice-scholarly-publishing

The subjects covered in the manuscripts submitted to the Journal for publication must be in accordance with the aim and scope of the Journal. Only those manuscripts approved by every individual author and that were not published before in or sent to another journal, are accepted for evaluation.

Changing the name of an author (omission, addition or order) in papers submitted to the Journal requires written permission of all declared authors.

Plagiarism, duplication, fraud authorship/denied authorship, research/data fabrication, salami slicing/salami publication, breaching of copyrights, prevailing conflict of interest are unethical behaviors. All manuscripts not in accordance with the accepted ethical standards will be removed from the publication. This also contains any possible malpractice discovered after the publication.

Plagiarism

Submitted manuscripts that pass preliminary control are scanned for plagiarism using iThenticate software. If plagiarism/self-plagiarism will be found authors will be informed. Editors may resubmit manuscript for similarity check at any peer-review or production stage if required. High similarity scores may lead to rejection of a manuscript before and even after acceptance. Depending on the type of article and the percentage of similarity score taken from each article, the overall similarity score is generally expected to be less than 15 or 20%.

Double Blind Peer-Review

After plagiarism check, the eligible ones are evaluated by the editors-in-chief for their originality, methodology, the importance of the subject covered and compliance with the journal scope. The editor provides a fair double-blind peer review of the submitted articles and hands over the papers matching

the formal rules to at least two national/international referees for evaluation and gives green light for publication upon modification by the authors in accordance with the referees' claims.

Open Access Statement

The journal is an open access journal and all content is freely available without charge to the user or his/her institution. Except for commercial purposes, users are allowed to read, download, copy, print, search, or link to the full texts of the articles in this journal without asking prior permission from the publisher or the author. This is in accordance with the BOAI definition of open access.

The open access articles in the journal are licensed under the terms of the Creative Commons Attribution-NonCommercial 4.0 International (CC BY-NC 4.0) license. (https://creativecommons.org/licenses/by-nc/4.0/deed.en)

Copyright Notice

Authors publishing with the journal retain the copyright to their work licensed under the Creative Commons Attribution-NonCommercial 4.0 International license (CC BY-NC 4.0) (https://creativecommons.org/licenses/by-nc/4.0/) which permits unrestricted, non-commercial use, distribution, and reproduction in any medium, provided the original work is properly cited.

Manuscript Preparation

The manuscripts should be prepared in accordance with ICMJE-Recommendations for the Conduct, Reporting, Editing, and Publication of Scholarly Work in Medical Journals (updated in December 2015 - http://www.icmje.org/icmje-recommendations.pdf). Author(s) are required to prepare manuscripts in accordance with the CONSORT guidelines for randomized research studies, STROBE guidelines for observational original research studies, STARD guidelines for studies on diagnostic accuracy, PRISMA guidelines for systematic reviews and meta-analysis, ARRIVE guidelines for experimental animal studies, and TREND guidelines for non-randomized public behavior.

Manuscripts can only be submitted through the journal's online manuscript submission and evaluation system, available at https://dergipark.org.tr/tr/pub/sabiad Manuscripts submitted via any other medium will not be evaluated.

Manuscripts submitted to the journal will first go through a technical evaluation process where the editorial office staff will ensure that the manuscript has been prepared and submitted in accordance with the journal's guidelines. Submissions that do not conform to the journal's guidelines will be returned to the submitting author with technical correction requests.

Author(s) are required to submit the following:

• **Copyright Agreement Form,**

Title page: A separate title page should be submitted with all submissions and this page should include:

• The full title of the manuscript as well as a short title (running head) of no more than 50 characters,

• Name(s), affiliations, highest academic degree(s) and ORCID ID(s) of the author(s),

• Grant information and detailed information on the other sources of support,

• Name, address, telephone (including the mobile phone number) and fax numbers, and email address of the corresponding author,

• Acknowledgment of the individuals who contributed to the preparation of the manuscript but who do not fulfil the authorship criteria.

Abstract: A Turkish and an English abstract should be submitted with all submissions except for Letters to the Editor. Submitting a Turkish abstract is not compulsory for international authors. The abstract of Original Articles should be structured with subheadings (Objective, Materials and Methods, Results, and Conclusion). Abstracts of Case Reports and Reviews should be unstructured. Please check Table 1 below for word count specifications.

Keywords: Each submission must be accompanied by a minimum of three to a maximum of six keywords for subject indexing at the end of the abstract. The keywords should be listed in full without abbreviations. The keywords should be selected from the National Library of Medicine, Medical Subject Headings database (http://www.nlm.nih.gov/mesh/MBrowser.html).

Manuscript Types

Original Articles: This is the most important type of article since it provides new information based on original research. The main text of original articles should be structured with Introduction, Material and Method, Results, Discussion, and Conclusion

Table 1: Limitations for each manuscript type

Type of manuscript	Word limit	Abstract word limit	Reference limit	Table limit	Figure limit
Original Article	3500	250 (Structured)	50	6	7 or total of 15 images
Invited Review Article	5000	250	50	6	10 or total of 20 images
Case Report	1000	200	15	No tables	10 or total of 20 images
Technical Note	1500	No abstract	15	No tables	10 or total of 20 images
Letter to the Editor	500	No abstract	5	No tables	No media

subheadings. Please check Table 1 for the limitations for Original Articles.

Statistical analysis to support conclusions is usually necessary. Statistical analyses must be conducted in accordance with international statistical reporting standards (Altman DG, Gore SM, Gardner MJ, Pocock SJ. Statistical guidelines for contributors to medical journals. Br Med J 1983: 7; 1489-93). Information on statistical analyses should be provided with a separate subheading under the Materials and Methods section and the statistical software that was used during the process must be specified.

Units should be prepared in accordance with the International System of Units (SI).

Editorial Comments: Editorial comments aim to provide a brief critical commentary by reviewers with expertise or with high reputation in the topic of the research article published in the journal. Authors are selected and invited by the journal to provide such comments. Abstract, Keywords, and Tables, Figures, Images, and other media are not included.

Invited Review Articles: Reviews prepared by authors who have extensive knowledge on a particular field and whose scientific background has been translated into a high volume of publications with a high citation potential are welcomed. These authors may even be invited by the journal. Reviews should describe, discuss, and evaluate the current level of knowledge of a topic in clinical practice and should guide future studies. The main text should contain Introduction, Clinical and Research Consequences, and Conclusion sections. Please check Table 1 for the limitations for Review Articles.

Case Reports: There is limited space for case reports in the journal and reports on rare cases or conditions that constitute challenges in diagnosis and treatment, those offering new therapies or revealing knowledge not included in the literature, and interesting and educative case reports are accepted for publication. The text should include Introduction, Case Presentation, Discussion, and Conclusion subheadings. Please check Table 1 for the limitations for Case Reports.

Letters to the Editor: This type of manuscript discusses important parts, overlooked aspects, or lacking parts of a previously published article. Articles on subjects within the scope of the journal that might attract the readers' attention, particularly educative cases, may also be submitted in the form of a "Letter to the Editor." Readers can also present their comments on the published manuscripts in the form of a "Letter to the Editor." Abstract, Keywords, and Tables, Figures, Images, and other media should not be included. The text should be unstructured. The manuscript that is being commented on must be properly cited within this manuscript.

Tables should be included in the main document, presented after the reference list, and they should be numbered consecutively in the order they are referred to within the main text. A descriptive title must be placed above the tables. Abbreviations used in the tables should be defined below the tables by footnotes (even if they are defined within the main text). Tables should be created using the "insert table" command of the word processing software and they should be arranged clearly to provide easy reading. Data presented in the tables should not be a repetition of the data presented within the main text but should be supporting the main text.

Figures and Figure Legends

Figures, graphics, and photographs should be submitted as separate files (in TIFF or JPEG format) through the submission system. The files should not

be embedded in a Word document or the main document. When there are figure subunits, the subunits should not be merged to form a single image. Each subunit should be submitted separately through the submission system. Images should not be labeled (a, b, c, etc.) to indicate figure subunits. Thick and thin arrows, arrowheads, stars, asterisks, and similar marks can be used on the images to support figure legends. Like the rest of the submission, the figures too should be blind. Any information within the images that may indicate an individual or institution should be blinded. The minimum resolution of each submitted figure should be 300 DPI. To prevent delays in the evaluation process, all submitted figures should be clear in resolution and large in size (minimum dimensions: 100 × 100 mm). Figure legends should be listed at the end of the main document.

All acronyms and abbreviations used in the manuscript should be defined at first use, both in the abstract and in the main text. The abbreviation should be provided in parentheses following the definition.

When a drug, product, hardware, or software program is mentioned within the main text, product information, including the name of the product, the producer of the product, and city and the country of the company (including the state if in USA), should be provided in parentheses in the following format: "Discovery St PET/CT scanner (General Electric, Milwaukee, WI, USA)"

All references, tables, and figures should be referred to within the main text, and they should be numbered consecutively in the order they are referred to within the main text.

Limitations, drawbacks, and the shortcomings of original articles should be mentioned in the Discussion section before the conclusion paragraph.

Revisions

When submitting a revised version of a paper, the author(s) must submit a detailed "Response to the reviewers" that states point by point how each issue raised by the reviewers has been covered and where it can be found (each reviewer's comment, followed by the author's reply and line numbers where the changes have been made) as well as an annotated copy of the main document. Revised manuscripts must be submitted within 30 days from the date of the decision letter. If the revised version of the manuscript is not submitted within the allocated time, the revision option may be canceled. If the submitting author(s) believe that additional time is required, they should request this extension before the initial 30-day period is over.

Accepted manuscripts are copy-edited for grammar, punctuation, and format. Once the publication process of a manuscript is completed, it is published online on the journal's webpage as an ahead-of-print publication before it is included in its scheduled issue. A PDF proof of the accepted manuscript is sent to the corresponding author(s) and their publication approval is requested within 2 days of their receipt of the proof.

References

While citing publications, preference should be given to the latest, most up-to-date publications. If an ahead-of-print publication is cited, the DOI number should be provided. Authors are responsible for the accuracy of references. Journal titles should be abbreviated in accordance with the journal abbreviations in Index Medicus/ MEDLINE/PubMed. When there are six or fewer authors, all authors should be listed. If there are seven or more authors, the first six authors should be listed followed by "et al." In the main text of the manuscript, references should be cited using Arabic numbers in parentheses. The reference styles for different types of publications are presented in the following examples.

Journal Article: Blasco V, Colavolpe JC, Antonini F, Zieleskiewicz L, Nafati C, Albanèse J, et al. Long-term out come in kidneyrecipients from do norstreated with hydroxyethylstarch 130/0.4 and hydroxyethylstarch 200/0.6. Br J Anaesth 2015;115(5):797-8.

Book Section: Suh KN, Keystone JS. Malaria and babesiosis. Gorbach SL, Barlett JG, Blacklow NR, editors. Infectious Diseases. Philadelphia: Lippincott Williams; 2004.p.2290-308.

Books with a Single Author: Sweetman SC. Martindale the Complete Drug Reference. 34th ed. London: Pharmaceutical Press; 2005.

Editor(s) as Author: Huizing EH, de Groot JAM, editors. Functional reconstructive nasal surgery. Stuttgart-New York: Thieme; 2003.

Conference Proceedings: Bengisson S. Sothemin BG. Enforcement of data protection, privacy and security in medical informatics. In: Lun KC, Degoulet P, Piemme TE, Rienhoff O, editors. MEDINFO 92. Proceedings of the 7th World Congress on Medical

Informatics; 1992 Sept 6-10; Geneva, Switzerland. Amsterdam: North-Holland; 1992. pp.1561-5.

Scientific or Technical Report: Cusick M, Chew EY, Hoogwerf B, Agrón E, Wu L, Lindley A, et al. Early Treatment Diabetic Retinopathy Study Research Group. Risk factors for renal replacement therapy in the Early Treatment Diabetic Retinopathy Study (ETDRS), Early Treatment Diabetic Retinopathy Study KidneyInt: 2004. Report No: 26.

Thesis: Yılmaz B. Ankara Üniversitesindeki Öğrencilerin Beslenme Durumları, Fiziksel Aktivitelerive Beden Kitle İndeksleri Kan Lipidleri Arasındaki Ilişkiler. H.Ü. SağlıkBilimleriEnstitüsü, DoktoraTezi. 2007.

Manuscripts Accepted for Publication, Not Published Yet: Slots J. The microflora of black stain on human primary teeth. Scand J Dent Res. 1974.

Epub Ahead of Print Articles: Cai L, Yeh BM, Westphalen AC, Roberts JP, Wang ZJ. Adult living donor liver imaging. DiagnIntervRadiol. 2016 Feb 24. doi: 10.5152/dir.2016.15323. [Epub ahead of print].

Manuscripts Published in Electronic Format: Morse SS. Factors in the emergence of infectious diseases. Emerg Infect Dis (serial online) 1995 Jan-Mar (cited 1996 June 5): 1(1): (24 screens). Available from: URL: http:/ www.cdc.gov/ncidodlElD/cid.htm.

Submission Checklist

- **Cover letter to the editor**
  - The category of the manuscript
  - Confirming that "the paper is not under consideration for publication in another journal".
  - Including disclosure of any commercial or financial involvement.
  - Confirming that the statistical design of the research article is reviewed.
  - Confirming that the references cited in the text and listed in the references section are in line with NLM.
- **Copyright Agreement Form**
- **Author Form**
- **Permission of previous published material if used in the present manuscript**
  - Acknowledgement of the study "in accordance with the ethical standards of the responsible committee on human experimentation (institutional and national) and with the Helsinki Declaration.
  - Statement that informed consent was obtained after the procedure(s) had been fully explained. Indicating whether the institutional and national guide for the care and use of laboratory animals was followed as in "Guide for the Care and Use of Laboratory Animals".
- **Title page**
  - The category of the manuscript
  - The title of the manuscript both in Turkish and in English
  - Short title (running head) both in Turkish and in English
  - All authors' names and affiliations (institution, faculty/department, city, country), e-mail addresses
  - Corresponding author's email address, full postal address, telephone and fax number
  - ORCIDs of all authors.
- **Main Manuscript Document**
  - The title of the manuscript both in Turkish and in English
  - Abstracts both in Turkish and in English (250 words). (Case report's abstract limit is 200 words)
  - Key words: 3 - 6 words both in Turkish and in English
  - Main article sections
  - References
  - Acknowledgement (if exists)
  - All tables, illustrations (figures) (including title, description, footnotes)

İstanbul University
İstanbul Üniversitesi

Dergi Adı: Sağlık Bilimlerinde İleri Araştırmalar Dergisi
Journal Name: Journal of Advanced Research in Healt Sciences

Telif Hakkı Anlaşması Formu
Copyright Agreement Form

Sorumlu Yazar *Responsible/Corresponding Author*	
Makalenin Başlığı *Title of Manuscript*	
Kabul Tarihi *Acceptance Date*	
Yazarların Listesi *List of Authors*	

Sıra No	**Adı-Soyadı** *Name - Surname*	**E-Posta** *E-Mail*	**İmza** *Signature*	**Tarih** *Date*
1				
2				
3				
4				
5				

Makalenin türü (Araştırma makalesi, Derleme, v.b.) *Manuscript Type (Research Article, Review, etc.)*	

Sorumlu Yazar:
Responsible/Corresponding Author:

Çalıştığı kurum	*University/company/institution*	
Posta adresi	*Address*	
E-posta	*E-mail*	
Telefon no; GSM no	*Phone; mobile phone*	

Yazar(lar) aşağıdaki hususları kabul eder::
Sunulan makalenin yazar(lar)ın orijinal çalışması olduğunu ve intihal yapmadıklarını,
Tüm yazarların bu çalışmaya asli olarak katılmış olduklarını ve bu çalışma için her türlü sorumluluğu aldıklarını,
Tüm yazarların sunulan makalenin son halini gördüklerini ve onayladıklarını,
Makalenin başka bir yerde basılmadığını veya basılmak için sunulmadığını,
Makalede bulunan metnin, şekillerin ve dokümanların diğer şahıslara ait olan Telif Haklarını ihlal etmediğini kabul ve taahhüt ederler.
İSTANBUL ÜNİVERSİTESİ'nin bu fikri eseri, Creative Commons Atıf-GayrıTicari 4.0 Uluslararası (CC BY-NC 4.0) lisansı ile yayınlamasına izin verirler. Creative Commons Atıf-GayrıTicari 4.0 Uluslararası (CC BY-NC 4.0) lisansı, eserin ticari kullanım dışında her boyut ve formatta paylaşılmasına, kopyalanmasına, çoğaltılmasına ve orijinal esere uygun şekilde atıfta bulunmak kaydıyla yeniden düzenleme, dönüştürme ve eserin üzerine inşa etme dâhil adapte edilmesine izin verir.
Yazar(lar)ın veya varsa yazar(lar)ın işvereninin telif dâhil patent hakları, fikri mülkiyet hakları saklıdır.
Ben/Biz, telif hakkı ihlali nedeniyle üçüncü şahıslarca vuku bulacak hak talebi veya açılacak davalarda İSTANBUL ÜNİVERSİTESİ ve Dergi Editörlerinin hiçbir sorumluluğunun olmadığını, tüm sorumluluğun yazarlara ait olduğunu taahhüt ederim/ederiz.
Ayrıca Ben/Biz makalede hiçbir suç unsuru veya kanuna aykırı ifade bulunmadığını, araştırma yapılırken kanuna aykırı herhangi bir malzeme ve yöntem kullanılmadığını taahhüt ederim/ederiz.
Bu Telif Hakkı Anlaşması Formu tüm yazarlar tarafından imzalanmalıdır/onaylanmalıdır. Form farklı kurumlarda bulunan yazarlar tarafından ayrı kopyalar halinde doldurularak sunulabilir. Ancak, tüm imzaların orijinal veya kanıtlanabilir şekilde onaylı olması gerekir.

The author(s) agrees that:
The manuscript submitted is his/her/their own original work and has not been plagiarized from any prior work,
all authors participated in the work in a substantive way and are prepared to take public responsibility for the work,
all authors have seen and approved the manuscript as submitted,
the manuscript has not been published and is not being submitted or considered for publication elsewhere,
the text, illustrations, and any other materials included in the manuscript do not infringe upon any existing copyright or other rights of anyone.
ISTANBUL UNIVERSITY will publish the content under Creative Commons Attribution-NonCommercial 4.0 International (CC BY-NC 4.0) license that gives permission to copy and redistribute the material in any medium or format other than commercial purposes as well as remix, transform and build upon the material by providing appropriate credit to the original work.
The Contributor(s) or, if applicable the Contributor's Employer, retain(s) all proprietary rights in addition to copyright, patent rights.
I/We indemnify ISTANBUL UNIVERSITY and the Editors of the Journals, and hold them harmless from any loss, expense or damage occasioned by a claim or suit by a third party for copyright infringement, or any suit arising out of any breach of the foregoing warranties as a result of publication of my/our article. I/We also warrant that the article contains no libelous or unlawful statements and does not contain material or instructions that might cause harm or injury.
This Copyright Agreement Form must be signed/ratified by all authors. Separate copies of the form (completed in full) may be submitted by authors located at different institutions; however, all signatures must be original and authenticated.

Sorumlu Yazar; *Responsible/Corresponding Author;*	**İmza** / *Signature*	**Tarih** / *Date*
		……../……../……


T.C. İSTANBUL ÜNİVERSİTESİ
1453


T.C. İSTANBUL ÜNİVERSİTESİ SAĞLIK BİLİMLERİ ENSTİTÜSÜ
1982